UNIVERSITAT
ROVIRA I VIRGILI

DEPARTAMENT DE QUIMICA ANALITICA
I QUIMICA ORGANICA

C/ Marcel.li Domingo s/n
Campus Sescelades
43007 Tarragona
Tel. 34 977 55 97 69
Fax 34 977 55 84 46
e-mail: secqaqo@urv.net

Dra. MARIA SOLEDAD LARRECHI GARCIA, profesora Titular de Universidad y Dr. F. XAVIER RIUS I FERRÚS, profesor Catedrático de Universidad del departament de Química Analítica i Química Orgànica de la Facultat de Química de la Universitat Rovira i Virgili,

CERTIFICAN: Que la presente memoria que tiene por título "Seguimiento cuantitativo de reacciones de resinas epoxi mediante espectroscopía de infrarrojo cercano y métodos de resolución de curvas", ha sido realizada por MARIANO ENRIQUE GARRIDO bajo nuestra dirección en el Área de Química Analítica de esta Universidad y que todos los resultados presentados son fruto de las experiencias realizadas por dicho doctorando.

Tarragona, 4 de octubre 2006

Dra. María Soledad Larrechi García

Dr. F. Xavier Rius i Ferrús

A Kari, porque sin ella esta aventura
transatlántica no hubiera tenido sentido.

Agradecimientos

Quiero agradecer a todas las personas que, en mayor o menor medida, han colaborado para que esta Tesis llegue a buen término.

A mis directores de Tesis, la Dra. Larrechi y el Dr. Rius, por su constante guía, y valiosos consejos, tanto en el plano científico como académico (los cuales me llevo en la maleta como un tesoro para el futuro), por alegrarse cada vez que he alcanzado un objetivo propuesto y por buscar soluciones conmigo cuando se presentaron problemas. Pero también agradezco muy especialmente a Marisol y a Xavier por la calidad humana excepcional que han demostrado continuamente y por todo el afecto que me han brindado (a mí y a mi familia) durante estos años.

A todos aquellos que me han prestado su ayuda, poniendo a mi disposición sus conocimientos y su tiempo:

A los miembros del grupo de polímeros de la Universitat Rovira i Virgili, particularmente a los doctores Marina Galià, Virginia Cádiz, Joan Carles Ronda y a todo el grupo de becarios que han tenido una paciencia infinita con alguien poco familiarizado con el campo de los polímeros. De manera especial quisiera agradecer a Luis Adolfo Mercado y a Gerard Lligadas por su ayuda en las tareas de síntesis y en diversos aspectos prácticos relacionados con las reacciones de resinas epoxi.

A los miembros del grupo de Cromatografía de la Universitat Rovira i Virgili, especialmente a las doctoras Marta Calull y Eva Pocurull por su asesoramiento en los trabajos de HPLC, y a todo el grupo de becarios por su continua disponibilidad.

Al Dr. Romà Tauler, por haber facilitado generosamente gran parte de los algoritmos utilizados en esta Tesis.

A los doctores Jordi Riu, Alicia Maroto y Ricard Boqué por sus valiosos comentarios acerca de la validación de métodos analíticos. Un agradecimiento especial al Dr. Santiago Macho, por estar siempre dispuesto a solucionar todo tipo de problemas.

A Valeria Russo, muchísimas gracias por la producción del diseño de la Tesis.

Además quisiera agradecer a todos los integrantes del grupo de Quimiometría, Cualimetría y Nanosensores, los que han pasado y los que están actualmente, por todo lo compartido: congresos, cafés, cenas, calçotadas, castañadas, charlas (de las científicas y de las otras), etc y por haber propiciado siempre un clima de trabajo agradable. Gracias Xavier, Marisol, Pili, Itziar, Joan, Ricard, Jordi, Alicia, Javi, Mari, Enric, Santi, Jaume, Eulàlia, Ignacio, Cristina C., Marc, Cristina B., Verónica, Alberto, Esther, Pablo, Marta, Paquita, Joe, Zayda, Néstor, Giselle, Gastón, Iolanda, Nicolás, Raquel, Rafa, Alí, Vanessa, Oleguer.

A los integrantes del Laboratorio FIA de la Universidad Nacional del Sur, especialmente a la Dra. Beatriz Fernández Band, porque comprensiva y generosamente me dejaron marchar y ahora me reciben de la misma manera.

Especialmente quiero dar un gran abrazo a mis amigos de aquí: Patri y Víctor, Iolanda, Pablo y Vale, Martita, Esther, Violeta y Enrique, Mabel y Miguel, Fernando y Elfi, Walter y Alba, Javier, Ignacio, Lola y Pepe, Carina y Daniel. Ya saben cuánto les agradezco y cuánto voy a echar de menos a los que se queden por aquí. Y a mis amigos de allá porque su esfuerzo de cultivar nuestra amistad, aún a la distancia, ha hecho que la lejanía y la añoranza fueran más llevaderas. No los nombraré a todos porque, afortunadamente, la lista es muy larga.

Quisiera expresar mi más profunda gratitud a mis padres porque me han dado todo lo que han podido y más. Sé que de alguna manera esta Tesis es la recompensa a su esfuerzo.

He dejado para el final Kari, mi esposa, porque fue ella quien me impulsó a emprender este proyecto, porque he recibido su apoyo constantemente, compartiendo los logros y también las angustias, ayudándome a mantener el equilibrio entre ciencia y familia. Y por amarnos a mi y a Manel de la forma en que lo hace.

A todos, gracias!

ÍNDICE

Objetivo

OBJETIVO

En esta Tesis doctoral que lleva por título: “Seguimiento cuantitativo de reacciones de resinas epoxi mediante espectroscopía de infrarrojo cercano y métodos de resolución de curvas” se han planteado dos objetivos generales. En el primer objetivo se ha propuesto evaluar la capacidad de la espectrosocopía de infrarrojo cercano, asistida mediante la Resolución Multivariante de Curvas basada en la optimización por Mínimos Cuadrados Alternados, para realizar el seguimiento cuantitativo de reacciones de resinas epoxi. Este objetivo plantea, en primer término, la necesidad de verificar si dicha combinación de técnicas (instrumentales y quimiométricas) permite detectar todas las fuentes de variación presentes en el sistema en estudio. Asimismo, en un segundo paso, implica la determinación cuantitativa de la evolución de las especies involucradas en la reacción a lo largo del tiempo, así como la obtención de información espectral de todos los compuestos (incluidos los intermedios de reacción). Esto supone, además, un estudio de la incertidumbre de los resultados obtenidos y la validación de los mismos.

En el segundo objetivo se ha planteado estimar las constantes cinéticas vinculadas a las reacciones de resinas epoxy. Esto supone profundizar en el conocimiento del mecanismo del proceso de curado y comprender las implicaciones del mismo en las propiedades del producto final de la polimerización.

La consecución de ambos objetivos requiere, por otra parte, llevar a cabo una adecuada documentación bibliográfica, tanto en lo que se refiere a la problemática inherente a las reacciones de curado, como en lo que concierne al mejor conocimiento de las técnicas instrumentales y quimiométricas utilizadas. Estos objetivos de generación y profundización de conocimientos se complementan con las competencias a adquirir para ser un buen investigador. Entre ellas podemos citar la capacidad de contextualizar la

investigación en el ámbito internacional del área de la especialidad, la habilidad para evaluar y sistematizar la bibliografía, con el objetivo de comprender los puntos clave del ámbito de conocimiento tratado, tanto desde un punto de vista disciplinar como multidisciplinar, la capacidad para analizar críticamente los cambios que se producen en el contexto de la disciplina, la capacidad para colaborar con otros investigadores, respetando y valorando sus contribuciones, para diseñar y ejecutar pequeños proyectos de investigación, para formular solicitudes de proyectos a los organismos adecuados, ya sea a la administración pública u otros organismos e instituciones, para gestionar de manera adecuada los recursos de la investigación, la propiedad intelectual y la comercialización de la innovación.

1. Introducción

Las resinas epoxi se hallan entre los compuestos más importantes dentro del grupo de los materiales poliméricos. Bajo el nombre de resina epoxi se suele designar tanto al prepolímero como al producto final del proceso de curado o polimerización, puesto que ambos contienen grupos epóxido en su estructura. El gran interés de las resinas epoxi se debe a la variedad extremadamente amplia de reacciones químicas en las que pueden tomar parte, y a la gran cantidad de materiales que pueden se utilizados como agentes de curado, lo que da lugar a diferentes propiedades en el polímero final. Dependiendo de la estructura química del agente de curado utilizado y de las condiciones del curado, es posible obtener polímeros con propiedades mecánicas que van desde la extrema flexibilidad hasta la completa dureza y rigidez, alto poder adhesivo, buena resistencia a la temperatura y altas propiedades aislantes [1,2]. Como resultado de esta versatilidad, estos productos han encontrado uso como adhesivos, pinturas y recubrimientos, textiles, aislantes eléctricos y como parte constituyente de materiales compuestos. Actualmente, la industria de las resinas epoxi tiene una producción mundial valorada en aproximadamente once mil millones de euros.

El proceso de curado de una resina epoxi afecta directamente las propiedades finales del polímero [2-3], razón por la cual surge la necesidad de desarrollar métodos analíticos capaces de monitorizar las reacciones que ocurren durante los procesos de curado. Por esta razón se han realizado numerosos estudios dedicados a la investigación del mecanismo de la reacción y a la cuantificación de los parámetros cinéticos correspondientes utilizando diferentes técnicas: Calorimetría Diferencial de Barrido (DSC) [4] Calorimetría Diferencial de Barrido con Temperatura Modulada (MTDSC) [5], Análisis Termogravimétrico (TGA) [6], Fluorescencia [7], espectroscopía Raman [8], Resonancia Magnética Nuclear (RMN) [9], Cromatografía Líquida de Alta Resolución (HPLC) [5,10], espectroscopía Infrarroja con Transformada de Fourier (FTIR) [11,12], y espectroscopía de Infrarrojo Cercano (NIR) [13-18].

La espectroscopía de Infrarrojo Cercano resulta una herramienta particularmente atractiva para el seguimiento de reacciones de curado puesto que, gracias a la baja absortividad molar de sus señales, permite el estudio *in situ* del proceso, sin la necesidad de aplicar tratamientos previos a la muestra [13,15,18]. Esto posibilita, además de controlar la calidad del producto de la polimerización en tiempo real, extraer información acerca de la reacción de curado. Sin embargo, la falta de especificidad en las señales de los espectros obtenidos mediante NIR no permite realizar el seguimiento de cada especie que interviene en el proceso de curado. Los espectros NIR normalmente se utilizan de manera univariante, monitorizando los cambios producidos en una banda característica (frente a otra de referencia, invariable) y relacionándolos con el avance global de la reacción [13,15,18]. Si bien este tipo de análisis permite obtener información útil para evaluar el grado de conversión total de los reactivos en productos, no ofrece información acerca del número de pasos involucrados en el proceso, de la concentración de cada una de las especies químicas a lo largo del tiempo ni sus correspondientes espectros.

El uso de los llamados Métodos de Resolución de Curvas [19-23] permite realizar un análisis multivariante de los datos espectrales, obteniendo mayor información acerca del sistema en estudio. Una condición necesaria para poder aplicar estos métodos, también llamados métodos de modelado blando, es que los datos deben tener una estructura bilineal o tendiente a la bilinealidad. Es decir, que la matriz de datos experimentales (matriz de intensidades de respuesta) pueda expresarse como el producto de una matriz de concentraciones por otra matriz que contenga la señal pura de las especies presentes [24]. Esta condición se satisface para la mayoría de las técnicas espectroscópicas si se cumple la Ley de Lambert-Beer. Así, mediante la descomposición de una matriz de datos, originados durante la monitorización de una reacción química (por ejemplo, una reacción de curado), es posible conocer la evolución de cada una de las especies que toman parte en el proceso, así como sus correspondientes espectros puros. Estos métodos han sido aplicados con éxito a diversas respuestas instrumentales registradas durante el curso de reacciones químicas [25-29]. En esta Tesis Doctoral, se aplicarán estas técnicas a datos obtenidos del

seguimiento de reacciones de resinas epoxi, mediante espectroscopía de infrarrojo cercano, con el fin de obtener información útil tanto cualitativa como cuantitativa, no sólo de la concentración de las especies en estudio sino también referida al mecanismo de reacción y a los parámetros cinéticos correspondientes.

A pesar de las ventajas que comporta el tratamiento multivariante de los datos espectrales existen algunos problemas típicos de la estructura de los datos registrados, como es el caso de la deficiencia de rango [30]. Cuando los datos espectroscópicos proceden de sistemas químicos en evolución, es frecuente encontrar esta *deficiencia de rango*, que tiene lugar cuando el número de fuentes de variabilidad observado es menor que el número de especies que absorben en esa región espectral [31]. Durante el desarrollo de esta Tesis se aplicarán dos estrategias diferentes para la resolución de este problema.

Otro inconveniente característico que se presenta cuando se realiza la descomposición de matrices de datos bilineales es la presencia de las llamadas ambigüedades rotacionales y de intensidad [21]. Esto implica que, en lugar de obtener soluciones únicas para la resolución de un determinado conjunto de datos, se obtiene un conjunto de soluciones, las cuales ajustan los datos experimentales con un mismo mínimo residual. Parte del trabajo realizado en esta Tesis está abocado a la estimación de dichas ambigüedades en las soluciones y a la minimización de las mismas.

Una de las ventajas de los métodos de modelado blando es que permiten obtener perfiles de la evolución de las concentraciones a lo largo del tiempo para las distintas especies involucradas en una reacción sin la necesidad de conocer el mecanismo de la misma ni establecer un modelo cinético [32]. Desde el punto de vista cualitativo, los métodos de modelado blando representan una valiosa información cualitativa que puede ser utilizada como soporte para el establecimiento de modelos cinéticos que describan las reacciones estudiadas [33]. Sin embargo, desde el punto de vista cuantitativo, es necesario

establecer la bondad de los resultados obtenidos mediante los métodos de modelado blando. En esta Tesis, los resultados obtenidos mediante la combinación de espectroscopía de infrarrojo cercano y métodos de modelado blando se han contrastado con técnicas de referencia ya establecidas para el seguimiento de este tipo de reacciones, como la cromatografía líquida de alta eficacia (HPLC) [5,10], y con otras técnicas cuyo uso en la monitorización cuantitativa de reacciones de resinas epoxi es inédita, como es el caso de la Resonancia Magnética Nuclear de ^{13}C.

Un estudio cinético de una reacción química comporta la identificación del mecanismo de reacción correcto y la obtención de los parámetros cinéticos asociados, es decir, las constantes de velocidad de reacción. Esto puede lograrse mediante la aplicación de métodos de ajuste no lineal directamente a los datos experimentales registrados durante la reacción, los que, usualmente, se denominan métodos de modelado duro [34]. Sin embargo los métodos de modelado duro encuentran dificultades cuando existe algún tipo de variabilidad en el espectro, por ejemplo, ruido o desplazamientos en la línea de base, o bien la presencia de especies absorbentes que no participan de la reacción estudiada [27,33,35]. En este sentido, la combinación de técnicas de modelado blando (que por si solas no permiten obtener las constantes cinéticas) con las técnicas de modelado duro, permite aunar las ventajas de ambas técnicas. Así, la rigidez de los métodos de modelado duro permite obtener soluciones sin ambigüedad y, al mismo tiempo, las constantes cinéticas, mientras que las características de los métodos blandos permiten resolver sistemas complejos en presencia de interferencias espectrales [33]. En esta Tesis estas dos técnicas se han combinado de diferente manera. Por una parte, se ha aplicado un paso de ajuste no-lineal sobre los perfiles de concentración obtenidos después de la aplicación del modelado blando. Por otro lado, se ha incluido un paso de ajuste no-lineal como una restricción durante el proceso iterativo del modelado blando. De la aplicación de ambas estrategias de combinación de los modelados blando y duro se han obtenido las constantes cinéticas para distintas reacciones de resinas epoxi.

Esta Tesis Doctoral se ha estructurado de la siguiente manera: inicialmente se han descrito los principales objetivos de la Tesis. En el presente capítulo (Capítulo 1) se han presentado los contenidos de la tesis, el interés del estudio de las resinas epoxi y las posibilidades de aplicación de los Métodos Multivariantes de Resolución de Curvas, así como los diferentes problemas abordados durante la investigación. En el Capítulo 2 se presentan los principales conceptos referentes a las reacciones de curado de resinas epoxi, así como también algunos aspectos teóricos relacionados con las técnicas instrumentales y quimiométricas utilizadas. El Capítulo 3 presenta, en líneas generales, los diferentes sistemas epoxi-amina estudiados y los procedimientos experimentales llevados a cabo. El Capítulo 4 está directamente relacionado con el primer objetivo general planteado en esta Tesis. En él se abordan problemáticas como la deficiencia de rango y la estimación y minimización de las ambigüedades para lograr la correcta cuantificación de la evolución, a lo largo del tiempo, de las especies involucradas en las reacciones de resinas epoxi. Asimismo, se incluye la validación de los resultados obtenidos. Todas las investigaciones llevadas a cabo en el Capítulo 4 han sido realizadas estudiando la reacción modelo (es decir, que no polimeriza) entre el fenilglicidiléter (PGE) y la anilina, de la cual se dispone abundante información en la bibliografía. El Capítulo 5 se refiere al establecimiento de modelos cinéticos para reacciones entre anilina y diferentes monómeros epoxídicos, y a la obtención de las constantes cinéticas correspondientes. En este capítulo se han estudiado, además del sistema PGE/anilina, sistemas modelo que involucran epóxidos no disponibles comercialmente, y cuyas constantes cinéticas no han sido reportadas en la literatura. El Capítulo 6 contiene una breve discusión acerca de las posibilidades de extrapolación de las técnicas empleadas en sistemas modelo a sistemas epoxy-amina que reaccionan formando una densa red entrecruzada. Los estudios realizados en este capítulo se llevaron a cabo para la reacción entre diglicidiléter de bisfenol A (DGEBA) y diaminodifenilmetano (DDM), ambos disponibles comercialmente. Finalmente, en el Capítulo 7 se exponen las conclusiones generales del trabajo realizado.

2. Fundamentos Teóricos

2.1 Reacciones de curado de resinas epoxi

2.1.1 Introducción

Las resinas epoxi son materiales que bajo determinadas condiciones (calor, radiación ultravioleta, presencia de un agente endurecedor), polimerizan dando lugar a materiales termoestables de notable resistencia que no pueden moldearse por la acción del calor. Una resina epoxi es capaz de reaccionar con un agente endurecedor (o simplemente *agente de curado*) originando polímeros formados por redes tridimensionales de cadenas ampliamente entrecruzadas. El proceso de polimerización también recibe el nombre de *curado* [36].

Las propiedades finales del polímero están ligadas al epóxido de partida y al agente de curado empleado, pero también a las condiciones bajo las cuales se realiza el proceso de curado [36]. Entre los agentes de curado más utilizados se encuentran las aminas debido a su gran reactividad [37]. Las resinas epoxi curadas con aminas se utilizan frecuentemente en la industria electrónica, aeroespacial y de la construcción, así como también en algunas aplicaciones en medicina y odontología [38-42]. El proceso de curado afecta la estructura química de la red tridimensional y, por lo tanto, determina las propiedades físicas finales del polímero [2,3,37].

2.1.2 Sistemas Epóxido/Amina

En forma general, la reacción de curado entre un epóxido y una amina primaria,

puede describirse en dos etapas (Fig. 2.1) [2,37]. En la primera etapa, se produce un ataque nucleófilo de la amina primaria al carbono menos sustituido del grupo oxirano produciéndose la apertura del anillo con la consiguiente formación de un grupo hidroxilo y la conversión de la amina primaria en secundaria.

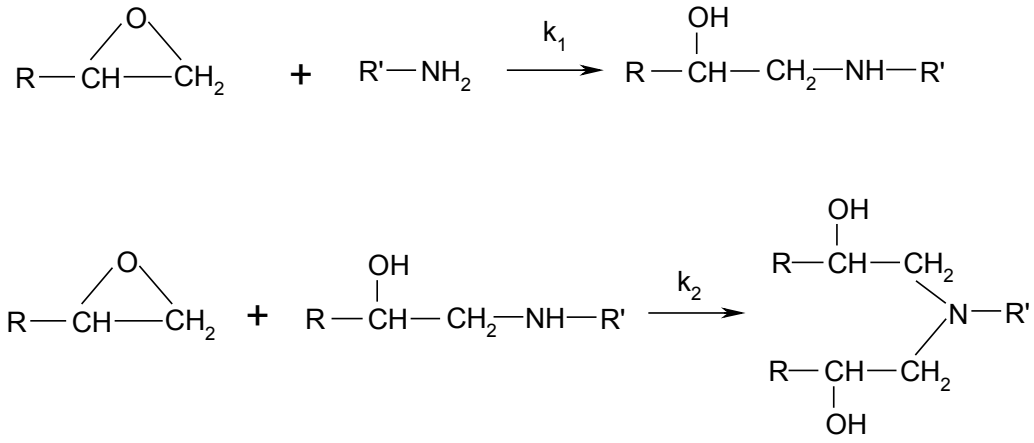

Fig. 2.1 Representación esquemática de las reacciones que tienen lugar durante el curado (con aminas) de una resina epoxi.

En la segunda etapa, la amina secundaria formada se consume reaccionando con el exceso de epóxido. Se produce un segundo ataque nucleófilo del grupo amino de la amina secundaria sobre el grupo oxirano, con la formación de un nuevo grupo hidroxilo debido a la apertura del anillo. La amina secundaria se transforma así en una amina terciaria.

Las etapas representadas en la Fig. 2.1 tienen lugar de forma mayoritaria pero, dependiendo de las condiciones de reacción (temperatura, concentración de los grupos

reactivos, presencia o ausencia de catalizadores), se pueden producir otras reacciones colaterales como la eterificación, la homopolimerización, reacciones de ciclación y de degradación [43].

En la eterificación (Fig. 2.2) el epóxido experimenta un ataque nucleófilo del grupo hidroxilo sobre el grupo oxirano, provocándose la apertura del anillo. Como resultado de esta reacción se obtiene un éter. La reacción de eterificación es usualmente más lenta que las reacciones epoxi-amina y solo es significativa en sistemas que poseen un exceso de epóxido, cuando los grupos amino se han consumido de forma considerable [44].

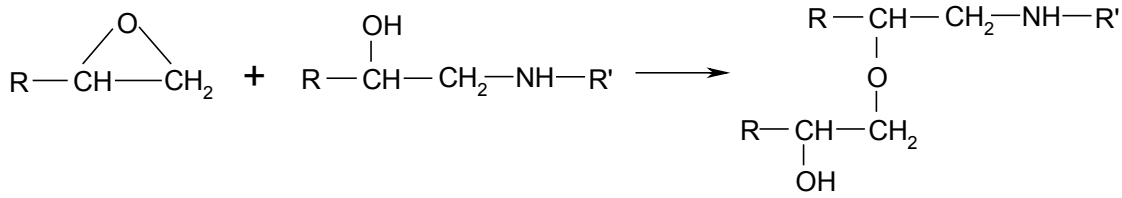

Fig. 2.2 Esquema de la reacción de eterificación.

La homopolimerización (Fig. 2.3) es la reacción de moléculas de epóxido entre sí para dar poliéteres y puede considerarse despreciable en ausencia de catalizadores como ácidos o bases de Lewis [45,46]. Que ocurra o no la reacción de ciclación dependerá de la longitud y la rigidez de los monómeros [36].

La reacción entre un epóxido y una amina presenta un mecanismo autocatalítico. Es decir, los grupos hidroxilo formados durante la reacción actúan catalizando la reacción entre el grupo oxirano y el grupo amino [37,47-49]. Si bien las reacciones descritas en la

Fig. 2.1 tienen lugar durante el curado de una resina epoxi, el mecanismo por el cual ocurren no está completamente establecido y existen diversas hipótesis planteadas al respecto [37,45,47-49].

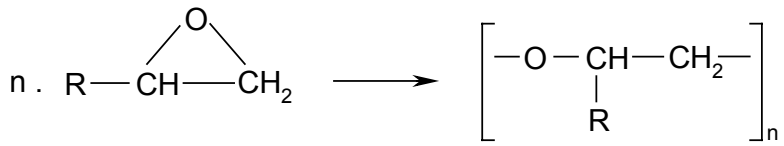

Fig. 2.3 Esquema de la reacción de homopolimerización.

Las constantes k_1 y k_2 (ver Fig. 2.1) que rigen la reacción de curado están relacionadas con los grupos funcionales amino primario y secundario, respectivamente. Para una reacción en la que los dos grupos amino (primario y secundario) poseen la misma reactividad, la relación entre las constantes $\rho = k_2/k_1$ debería ser igual a ½, puesto que la capacidad de combinación del grupo amino primario es el doble que la del grupo amino secundario.

Generalmente, los valores de ρ son menores que 0,5 porque el grupo amino secundario es mucho menos reactivo que el grupo amino primario a causa de impedimentos estéricos, por lo tanto existe un *efecto de sustitución negativo* [43]. Este hecho se destaca sobre todo en aminas aromáticas para las que los valores de ρ oscilan entre 0,15 y 0,25 [36,46]. Así, la reacción de la amina primaria es más rápida que la que involucra a la amina secundaria, pero no lo suficiente como para que sean consecutivas. Una consecuencia evidente de esta circunstancia se puede apreciar en la construcción del polímero (ver Fig. 2.4), ya que se produce una diferenciación entre las dos etapas anteriormente descritas (Fig. 2.1).

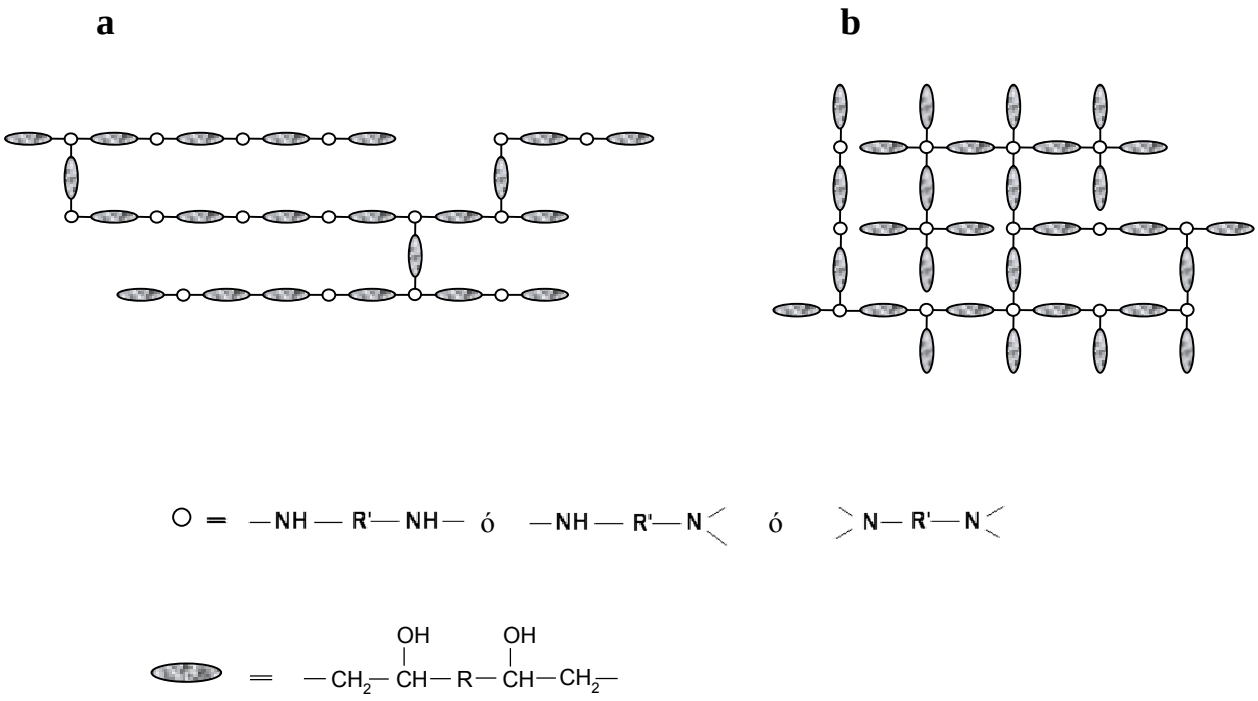

Fig. 2.4 Esquema de la reacción entre un epóxido y una amina bifuncionales. a) Los grupos amino primarios reaccionan en primer término para formar oligómeros lineales. b) Las reacciones epóxido-amina primaria y epóxido-amina secundaria se desarrollan a velocidad similar, por lo que se forma una densa red entrecruzada desde el inicio de la reacción.

En presencia de efecto de sustitución negativo, la reacción de la amina primaria tiene preponderancia sobre la de la amina secundaria, dando lugar a la formación de cadenas lineales, mientras que la ramificación y entrecruzamiento, correspondientes a la reacción de la amina secundaria, quedan retrasados (Fig. 2.4 a) [43]. Contrariamente, cuando la reactividad de la amina primaria es similar a la de la amina secundaria ($\rho \sim 0{,}5$),

se producen polímeros en los que la red está extensamente entrecruzada desde el inicio de la reacción (Fig. 2.4 b). El valor de efecto de sustitución depende de la amina utilizada como endurecedor, por eso es importante seleccionarla adecuadamente, en relación con las propiedades deseadas en el polímero final.

2.1.3 Modificaciones físicas durante el proceso de curado

A lo largo del proceso de curado, el sistema sufre distintas transformaciones que están relacionadas con las propiedades físicas del polímero en formación. Estas transformaciones están marcadas por dos fenómenos característicos de los polímeros amorfos: la gelificación y la vitrificación.

La gelificación es el cambio irreversible que experimenta el polímero desde un estado líquido-viscoso (sol) a un gel elástico que representa la aparición de una red tridimensional entrecruzada. El paso de sol a gel está identificado por el llamado *punto gel*. Antes de la gelificación el sistema es soluble pero, una vez atravesado el punto gel, parte del polímero se vuelve insoluble debido al extenso entrecruzamiento entre las cadenas formadas. A medida que el polímero se acerca a la gelificación, la viscosidad se incrementa abruptamente y el peso molecular del polímero crece de forma drástica [50].

La vitrificación es un proceso termo-reversible, que implica el cambio desde un estado líquido o gel a un estado vítreo, en el que el material se vuelve rígido [51]. La temperatura a la cual se produce este fenómeno se denomina *temperatura de transición vítrea* (Tg). La vitrificación ocurre cuando la temperatura de curado es inferior a la Tg del material que está curando [52]. A medida que el polímero avanza en su grado de curado, también se modifica la Tg produciéndose un aumento de la misma [36].

Siempre que la temperatura de curado se encuentre por encima de la Tg del polímero (en cualquier estado del curado) la reacción evolucionará normalmente. En el momento en el cual el polímero alcance un grado de curado tal que su Tg supere la temperatura de curado, la reacción se detendrá debido al impedimento en la movilidad de las cadenas, necesaria para que la reacción se produzca [53,54]. En lugar de punto de vitrificación, es común hablar de una *región de vitrificación* en la cual la reacción comienza a hacerse más lenta para, finalmente, detenerse por completo [36].

El análisis de la evolución del proceso de curado es complicado dado que los cambios químicos ocurridos en el sistema, debidos a la reactividad química de los grupos funcionales, están íntimamente relacionados con los cambios físicos que se acaban de describir. Normalmente, para estudiar el proceso de curado se utilizan sistemas modelo epoxi/amina con bajas temperaturas de transición vítrea o sistemas para los cuales tienen lugar las reacciones de la Fig. 2.1 pero que no evolucionan hacia productos entrecruzados, evitando así la gelificación [55]. En esta Tesis se utilizan tres sistemas modelo que involucran la reacción de la anilina con tres monómeros epoxídicos diferentes (fenilglicidiléter (PGE), fenilglicidiloxidimetilsilano (GDMPS), y fenilglicidiltioéter (PGTE)), cuyos respectivos productos de reacción no forman redes entrecruzadas. Asimismo se ha estudiado la reacción entre diglicidiléter de bisfenol A (DGEBA) con diaminodifenilmetano (DDM), a fin de evaluar la posibilidad de extrapolar los métodos utilizados en sistemas modelo a sistemas cuyo producto final es un polímero termoestable.

2.2 Técnicas Instrumentales

En esta sección se presentan algunos conceptos téoricos relacionados con la

aplicación práctica de las técnicas instrumentales utilizadas en este trabajo de investigación. Los fundamentos de las técnicas han sido omitidos a fin de no extender innecesariamente la Tesis con contenidos que pueden encontrarse en libros de texto. Sin embargo algunos temas han sido incluidos para facilitar la lectura y comprensión de ciertos procedimientos experimentales empleados. Así, en el apartado 2.2.1, se hace mención a los tipos de medida en la espectroscopía de infrarrojo cercano. En el apartado 2.2.2. se recogen los principios referentes a los procesos de relajación que experimentan los núcleos cuando son irradiados con energía de radiofrecuencia durante los experimentos de resonancia magnética nuclear. También se detallan algunas características de la resonancia magnética nuclear de Carbono 13, puesto que además de proveer información complementaria a la espectroscopía de infrarrojo cercano (ver capítulo 4, sección 4.3), también se ha utilizado como técnica de referencia para contrastar los resultados obtenidos mediante la combinación de espectroscopía de infrarrojo cercano con técnicas quimiométricas (ver Capìtulo 5, sección 5.4). Al final de esta sección (apartado 2.2.3) se hace una breve mención al Análisis Térmico Dinamomecánico (DMA), usado para estudiar el comportamiento viscoelástico de las resinas epoxi en el Capítulo 6.

2.2.1 Tipos de medida en la espectroscopía de Infrarrojo Cercano

Al incidir sobre una muestra, la radiación infrarroja puede sufrir diferentes fenómenos: absorción, transmisión y reflexión (Ver Fig. 2.5). Así, de la intensidad de radiación incidente (P_0), una parte es transmitida (P_T), otra parte es reflejada (P_R) mientras que otra parte es absorbida por la sustancia (P_A). En líneas generales, las mediciones en el NIR pueden realizarse teniendo en cuenta la radiación transmitida/absorbida (medidas por transmisión), la radiación reflejada (reflectancia difusa, reflectancia total interna) o ambas a la vez (transflectancia). En esta tesis, las medidas realizadas se llevaron a cabo en modo de transflectancia.

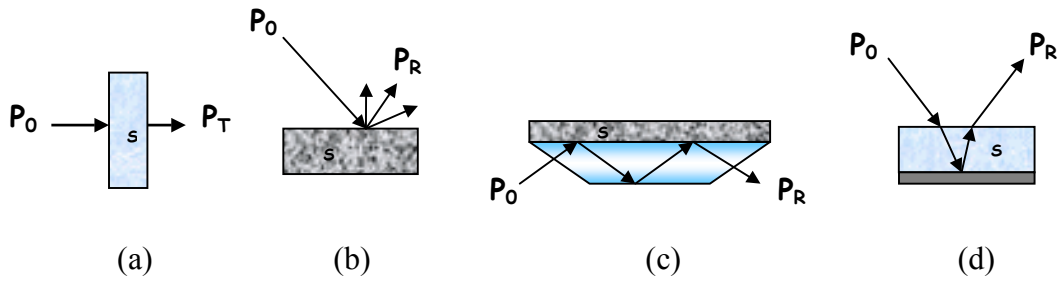

(a) (b) (c) (d)

Fig. 2.5 Diferentes tipos de medida en la región del infrarrojo cercano. (a) Transmisión, (b) Reflectancia difusa, (c) Reflectancia total interna, (d) Transflectancia. S: muestra, P_0: potencia de radiación incidente, P_T: potencia de radiación transmitida, P_R: potencia de radiación reflejada.

Los instrumentos diseñados para medir reflectancia difusa, también pueden adaptarse para realizar mediciones en muestras líquidas, utilizando las llamadas celdas de transflectancia. En una medida de transflectancia la radiación pasa a través de la muestra hacia una superficie reflectante (que puede ser de cerámica, oro o acero inoxidable) donde es reflejada y regresa atravesando nuevamente la muestra y alcanzando el detector (Fig. 2.5 d). Como resultado, el paso óptico es aproximadamente el doble de la distancia entre el punto de entrada de la radiación y el material reflectante. La intensidad de radiación absorbida será proporcional a la concentración, y seguirá la ley de Lambert-Beer si en la muestra no existen partículas o turbidez que ocasionen la dispersión de la radiación [56].

2.2.2 Resonancia Magnética Nuclear

2.2.2.1 Proceso de relajación

Existen dos tipos principales de procesos de relajación de los núcleos que han absorbido energía de radiofrecuencia. El primero, llamado relajación longitudinal o spin-lattice, corresponde al intercambio energético entre el núcleo excitado y el entorno. Este entorno se entiende como un conjunto de núcleos de la misma molécula, moléculas vecinas o moléculas del solvente. Por definición, este tipo de relajación reduce la energía total del sistema nuclear excitado, conduciendo a la recuperación del estado de equilibrio. El proceso de relajación posee una constante de velocidad llamada "tiempo de relajación de spin-lattice", T_1. En sólidos y líquidos viscosos los tiempos de relajación son del orden de horas, mientras que para soluciones en solventes orgánicos el tiempo oscila entre 0.01 y 100 segundos.

En contraste, la segunda vía de relajación, llamada relajación transversal o spin-spin, tiene un carácter entrópico: dos núcleos del mismo tipo con spins idénticos pero con diferente orientación con respecto al campo magnético externo sufren movimientos de "flip-flop", como se muestra en la Fig. 2.6, debido a la transferencia de energía entre ellos.

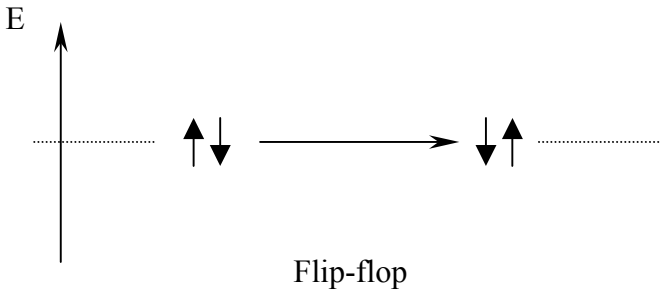

Fig. 2.6 Movimientos de "flip-flop" que causan la relajación spin-spin.

Es obvio que la energía total del sistema nuclear permanece constante, aunque los tiempos de vida de los núcleos excitados decrece, por lo tanto el sistema nuclear se relaja. Este proceso posee un tiempo de relajación llamado de *spin-spin* o T_2.

Fenomenológicamente, los tiempos T_1 y T_2 caracterizan dos procesos diferentes y, por lo tanto, lo normal es que $T_1 \neq T_2$. De hecho, $T_1 > T_2$ en sólidos donde los movimientos moleculares están fuertemente restringidos. Por el contrario, en líquidos y gases en los que la difusión y la rotación son procesos rápidos, T_1 y T_2 son esencialmente iguales [57].

Los tiempos de relajación son utilizados principalmente para decidir acerca del tiempo de retardo necesario entre dos adquisiciones de datos. Para la obtención de datos cuantitativos fiables, el tiempo entre adquisiciones de datos debe ser, como mínimo, cincoveces T_1. Los tiempos de relajación se determinan mediante experimentos especialmente preparados y pueden realizarse de diversas maneras [57]. Sin embargo, el modo más usual de obtener esta información es mediante el método de recuperación de la inversión. Estemétodo consiste en aplicar una secuencia de pulsos de radiofrecuencia de duración variable (τ) en dirección perpendicular al campo magnético aplicado. El experimento se realiza aumentando el tiempo τ y registrando la señal de RMN obtenida después de la aplicación del pulso de radiofrecuencia. Así se obtienen curvas como la de la Fig. 2.7. En el punto en el cual la señal de RMN se hace cero, se cumple la siguiente igualdad: $T_1 = \tau / \ln 2$.

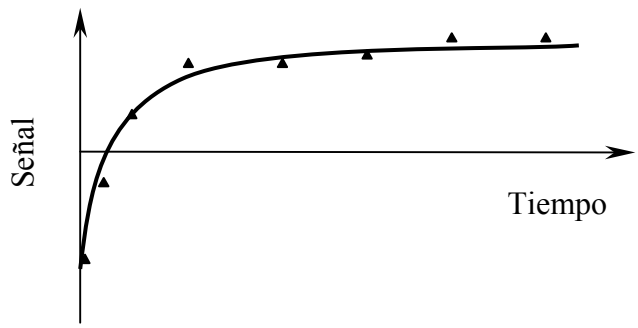

Fig. 2.7 Datos experimentales de recuperación de la inversión (▲) y curvas correspondientes calculadas mediante ajuste no lineal (——).

2.2.2.2 Resonancia Magnética Nuclear de ^{13}C

Aproximadamente el 99% de los átomos de carbono en una muestra natural corresponden al isótopo ^{12}C. Este isótopo posee un número par de protones y un número par de neutrones, por tanto, no tiene espín magnético y no puede dar lugar a señales de resonancia magnética nuclear. El isótopo de ^{13}C, aunque menos abundante, tiene un número impar de neutrones, lo que le confiere un espín magnético que permite la absorción de radiofrecuencia por parte del núcleo. Debido a que la abundancia de esta forma isotópica es de sólo un 1%, la sensibilidad de esta técnica es mucho menor comparada, por ejemplo, con la sensibilidad de ^{1}H RMN. A esto se debe también la cantidad relativamente grande de muestra (más de 100 mg) que, en ocasiones, debe utilizarse para obtener espectros de ^{13}C. A pesar de esto, ^{13}C RMN posee una serie de interesantes ventajas [58]:

- posee una mayor resolución, puesto que el rango de desplazamientos es aproximadamente de 200 ppm para la mayoría de las moléculas orgánicas (contra un intervalo de unos 10 ppm para ^{1}H RMN).

- los carbonos que no tiene hidrógenos unidos son directamente visibles, lo cual representa una ventaja desde el punto de vista de la dilucidación de la estructura química de las moléculas.

- el efecto spin-spin homonuclear (es decir, el desdoblamiento de la señal por la cercanía de otros núcleos) es despreciable, puesto que debido a la baja abundancia de núcleos que entran en resonancia es poco probable que dos núcleos de ^{13}C sean adyacentes. Esto hace que los espectros sean considerablemente más simples.

Es usual, cuando se trabaja con ^{13}C RMN, eliminar el efecto del acoplamiento spin-spin heteronuclear que tiene lugar entre ^{1}H y ^{13}C. El procedimiento se denomina

desacoplamiento de spin y se logra irradiando la muestra con un segundo campo de radiofrecuencia fuerte, perpendicular a H_0, de un ancho de banda que incluya la frecuencia de precesión de los núcleos cuyo efecto se desea eliminar (en este caso, ^1H) [59]. Como resultado, se producen transiciones nucleares en los ^1H vecinos que eliminan el acoplamiento spin-spin. De esta forma desaparecen todas las señales múltiples, aumentando la sensibilidad (puesto que el área bajo los multipletes se encuentra ahora bajo un singlete) y la simplicidad del espectro. Sin embargo, el aumento en sensibilidad en las señales de ^{13}C es mayor que el esperado debido a la aparición del llamado Efecto Nuclear Overhauser (NOE) [59]. En el proceso de desacoplamiento, los núcleos ^1H son irradiados mientras se observa la resonancia de los núcleos ^{13}C. Debido a la fuerza del campo aplicado, los procesos de relajación de los protones no son suficientes para restablecer el equilibrio en la población, por lo que los ^1H transfieren su energía a los núcleos ^{13}C a través de interacciones dipolo-dipolo. Los carbonos reciben esta energía suplementaria y actúan como si hubieran sido irradiados, con el consiguiente proceso de relajación. Como consecuencia, la población del nivel de energía más bajo de los núcleos ^{13}C se incrementa, y la intensidad de la señal se ve incrementada. Este efecto es benéfico cuando se trabaja en un sentido cualitativo, pero debe eliminarse cuando se requiere realizar un análisis cuantitativo. Una manera de eliminar el NOE es aplicar la técnica de "inverse-gated decoupling" que consiste en activar el desacoplamiento sólo durante la adquisición, y aumentar el tiempo de espera entre adquisiciones. Por lo general se suele utilizar tiempos de recuperación entre cinco y diez veces el tiempo de relajación T_1 del núcleo que relaja más lentamente [60].

2.2.3 Análisis Térmico Dinamomecánico

El análisis térmico Dinamomecánico (DMA) es uno de los métodos más empleados para estudiar el comportamiento viscoelástico de ciertos materiales [61].

Durante el proceso de curado, y dependiendo del avance del mismo, las resinas epoxi exhiben un comportamiento viscoelástico, es decir, poseen características tanto de los sólidos elásticos como de los líquidos viscosos [62]. El estudio de la viscoelasticidad se realiza aplicando sobre la muestra una tensión oscilatoria (sinusoidal) en función del tiempo (es decir, caracterizada por una determinada frecuencia) y registrando la deformación sufrida por el material. La respuesta a la tensión aplicada también es de tipo sinusoidal pero, dado que el material no responde instantáneamente a la tensión impuesta, la deformación resultante se ve retrasada con relación a la tensión en una cantidad que depende del comportamiento viscoelástico del elemento (ver Fig. 2.8).

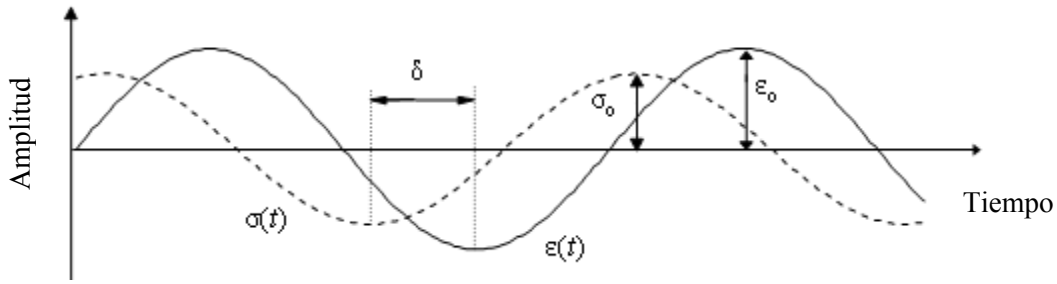

Fig. 2.8 Representación del desfase entre la tensión impuesta (línea continua) y la deformación resultante (línea punteada) en un ensayo de DMA, donde σ_o representa la máxima deformación sufrida por el material, ε_o es la tensión máxima aplicada y δ es el ángulo de desfase.

La respuesta del material puede expresarse como una función de variables complejas:

$$\sigma(t) = \sigma_0 (sen\ \omega t\ cos\ \delta\ + i\ cos \omega t\ sen\ \delta) \qquad \text{Ec.(2.1)}$$

y en base a esta expresión se puede definir el llamado módulo complejo E*, que está constituido por dos partes: una real, E' (o módulo de almacenamiento) y otra imaginaria E'' (o módulo de pérdida):

$$E'(\omega) = \frac{\sigma_0}{\varepsilon_0} cos\,\delta \qquad E''(\omega) = i\frac{\sigma_0}{\varepsilon_0} sen\,\delta \qquad \text{Ec. (2.2)}$$

El módulo de almacenamiento (E') representa la energía mecánica que el material almacena como consecuencia de la deformación, de forma completamente reversible; mientras que el módulo de pérdida (E'') corresponde a la energía que se disipa, de manera irreversible, en forma de calor a causa de la fricción intermolecular de las cadenas durante la deformación.

Los módulos complejo, de almacenamiento y de pérdida están relacionados directamente con distintos tipos de viscosidad. Si se divide el módulo de pérdida por la frecuencia de la tensión sinusoidal aplicada (ω), se obtiene la viscosidad dinámica, η'. Asimismo, si se divide el módulo de almacenamiento por la frecuencia ω se obtiene la viscosidad fuera de fase, η''. La llamada viscosidad compleja posee dos componentes: una componente real que es la viscosidad dinámica y una componente compleja que es la viscosidad fuera de fase, $\eta^* = \eta' + i\eta''$ [63].

A partir de estos módulos se puede definir la llamada tangente de pérdida, según la siguiente ecuación:

$$tan\,\delta = E''/E' \qquad \text{Ec.(2.3)}$$

Este parámetro es muy sensible a los cambios viscoelásticos que tienen lugar cuando un material está experimentando diferentes transformaciones estructurales (por ejemplo, un polímero que sufre un proceso de curado). En el caso del curado de un polímero, la aparición de un máximo en la tan δ indica que se ha producido una diferencia muy importante entre el comportamiento viscoso y elástico del polímero [62]. Esto se relaciona con el paso del estado sol al estado gel, en el cual el polímero se vuelve insoluble, debido a la aparición de una red tridimensional entrecruzada. El máximo en tan δ indica el punto gel, en el cual tiene lugar esta transición. Otra transición que puede visualizarse mediante un máximo en tan δ corresponde al punto de vitrificación, en el cual la reacción de polimerización se detiene y el polímero se vuelve rígido, con características vítreas. Esto ocurre en curados isotérmicos, cuando la temperatura del sistema que está reaccionando se encuentra por debajo de la temperatura de transición vítrea (Tg) del material que está curando.

2.3 Técnicas Quimiométricas

2.3.1 Introducción

En los últimos años, los avances instrumentales, la automatización de métodos analíticos y la incorporación de sistemas informáticos con mayor capacidad de procesamiento, han hecho posible la obtención de gran cantidad de datos en tiempos muy reducidos. La aplicación de estos avances a problemas químicos, permite obtener grandes cantidades de datos. La extracción de información relevante para la resolución de un determinado problema requiere la utilización de herramientas matemáticas y estadísticas. La disciplina química que emplea el conjunto de estas técnicas se denomina Quimiometría [64].

Especialmente, en lo que concierne al seguimiento y monitorización de procesos químicos, la Quimiometría cobra vital importancia. El desarrollo y aplicación de métodos de calibración multivariante [65-68] ha permitido relacionar una propiedad a determinar con un conjunto de múltiples variables obtenidas como respuesta analítica para extraer, finalmente, información cuantitativa relacionada con la propiedad de interés. Esto requiere establecer un modelo o matriz de calibración constituido por patrones, de los cuales se conoce el valor de la propiedad a determinar. Sin embargo, en ocasiones no existe información previa disponible para realizar una calibración. Esto puede ocurrir en sistemas donde uno o más parámetros (temperatura, pH, concentración de los reactivos) cambian a lo largo del tiempo [69].

Una manera de solucionar este problema es la aplicación de los llamados *Métodos Multivariantes de Resolución de Curvas* [70,71]. Este conjunto de distintas técnicas quimiométricas permite obtener una aproximación del comportamiento del sistema a partir

del análisis matemático de los datos experimentales haciendo muy pocas (o ninguna) asunciones previas sobre la naturaleza o la composición del sistema en estudio.

A continuación se detallan los fundamentos teóricos de las técnicas quimiométricas empleadas en esta Tesis. En primer lugar se realiza un resumen del análisis de componentes principales, puesto que la mayoría de las técnicas empleadas involucran esta descomposición (apartado 2.3.2). El apartado 2.3.3 se refiere a la regresión por componentes principales (utilizada en el capítulo 6). Otras técnicas como el análisis de factores emergentes (empleada para el estudio del rango de las matrices de datos experimentales) y SIMPLISMA (utilizada como herramienta para la construcción de la estima inicial para el método de mínimos cuadrados alternados) se detallan en los apartados 2.3.4 y 2.3.5, respectivamente. Finalmente, en el apartado 2.3.6 se describe la resolución de curvas multivariante optimizada mediante mínimos cuadrados alternados, en la que se ha hecho especial hincapié por ser la principal técnica quimiométrica utilizada en esta Tesis.

2.3.2 Análisis de componentes principales

La descomposición en componentes principales (*Principal component Análisis,* PCA) permite representar, en unos pocos factores o componentes principales, la variabilidad presente en la matriz de respuestas de un determinado sistema. Dichos factores son combinaciones lineales de las variables originales [72].

La técnica consiste en una transformación matemática abstracta de la matriz de respuestas experimentales **R** (*I*x*J*) (compuesta por las respuestas de *I* muestras analizadas para *J* variables), como se muestra en la Fig. 2.9, donde **T** (*I*x*N*, con *N* = número de componentes principales significativos) es la matriz de *scores* que posee información sobre las filas de la matriz **R**, por lo que expresará las relaciones entre los objetos (muestras); **P** (*J*x*N*) es la

matriz de *loadings* que contiene información referida a las columnas de la matriz **R,** y por lo tanto refleja la relación existente entre las variables; y **E** es la matriz de los residuales, en la que se encuentra la porción de información no recogida por el producto $\mathbf{TP}^T$. Las filas de la matriz $\mathbf{P}^T$ son los llamados componentes principales de **R**, y son combinaciones lineales de las *J* variables originales. Los elementos de cada una de esas filas representan las componentes de vectores linealmente independientes que son ortogonales entre sí y además están normalizados (llamados también vectores propios).

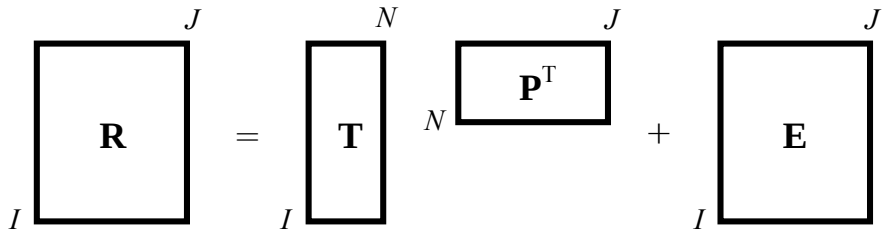

Fig. 2.9 Representación matricial de la descomposición en componentes principales.

Si se desea recomponer la matriz de respuestas, cada fila de la matriz **R** puede ser representada por una combinación lineal de todos los componentes principales de la matriz de loadings; los factores multiplicativos o coeficientes de esa combinación lineal para una dada fila r_i, estarán dados por la correspondiente fila t_i de la matriz de scores.

La cantidad de componentes principales o factores abstractos siempre será menor o igual que el mínimo valor entre *I* y *J*. Pero no todos los componentes principales son realmente significativos. Dicho de otro modo, no todos los componentes principales aportan información relevante. De hecho, solo algunos explican significativamente la

variabilidad de los datos de la matriz original debido a que existe cierta colinealidad entre los datos experimentales. Por los tanto, la información principal presente en la matriz **R** puede ser condensada en un conjunto más pequeño de *N* variables, representadas por los componentes principales significativos.

El primer factor o componente principal $\mathbf{p}_1$ es aquel que recoge la mayor cantidad de información contenida en **R** (de manera que se maximiza la expresión: $\mathbf{p}_1^T \mathbf{R}^T \mathbf{R}\mathbf{p}_1 = \mathbf{t}_1^T \mathbf{t}_1$), donde las letras **p** y **t** indican las correspondientes filas (vectores) de las matrices **P** y **T**, respectivamente). El siguiente factor $\mathbf{p}_2$, recoge la máxima información de **R** no contenida en $\mathbf{p}_1$ (maximiza $\mathbf{p}_2^T \mathbf{R}^T \mathbf{R}\mathbf{p}_2 = \mathbf{t}_2^T \mathbf{t}_2$ pero es ortogonal al primer componente principal, es decir $\mathbf{t}_1^T \mathbf{t}_2 = 0$), y así sucesivamente. Los vectores $\mathbf{p}_n$ son también llamados *vectores propios* y tienen asociado un *valor propio* λ_n

$$\lambda_n = \mathbf{t}_n^T \mathbf{t}_n \qquad \text{con } n = 1, 2 \ldots N \qquad \text{Ec. (2.4)}$$

de forma que se cumple la siguiente ecuación

$$\mathbf{R}^T \mathbf{R}\mathbf{p}_n = \mathbf{p}_n \lambda_n \qquad \text{Ec. (2.5)}$$

La magnitud de los valores propios indica la cantidad de variabilidad (información) retenida por cada uno de los vectores propios o componentes principales.

Descomposición en valores singulares

El análisis de componentes principales de una matriz de datos puede llevarse a cabo utilizando diferentes algoritmos [73]. Entre ellos, la descomposición en valores singulares (*Singular Value Decomposition,* SVD) ha sido utilizada particularmente en esta Tesis para el análisis del número de fuentes de variabilidad presentes en los datos experimentales.

Este algoritmo se basa en el teorema del álgebra matricial que establece que una matriz **R** de dimensiones *I*x*J* puede descomponerse en el producto de tres matrices **U** (*I*x*K*), **W** (*K*x*K*) y $\mathbf{V}^T$ (*K*x*J*), siendo *K* igual al menor valor entre *I* y *J*.

$$\mathbf{R} = \mathbf{U}\mathbf{W}\mathbf{V}^T \qquad \text{Ec. (2.6)}$$

Los elementos de la diagonal de **W** están definidos como valores positivos, mientras que los valores fuera de la diagonal son cero. Los vectores (columnas) de las matrices **U** y **V** son ortonormales, lo que implica que los productos $\mathbf{U}^T\mathbf{U}$ y $\mathbf{V}^T\mathbf{V}$ son iguales a la matriz identidad [73].

El producto de las matrices **U** y **W** sería equivalente a la matriz de scores mencionada con anterioridad, mientras que la matriz $\mathbf{V}^T$ equivale a la matriz de loadings. Los valores de la diagonal de la matriz **W** son llamados *valores singulares*, están ordenados de mayor a menor y corresponden a la raíz cuadrada de los valores propios (λ).

Cuando los valores singulares se representan frente al número de componentes, es posible extraer información acerca del número de factores o componentes que contienen

información útil sobre el sistema en estudio. Aquellos factores que tengan asociados valores singulares bajos, generalmente recogen información sobre el ruido asociado a las medidas experimentales (Fig. 2.10). De esta manera puede determinarse el *rango de la matriz* de datos. El rango de una matriz es igual al número de vectores linealmente independientes a partir de los cuales, mediante combinaciones lineales de ellos, pueden reconstruirse todas las columnas (o filas) de la matriz [73].

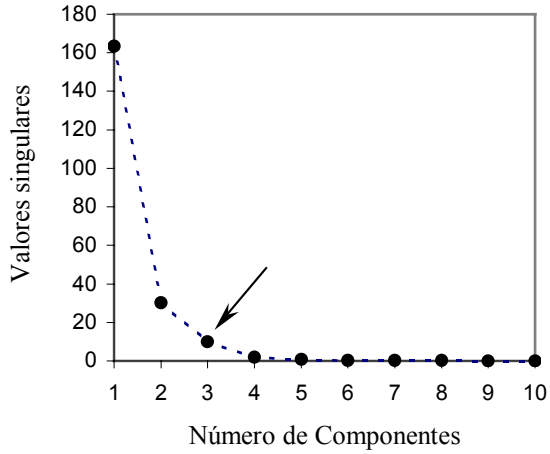

Fig. 2.10 Descomposición en valores singulares de una matriz de datos. La flecha indica el número de componentes principales significativos.

El número de factores significativos sería *aproximadamente* igual al rango de la matriz, puesto que la reconstrucción de la matriz de datos a partir de éstos no ocasiona pérdida de información relevante. Cabe resaltar que en algunas ocasiones existen diferencias en la definición del rango matemáticamente exacto (que involucra el número de componentes que permite reconstruir el conjunto de datos sin residual), y el rango aproximado (también llamado *rango químico* cuando se analizan matrices de datos

procedentes de respuestas experimentales correspondientes a un sistema químico) que corresponde al número de componentes significativos del conjunto de datos [74].

La importancia de la determinación del rango de la matriz radica en que se asume que el rango químico corresponde al número de especies químicas que ocasionan la variabilidad en la matriz de respuestas.

2.3.3 Regresión en componentes principales (PCR)

Un procedimiento de calibración tiene como objetivo la predicción de una propiedad determinada en una muestra incógnita, en base a la respuesta obtenida para dicha muestra y para un conjunto de estándares de calibración mediante alguna técnica analítica. Si la propiedad a determinar tiene un comportamiento lineal en función de la respuesta obtenida, se puede expresar el siguiente modelo en notación matricial:

$$\mathbf{Y} = \mathbf{RB} + \mathbf{E} \qquad \text{Ec. (2.7)}$$

Donde **Y** es la matriz correspondiente a la propiedad que se quiere determinar, **R** es la matriz de respuestas, **B** es la matriz de los coeficientes de regresión y **E** la matriz de residuales.

En la regresión en componentes principales, en lugar de realizarse la regresión sobre la matriz **R** de respuestas, se realiza sobre los scores (matriz **T**, ver Fig. 2.9) obtenidos por la aplicación del análisis de componentes principales a la matriz **R** [75]:

$$\mathbf{Y} = \mathbf{TB} + \mathbf{E} \qquad \text{Ec. (2.8)}$$

Por lo tanto, el primer paso de la regresión en componentes principales es la reducción de dimensión de la matriz de respuesta mediante PCA. A partir de la matriz de scores se obtiene la matriz **B** de regresores mediante el método de mínimos cuadrados, utilizando un conjunto de muestras de calibración para las cuales se conoce el valor de la propiedad estudiada (por ejemplo, la concentración).

$$\hat{\mathbf{B}} = (\mathbf{T}^T \mathbf{T})^{-1} \mathbf{T}^T \mathbf{Y} \qquad \text{Ec. (2.9)}$$

Una vez calculados los coeficientes de regresión y, por lo tanto, establecido el modelo de calibración, se puede predecir la propiedad de interés para nuevas muestras de la siguiente manera: a partir de la matriz de loadings **P**, calculada en la etapa de calibración, se calculan los scores de las muestras de predicción:

$$\mathbf{T}^* = \mathbf{R}^* \mathbf{P} \qquad \text{Ec. (2.10)}$$

Siendo $\mathbf{R}^*$ la matriz de respuestas del conjunto de muestras de predicción. Finalmente se estima la propiedad de interés en las muestras desconocidas.

$$\mathbf{Y}^* = \mathbf{T}^* \hat{\mathbf{B}} \qquad \text{Ec. (2.11)}$$

2.3.4 Análisis de factores emergentes

Cuando el análisis de componentes principales se realiza en sistemas cuyas respuestas varían a incrementos discretos de alguna variable controlada (tiempo, pH, potencial), la evolución de los factores o componentes del sistema puede expresarse como función de dicha variable.

Uno de los métodos que permite estimar esta evolución es el análisis de factores emergentes (*Evolving Factor Análisis*, EFA) [76,77]. La idea fundamental de EFA es analizar el cambio en el rango de la matriz de datos realizando un análisis de componentes principales de la primera fila (o bien escogiendo unas pocas filas) de la matriz, y calculando el número de factores para las submatrices que resultan de agregar una nueva fila sucesivamente. Así, hasta completar el total de filas que componen la matriz de datos.

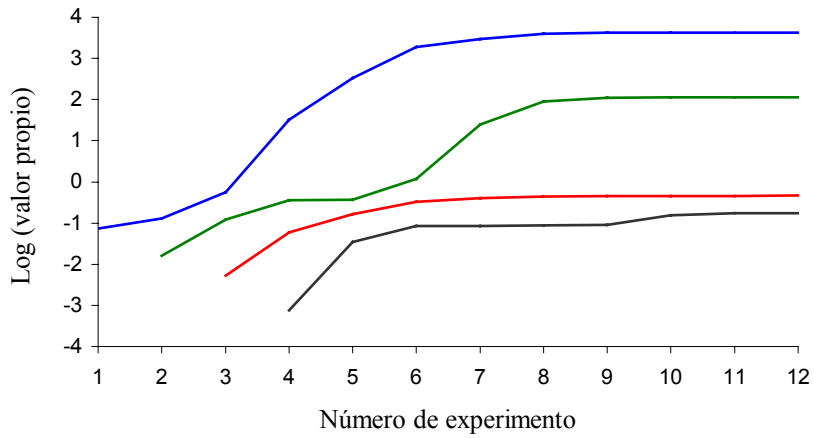

Fig. 2.11 Análisis EFA (sólo *hacia adelante*) de una matriz de datos.

El proceso descrito se llama usualmente *forward* EFA o *hacia adelante*, es decir, en el sentido del avance del experimento realizado. El mismo proceso se repite en la dirección contraria (partiendo de la última fila de la matriz de datos), lo que se denomina *backward* EFA o *hacia atrás*. Los valores propios (o, más frecuentemente, sus logaritmos decimales) calculados para cada submatriz pueden representarse en función de la variable para la cual se estudia la evolución. Los valores propios obtenidos para el primer componente principal de cada submatriz se unen con una línea, con el objeto de analizar correctamente su evolución, y lo mismo se realiza para los factores que siguen en jerarquía (Fig. 2.11).

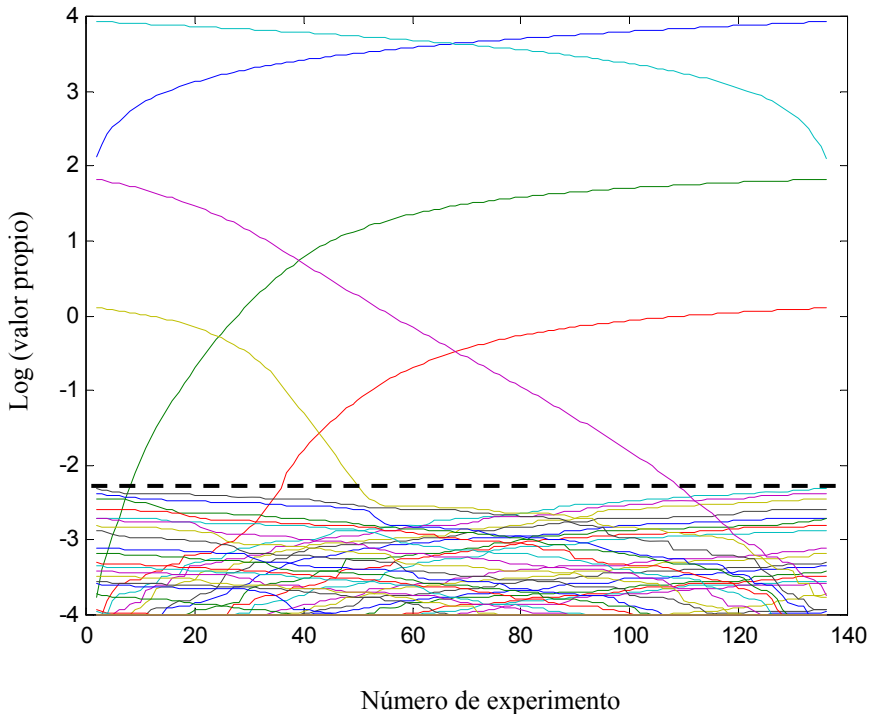

Fig. 2.12 Análisis EFA de una matriz de datos. Tres componentes principales se destacan del ruido (marcado con la línea punteada).

Una vez obtenido el gráfico del análisis EFA (ver Fig. 2.12), además de observar la variación de los factores a lo largo del proceso en evolución, es posible estimar visualmente el número de componentes presentes que contribuyen a la variabilidad de los datos experimentales. Los valores propios relacionados con los componentes significativos son de mayor magnitud y se diferencian claramente del ruido. Además de ser utilizado para la determinación del número de componentes, EFA puede ser empleado como herramienta para el análisis exploratorio de la matriz de datos en busca de regiones de selectividad (donde puede hallarse sólo un componente) o información del rango de forma localizada, indicando, a lo largo del conjunto de datos, regiones donde ciertos componentes pueden encontrarse ausentes. También, mediante EFA puede construirse una estima inicial para el algoritmo de mínimos cuadrados alternados.

2.3.5 SIMPLISMA

Este método (cuyo acrónimo, SIMPLISMA, corresponde a la expresión inglesa SIMPLe-to-use Interactive Self-modelling Mixture Analysis [78]) permite hallar variables puras en un conjunto de datos experimentales sin la necesidad de realizar el análisis de componentes principales. El procedimiento se basa en la evaluación de la desviación estándar relativa de las columnas de la matriz de datos:

$$p_i = \frac{S_i}{m_i} \qquad \text{Ec. (2.12)}$$

siendo p la desviación estándar relativa, S la desviación estándar y m la media para un columna i. Una desviación estándar relativa grande indica una alta pureza para esa columna. Con el fin de evitar la sobrevaloración de columnas con un valor medio pequeño (generalmente correspondientes al ruido) se introduce un factor de corrección f (normalmente 0.1 o 1 según el nivel de ruido aceptado):

$$p_i = \frac{S_i}{m_i + f} \qquad \text{Ec. (2.13)}$$

El procedimiento [78] consiste, en primer lugar, en hallar la columna con la mayor desviación estándar relativa. Seguidamente, se procede a la normalización de dicha columna. La segunda variable de mayor pureza, además de poseer la mayor desviación estándar, deberá presentar la mínima correlación con la primera variable pura encontrada. Por lo tanto se calcula un factor de ponderación, *w*, de la siguiente manera:

$$w_i = \det(\mathbf{Y}_i{}^T \mathbf{Y}_i) \qquad \text{Ec. (2.14)}$$

donde **Y** es la matriz compuesta por las variables puras halladas y cada *i*-ésima columna de la matriz de datos que aún no ha sido seleccionada. El valor calculado para el determinante será proporcional a la independencia que haya entre la variables puras halladas y la fila *i*-ésima que se ha utilizado para construir la matriz $\mathbf{Y}_i$. Así, el determinante tendrá un valor más alto en la medida que las variables no estén correlacionadas, mientras que para variables correlacionadas dará un valor cercano a cero [78].

Así, para las siguientes variables a analizar, se aplica el factor de ponderación de forma que la expresión de la Ec. (2.13) cambia ligeramente,

$$p_i = w_i \left(\frac{S_i}{m_i + f} \right) \qquad \text{Ec. (2.15)}$$

El algoritmo seleccionará el máximo p_i, que corresponderá a la siguiente variable de mayor pureza, y así sucesivamente hasta hallar la totalidad de variables puras.

2.3.6 Resolución Multivariante de Curvas. Optimización mediante Mínimos Cuadrados Alternados (MCR-ALS)

La Resolución Multivariante de Curvas tiene como finalidad aislar, resolver y cuantificar las fuentes variabilidad presentes en un determinado conjunto de datos. A diferencia de los métodos univariantes, que utilizan la información puntual suministrada por la respuesta del sistema en estudio para una única variable (ej. la respuesta para una sola longitud de onda, si se trata de datos espectroscópicos), los métodos multivariantes analizan la respuesta para múltiples variables (ej. todo el espectro). La Resolución Multivariante de Curvas se utiliza comúnmente para resolver componentes presentes en muestras de naturaleza y composición desconocida [19,20,23,79], pero también puede emplearse para la descripción e identificación de especies presentes en sistemas (total o parcialmente desconocidos) que involucran procesos y reacciones químicas, en los cuales existen compuestos intermediarios desconocidos o las especies que intervienen no pueden ser fácilmente aisladas [80].

La condición habitual, cuando se utiliza MCR, es que los datos sigan un modelo lineal [81] (ej. la ley de Lambert-Beer para datos espectroscópicos), lo cual puede expresarse como

$$\mathbf{D} = \mathbf{C}\,\mathbf{S}^{T} + \mathbf{E} \qquad \text{Ec. (2.16)}$$

donde **D** es la matriz de datos adquiridos a diferentes valores de cierta variable (tiempo, pH, concentración, potencial, etc.) durante una reacción o proceso químico, **C** y $\mathbf{S}^T$ están relacionadas con las concentraciones y los perfiles de respuesta puros de las variables presentes en el sistema, respectivamente, y **E** es la matriz de los residuales, que contiene información no explicada por el producto $\mathbf{CS}^T$. Las dimensiones de las cuatro matrices son: **D** (I x J), **C** (I x N), **S** (J x N) y **E** (I x J), donde I es el número de mediciones realizadas (ej. número de espectros), J es el número de variables registradas para cada medición (ej. número de longitudes de onda) y N es el número de especies químicas presentes.

Para conseguir la descomposición descrita en la Ec. (2.16), se implementan distintas técnicas de análisis multivariante, ensambladas en un solo método que consta de diferentes partes [80]:

- Determinación del número de componentes

En primer lugar se determina el número de componentes que contribuyen significativamente a la respuesta del sistema. Si las especies químicas presentes poseen una contribución a la varianza de los datos mayor que el ruido, el número de componentes o factores puede estimarse directamente evaluando los respectivos valores singulares.

- Construcción de la estima inicial

Las matrices **C** y $\mathbf{S}^T$ (Ec. (2.16)) se determinan mediante la aplicación de un algoritmo de optimización (ver más adelante "Mínimos Cuadrados Alternados" en este

mismo apartado) que requiere establecer una estima inicial para **C** o $\mathbf{S}^T$ como punto de partida. Dichas estimas pueden obtenerse a partir de técnicas basadas en la detección de variables puras (SIMPLISMA) o en el análisis de factores emergentes (EFA), entre otras.

- Mínimos Cuadrados Alternados

Las estimas iniciales para **C** o $\mathbf{S}^T$ se optimizan resolviendo la Ec. (2.16) iterativamente mediante el método de Mínimos Cuadrados Alternados. A cada iteración del proceso de optimización se obtienen nuevas estimas de las matrices **C** y $\mathbf{S}^T$:

$$\mathbf{C}^{+}\mathbf{D}^{*} = \mathbf{C}^{+}\mathbf{C}\mathbf{S}^{T} = \mathbf{S}^{T} \qquad \text{Ec. (2.17)}$$

y

$$\mathbf{D}^{*}(\mathbf{S}^{\mathrm{T}})^{+} = \mathbf{C}(\mathbf{S}^{T})(\mathbf{S}^{T})^{+} = \mathbf{C} \qquad \text{Ec. (2.18)}$$

dónde la matriz $\mathbf{D}^*$ es la matriz de los datos experimentales reproducida mediante PCA para el número de componentes seleccionados. El uso de esta matriz en lugar de la matriz experimental **D** mejora la estabilidad de los cálculos, puesto que mediante PCA se elimina la mayor cantidad de ruido en los datos experimentales. $\mathbf{C}^+$ es la pseudoinversa [82] de la matriz **C** y $(\mathbf{S}^T)^+$ es la pseudoinversa de la matriz $\mathbf{S}^T$.

Desafortunadamente, cuando se trabaja con datos bilineales, no existen soluciones únicas para la descomposición planteada en la Ec. (2.16). En ausencia de otra información,

C y $\mathbf{S}^T$ no se pueden distinguirde otras matrices **C**' y $\mathbf{S}^T$' que permiten obtener la misma matriz de residuales **E**, puesto que todas las soluciones para la descomposición de **D** son combinaciones lineales unas de otras [83,84]. Mediante la utilización de información adicional en forma de restricciones, basadas en el conocimiento físico-químico del sistema en estudio, es posible reducir considerablemente el número de soluciones posibles e incluso obtener una solución única al problema. Una restricción puede ser definida como cualquier propiedad matemática o química que es sistemáticamente satisfecha por el sistema completo o por algunas de sus contribuciones puras [85]. Básicamente, el algoritmo ALS permite obtener soluciones con significado químico, a partir de estimaciones iniciales que evolucionan, bajo determinadas restricciones (aplicadas en las matrices **C** y/o $\mathbf{S}^T$), a cada paso del proceso de optimización. Las restricciones aplicadas pueden proceder de la naturaleza misma del sistema químico:

- *No negatividad*: Puede aplicarse a todos los perfiles de concentración y a algunos tipos de respuesta instrumental (ej. espectros UV, infrarrojos, etc.). Esta restricción obliga a que todos los valores de un perfil (de concentración o respuesta) sean mayores o iguales a cero [19,70,86,87].

- *Sistema Cerrado*: Esta restricción implica que, en todo momento, la suma de las concentraciones de las especies presentes en el sistema en estudio (o algunas de ellas) sea igual a una constante [19,21].

- *Unimodalidad*: Por medio de esta restricción se impone la existencia de un único máximo (máximo absoluto) en cada perfil de respuesta [85]. Es aplicable a perfiles de concentración relacionados con procesos de separación (ej. perfiles cromatográficos) o reacciones químicas [88]. Algunos tipos de respuesta, como las señales voltamperométricas, también admiten este tipo de restricción [80].

Pero también pueden aplicarse otras restricciones si se posee información adicional acerca del sistema. Por ejemplo, si se conocen *a priori* los espectros puros o perfiles de concentración (o parte de ellos) de alguna de las especies presentes, en cada iteración los perfiles conocidos pueden mantenerse invariables [76,81,84]. Otras restricciones están relacionadas con aspectos matemáticos, y son independientes de la naturaleza química. Las restricciones de este tipo están asociadas al concepto de rango local, es decir, de qué manera varía, localmente, el número y la distribución de los componentes en el conjunto de datos. Por ejemplo, la restricción de *selectividad* implica la existencia de regiones (ya sea en los perfiles de concentración como en los espectrales) en las que sólo una especie está presente [81,84]. También pueden aplicarse restricciones relacionadas con información de *rango local*, mediante las cuales se especifica la ausencia de alguna de las especies a lo largo de alguno de los perfiles [81,84].

Cuando, mediante ALS, se analizan simultáneamente distintos conjuntos de datos correspondientes a un mismo problema en estudio, se pueden aplicar restricciones adicionales con el fin de establecer correspondencias entre las mismas especies presentes en los diferentes conjuntos de datos, o que especies comunes en las distintas matrices de datos tengan el mismo perfil de respuesta [19,20].

- Parámetros de calidad del ajuste

Existen diferentes parámetros a partir de los cuales se puede obtener información acerca de la bondad del ajuste realizado mediante MCR-ALS. Uno de ellos se denomina falta de ajuste (*lof*, del inglés "lack of fit") y está definido por la Ec. (2.19):

$$lof = \sqrt{\frac{\sum_i \sum_j (d_{ij} - \hat{d}_{ij})^2}{\sum_i \sum_j d_{ij}^2}} \qquad \text{Ec. (2.19)}$$

dónde d_{ij} representa a cada uno de los elementos de la matriz experimental **D** y $\hat{d}_{ij}$ representa los elementos calculados por el modelo para el producto $\mathbf{CS}^T$.

Otro parámetro, que ofrece una información similar al anterior, es el porcentaje de varianza explicada por el producto $\mathbf{CS}^T$:

$$R^2 = \frac{\sum_i \sum_j \hat{d}_{ij}^2}{\sum_i \sum_j d_{ij}^2} \qquad \text{Ec. (2.20)}$$

Por otra parte, si se desea evaluar la calidad de los perfiles obtenidos, en el caso en que se posea información acerca de los perfiles reales, es conveniente utilizar el llamado criterio de similitud, que calcula la correlación existente entre los perfiles recuperados por el modelo y los perfiles reales (ver Ec. (2.21)).

$$r = \cos\gamma = \frac{\mathbf{s}_i^T \hat{\mathbf{s}}_i}{\|\mathbf{s}_i\| \cdot \|\hat{\mathbf{s}}_i\|} \qquad \text{Ec. (2.21)}$$

dónde γ es el ángulo definido por los vectores asociados al perfil recuperado mediante MCR-ALS ($\hat{s}_i$) y al perfil real (s_i), para una determinada especie *i* estudiada.

3. Parte Experimental

3.1 Sistemas químicos estudiados

Como ya se ha comentado al final de la sección 2.1, a lo largo de esta Tesis se han estudiado diferentes reacciones de resinas epoxi con aminas. La mayoría de estas reacciones son sistemas modelo, puesto que no evolucionan hacia productos sólidos. De esta manera, el estudio de la cinética y la reactividad de las especies implicadas en la reacción se puede llevar a cabo sin considerar los cambios físicos que tienen lugar durante la polimerización. Entre estas reacciones, se ha puesto especial atención en aquella que involucra el fenilglicidiléter (PGE) y la anilina, principalmente debido a la gran similitud del PGE con resinas epoxi utilizadas normalmente a nivel industrial. Los resultados obtenidos del estudio de esta reacción se recogen en el Capítulo 4 y en la sección 5.1 del Capítulo 5. El PGE (ver Fig. 3.1 a) empleado en este trabajo ha sido suministrado por Aldrich. La anilina (Aldrich) ha sido destilada antes de su utilización.

Otros monómeros epoxídicos estudiados no están disponibles comercialmente y han sido sintetizados por el Grupo de Polímeros del Departamento de Química Analítica y Química Orgánica de la Universidad Rovira i Virgili. Es el caso del fenilglicidiloxidimetilsilano (GDMPS) y el fenilglicidiltioéter (PGTE) (ver Fig. 3.1 c y d, respectivamente). La preparación de estos monómeros, y su reacción con anilina, ha sido estudiada en el Capítulo 5.

Asimismo, los estudios llevados a cabo en el Capítulo 6 se basan en la reacción entre diglicidiléter de bisfenol A (DGEBA, Fig. 3.1 e) y diaminodifenilmetano (DDM) (Fig. 3.1 f), ambos compuestos bifuncionales que al reaccionar forman una densa red entrecruzada.

a

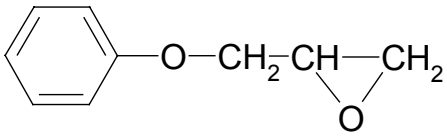

PGE

b

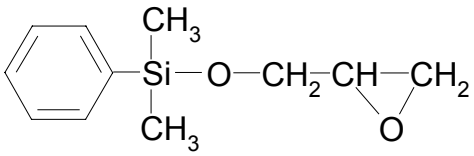

GDMPS

c

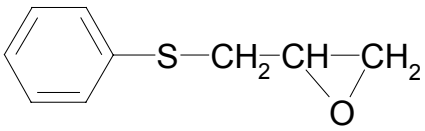

PGTE

d

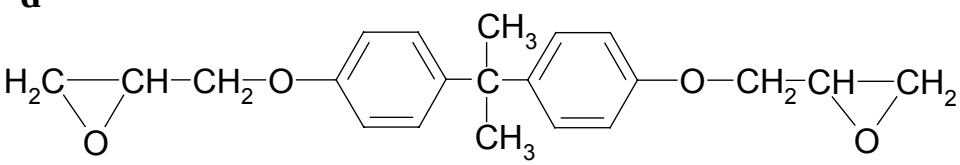

DGEBA

e

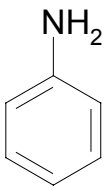

Anilina

f

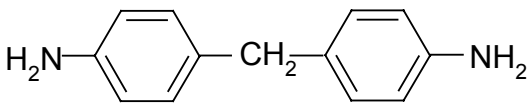

DDM

Fig. 3.1 Epóxidos (a-d) y aminas (e y f) utilizados.

3.2 Procedimiento experimental

3.2.1 Preparación de la mezcla de reacción

Todos los compuestos modelo utilizados (es decir, PGE, PGTE y GDMPS) al igual que la anilina son líquidos a temperatura ambiente. El procedimiento experimental para la preparación de las mezclas de reacción consistió en pesar las cantidades adecuadas, de acuerdo a la relación molar epóxido/anilina deseada, de cada uno de los reactivos en una balanza analítica y, posteriormente, mezclarlos hasta obtener un sistema homogéneo.

Por otra parte, tanto el DGEBA como el DDM son sólidos; el primero de consistencia pastosa mientras el segundo se presenta en forma de polvo. En este caso, una vez pesadas las cantidades necesarias de cada reactivo, se procedió al mezclado mecánico de ambos sólidos con ayuda de un mortero hasta lograr una pasta homogénea.

Cabe destacar que todas las reacciones estudiadas son muy lentas a temperatura ambiente, por lo que el avance de las mismas durante el procedimiento de mezclado puede considerarse despreciable.

3.2.2 Procedimiento para las medidas en NIR

Las medidas de infrarrojo cercano se realizaron en un espectrofotómetro InfraAlizer 500 de Bran+Luebbe. En el caso de mezclas de reacción correspondientes a los sistemas modelo, el procedimiento consistió en inyectar 1 mL de la mezcla dentro de la celda para líquidos del espectrofotómetro, previamente termostatizada a la temperatura

adecuada mediante un baño termostático PolyScience, USA (Ver Fig. 3.2). Dada la escasa cantidad de muestra inyectada, se considera que el proceso de estabilización de la temperatura de la mezcla de reacción es rápido, por lo que el primer espectro se registró inmediatamente después de la inyección. El resto de los espectros se registró automáticamente cada 5 minutos hasta que no existieron diferencias significativas entre dos espectros consecutivos.

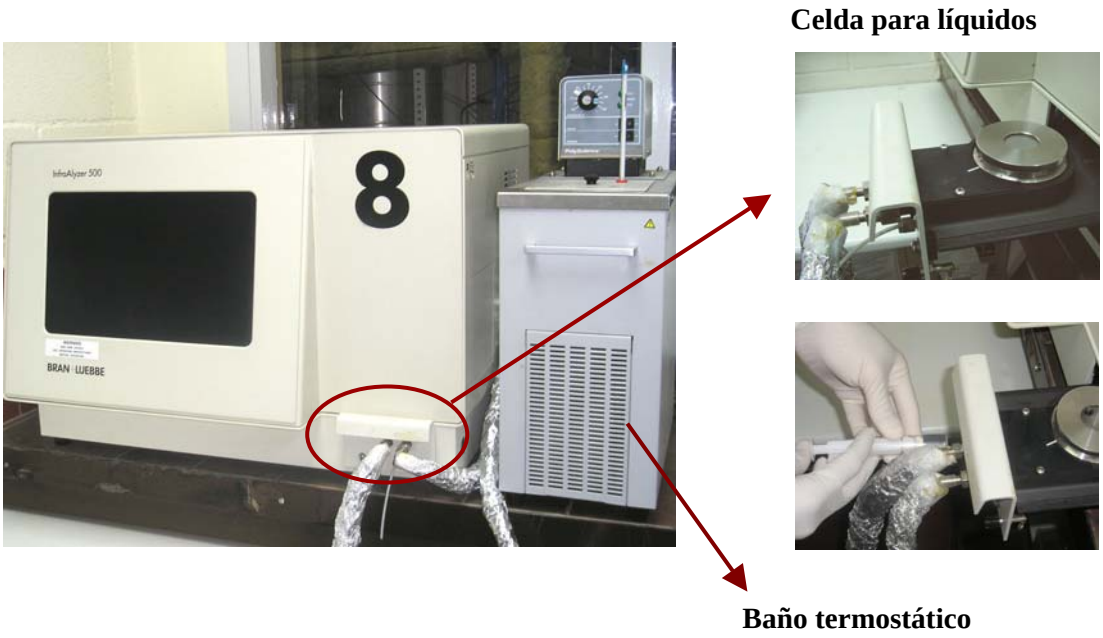

Fig. 3.2 Espectrofotómetro NIR y celda para líquidos.

El procedimiento para el sistema DGEBA/DDM fue ligeramente diferente debido a que el producto de reacción es un sólido insoluble. Por esta razón, y para salvaguardar la integridad de la celda para líquidos, se depositó una gota de la mezcla de reacción sobre una superficie delgada (0,2 mm de espesor) de vidrio circular de 1,5 cm de diámetro, que a su vez se colocó sobre la superficie reflectante de acero inoxidable de la celda para líquidos. Finalmente, la celda se cerró con una ventana de cuarzo (ver Fig. 3.3). Los espectros se registraron de igual manera que para los sistemas modelo.

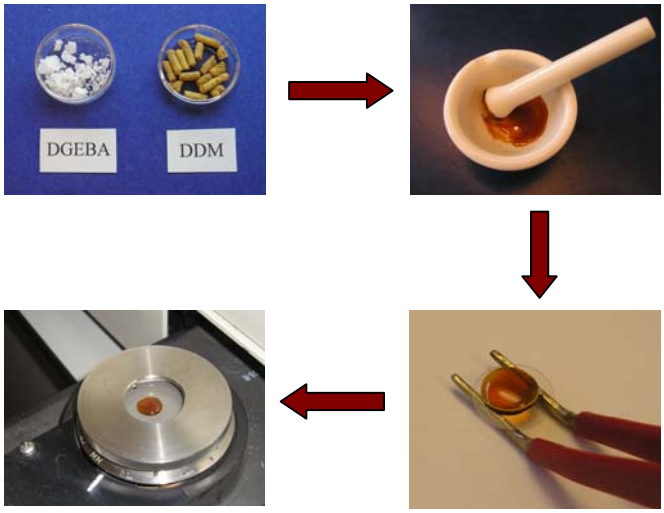

Fig. 3.3 Procedimiento para las medidas NIR del sistema DGEBA/DDM.

3.2.3 Procedimiento para las medidas en ^{13}C RMN

Las medidas de resonancia magnética nuclear se realizaron sólo para los sistemas modelo PGE/anilina y GDMPS/anilina. El procedimiento (ver Fig. 3.4) consistió en colocar, en primer término, volúmenes iguales (300 μL) de la mezcla de reacción en pequeños tubos de ensayo Pyrex ® (uno por cada tiempo de reacción para el cual quiere realizarse el espectro de resonancia). A continuación, la serie de tubos fue sumergida en un baño termostático (PolyScience, USA) y la temperatura fue controlada mediante una sonda de temperatura (Crison). Cada tubo se retiró al tiempo de reacción deseado y fue rápidamente enfriado en una mezcla de agua y hielo a fin de detener la reacción. Una pequeña porción (alrededor de 150 mg) de la mezcla de reacción se transfirió a un tubo de resonancia magnética nuclear y fue disuelta en una cantidad adecuada de cloroformo deuterado (700 μL). Los espectros de resonancia de ^{13}C se registranron a temperatura ambiente utilizando desacoplamiento para la señal de los protones. A fin de obtener

resultados cuantiativos los espectros se adquirieron utilizando "*inverse-gated decoupling*" (ver Sección 2.2.2.2) y tiempos de recuperación de aproximadamente cinco veces el tiempo de relajación de los núcleos que relajan más lentamente. El número de barridos realizados varía en relación a la cantidad de muestra utilizada. En todos los casos, 64 barridos fueron suficientes para obtener espectros satisfactorios.

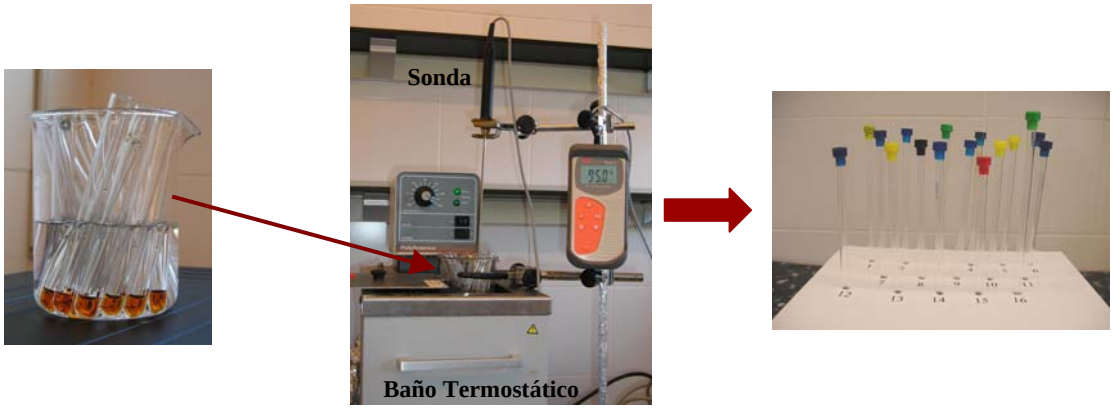

Fig. 3.4 Procedimiento para el seguimiento de reacciones modelo mediante RMN.

3.2.4 Separación Cromatográfica

Los experimentos realizados en cromatografía líquida se diseñaron para estudiar la reacción entre el PGE y la anilina. La preparación de la reacción y el procedimiento para llevar a cabo la toma de muestras se realizó de igual manera que para los experimentos de resonancia magnética nuclear (apartado 3.2.3). Se pesaron porciones de la mezcla de reacción (alrededor de 15 mg) y se llevaron a un volumen de 10 mL con metanol en matraces aforados. Las muestras así preparadas se conservaron a baja temperatura hasta el momento de la inyección al cromatógrafo.

La cromatografía líquida de alta eficacia (HPLC) se llevó a cabo en fase inversa en un cromatógrafo Hewlett Packard series 1100, equipado con un detector UV-Vis para la monitorización de las especies eluídas. La separación cromatográfica se realizó en una columna analítica Hypersil ODS para fase inversa, con dimensiones de 200 mm de largo y 4, 6 mm de diámetro interno, y rellena con partículas de 5 μm de diámetro. La temperatura de la columna fue termostatizada a 20 ºC.

El análisis por HPLC se realizó en gradiente de elución de metanol/agua (ambos solventes de grado HPLC gradiente, adquiridos a SDS), con una velocidad de flujo de 1,75 mL min^{-1}. El gradiente comenzó con una mezcla de 20 % de metanol y 80 % de agua, la cual se fue modificando de manera continua hasta llegar a un 100% de metanol, al cabo de 10 minutos.

La concentración de las especies estudiadas se calculó por interpolación de las áreas obtenidas para los correspondientes picos cromatográficos en las rectas de calibrado construidas a partir de soluciones estándar de los compuestos puros. Como se ha dicho anteriormente, tanto el PGE como la anilina están disponibles comercialmente. La amina secundaria se ha preparado haciendo reaccionar PGE con un exceso de anilina (en relación molar PGE/anilina de 1:10) a 80 ºC durante 12 horas. El exceso de anilina fue destilado en condiciones de alta presión. La amina terciaria se obtuvo haciendo reaccionar PGE y anilina en proporciones estequiométricas (es decir, en una relación molar PGE/anilina de 2:1) a 120 ºC durante 20 horas.

3.2.5 Medidas dinamomecánicas

Las medidas de viscosidad compleja realizadas para el sistema DGEBA/DDM discutidas en el capítulo 6 se llevaron a cabo en un analizador dinamomecánico 2980 DMA V1.40 de TA Instruments. Los anásis se realizaron en modo de

cizalla con una mordaza de tipo sándwich, aplicando una deformación con una frecuencia fija de 1 Hz y una amplitud de 30 μm. Las medidas se llevaron a cabo en régimen isotérmico a 70 ºC. El procedimiento para la preparación de la muestra consitió en impregnar con la mezcla de reacción un soporte de fibra de vidrio (10 x 10 x 0,34 mm^3). Una vez impregnado, el soporte fue cuidadosamente colocado en la mordaza del DMA, cuya temperatura fue previamente ajustada según los requierimientos del experimento.

3.3 Software utilizado

Todos los tratamientos quimiométricos realizados en esta Tesis se llevaron a cabo empleando el programa MATLAB® [89], en su versión 6.5.

Los espectros NIR, registrados mediante el software SESAME 3.01 de Bran+Luebbe, se exportaron como archivos JCAMP-DX. Mediante el uso de The Unscrambler [90], versión 9.0, estos archivos se convirtieron a archivos compatibles con el formato utilizado por MATLAB. Los espectros de resonancia magnética nuclear se trataron mediante el programa MestRe-C 2.3a [91].

Las subrutinas utilizadas para aplicar MCR-ALS fueron suministradas por el Grupo de Quiometría y Equilibrio en Solución de la Universidad de Barcelona. Las mismas se pueden obtener de forma gratuita en Internet [92]. La subrutina para el cálculo de los límites de las bandas de soluciones factibles obtenidas mediante MCR-ALS, ha sido gentilmente proporcionada por el profesor Romà Tauler. Las subrutinas utilizadas para la obtención de las constantes cinéticas han sido creadas en nuestro laboratorio. Esto incluye tanto nuevas subrutinas como modificaciones realizadas sobre el algoritmo de optimización por mínimos cuadrados alternados [92].

4. Seguimiento de Reacciones de Resinas Epoxi

4.1 Introducción

El conjunto de datos obtenidos de la monitorización de cualquiera de las reacciones estudiadas mediante espectroscopía NIR consiste en una acumulación de espectros registrados a lo largo del tiempo de reacción. Estos datos se han dispuesto en una matriz de respuestas en las que las filas corresponden a los diferentes tiempos de reacción para los cuales se registran los espectros y las columnas representan las diferentes longitudes de onda NIR (ver Fig. 4.1).

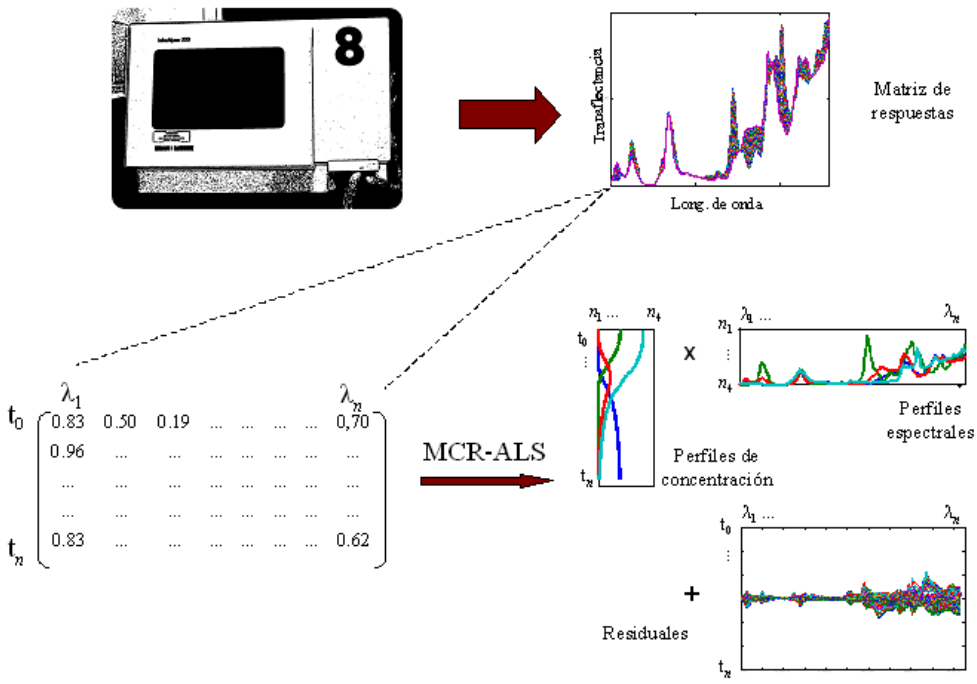

Fig. 4.1. Descomposición mediante MCR-ALS

Así, el problema que se plantea es obtener, a partir de la matriz de respuestas, la información necesaria para identificar cada una de las *n* especies involucradas en el proceso de reacción (es decir, los espectros puros de cada compuesto) y, por otra parte, la evolución de la concentración de esas especies a lo largo del tiempo (perfiles de concentración). La extracción de esta información se realiza a través la resolución de curvas multivariante optimizada mediante mínimos cuadrados alternados (ver Fig. 4.1).

Uno de los aspectos primordiales en la aplicación de los Métodos de Resolución de Curvas es la determinación del número de factores que causan la variabilidad observada en los datos experimentales, lo cual puede asumirse como el rango químico de la matriz de respuestas, como ya se ha establecido en la Sección 2.3.2. La descomposición descrita en la Ec. (2.16) sólo es posible si se asume que el rango de la matriz de datos es igual al número de especies que generan esas de respuestas, cuando otras contribuciones, como el ruido instrumental, no son importantes [31].

Puesto que la matriz de datos puede considerarse como el producto de dos matrices ($\mathbf{D} = \mathbf{C}\,\mathbf{S}^T$), el rango obtenido para la matriz **D** puede comprenderse a partir de la siguiente propiedad del rango de una matriz [21]:

$$\text{rango}\,(\mathbf{D}) \leq \min\,(\text{rango}\,(\mathbf{C}), \text{rango}\,(\mathbf{S}^T)) \qquad \text{Ec. (4.1)}$$

Así, si una de las dos matrices (**C** o $\mathbf{S}^T$) es de rango completo, es suficiente estudiar el rango de la otra matriz para obtener el rango de **D**. Cuando el sistema analizado proviene de procesos en evolución (ej. reacciones químicas), el conjunto de datos obtenido frecuentemente resulta deficiente de rango, es decir, el número de contribuciones

significativas a la varianza de los datos (estimada por medio de SVD u otro técnica) es menor que el número real de especies químicas presentes en el sistema [30,31].

En el caso de reacciones químicas, la deficiencia de rango puede aparecer en la matriz de concentraciones, **C**, por varias razones [31]. Los perfiles de concentración pueden ser linealmente dependientes, a causa del sistema de ecuaciones químicas subyacentes. Ha sido demostrado [93] que para reacciones a volumen constante se cumple que:

$$\text{rango}\,(\mathbf{C}) = \min\,(R + 1, N) \qquad \text{Ec. (4.2)}$$

dónde R es el número de reacciones independientes presentes en el sistema y N es el número total de especies.

La deficiencia de rango también puede estar causada por las ecuaciones de balance de masa derivadas de las reacciones químicas (deficiencia de rango causado por sistema cerrado o por balance de masa) [21]. Otra causa de la deficiencia de rango es el llamado solapamiento de rango, el cual tiene lugar cuando varias especies tienen perfiles en común en cualquiera de los dos órdenes de medida (perfiles de concentración o de respuesta). Este puede ser el caso de procesos en los cuales dos o más productos se forman o se consumen durante la reacción a igual velocidad, produciendo perfiles de concentración de igual forma.

La deficiencia de rango (en cualquiera de sus formas mencionadas), puede resolverse siguiendo dos metodologías [20,93]: (a) construcción de una matriz aumentada, ensamblando distintas submatrices correspondientes al análisis del proceso bajo distintas condiciones iniciales linealmente independientes (ej.concentraciones de partida diferentes); (b) perturbación de la matriz de datos por el añadido de un componente (reactivo o producto) o una mezcla de ellos durante el proceso.

Los datos experimentales procedentes de la monitorización de resinas epoxi presentan deficiencia de rango. Este problema se ha abordado aplicado la primera de estas estrategias, pero con dos variantes diferentes. En la sección 4.2, para la construcción de la matriz aumentada, se han utilizando matrices de datos correspondientes a la monitorización del mismo proceso químico pero partiendo de relaciones molares diferentes para los reactivos de partida. Por otra parte, en la sección 4.3 se presenta otra variante de la estrategia de matrices aumentadas que utiliza conocimiento químico previo acerca del sistema. En este caso la matriz de datos es aumentada con los espectros puros de los reactivos de partida.

Uno de los inconvenientes de la descomposición de datos bilineales es que, frecuentemente, las soluciones halladas no son únicas. Por el contrario, se obtiene un conjunto de soluciones, todas ellas factibles, que permiten obtener el mismo mínimo residual. Este problema, conocido como el nombre de ambigüedad, puede ser de dos tipos: ambigüedad de intesidad y ambigüedad rotacional.

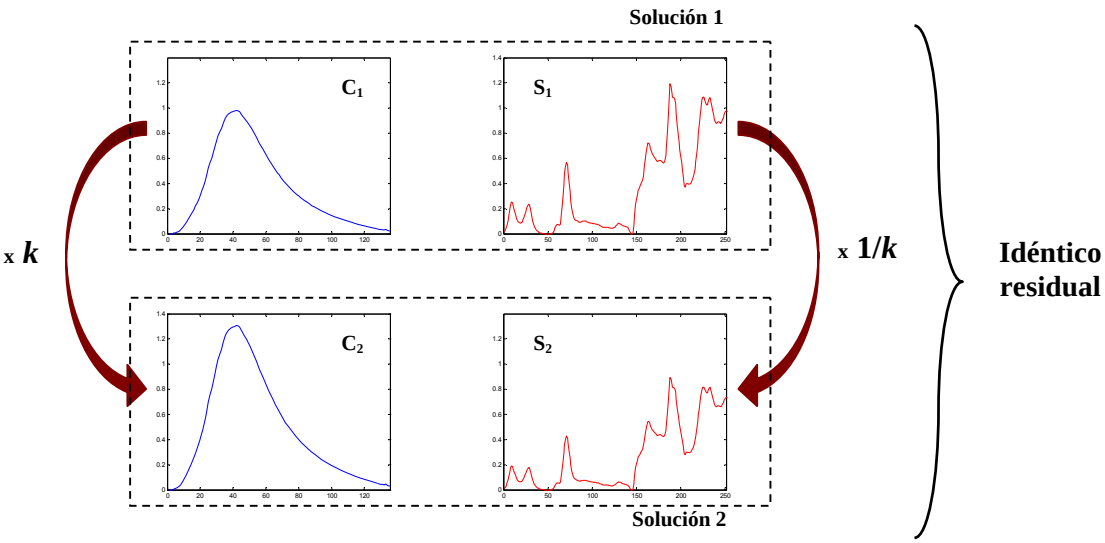

Fig. 4.2 Ambigüedad de intensidad en las soluciones de MCR-ALS

La ambigüedad de intensidad se manifiesta cuando es posible multiplicar por un escalar (*k*) y su recíproco (*1/k*) las soluciones obtenidas mediante alguno de los métodos de resolución de curvas, en nuestro caso MCR-ALS (ver Fig. 4.2). De esta manera, resultan nuevas soluciones que conservan la forma de los perfiles pero no la misma magnitud. Este tipo de ambigüedad dificulta la obtención de información cuantitativa. Normalmente la ambigüedad de intensidad en datos bilineales puede eliminarse utilizando restricciones de sistema cerrado para las concentraciones, normalización o restricciones de igualdad (conocimiento externo, ya sea acerca de los espectros o de los perfiles de concentración).

La descomposición de la matriz de respuestas también se ve afectada por la ambigüedad rotacional. Si no existen restricciones, existe un número infinito de soluciones para dicha descomposición o, dicho en otras palabras, existe libertad rotacional en las soluciones de la Ec. (2.16) [84]. De forma análoga a lo explicado para la ambigüedad de intensidad, las soluciones obtenidas mediante MCR-ALS pueden multiplicarse por una matriz de rotación **T** y por su inversa ($\mathbf{T}^{-1}$) para obtener soluciones diferentes (con un mismo residual). La Ec. (4.3) muestra una expresión matemática para el problema de la ambigüedad rotacional:

$$\mathbf{D} = \mathbf{C}\mathbf{S}^{\mathbf{T}} = (\mathbf{C} \times \mathbf{T})(\mathbf{T}^{-1} \times \mathbf{S}^{\mathbf{T}}) = \mathbf{C'S'}^{\mathbf{T}} \qquad \text{Ec. (4.3)}$$

donde **T** puede ser cualquier matriz no singular para la cual pueda calcularse la inversa. En este caso, también la forma de los perfiles se verá afectada.

La utilización de restricciones como no negatividad, condición de sistema cerrado o unimodalidad permite reducir considerablemente el número de posibles soluciones. Sin embargo las únicas restricciones que pueden limitar severamente las ambigüedades son aquellas relacionadas con regiones de selectividad o rango local (ver cap. 2, apartado 2.3.6).

En el caso en que el problema químico no permita aplicar ese tipo de restricciones, las soluciones obtenidas se verán inevitablemente afectadas por la ambigüedad. Por lo tanto, surge la necesidad de estimar el intervalo o banda de posibles soluciones obtenidas. Este aspecto es estudiado en la sección 4.4 de este capítulo. Si, eventualmente, se dispone de información externa que pueda utilizarse como restricción de igualdad, es posible obtener soluciones únicas tanto en el modo espectral como en los perfiles de concentración. Es el caso estudiado en el la sección 4.3, en la que se utiliza información suplementaria obtenida mediante ^{13}C RMN para algunos perfiles de concentración y que permite recuperar perfiles libres de ambigüedad.

Los resultados obtenidos aplicando MCR-ALS a los datos NIR procedentes de la monitorización de reacciones de resinas epoxi se validaron utilizando HPLC como técnica de referencia. En la sección 4.5 se muestra un estudio detallado de la validación para distintos parámetros analíticos como la veracidad, la precisión, la incertidumbre, así como una valoración de otros aspectos operacionales del método propuesto en la sección 4.2.

4.2 Multivariate resolution of rank-deficient near infrared spectroscopy data from the reaction of curing epoxy resins using the rank augmentation strategy and multivariate curve resolution-alternating least square approach

Analytica Chimica Acta, 515, **2004**, 65-73

M. Garrido, I. Lázaro, M.S. Larrechi and F.X. Rius*

Department of Analytical and Organic Chemistry, Faculty of Chemistry, Rovira i Virgili University, Pl. Imperial Tàrraco, 1, 43005 Tarragona (Spain)

(Received 24 July 2003; received in revised form 24 October 2003; accepted 30 October 2003
Available online 18 December 2003)

Abstract

A model of the curing reaction between phenyl glycidyl ether (PGE) and aniline as the curing agent was studied isothermally at 95 ºC and monitored *in situ* by near-infrared spectroscopy (NIR). The spectra were recorded every 5 minutes. The ubiquitous problem of rank deficiency in reaction network systems was solved by assembling an augmented column-wise matrix containing five process runs from different initial conditions. The data were analyzed using a two-way multivariate curve resolution alternating least squares method (MCR-ALS). Initial estimates of spectra required by MCR-ALS were given by a SIMPLe-to-use Interactive Self-modelling Mixture Analysis (SIMPLISMA) approach. The reactant, product and intermediate spectra were successfully resolved and the concentration profiles properly represented the system studied. The performance of the model was evaluated by two parameters: ALS lack of fit (lof = 0.88%) and explained variance (R^2 = 99.99%). To validate the MCR-ALS results, the similarity coefficients (r) between the

recovered spectra and the pure species spectra were calculated. These were: PGE (r = 0.998), aniline (r = 0.994) and tertiary amine (r = 0.999).

1. Introduction

Near Infrared Spectroscopy (NIR) is an interesting tool for *in situ* monitoring polymerization reactions such as the curing of epoxy resins [1-4]. The quality of the final polymerization product can be controlled, and the process can be carried out in real time, which means that relevant information about the chemistry of the reaction can be obtained.

The spectral data obtained with NIR are normally used univariately [1,2], so the information obtained is only about the degree of conversion of the reactants in the final product but there is no knowledge about how many compounds are involved or how they evolve over time. The use of the so-called multivariate curve resolution methods [5-9] allows us to find out more about the process that is being carried out. Several studies in the literature use these methods to analyze chemical reactions in which a variety of instrumental techniques were used [10-12].

Larrechi and Rius have recently shown the use of multivariate analysis methods, specifically Alternating Least Squares (MCR-ALS) [13], to study the curing reactions of epoxy resins and obtain a profile of the concentrations, as a function of time, of the chemical species involved in the reaction and their corresponding spectra [14]. The present study uses a different strategy in the application of MCR-ALS to NIR data obtained in the analysis of the model reaction between phenylglycidylether (PGE) and aniline [15].

When using multivariate curve resolution methods, it is neccesary to take into

account the rank deficiency, which is not always present but it is often found in experimental data obtained from a chemical reaction [16]. The rank of the experimental matrix, when there is no noise or any other cause of variability, should be equal to the number of absorbent chemical species. However, when the number of species in the data set exceeds the number of reactions plus one, there is rank deficiency [17]. Different ways to solve this have been proposed by Amrhein *et al*. [17] and Tauler and coworkers [18].

In the previous study [14], the strategy to solve rank deficiency was based on chemical knowledge of the process and carried out by incorporating spectral information about three of the four species involved in the chemical reaction. Specifically, these were the spectra of the reactants and final product. This is a very specific situation because, although it is feasible to have information about the reactants for any reaction, this is not true for the final product. This is because the reactions sometimes evolve towards solid products, which makes it impossible to take certain measurements.

The aim of our present study is to overcome rank deficiency by increasing the number of experimental matrices [17]. To do this, the reaction is carried out at several stoichiometric proportions, which ensure that only the reactions under study are produced [19]. This allows us to calculate the concentration profiles and spectra for each experiment. To do this, the ALS method needs an initial estimate of the spectra considered in the adjustment, and this is obtained by selecting the purest components of the system using SIMPLe-to-use Interactive Self-modeling Mixture Analysis (SIMPLISMA) [20].

The results are evaluated by studying the residuals and parameters such as lack of fit (*lof*), the percentage of explained variance and the coefficient of similarity (r) between the recovered spectra and the spectra of the pure species. A qualitative evaluation of the correspondence between the ALS solution and the chemistry of the proposed system is also made.

2. Theory

The aim of the MCR-ALS method is the bilinear decomposition of the experimental data set **D**, coming from the iterative optimization of some C-type or S^T-type initial guesses, in order to obtain matrices **C** and $\mathbf{S}^T$, which have a real chemical significance, according to Eq. (1):

$$\mathbf{D} = \mathbf{C}\mathbf{S}^T + \mathbf{E} \qquad \text{Eq. (1)}$$

in which matrix **C** (*n* x *c*) has column vectors corresponding to the profiles of the *c* pure components that are present in matrix **D**. The row vectors of matrix $\mathbf{S}^T$ (*c* x *m*) correspond to the spectra of the *c* pure components and **E** is the matrix of the residuals.

Specifically, MCR-ALS is an iterative method that at each cycle calculates new matrices **C** and $\mathbf{S}^T$ and incorporates a set of constraints arising from chemical knowledge of the system in the study (non-negativity, closure, etc.) so that the value of **E** is minimum. The constraints imposed on the algorithm are intended to reduce the intensity and rotational ambiguities [13] of techniques that are based on factor analysis.

Analysis of the rank associated with matrices of data obtained in the study of a chemical reaction has been widely discussed by Amrhein *et al*. [17], who showed that in this type of matrix the rank is equal to *min(r*+1*, c)*, where *r* is the number of independent reactions in the chemical system and *c* is the number of absorbent species. Therefore, when $r+1 < c$, there is rank deficiency. These authors also showed that the rank can be increased by augmenting the data matrix. For each additional matrix corresponding to an independent

initial condition, the rank of the augmented matrix increases by one until its value is the same as the number of absorbent species.

The optimization of Eq. (1) requires an initial estimate either of the spectra in $\mathbf{S}^T$ or of the concentration profiles associated with these spectra. This estimate is obtained with the SIMPLISMA approach [20]. This is based on the use of real variables and finds the purest or most representative contributions to the data matrix. The algorithm evaluates the relative standard deviation for each variable and selects as the first purest variable the one with the highest relative standard deviation.

The next purest contribution must have the highest relative standard deviation and be as independent as possible from the first purest variable, and so on with the remaining variables. The independence between variables is evaluated using a function for calculating determinants.

One way to evaluate the quality of the recovered profiles is to use the criterion of similarity, by comparing the true spectra (if there are any) with the spectra obtained from the MCR-ALS algorithm, in accordance with the following equation:

$$r = \cos\gamma = \frac{\boldsymbol{s}_i^T \hat{\boldsymbol{s}}_i}{\|\boldsymbol{s}_i\| \cdot \|\hat{\boldsymbol{s}}_i\|} \qquad \text{Eq. (2)}$$

where γ is the angle defined by the vectors associated with the recovered spectra ($\hat{s}_i$) and the real spectra (s_i) of the compound studied. Also used as parameters in the evaluation are lack of fit, which is the lack of adjustment of the model proposed in Eq. (1), and R^2, which is the explained variance reported by the product $\mathbf{C}\cdot\mathbf{S}^T$.

$$R^2 = \frac{\sum_i \sum_j \hat{d}_{i,j}^2}{\sum_i \sum_j d_{i,j}^2} \qquad \text{Eq. (3)}$$

$$lof = \sqrt{\frac{\sum_i \sum_j (d_{i,j} - \hat{d}_{i,j})^2}{\sum_i \sum_j d_{i,j}^2}} \qquad \text{Eq. (4)}$$

where d_{ij} represent the elements of the experimental matrix **D**, and $\hat{d}_{ij}$ are the values calculated by the model in Eq. (1).

3. Experimental

3.1 Reaction conditions and procedure

The reaction studied in this paper is the one between PGE and aniline, which acts as the curing agent (Fig. 1). The reaction was performed at 95º C. The molar ratio between PGE and aniline was chosen to ensure that only the reaction under study took place and that there were no collateral etherification or homopolymerization reactions [3,15,19,21]. Five experiments were performed. In these experiments the molar ratios between the reactants were varied to obtain the following PGE/aniline ratios: 1:1, 1.25:1, 1.5:1, 1.75:1 and 2:1. More experiments than were needed to break the rank deficiency of data were performed,

but this extra information helped reduce the uncertainty of the results. Also, the simple technique did not require too much experimental effort. The procedure involved mixing the necessary amounts of aniline and PGE at room temperature to obtain the desired molar ratio and, immediately after, injecting 1 mL of this mixture into the liquid cell of the NIR spectrophotometer. The cell temperature was set at 95ºC.

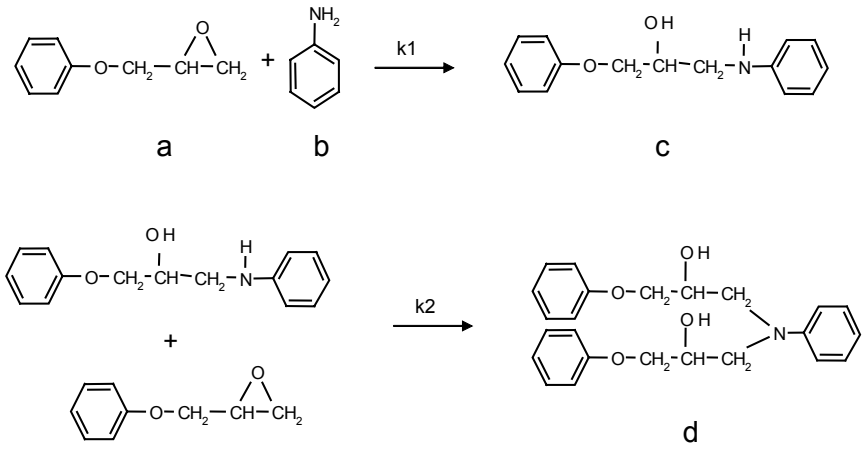

Fig. 1. Curing reaction between phenylglycidylether (PGE) and aniline at T=95ºC. (a) PGE, (b) aniline, (c) secondary amine, (d) tertiary amine.

3.2 Data acquisition

The data obtained correspond to the NIR spectra recorded every 4nm between 1100 and 2500 nm in an InfraAlyzer 500 Bran-Luebbe spectrophotometer.

For each experiment, data at intervals of 5 min until the end of the reaction were acquired. As a reference the band at 2208 nm, which is characteristic of the oxirane

group [1] was chosen. The reaction was considered to be completed when this band disappeared. In this way, the times during which spectra were recorded for each experiment, in increasing order with respect to the proportion of epoxide, were: 230, 300, 390, 480 and 675 min.

The experimental data were arranged in matrices whose rows were the number of recorded spectra and whose columns were the wavelengths. The following matrices were thus obtained: $\mathbf{A_1}$ (47 x 351), $\mathbf{A_2}$ (61 x 351), $\mathbf{A_3}$ (79 x 351), $\mathbf{A_4}$ (97 x 351) and $\mathbf{A_5}$ (136 x 351), corresponding to the experiments with PGE/Aniline molar ratios of 1:1, 1.25:1, 1.5:1, 1.75:1 and 2:1, respectively.

In the same conditions, the NIR spectra of the pure reactants were also recorded. The spectra recorded in the InfraAlyzer 500 were exported and converted into MATLAB binary files [22,23].

3.3 Data Analysis

This section describes the procedure for applying the MCR-ALS method to the study of this reaction.

3.3.1 Data preprocessing and data matrices

3.3.1.1 Offset correction. All the original spectra were corrected. This was to eliminate any vertical shift in the spectra during the course of the experiment caused by using a NIR spectrophotometer with only one light beam. This pre-treatment involves subtracting from the values of reflectance, recorded at each wavelength, the lowest value of reflectance for each individual spectrum [24].

3.3.1.2 Wavelength selection. Another treatment applied to the experimental data involves selecting the wavelengths of interest and ignoring those in which no variation over time was observed because these provide no information about the reaction under study. The regions of the spectrum in which only noise was detected were also eliminated. The selected wavelengths ranged from 1400 to 2432 nm.

3.3.1.3 Arrangement of the augmented matrix. A column-wise augmented data matrix (420 x 259 in size) was constructed with the five sets of data (corresponding to the 5 experiments) corrected and ordered from greatest to least in terms of decreasing proportions of epoxide.

3.3.2 Rank analysis

The rank of the individual matrices and the augmented matrix were analyzed with singular value decomposition (SVD) [25]. Considering that the chemical components made a much larger contribution to the data variance than noise, it was enough estimates the number of factors by simple inspecting the tables of singular values.

3.3.3 Initial profile estimates

The initial estimate was constructed in three phases. First, the SIMPLISMA algorithm was applied to all the rows in the augmented matrix to search for an estimate for matrix $\mathbf{S}^T$. In this way, we obtained an approximation of a spectral profile for the components that intervene in the reaction. Second, Eq. (1) was fitted with the estimate provided by SIMPLISMA and optimized in order to minimize the residual matrix **E**. In this optimization, were used the non-negativity and closure constraints. This led to a new set of spectra and kinetic profiles for each compound. Although these profiles do not correctly

describe the evolution of each species as a function of time, they are a satisfactory approximation of the behavior expected for the intermediate and final compounds of the reaction. Finally, the initial estimate was made up of the spectra for the secondary and tertiary amines, recovered in the optimization of the second phase above mentioned, whereas for the aniline and the PGE, the spectra of the pure compounds recorded previously were used.

3.3.4 Alternating least squares (ALS) optimization

The ALS algorithm was iterated by applying a series of constraints in an attempt to obtain a solution that was consistent with the chemical problem and restrict the number of possible solutions. These constraints were the following:

a) The values of the spectra of each component must be non-negative.

b) The values of the concentration profiles as a function of time must be non-negative.

c) The system must be closed related to the total analytic concentration.

d) Each concentration profile must have only one maximum (unimodality).

It is important to clarify that the pure spectra used in the construction of the initial estimate have not been fixed through the resolution process.

3.3.5. Validation of the results

To validate the results, we compared the pure spectra and the spectra recovered by MCR-ALS using the similarity criterion in Eq. (2). As far as the reagents are concerned, we used the pure spectra of aniline and PGE, different from those used during the optimization, and the last spectrum recorded for the tertiary amine when the PGE/aniline molar ratio was 2:1 because we considered the reaction to be complete.

Other parameters related to the quality of the result were also applied: the percentage of explained variance (Eq. (3)) and the lack of fit (Eq. (4)). Finally, a qualitative analysis of the residuals derived from the fitting process by ALS was made.

4. Results and discussion

Fig. 2 shows the NIR spectra obtained from the experiment with a PGE/aniline molar ratio of 2:1, after wavelength selection and off-set correction. We can see that the characteristic bands of the oxirane group (2208 nm) and the primary (1978 nm and 1500 nm) and secondary (1500 nm) amines disappear as the reaction progresses, and that the band corresponding to the hydroxilic group (1431 nm) appears.

Rank analysis of the individual data matrices from the experiments in which the PGE/aniline ratio was varied showed that there were three significant contributions for all the matrices not four, which was the number of species that intervene in the process and absorb in the spectral zone ($c = 4$). In this study, two reactions ($r = 2$) were postulated, so the rank was $\min(r + 1, c)$ i.e. 3. The reason for this rank deficiency is that the

concentration profiles of the absorbing species are not linearly independent, as they usually are in this type of chemical reaction. To eliminate this rank deficiency, a column-wise augmented matrix with the data from all the experiments was constructed. As an example, Table 1 shows the first six singular values associated to the SVD for the experiment in which the PGE/aniline molar ratio is 2:1 and for the augmented matrix.

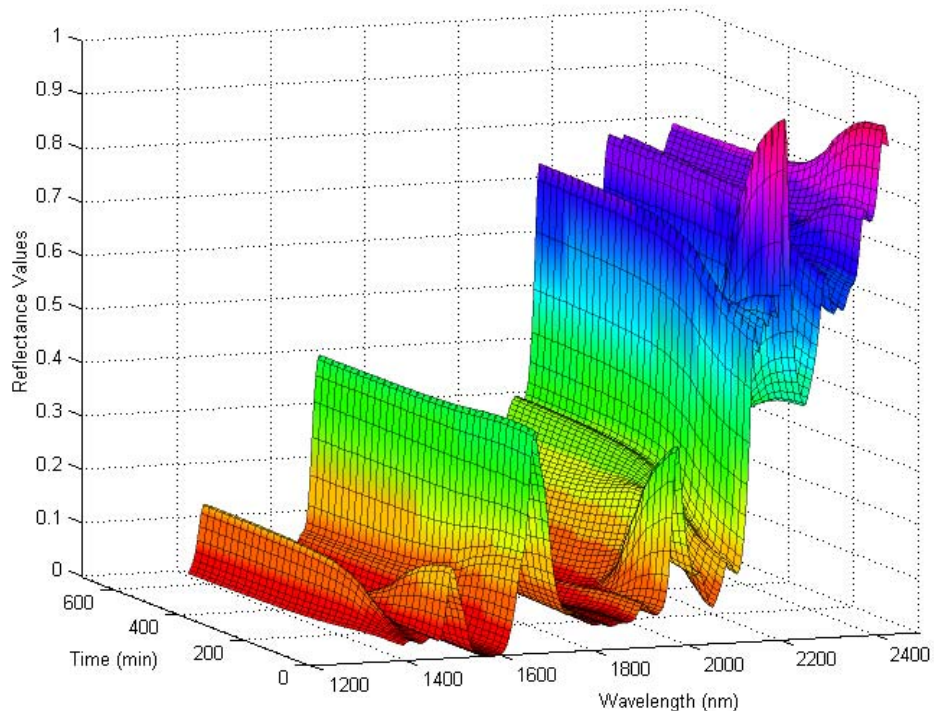

Fig. 2. Three-dimensional representation of NIR data (Reflectance-Wavelength-Time) relative to the PGE/aniline 2:1 system at 95ºC, after the application of data preprocessing.

Number of factor	Singular values of the $\mathbf{A_5}$ matrix	Singular values of the augmented matrix
1	66.94	78.31
2	8.00	9.86
3	1.06	3.78
4	0.06	1.35
5	0.01	0.15
6	< 0.01	0.09

Table 1. Rank analysis of matrix $\mathbf{A_5}$ and the column-wise augmented matrix . The first six singular values are shown.

When we calculated the singular values for the augmented matrix, there was a considerable increase in the fourth singular value, whose magnitude was similar to the third singular value of the individual matrix. The rank deficiency, therefore, is broken because the rank of the new matrix matched the number of absorbing species.

Fig. 3 shows the spectra selected when SIMPLISMA was applied to the augmented data matrix. The variables selected, in decreasing order of purity, were the spectra (rows) 136, 374, 420, and 33. Spectrum 136 was the last spectrum of the experiment that was carried out with a 2:1 molar ratio (675 min.). At this time the reaction was considered to be completely finished, so only the tertiary amine was present. In the spectrum of Fig. 3, only the band corresponding to the OH group (1431 nm) of the final reaction product was

observed: the bands that identify the epoxide (2208 nm) and the primary (1500 nm and 1978 nm) and secondary (1500 nm) amines disappeared. Spectrum 374 had the characteristic aniline bands and was the first spectrum of the 1:1 experiment. At this point, the only species present were PGE and aniline, and the ratio of the latter with respect to the epoxide was higher than in other experiments.

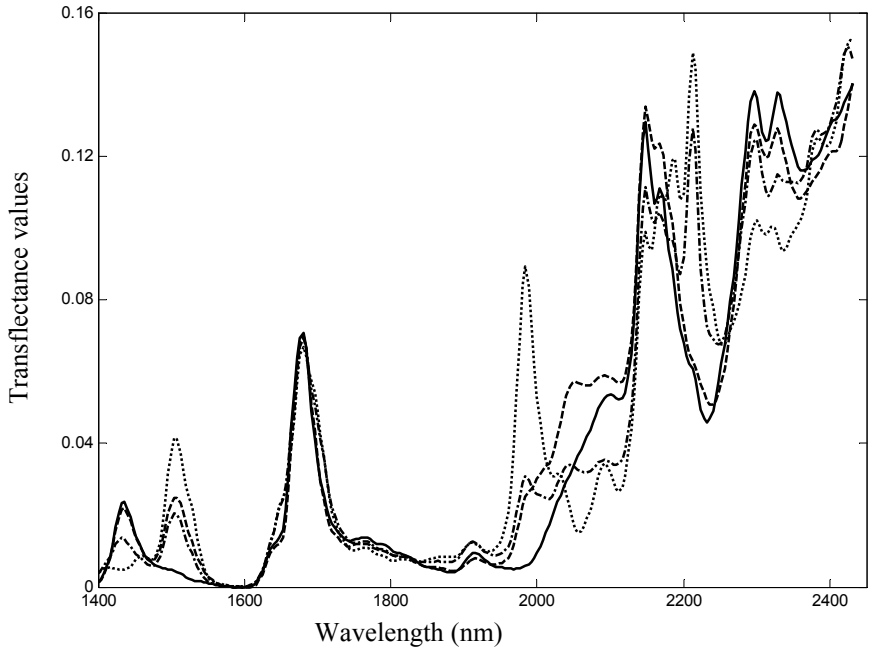

Fig. 3. Selected spectra by SIMPLISMA for the augmented column-wise data matrix. Solid line: spectrum Nº 136, dotted line: spectrum Nº 374, dashed line: spectrum Nº 420, dash-dot line: spectrum Nº 33.

Spectrum 420, the last spectrum of experiment 1:1, was a good estimate of the

reaction intermediate (see Fig. 3). The spectrum showed that the band corresponding to theepoxy group disappeared and the peak at 1978 nm that characterizes the aniline also practically disappeared. Spectrum 33 was selected from experiment 2:1, in which the ratio of PGE was larger than in the other experiments. Although bands other than those that are characteristic of PGE appeared in the spectrum, we can see that the band that characterizes the primary amine is not particularly intense and that in the time before spectrum 33 (160 min), the contribution of the tertiary amine to the spectrum could be considered to be negligible. These spectra were used as an initial estimate for a first ALS optimization, which led to another set of four spectra. The recovered spectra that estimated the reagents were discarded and replaced by the corresponding pure spectra. This new set of spectra made a better initial estimate, which was used to begin the MCR-ALS iteration. The spectra of the pure reagents constituted the only additional information supplied to carry out the optimization.

The process incorporated the constraints mentioned in section 3.3.4 and produced the following matrices: matrix **C** (420 x 4), which contained the concentration profiles for the four compounds that intervened in the reaction for each of the five experimental situations; and matrix $\mathbf{S}^T$ (4 x 259), which consisted of the spectra recovered for each of the four species that formed a single spectral matrix for the five experimental situations. The concentration profiles obtained satisfactorily reproduced the molar ratio that was initially used in each experiment (Fig. 4 a-e).

It is clear that for the first 200 minutes of reaction, the variations in PGE and aniline were similar and the concentration of these reactants decreased in a practically parallel fashion. Once the aniline was consumed, the variation in PGE entered into a second stage and the decrease was less pronounced. In experiment 2:1, it is clear that the PGE evolved in a similar way to the secondary amine.

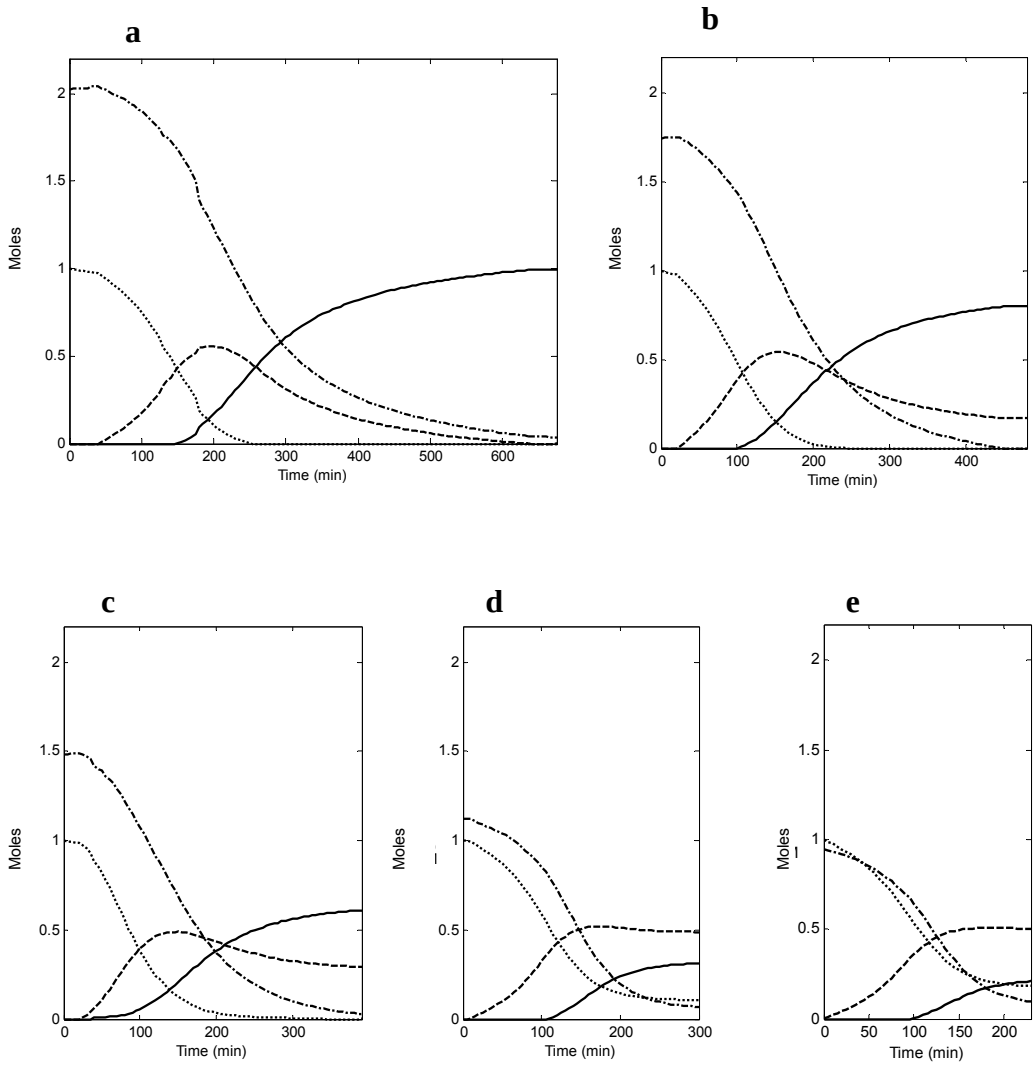

Fig. 4. Concentration profiles for the different PGE/Aniline molar ratios a) 2:1, b) 1.75:1, c) 1.5:1, d) 1.25:1 and e) 1:1. Aniline (dotted line), PGE (dash-dot line), secondary amine (dashed line) and tertiary amine (solid line).

From the moment that the aniline was totally reacted, in experiments 2:1, 1.75:1 and 1.5:1 we can see that the variation in the tertiary amine profile was the same but opposite to that of the secondary amine since, as in the second stage of the reaction, the secondary amine was consumed as the tertiary amine was produced. This is not seen so clearly in experiments 1.25:1 and 1:1 because the aniline was not totally consumed. In experiment 2:1, the final value for the tertiary amine was the one predicted by the stoichiometry of the reaction. One aspect to be improved is that the PGE profile should show that this species has been totally consumed by the end of each experiment.

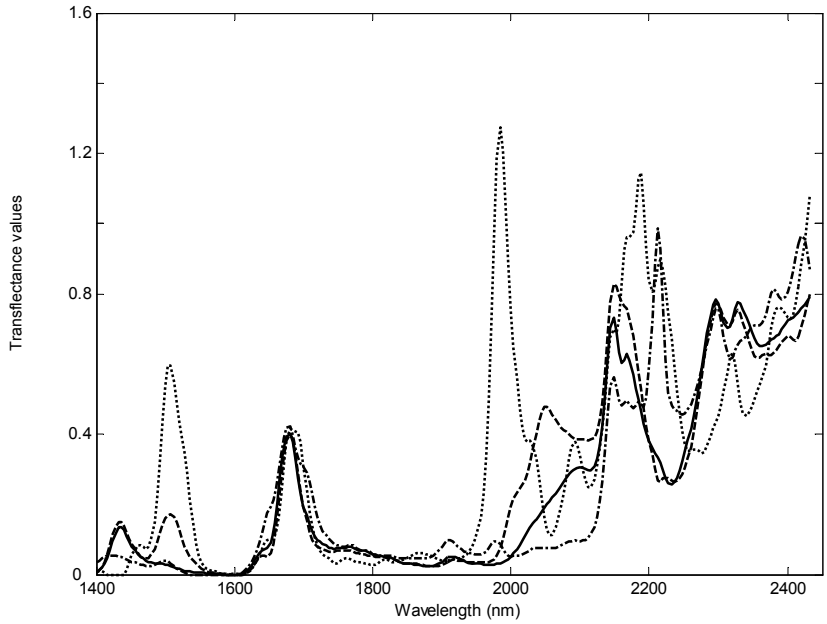

Fig. 5. Recovered spectra relative to aniline (dotted line), PGE (dash-dot line), secondary amine (dashed line) and tertiary amine (solid line).

Matrix $\mathbf{S}^T$ contained the spectra recovered after the process of MCR-ALS optimization (Fig. 5) and the characteristic spectral bands of each compound can be

assigned in the same way as in the previous study [14]. The spectral profiles were evaluated quantitatively with Eq. (2). The similarity coefficient r was calculated and the values obtained were 0.998 for PGE, 0.994 for aniline and 0.999 for the tertiary amine. The recovered spectrum of the tertiary amine was compared with the last spectrum of the experiment in which the PGE/aniline molar ratio was 2:1, because it was assumed that the reaction was finished.

The similarity between the recovered and the pure spectra was high in all cases, although a little less for aniline. This suggested that the recovered spectrum of the secondary amine was similar to the real spectrum.

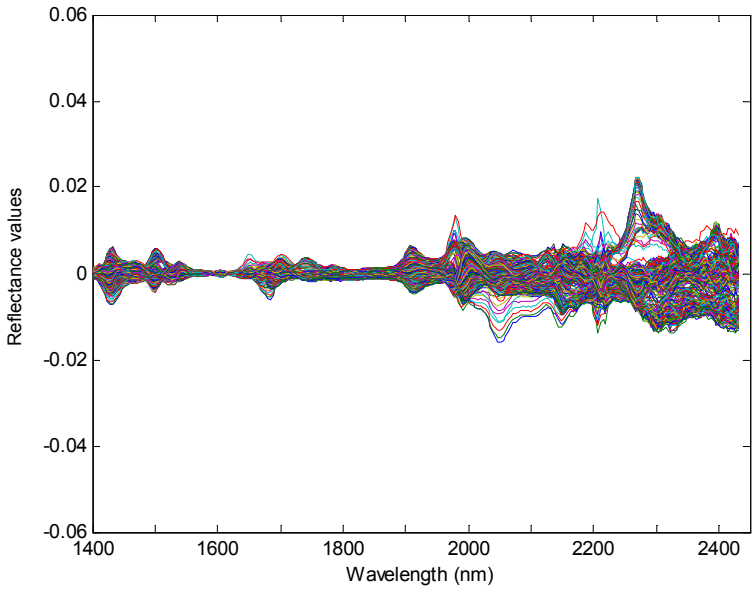

Fig. 6. Spectral residuals plot obtained after the ALS adjustment.

In accordance with Eq. (3), the product of the spectral and concentration profiles expressed 99.99% of the variance associated to the augmented data matrix. Another of the

parameters that was used to evaluate the fit was the percentage of lack of fit (Eq. (4)), which had a value of 0.88%. This indicated that, although this parameter provided a global measure of the residual, most of the variability in the experimental data was represented in the product $\mathbf{C}\cdot\mathbf{S}^T$. Fig. 6 shows the distribution of the residuals throughout the range of wavelengths that was considered. The magnitude of these residuals was comparable with the experimental error in NIR reflectance measurements. This matched the values obtained for the percentage of *lof* and for the percentage of explained variance.

5. Conclusions

Curve-resolution methods, especially MCR-ALS, are good for carrying out quantitative studies of curing reactions of epoxy resins using NIR spectroscopy.

Rank deficiency in this type of experimental data has been successfully resolved by applying the strategy proposed by Amrhein et al.

Results of studies using SIMPLISMA to obtain the initial estimate of the ALS algorithm satisfactorily describe the evolution over time of the species involved in the chemical reaction. These studies also produce an estimate for the spectrum of the intermediate compound in the reaction that is impossible to obtain with instrumental methods.

It should be stressed that it is important to obtain the individual concentration profiles of each species, especially the ones that correspond to the reactants (PGE and aniline) because they are linearly dependent at all times.

As rotational and intensity ambiguities exist, it may be supposed that the solution found is one of a number of possible solutions, despite the restrictions imposed on the system. Finding the unique solution may involve other techniques such as the combination of hard-modelling and soft-modelling strategies.

6. Acknowledgements

We would like to thank Romà Tauler, from the University of Barcelona, and Virginia Cádiz and Marina Galià from the Area of Organic Chemistry of the Rovira i Virgili University, for their collaboration in the preparation of this paper. Likewise, we would like to acknowledge the economic suport provided by the MCyT (project Nº BQU 2000-1256).

References

[1] J. Mijovic and S. Andjelic, Macromolecules 28, (1995), 2787-2796.

[2] K. Dean, W. Cook, L. Rey, J. Galy and H. Sautereau, Macromolecules 34, (2001), 6623-6630.

[3] C. Billaud, M. Vandeuren, R. Legras and V. Carlier, Appl. Spectrosc. 56, (2002), 1413-1421.

[4] D. Hill, G. George and D. Rogers, Polym. Adv. Technol. 13, (2002), 353-362.

[5] R. Tauler, A. Izquierdo-Ridorsa and E. Casassas, Chemom. Intell. Lab. Syst. 18, (1993), 293-300.

[6] A. Izquierdo-Ridorsa, J. Saurina, S. Hernández-Cassou and R. Tauler. Chemom. Intell. Lab. Syst. 38, (1997), 183-196.

[7] A. Cladera, E. Gomez, J. M. Estela and V. Cerdà, Anal. Chem. 65, (1993), 707-715.

[8] M. Gui, S. C. Rutan and A. Agbodjan, Anal Chem. 67, (1995), 3293-3299.

[9] J. Saurina, S. Hernández-Cassou and R. Tauler, Anal Chem 69, (1997), 2329-2336.

[10] M. Amrhein, B. Srinivasan, D. Bonvin and M. M. Schumacher, Chemom. Intell. Lab. Syst. 46, (1999), 249-264.

[11] A. K. Smilde, Y. Wang and B. R. Kowalsky, J. Chemometrics 8, (1994), 21-36.

[12] P. J. Gemperline, K. H. Miller, T. L. West, J. E. Weinsteim, J. G. Hamilton and J. T. Bray, Anal. Chem. 64, (1992), 523A-532A.

[13] R. Tauler, A. Smilde and R. Kowalsky, J. Chemometrics 9, (1995), 31-58.

[14] M. S. Larrechi and F. X. Rius, Appl. Spectrosc. 58, (2004), 47-53.

[15] J. Mijovic, A. Fishbain and J. Wijaya, Macromolecules 25, (1992), 979-985.

[16] E. R. Malinowski, Factor Analysis in Chemistry ,3rd Edn., Wiley, New York, 2002.

[17] M. Amrhein, B. Srinivasan, D. Bonvin and M. M. Schumacher, Chemom. Intell. Lab. Syst. 33, (1996), 17-33.

[18] J. Saurina, S. Hernández-Cassou, R. Tauler and A. Izquierdo-Ridorsa, J. Chemometrics 12, (1998), 183-203.

[19] L. Matějka and K. Dušek, J. Polym. Sci. Part A: Polym. Chem. 33, (1995), 461-472.

[20] W. Windig and J. Guilment, Anal Chem. 63, (1991), 1425-1432.

[21] C.A. May, Epoxy resins:chemistry and technology, Marcel Dekker, New York, 1988, pp.293-305.

[22] The Mathworks, MATLAB Version 6.5, Natick, MA, 2002.

[23] The Mathworks, Optimization Toolbox, 2.0 version, Natick, MA, 1998.

[24] J.J. Kelly, C. H. Barlow, T. M. Jinguji and J. B. Callis, Anal. Chem. 61, (1989), 313-320.

[25] D. L. Massart, B. Vandeginste, L. Buydens, S. de Jong, P. Lewi and J. Smeyers-Verbeke, Handbook of Chemometrics and Qualimetrics : Part A, Elsevier, Amsterdam, 1997.

4.3 Integration of Near infrared spectroscopy and ^{13}C-NMR with Multivariate Curve Resolution-Alternating Least Squares for monitoring epoxy resins reactions

submitted

M. Garrido, M.S. Larrechi and F.X. Rius*

Department of Analytical and Organic Chemistry, Faculty of Chemistry, Rovira i Virgili University, Marcel·lí Domingo s/n (43007), Tarragona, Spain

Summary

This paper describes how data from two instrumental techniques─near infrared spectroscopy and ^{13}C nuclear magnetic resonance─are combined by means of Multivariate Curve Resolution-Alternating Least Squares to obtain concentration and spectral profiles for the reaction between phenylglycidylether and aniline. The reaction, in stoichiometric proportions, was monitored by both spectroscopic techniques at 95 ºC. The concentration values obtained by ^{13}C nuclear magnetic resonance were used as an equality constraint during the multivariate curve resolution of the near infrared data. The results obtained were recovered without ambiguities: that is to say, there was a unique solution. The goodness of the results was tested by comparing the recovered concentration profiles with the values obtained by high performance liquid chromatography as a reference technique. The statistical tests showed that there were no significant differences between the results of both methods (α = 5%). Also, the recovered spectra were compared with the experimentally recorded spectra for the reagents (i.e. phenylglycidylether and aniline) and the final product and the correlation coefficients were, in all cases, higher than 0.998.

1. Introduction

Near infrared spectroscopy (NIR) in combination with multivariate curve resolution methods has demonstrated to be a useful technique in many analytical applications due to the combination of an instrumental technique that incorporates an easy-to-obtain analytical signal with a powerful chemometric technique that can achieve the necessary spectral resolution [1-4]. Soft-modelling methods, in particular the Multivariate Curve Resolution-Alternating Least Squares method (MCR-ALS), have great potential when applied to spectroscopic data obtained from monitoring a chemical reaction, so the concentration profiles of each species involved in the reaction and the corresponding pure spectra can be estimated [5-7]. However, the presence of rotational and intensity ambiguities [8] is a characteristic problem in factor analysis decompositions of some bilinear data matrices and makes it difficult to obtain unique solutions. Instead of unique solutions, a band of feasible solutions are obtained that fit the experimental data equally well. The number of feasible solutions can be drastically reduced when constraints, which are inherent to and characteristic of the chemical system being studied, are applied to estimate concentration and spectra profiles (e. g. non-negativity, closure and unimodality constraints) [9,10]. Other constraints related to selectivity in concentration or spectral regions [8] and knowledge of local rank conditions [11] make it possible to obtain solutions that are nearly unique or totally eliminate the ambiguities. In addition, when the concentration and/or spectral profiles (totally or partially) are known for some of the species, they can be used as an equality constraint (i.e. the known values are set to be invariant during the iterative process) [12].

Unfortunately, in data matrices obtained from the spectroscopic monitoring of chemical reactions, knowledge of local rank conditions and selectivity regions are not usually expected. Furthermore, the spectral profiles of the reactants may usually be available for use as an equality constraint, but it is not always possible to have the spectra

of the intermediate or final products. It is also uncommon to know how the concentration of some of the species evolves over time.

In some circumstances, a complementary technique of analysis can provide supplementary information that helps to resolve the system being studied successfully. Multivariate curve resolution has been used to combine such spectroscopic techniques as fluorescence and circular dichroism [13], near infrared and mid infrared [4], and mass spectrometry and circular dichroism [14]. It also makes it possible to combine UV-Vis and near infrared with calorimetric techniques [15,16].

This study uses multivariate curve resolution methods to combine the information supplied by two spectroscopic techniques─near infrared spectroscopy and ^{13}C nuclear magnetic resonance (^{13}C NMR)─when they are used to monitor an epoxy resin reaction. NMR has several advantages that make it suitable for monitoring reactions involving organic compounds: it is rapid, requires small amounts of sample and provides structural information of the investigated compounds because of the high selectivity of the signals. NMR spectroscopy has been used to characterize epoxy resins [17-20], usually to analyze either the final product structure or the influence of the molecular structure on the physical relaxations of the epoxy resin systems. However, to our knowledge, it has never been used to study the changes in the concentration of the species throughout the reaction process. Specially, ^{13}C NMR presents a relatively simple pattern of signals that are hardly affected by the solvents used [20]. However, quantitative analysis may be unreliable due to the fact that the relaxation time for some atoms is long. Therefore, it is not always possible to obtain quantitative information about all the species.

Other techniques, such as HPLC, have been used to obtain quantitative individual information about the evolution of each species in epoxy resins, but these procedures are usually laborious and time-consuming [21,22].

In the present paper, MCR-ALS has been applied to the near infrared data obtained from the on-line monitoring of the reaction between phenylglycidylether and aniline at 95 ºC, in order to obtain the corresponding spectral and concentration profiles. The resolution was improved by imposing an equality constraint, which consisted of the concentration values for some of the species involved in the reaction, obtained by at-line monitoring of the reaction using ^{13}C NMR. To the best of our knowledge, no studies have been published on the use of ^{13}C NMR for the quantitative monitoring of epoxy resins reactions.

In order to verify the validity of the concentration profiles obtained, the recovered spectra were compared with the recorded near infrared spectra of both the reactants (phenylglycidylether and aniline) and the final product of the reaction, in terms of correlation coefficient. The reaction was also monitored by High Performance Liquid Chromatography (HPLC) and the results obtained were compared to those obtained by the NIR/NMR and MCR-ALS procedure.

2. Experimental

The reactions that take place between PGE and aniline are depicted in Scheme 1. Primary amine reacts with the epoxide to form a secondary amine and, in a further reaction, the secondary amine reacts with epoxide to form a tertiary amine. The experimental procedure for the reaction involved mixing the necessary amounts of aniline (Aldrich, distilled before using it) and PGE (Aldrich) at room temperature to obtain a molar ratio of 2.1. The reaction was carried out at 95 ºC and the epoxide concentration was not in excess to ensure that the reactions being studied were the only ones taking place and that there was no collateral etherification or homopolymerization reaction [21,23].

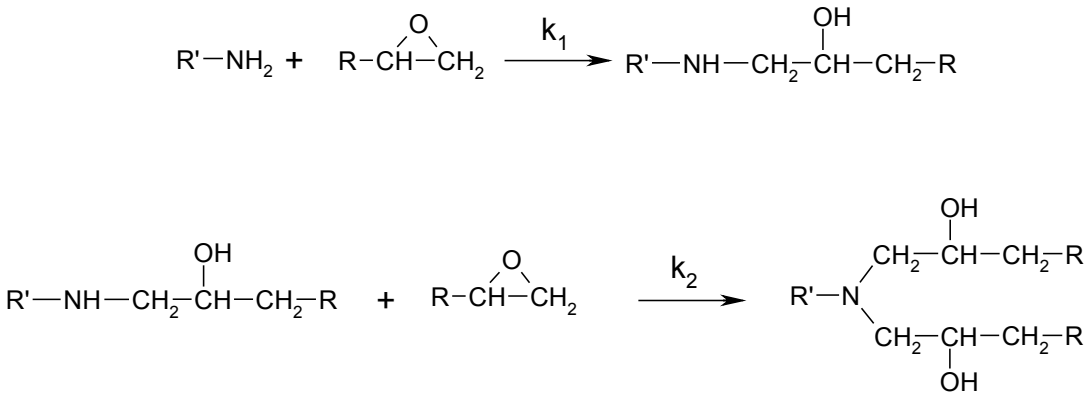

Scheme 1. Chemical reaction between phenylglycidylether (PGE) and aniline.

2.1 NIR monitoring

Typically, 1 mL of the reacting mixture was injected into the cell for liquids of the NIR spectrophotometer. The cell temperature was set at 95ºC. The NIR spectra were recorded throughout the reaction every 4 nm, between 1100 and 2500 nm with an InfraAlizer 500 spectrophotometer from Bran-Luebbe. For each experiment, we automatically acquired data at intervals of 5 minutes until the end of the reaction. The reaction was considered to be complete when no change was observed in the spectra throughout the time. NIR spectra of the pure reactants (aniline and PGE) were also recorded in the same experimental conditions. The recorded spectra were exported and converted into MATLAB binary files [24].

2.2 ^{13}C NMR analysis

The reaction was carried out under stoichiometric proportions (*i.e.* PGE/aniline molar ratio of 2:1) in a thermostatic bath (PolyScience, USA) at 95 ± 0.2 ºC, and the temperature of the reacting mixture was controlled with an immersion probe thermometer (Crison). Eighteen samples of the reacting mixture (about 150 mg) were withdrawn at different reaction times and immediately dissolved with $CDCl_3$. They were then kept at 20ºC. In this way, the reaction can be considered to have stopped. A chronometer was used to synchronize the sampling in the ^{13}C NMR experiment with the NIR measurements. ^{13}C NMR spectra of the samples were recorded at room temperature at 75.4 M Hz in a Varian Gemini 300 NMR spectrometer with proton noise decoupling.

In order to quantitatively integrate the signals, the NMR spectra were acquired using inverse-gated decoupling and a relaxation time delay of about $5T_1$. This value (T_1) was the relaxation time of the carbons located in the *para* position with respect to the ether group of the PGE, which was used as the reference signal (see Fig. 1, signal 7). It was the slowest relaxing nucleus of all the signals used in the quantification.

Relative quantification was carried out using the invariable signal of the reference carbon and assuming that, in all spectra, this signal had a concentration of 5.09 mol kg^{-1} (of the amount of PGE that was initially present in the 2:1 PGE/aniline reacting mixture).

2.3 High Performance Liquid Chromatography

For monitoring by HPLC, the reaction was carried out under stoichiometric proportions (i.e. PGE/aniline molar ratio of 2:1) in a thermostatic bath (PolyScience, USA) at 95 ± 0.2 ºC. The temperature of the reacting mixture was controlled with an immersion probe thermometer (Crison).

The chromatographic separation was performed by reversed-phase HPLC using a Hewlett Packard series 1100 chromatographic system with a UV detector set at 254 nm to monitor the eluted species. The samples (nineteen samples withdrawn from the reacting mixture at different times, analyzed in triplicate) were prepared by weighing 10-25 mg of reacting mixture and dissolving them with methanol to 10 mL. Aliquots of this solution (20 μL) were injected into an analytical Hypersil ODS reverse-phase column (5 μm particle size), 200 mm x 4.6 mm i.d. (Agilent Technologies). The temperature of the column was kept at 20 ºC. HPLC analyses were carried out by gradient elution of the methanol-water system (both HPLC grade solvents from SDS) with a flow rate of 1.75 mL min^{-1}. The gradient ranged from 20% to 100% of methanol within 10 min.

The concentration of the species under study was calculated from the peak areas using the calibration curves of pure compounds. PGE and aniline were commercially available. The secondary amine product was prepared by reacting PGE with excess aniline (1:10 molar ratio) at 80 ºC for 12 h. The excess aniline was distilled off under reduced pressure. Tertiary amine was obtained from the stoichiometric mixture (i.e. PGE/aniline 2:1) reacted at 120 ºC for 20 h. The standard solutions for the calibration curves were made in triplicate and tood into account the range of concentration of each species throughout the process. The areas of the chromatographic peaks had a linear relationship with respect to the concentration of the species in the mobile phase.

2.4 MCR-ALS optimization

In order to eliminate the vertical shift caused by using a NIR spectrophotometer with only one light beam, all the spectra were pretreated with an *off-set* correction [25]. The wavelengths of interest were selected and those in which no variation over time was observed were ignored because they provided no information about the reaction under

study. The regions of the spectrum in which only noise was detected were also eliminated. The pretreated spectra were arranged in an experimental data matrix **D**.

Rank analysis was performed by singular value decomposition (SVD) [26]. In order to overcome the rank deficiency of matrix **D**, a column-wise augmented matrix **M** was built with experimental data matrix **D** and the NIR spectra recorded for PGE and aniline (i.e. the reactants). The initial estimate for the ALS algorithm was constructed using SIMPLISMA [27] as mentioned elsewhere [28].

The MCR-ALS optimization was carried out under the following constraints: non-negativity for both the spectral and the concentration profiles, unimodality for the concentration profiles and closure constraints for the concentration profiles. Likewise, an equality constraint was applied for the concentration profiles, by imposing that some concentration values, known by ^{13}C NMR for certain reaction times, were fixed at each step of the optimization process.

3. Results and Discussion

As can be seen in Scheme 1, four sources of variability were expected, one for each of the four species involved in the reaction: PGE, aniline, the secondary amine and the tertiary amine. Rank analysis of matrix **D** showed that only three significant contributions were present. In order to eliminate this rank deficiency, the column-wise augmented matrix **M** was built by adding the row vectors corresponding to the spectra of the reactants (i.e. PGE and aniline) to the experimental data matrix **D**. In this way, the rank deficiency was broken because the rank of the new matrix matched the number of absorbing species.

After the rank deficiency had been overcome, MCR-ALS was applied to augmented matrix **M**. When only non-negativity, unimodality and closure constraints were implemented, the results obtained were strongly affected by the intensity and rotational ambiguities and. Therefore, a set of feasible solutions was obtained, as has been discussed in a previous article [7]. In order to minimize or totally eliminate the ambiguities, more forceful constraints are needed. External knowledge, consisting of the spectra of the reactants, was fixed throughout the iteration process, but it was not effective at diminishing the ambiguities and the results were approximately the same when this constraint was not applied.

Fig. 1 shows, as an example, the ^{13}C NMR spectra for the reaction between PGE and aniline at three different times. The signals were assigned in accordance with the spectra reported in the literature for the same reaction [17,20]. Fig. 1 a) shows the spectrum obtained at the beginning of the reaction, when PGE and aniline have still not significantly reacted. When the secondary amine starts to form, new signals are detected (Fig. 1b)) but by the end of the reaction they had totally disappeared (Fig. 1 c)), and the tertiary amine had formed almost completely.

The evolution of PGE was monitored by two signals, 1 and 2. The secondary amine was monitored through the signals 22 and 23 and the tertiary amine was monitored through signals 25, 26 and 27 (see Fig. 1). The 25, 26 and 27 carbons led to double peaks because of the different stereoisomeric forms of the tertiary amine. The tertiary amine consists of a mixture of RR, RS and SS stereoisomers at a molar ratio of 1:2:1. The RR and SS isomers produce the same NMR spectra, which are different from those produced by the RS isomer. Therefore, Fig. 1 c) shows two signals of similar intensities in several carbons of the tertiary amine [20]. This indicates that the reaction is not steroeselective. So, to calculate the concentration vales of the tertiary amine, the signals of the L, M and N carbons were added together.

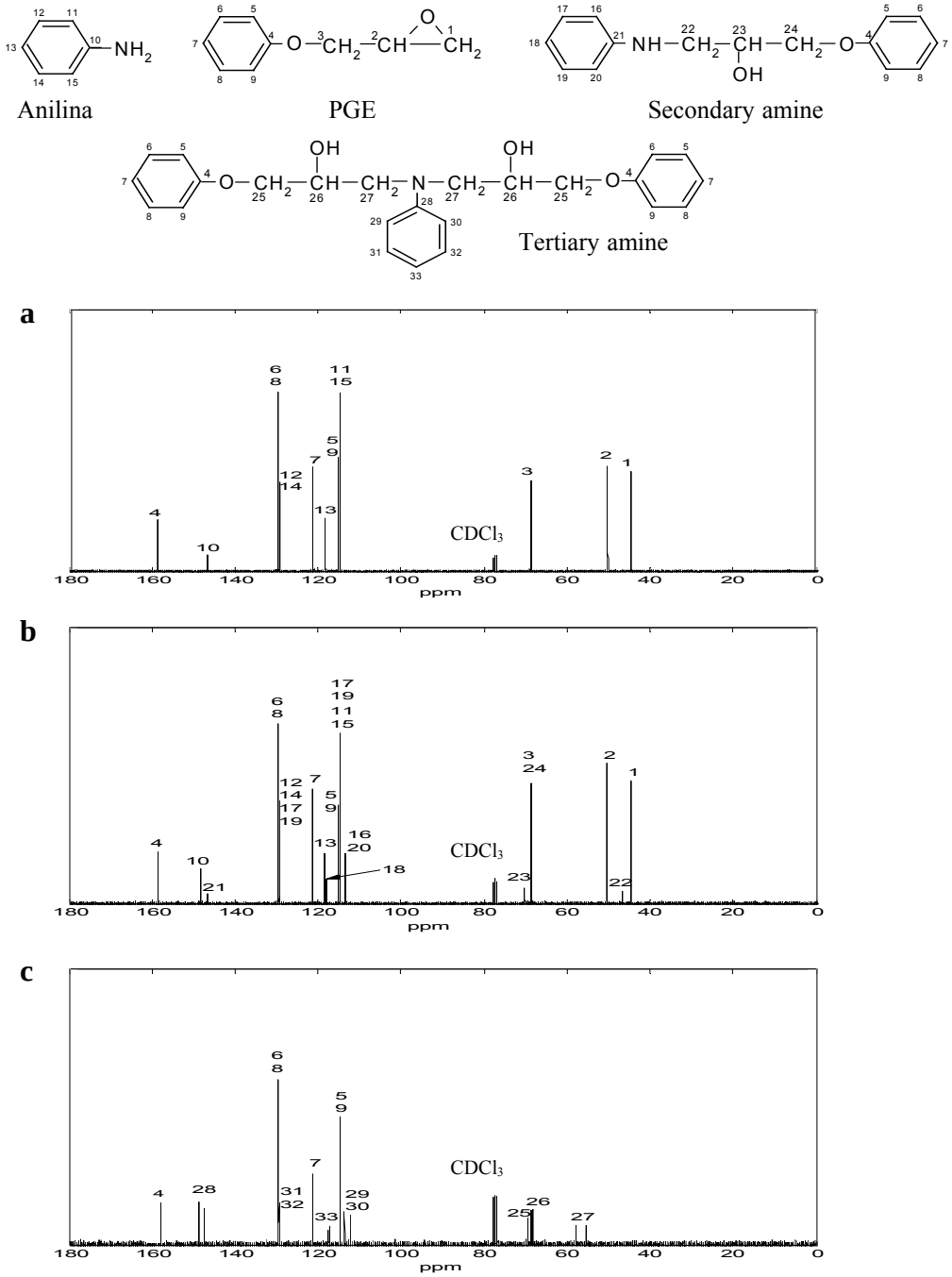

Fig. 1. ^{13}C NMR spectra of the reacting mixture at different reaction times a) 0 min, b) 45 min and c) 675 min. The numbers corresponding to the signals have been assigned to the different carbon atoms in the upper part of the figure.

Signals 10 to 15 could be useful for monitoring aniline, but their relaxation times are so long that the quantitative results would not be trustworthy (relaxation times > 5 s). Therefore, ^{13}C NMR can reliably monitor only the profiles for PGE, the secondary amine and the tertiary amine.

New external information provided by ^{13}C NMR consisted of eighteen concentration values corresponding to the quantified species (i.e. PGE, the secondary amine and the tertiary amine) at different reaction times. These values were fixed and imposed as an equality constraint during the MCR-ALS optimization.

The spectra of the four species after MCR-ALS had been applied are shown in Fig. 2. The goodness of the spectral profiles was evaluated by calculating the similarity coefficients [28] between the recovered spectra and the spectra recorded for the reactants (i.e. PGE and aniline), respectively. The values were 0.9986 for the PGE and 0.9999 for the aniline. In the same way, the recovered spectrum for the tertiary amine was compared with the last spectrum recorded for the reacting system, assuming that the conversion was almost 100 %. The similarity coefficient for the tertiary amine was 0.9999. The similarity coefficient was high in all cases, which suggests that the recovered spectrum of the secondary amine was similar to its real spectrum. When the equality constraint (based on the NMR known concentration values) was not used, the correlation coefficients were worse.

The concentration profile of each species, recovered in % w/w, was divided by the corresponding molecular weight in order to express the concentrations in mol kg^{-1} (see Fig. 3). The initial concentration values corresponded well to the molar ratio used in the reaction (PGE/aniline molar ratio of 2:1). Likewise, the concentration of the tertiary amine at the end of the reaction reached the value predicted by the stoichiometry.

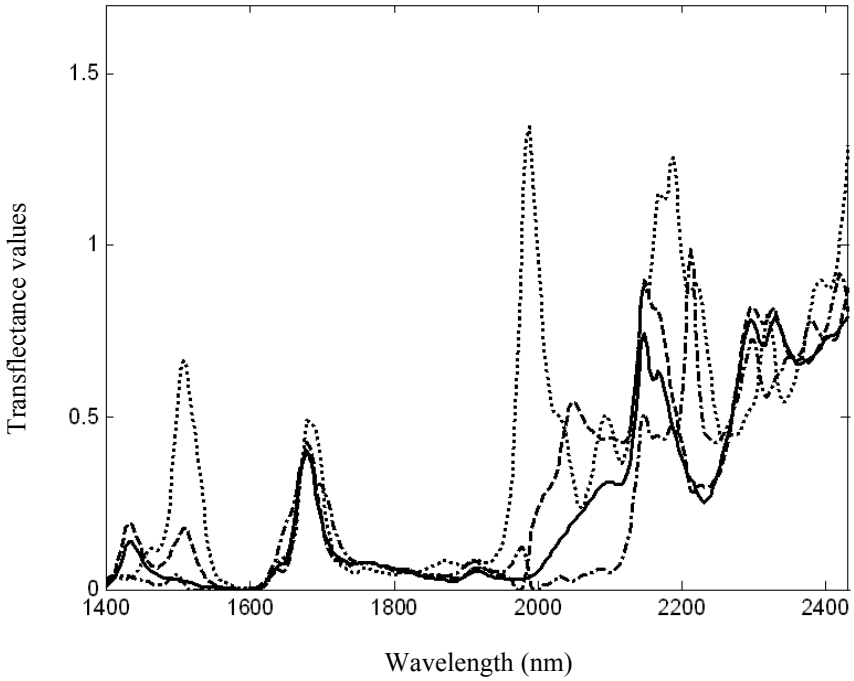

Fig. 2. Spectra recovered by MCR-ALS: aniline (dotted line), PGE (dash-dot line), secondary amine (dashed line) and tertiary amine (solid line).

Fig. 3 shows that PGE was not totally consumed, contrary to what was expected at the end of the experiment. One possible explanation for this is that the NIR spectra for each experiment were recorded until the band corresponding to the oxirane group (2208 nm) disappeared. At this point, the reaction is considered to have finished. The NIR spectra may show that the band disappears at 2208 nm, but the reaction has not really stopped, and a small quantity of epoxide has still not reacted.

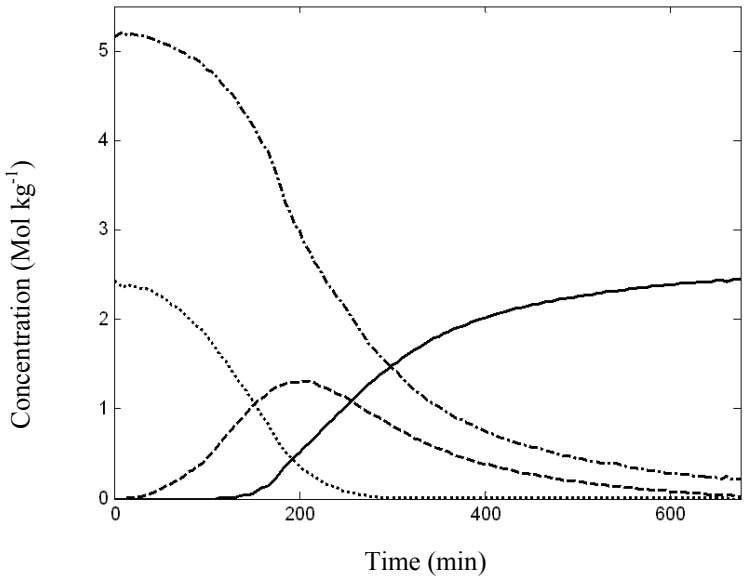

Fig. 3. Concentration profiles recovered by MCR-ALS: Aniline (dotted line), PGE (dash-dot line), secondary amine (dashed line) and tertiary amine (solid line).

This clearly indicates the disadvantages of using a univariate approach for the near infrared monitoring of this kind of reaction since, in the last stages of the reaction it is difficult to say when a band has totally disappeared. Likewise, when a band has nearly disappeared, it is not easy to integrate its area to quantify the extent of the reaction.

Known concentration values were used as a constraint during the ALS optimization process and, even though only a few of them were available and they corresponded to only three of the four species involved, unique solutions were obtained both for the concentration and the spectral profiles.

In order to further assess the validity of the results obtained by MCR-ALS, the recovered concentration profiles were compared with the concentration values obtained by

HPLC (see Fig. 4). A preliminary visual inspection made it possible to conclude that there is a good correspondence between the MCR-ALS concentration profiles and those obtained by liquid chromatography. However, the equivalence between data needs to be quantified.

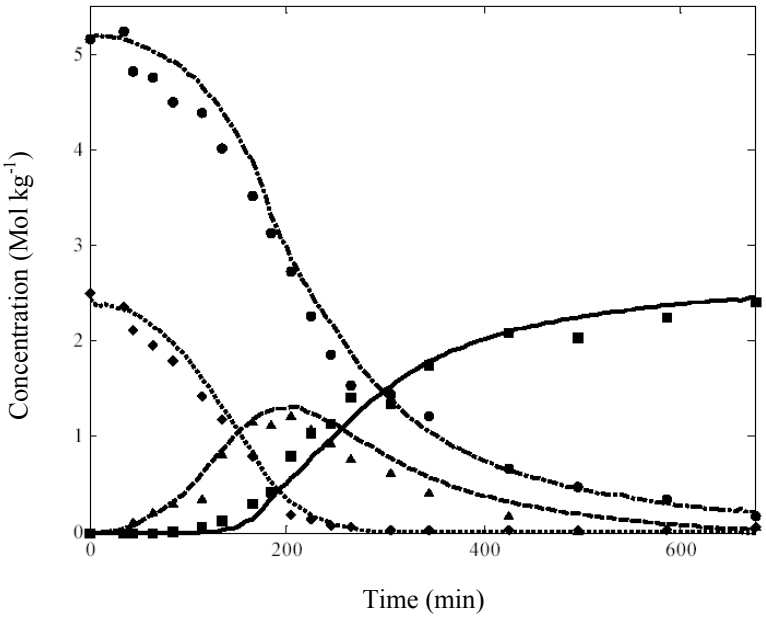

Fig. 4. Superposition of the concentration profiles recovered by MCR-ALS and the experimental values obtained by HPLC for the reaction between PGE and aniline (molar ratio of 2:1). For the MCR-ALS concentration profiles: aniline (dotted line), PGE (dash-dot line), secondary amine (dashed line) and tertiary amine (solid line). HPLC experimentally determined results: (♦) aniline, (●) PGE, (▲) secondary amine and (■) tertiary amine.

Since the evolution of the species is related to one another by the underlying mass balance, the concentration profiles were jointly analyzed for the four species. When the

concentrations recovered by MCR-ALS were plotted vs. the concentrations recovered byHPLC, a straight regression line was obtained, with a slope near to 1 and an intercept near to 0 (y = 0.99x - 0.02). The qualitative similarity between the profiles obtained by both methods was evaluated in terms of the correlation coefficient of this straight line. The value obtained was 0.998.

The statistical joint interval test of slope and intercept was used to test for the presence of bias [29]. The results show that there are no significant differences between the concentration profiles obtained by the two techniques (α = 5%).

4. Conclusions

Combining the results of two spectroscopic techniques─near infrared and ^{13}C nuclear magnetic resonance─ by means of Multivariate Curve Resolution-Alternating Least Squares led to spectral and concentration profiles that adequately described the species studied and their evolution over time. Furthermore, the concentrations obtained by ^{13}C NMR for some of the species involved in the reaction at a given reaction time were used as equality constraint, which made it possible to obtain unique solutions for both concentration and spectral profiles.

The validation process showed that the recovered concentration profiles were not significantly different from the values of concentration obtained by HPLC used as a reference technique (α = 5%). On the other hand, the recovered spectra showed high similarity coefficients (>0.998) when they were compared with the spectra of the experimentally recorded pure compounds.

Although the proposed strategy involves using a complementary spectroscopic technique to achieve results free of ambiguities, the concentrations obtained by ^{13}C NMR are easily determined and effortlessly incorporated as an equality constraint into the MCR-ALS algorithm, which mean that this method is a satisfactory tool for monitoring epoxy resins reactions.

Acknowledgements

The authors acknowledge economic support from the MCyT (project nº BQU2003-1142).

References

[1] Puxty G, Maeder M, Radack HP, Gemperline PJ. Equilibrium modeling of mixtures of methanol and water. *Appl. Spectrosc.* 2005; **59**:329-334.

[2] Czarnik-Matusewics B, Pilorz S, Hawranek JP. Temperature-dependent water structural transitions examined by near-IR and mid-IR spectra analyzed by multivariate curve resolution and two-dimensional correlation spectroscopy. *Anal. Chim. Acta* 2005; **544**:15-25.

[3] Blanco M, Alcala M, González JM, Torras E. Near infrared spectroscopy in the study of polymorphic transformations. *Anal. Chim. Acta* 2006; **567**:262-268.

[4] Navea S, de Juan A, Tauler R. Modeling Temperature-Dependent Protein Structural Transitions by Combined Near-IR and Mid-IR Spectroscopies and Multivariate Curve Resolution. *Anal. Chem.* 2006; **75**:5592-5601.

[5] Tauler R, Izquierdo-Ridorsa A, Casassas E. Simultaneous analysis of several spectroscopic titrations with self-modeling curve resolution. *Chemom. Intell. Lab. Syst.* 1993; **18**:293-300.

[6] Izquierdo-Ridorsa A, Saurina J, Hernandez-Cassou S, Tauler R. Second-order multivariate curve resolution applied to rank-deficient data obtained from acid-base spectrophotometric titrations of mixtures of nucleic bases. *Chemom. Intell. Lab. Syst.* 1997; **38**:183-196.

[7] Larrechi MS, Rius FX. Spectra and concentration profiles throughout the reaction of curing epoxy resins from near-infrared spectroscopy and multivariate curve resolution methods. *Appl. Spectrosc.* 2004; **58**:47-53.

[8] Tauler R, Smilde A, Kowalski B. Selectivity, local rank, 3-way data-analysis and ambiguity in multivariate curve resolution. *J. Chemometrics* 1995; **9**:31-58.

[9] Gargallo R, Tauler R, Cuesta-Sanchez F, Massart DL. Validation of alternating least-squares multivariate curve resolution for chromatographic resolution and quantitation. *Trends Anal. Chem.* 1996; **15**:279-286.

[10] de Juan A, Vander Heyden Y, Tauler R, Massart DL. Assessment of new constraints applied to the alternating least squares method. *Anal. Chim. Acta* 1997; **346**:307-318.

[11] Manne R, On the resolution problem in hyphenated chromatography. *Chemom. Intell. Lab. Syst.* 1995; **27**:89-94.

[12] de Juan A, Tauler R. Chemometrics applied to unravel multicomponent processes and mixtures - Revisiting latest trends in multivariate resolution. *Anal. Chim. Acta* 2003; **500**:195-210.

[13] Navea S, de Juan A, Tauler R. Detection and Resolution of Intermediate Species in Protein Folding Processes Using Fluorescence and Circular Dichroism Spectroscopies and Multivariate Curve Resolution. *Anal. Chem.* 2002; **74**:6031-6039.

[14] Navea S, Tauler R, de Juan A. Monitoring and Modeling of Protein Processes Using Mass Spectrometry, Circular Dichroism, and Multivariate Curve Resolution Methods. *Anal. Chem.* 2006; **78**:4768-4778.

[15] Zogg A, Fischer U, Hungerbühler K. A new approach for a combined evaluation of calorimetric and online infrared data to identify kinetic and thermodynamic parameters of a chemical reaction. *Chemom. Intell. Lab. Syst.* 2004; **71**:165-176.

[16] Ma B, Gemperline PJ, Cash E, Bosserman M, Comas E. Characterizing batch reactions with in situ spectroscopic measurements, calorimetry and dynamic modeling. *J. Chemometrics* 2003; **17**:470-479.

[17] Jullien H, Petit A, Merienne C. The microwave reaction of phenyl glycidyl ether with aniline on inorganic supports: A model for the microwave crosslinking of epoxy resins. *Polymer* 1996; **37**:3319-3330.

[18] Oommen C, Amanulla S, Jain SR. Characterization of diglycidylamine epoxy resins based on bis-hydrazones. *Eur. Polym. J.* 2000; **36**:779-782.

[19] Xu K, Chen MC, Zhang K, Hu JW. Synthesis and characterization of novel epoxy resin bearing naphthyl and limonene moieties, and its cured polymer. *Polymer* 2004; **45**:1133-1140.

[20] Dyakonov T, Chen Y, Holland K, Drbohlav J, Burns D,Vander Velde D, Seib L, Soloski EJ, Kuhn J, Mann PJ, Stevenson WTK, Thermal analysis of some aromatic

amine cured model epoxy resin systems—I: Materials synthesis and characterization, cure and post-cure. *Polym. Degrad. Stabil.* 1996; **53**:217-242.

[21] Mijovic J, Fishbain A, Wijaya J. Mechanistic modeling of epoxy amine kinetics.1. Model-compound study. *Macromolecules* 1992; **25**:979-985.

[22] Swier S, Van Mele B. Mechanistic modeling of the reaction kinetics of phenyl glycidyl ether (PGE) plus aniline using heat flow and heat capacity profiles from modulated temperature DSC. *Termochim. Acta* 2004; **411**:149-169.

[23] May CA, *Epoxy Resins*, Marcel Dekker: New York, 1988.

[24] The Mathworks, MATLAB Version 6.5, Natick, MA, 2002.

[25] Kelly JJ, Barlow CH, Jinguji TM, Callis JB. Prediction of gasoline octane numbers from near-infrared spectral features in the range 660-1215 nm. *Anal. Chem.* 1989; **61**:313-320.

[26] Massart DL, Vandeginste BGM, Buydens LMC, de Jong S, Lewi PJ, Smeyers-Verbeke J, *Handbook of Chemometrics and Qualimetrics : Part A*. Elsevier: Amsterdam, 1997.

[27] Windig W, Guilment J. Interactive self-modeling mixture analysis. *Anal Chem.* 1991; **63**:1425-1432.

[28] Garrido M, Lazaro I, Larrechi MS, Rius FX. Multivariate resolution of rank-deficient near-infrared spectroscopy data from the reaction of curing epoxy resins using the rank augmentation strategy and multivariate curve resolution alternating least squares approach. *Anal. Chim. Acta* 2004; **515**:65-73.

[29] Riu J, Rius FX. Assessing the accuracy of analytical methods using linear regression with errors in both axes. *Anal. Chem.* 1996; **68**:1851-1857.

4.4 Calculation of band boundaries of feasible solutions obtained by Multivariate Curve Resolution-Alternating Least Squares of multiple runs of a reaction monitored by NIR spectroscopy

Chemometrics and Intelligent Laboratory Systems, 76, **2005**, 111-120

M. Garrido[a], M.S. Larrechi[a], F.X. Rius[a] and R. Tauler[b]*

[a] Department of Analytical and Organic Chemistry, Faculty of Chemistry, Rovira i Virgili University, Pl. Imperial Tàrraco, 1, 43005 Tarragona (Spain)
[b]Institute of Chemical and Environmental Research, CSIC, Jordi Girona 18-24, Barcelona 08034, Spain

(Received 1 September 2004; accepted 1 October 2004
Available online 6 November 2004)

Abstract

This study describes a method for calculating the band boundaries of feasible solutions for spectra and concentration profiles obtained by Multivariate Curve Resolution-Alternating Least Squares (MCR-ALS) analysis of a spectroscopic NIR data set. The data set is obtained by monitoring *in situ* the model reaction between phenyl glycidyl ether (PGE) and aniline. As this system happened to be rank-deficient, the resolution strategy used matrix augmentation. The calculation of band boundaries of feasible solutions is extended here to the simultaneous analysis of multiple data matrices. The boundaries were obtained by a non-linear constrained non-linear optimization. The influence that the

number and type of data matrices in the simultaneous analysis have on the amplitude of band boundaries is also discussed.

1. Introduction

Different soft-modelling methods have been proposed for resolving concentration and spectra profiles of the species present in complex unknown reaction network systems [1,2]. These soft modelling methods, such as the Multivariate Curve Resolution-Alternating Least Squares method (MCR-ALS) [3,4], do not need a chemical model to be previously postulated. When they are applied to bilinear spectroscopic data obtained from monitoring a chemical reaction, they make it possible to estimate the concentration profiles of each component in the reaction as well as the corresponding pure spectra [5]. This is only possible if rank deficiency problems [6] are not present or have been appropriately solved, as already discussed in the bibliography. [4,7].

The solutions obtained by MCR-ALS, are often not unique because of the rotational and intensity ambiguities [8] that are ubiquitously present in factor analysis decompositions of bilinear data matrices. Instead of unique solutions, a band of feasible solutions that fit the experimental data equally well are obtained. These bands of feasible solutions can be drastically reduced when constraints that are inherent and characteristic of the chemical system being studied, are applied during the estimation of concentration and spectra profiles. Non-negativity, closure and unimodality [9,10] are the constraints that are typically imposed. Furthermore, constraints related to selectivity in concentration or spectral regions [8] and knowledge of local rank conditions [11] often make it possible to obtain solutions which are nearly or completely unique. Unfortunately, this is not the most

common situation when data matrices obtained from the spectroscopic monitoring of chemical reactions are analyzed.

Although several procedures have already been described in the literature about how to find the bands of feasible solutions associated to multivariate curve resolution procedures [12-16], few of them have been used to solve complex chemical systems with more than three overlapping components. In this respect, Gemperline [15] and Tauler [16] have reported a procedure for optimizing the calculation of the band boundaries of feasible solutions for a variety of systems, including chromatographic coelution systems, reaction equilibrium systems, and batch first order reaction systems. Larrechi and Rius [17] also used Tauler's strategy [16] to calculate the band boundaries of feasible solutions for species profiles obtained by MCR-ALS from NIR data, which had been obtained in turn from the monitoring of a curing reaction, which followed a second order kinetics.

Unlike in the previous study [17], which analyzed a single data matrix, the present paper calculates band boundaries of feasible solutions, using the strategy proposed by Tauler [16], for the case in which several spectral data matrices, arranged in an augmented data matrix, are simultaneously analyzed.

The system studied is the curing reaction between phenyl glycidyl ether (PGE) and aniline, which has already been analyzed by means of MCR-ALS [17,18]. The augmented matrices strategy for solving the rank deficiency problems in the system [7,18] implies the simultaneous analysis of a set of data matrices (forming an augmented data matrix) obtained by near infrared monitoring of the reaction starting from several initial molar ratios for the reagents. The algorithm used to calculate the band boundaries of feasible solutions [16] was adapted so that the ambiguity of all the profiles obtained when an augmented matrix is analyzed could be evaluated simultaneously. The effects that the number and type of data matrices in the simultaneous analysis have on the amplitude of band boundaries were also studied.

2. Theory

In Multivariate Curve Resolution a bilinear decomposition of the experimental data matrix is performed using the following model equation:

$$\mathbf{D} = \mathbf{C}\,\mathbf{S}^{\mathbf{T}} + \mathbf{E} \qquad \text{Eq. (1)}$$

where the dimensions of the matrices are: **D**(NR,NC), **C**(NR,N), $\mathbf{S}^{\mathbf{T}}$(N,NC); **E**(NR,NC); and N is the number of components considered (chemical species contributing to the signal), NR is the number of rows (in spectroscopic data NR is the number of spectra) in data matrix **D;** and NC is the number of columns (in spectroscopic data NC is the number of wavelengths) in data matrix **D. C** is the matrix describing how the contribution of the N species change in the different NR rows of the data matrix (concentration profiles). $\mathbf{S}^{\mathbf{T}}$ is the matrix describing how the response of these N species changes in the NC columns of the data matrix (pure spectra profiles). **E** is the residual matrix with the data variance unexplained by $\mathbf{C}\,\mathbf{S}^{\mathbf{T}}$.

The problem to solve in multivariate curve resolution may be mathematically stated in the following way: given data matrix **D,** find: 1) N, the number of chemical components or species causing the observed data variance; 2) find the (row) concentration profiles of these species, i.e. matrix **C;** and 3) find the (column) pure response or spectra profiles of these species, i.e. matrix $\mathbf{S}^{\mathbf{T}}$.

This is possible if it is assumed that the rank of the data matrix (chemical rank) is equal to the number of absorbing species, when no other contributions, such as instrumental

noise, are present. Since matrix **D** can be considered as the product of two matrices (**D** = **C** $\mathbf{S}^T$), the rank obtained for matrix **D** can be understood from the following mathematical property of the rank: when matrix **D** can be decomposed into the product of two matrices, **C** and $\mathbf{S}^T$, then rank(**D**) ≤ min (rank(**C**), rank($\mathbf{S}^T$)). Thus, if one of the two matrices is full rank, it is sufficient to look into the rank of the other matrix to analyze the rank of **D**. When the systems analyzed come from processes in evolution, the data sets are often rank-deficient, i.e. their chemical rank is lower than the total number of absorbing compounds. In the case of reacting mixtures, a rank-deficiency can appear in concentration matrix **C** for several reasons. The concentration profiles of the absorbing species may be not linearly independent because of the underlying reaction network. It has been proven for constant-volume batch reaction systems with constant density [7] that: rank (**C**) = min (R+1,N), where R is the number of independent reactions present in the system and N is the total number of species. Rank-deficiency can also be caused by the mass balance equations derived from the reactions (rank-deficiency caused by closure and mass balance equations) [5]. Another cause of rank deficiency is the so-called rank-overlap, which comes about when various chemical species have common profiles in one of the two orders of measurement. This would be the case of a process in which two or more products are formed or consumed during the reaction at equal rates, producing concentration profiles also of equal shapes, e.g. a second order reaction X + Y → Z, [X] = [Y]. When rank-overlap is present in the concentration profiles, the rank of the matrix **D** is equal to the number of independent concentration profiles. The rank-deficiency due to closure, mass-balance equations or rank overlap in concentration profiles can be broken by column-wise matrix augmentation, as has already been demonstrated [5,7]. In all cases, the success of rank augmentation is linked with the strategy of choosing which individual data matrices must be included in the augmented one.

The solution to Eq. (1) for **C** and $\mathbf{S}^T$ is ambiguous if no additional information is available: in other words, this solution contains rotational and scale freedom. The literature

often refers to this problem as the factor analysis ambiguity problem [3-5,7-9]. Rotational and intensity ambiguities can be easily shown by the equation:

$$\mathbf{D} = \mathbf{C}_{old}\,\mathbf{S}_{old}^{T} = (\mathbf{C}_{old}\mathbf{T})\,(\mathbf{T}^{-1}\,\mathbf{S}_{old}^{T}) = \mathbf{C}_{new}\mathbf{S}_{new}^{T} \qquad \text{Eq. (2)}$$

If no constraints are considered it is clear that there are an infinite number of possible solutions to Eq. (2) for any non-singular matrix **T:** i.e. **T** should be invertible. But this is accomplished by an infinite number of matrices **T**. Interestingly, however, **T** have reduced dimensions **T**(N,N), much smaller than the dimensions of **C, S**^{T} or **D**.

This infinite number of possible solutions can usually be considerably reduced by means of constraints derived from the physical nature and previous knowledge of the system under study. For instance, only positive values for the concentrations of the chemical components in the mixture have physical meaning; in many spectroscopies, only positive values are allowed in the spectra; concentration profiles are often unimodal; and closure or mass-balance equations should be fulfilled for reaction based systems.

For a particular species profile, the set of feasible solutions under constraints defines a range or band of feasible solutions, and this band may be delimited by maximum and minimum band boundaries. These boundaries can be defined in different ways. One of the simplest has recently been proposed by Gemperline [15] in terms of the maximum and minimum signal contribution of each species to the whole measured signal (see below). These boundaries will be related to specific rotation matrices **T** for each species *k***,** which will be called $\mathbf{T}_{max,k}$ and $\mathbf{T}_{min,k}$. Consider a particular set of solutions to Eq. (1), which fulfills the constraints defined by the problem, $\mathbf{C}_{inic}$ and $\mathbf{S}_{inic}^{T}$. The maximum band boundaries, $\mathbf{C}_{max,k}$ (for the concentration profiles) and $\mathbf{S}_{max,k}^{T}$ (for the spectra profiles), and

the minimum band boundaries, $\mathbf{C}_{min,k}$ (for the concentration profiles) and $\mathbf{S}_{min,k}^{T}$,(for the spectra profiles) may be defined, respectively, by the following equation:

$$\mathbf{D} = \mathbf{C}_{inic}\,\mathbf{S}_{inic}^{T} = \mathbf{C}_{inic}\,\mathbf{T}_{min}\,\mathbf{T}_{min}^{-1}\,\mathbf{S}_{inic}^{T} = \mathbf{C}_{min,k}\,\mathbf{S}_{min,k}^{T} = \\ = \mathbf{C}_{inic}\,\mathbf{T}_{max,k}\,\mathbf{T}_{max,k}^{-1}\,\mathbf{S}_{inic}^{T} = \mathbf{C}_{max,k}\,\mathbf{S}_{max,k}^{T} \qquad \text{(eq. 3)}$$

The goal of the method described here is to find a way to calculating the values of $\mathbf{T}_{max,k}$ and $\mathbf{T}_{min,k}$ which define the maximum and minimum band boundaries of feasible solutions for the profiles of each *k* species under a set of constraints defined for a particular data set.

A previous study has described in detail the optimization algorithm for calculating the band boundaries of feasible solutions obtained by MCR-ALS analysis of a two-way data matrix [16]. The method is based on a non-linear constrained optimization of an objective function defined by the ratio between the signal contribution of a particular species and the whole measured signal. Implementing different constraints during the optimization considerably reduce the width of the bands of feasible solutions.

Maximum and minimum band boundaries have been calculated for different simulated and real two-way data examples of increasing complexity [16]. In the present study, the same approach is extended to analyze column-wise augmented data matrices obtained by joining individual data matrices from different kinetic runs. In principle, as happens for the MCR-ALS algorithm [19], the band boundaries for augmented data matrices are calculated in a similar way to those of individual two-way data matrices and there are no fundamental differences in the implementation of the algorithm with respect to the procedure described previously [16]. It should be taken into account, however, that the number of rows (reaction times) of the individual data matrices can be different and,

consequently, the resolved concentration profiles for the different data matrices will also be of different sizes. Accordingly, constraints on concentration profiles should be algorithmically implemented separately for each data matrix in agreement with their different size.

3. Experimental

3.1 Reaction conditions and procedure

Fig. 1 shows the reactions that take place between PGE and aniline, which acts as the curing agent. The temperature for the isothermal curing of the epoxy resin was 95ºC. Initial molar ratios between PGE and aniline were chosen to ensure that the reaction under study was the only one taking place and that there were no collateral etherification or homopolymerization reactions [20-23].

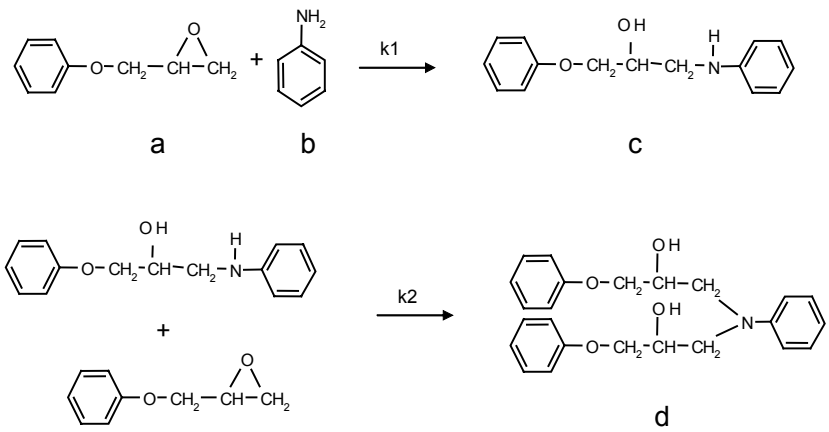

Fig. 1. Curing reaction between phenylglycidylether (PGE) and aniline at T = 95ºC, (k1 > k2). (a) PGE, (b) aniline, (c) secondary amine, (d) tertiary amine.

Five experiments were performed. In these experiments, the molar ratios between the reactants were varied to obtain the following PGE/aniline ratios: 1:1, 1.25:1, 1.5:1, 1.75:1 and 2:1. The experimental procedure involved mixing the necessary amounts of aniline and PGE at room temperature to obtain the desired molar ratio and, immediately after, injecting 1 mL of this mixture into the liquid cell of the NIR spectrophotometer. The transflectance measurements were performed by using a "home-made" cell consisting in a thin plate of glass (where a drop of sample is placed) that is located on a stainless steel diffuse reflecting surface. The cell is closed by using a quartz window and its temperature was set at 95ºC.

3.2 Data acquisition

Detection was performed using an InfraAlyzer 500 Bran-Luebbe Near Infrared spectrophotometer equipped with a liquid cell. Transflectance spectra were initially recorded from 1100 to 2500 nm, every 4 nm. For each experiment, data were acquired at intervals of 5 minutes until the end of the reaction. The reaction was considered to be complete when the reference band at 2208 nm, which is characteristic of the oxirane group [24], disappeared. Spectra of the mixtures at different initial ratios of the reagents (PGE and aniline) were acquired at different reaction times: 230, 300, 390, 480 and 675 min, in increasing order with respect to the proportion of epoxide (see above). NIR spectra of the pure reactants were also recorded in the same experimental conditions. Spectra recorded in the InfraAlyzer 500 were exported and converted into MATLAB binary files [25,26].

3.3 Data Analysis

3.3 1 Data matrices and data preprocessing

Experimental data were arranged in five matrices whose rows were the spectra

recorded at different reaction times and whose columns were the wavelengths. The following matrices were obtained: $\mathbf{A_1}$ (47 x 351), $\mathbf{A_2}$ (61 x 351), $\mathbf{A_3}$ (79 x 351), $\mathbf{A_4}$ (97 x 351) and $\mathbf{A_5}$ (136 x 351), corresponding to the experiments with PGE/aniline molar ratios of 1:1, 1.25:1, 1.5:1, 1.75:1 and 2:1, respectively. The number of rows in the matrices depends on the different reaction times in each experiment. The higher the proportion of PGE, the more rows there are. The same number of columns for all the matrices refers to the 351 NIR wavelengths from 1100 to 2500 nm, every 4 nm.

3.3.1.1 Offset correction

All experimental spectra were corrected so that any vertical shift in the spectra caused by the single beam NIR spectrophotometer was eliminated. For each individual spectrum, this pre-treatment involved subtracting the lowest log (1/R) value from all the other log (1/R) values at each wavelength [27].

3.3.1.2 Wavelength selection

Another pretreatment applied to experimental data involved selecting the wavelengths of interest and ignoring those in which no variation over time was observed. The latter wavelengths provide no information about the reaction under study. The regions of the spectrum in which only noise was detected were also eliminated. The wavelengths that were finally selected ranged from 1400 to 2432 nm.

3.3.1.3 Arrangement of the augmented matrices

Two column-wise augmented data matrices $\mathbf{M_1}$ (420 x 259 in size) and $\mathbf{M_2}$ (183 x 259 in size) were constructed with the five sets of data (corresponding to the 5 experiments $\mathbf{A_1}$, $\mathbf{A_2}$, $\mathbf{A_3}$, $\mathbf{A_4}$ and $\mathbf{A_5}$) and with the first and last sets of data ($\mathbf{A_1}$ and $\mathbf{A_5}$), respectively, to

which the offset correction and wavelength selection had been applied. The individual matrices were ordered according to the increasing proportions of epoxide.

3.3.2 Rank analysis

The rank of the individual and augmented matrices was analyzed by means of the singular value decomposition (SVD) procedure [28]. The number of chemical components was estimated by inspecting of the size of the singular values. It is assumed that the singular values associated to the chemical components are much larger than other possible contributions such as instrumental drift or experimental error. Therefore, the chemical rank was estimated by simply inspecting of the tables of singular values for each data matrix analyzed.

3.3.3 Initial estimates of the pure spectra

Initial estimates of the pure spectra were obtained in three stages. First, the SIMPLe-to-use Interactive Self-modelling Mixture Analysis (SIMPLISMA) algorithm, a technique based on detecting of the purest variables [29], was applied to the corresponding augmented matrix to search for spectral estimates of the various reaction components. Second, the ALS algorithm (see below) optimized the SIMPLISMA initial estimates and led to a new set of spectra and concentration profiles for each reaction component. Although the corresponding concentration profiles did not correctly describe the evolution of the species as a function of time, they were a satisfactory approximation of the behaviour expected for the intermediate and final compounds of the reaction. Finally, initial spectral estimates were obtained for the secondary and tertiary amines as described above. For the aniline and the PGE, however, the previously recorded spectra of the pure compounds were used.

3.3.4 Alternating Least Square (ALS) optimization

The ALS optimization algorithm for curve resolution has been described in detail in previous papers [3,9,19]. A series of constraints was applied in an attempt toimprove the optimization and to restrict the number of possible solutions: a) the pure spectra of each component must be non-negative; b) the concentration profiles of each component must be non-negative; c) the concentration profiles must fulfill a mass balance condition, i.e. a closure constraint with respect to total mass was applied (see section 4); d) each concentration profile must have only one maximum (unimodality).

When multiple kinetic runs are simultaneously analyzed by MCR-ALS by column-wise matrix augmentation, additional constraints can be applied: e) the pure spectra of common components in the different kinetic runs are equal; f) correspondence of common components between runs and g) selectivity constraint: the absent components in a run or in a time interval are forced to have a concentration value of zero. The e) constraint is fulfilled whenever there are no changes in physical properties such as solvent composition or temperature between runs. The f) constraint is fulfilled for the augmented data matrices from different kinetic runs that have common components. The selectivity constraint within a kinetic run can only be implemented to analyze a single reaction system and for the first point of the kinetic concentration profiles, since at this point the two reagents (aniline and PGE) are the only species present. However, this constraint is only an approximation because, in the actual experimental conditions, the first spectrum is measured when the reaction has already started, so it does not correspond only to the mixture of the initial reagents. Accordingly, in the present study, no selectivity constraints were applied during the ALS optimization. The trilinearity constraint was not applied in this case because the reaction is performed under second-order conditions and trilinearity can only be assured for strictly first-order kinetic conditions.

3.3.5 Band boundaries of feasible solutions

The optimization algorithm used to find the band boundaries of feasible solutions (see Theory section) was reported by Tauler [16]. The profiles used as initial estimates for the non-linear optimization were the solutions obtained by MCR-ALS. In an attempt to compare the effects that the number and type of data matrices have on the amplitude of band boundaries in the simultaneous analysis, the band boundaries of feasible solutions were calculated for the recovered concentration and spectra profiles obtained for $\mathbf{M_1}$ and $\mathbf{M_2}$ matrices. The non-negativity and closure constraints were applied.

4. Results and discussion

The rank analysis of individual data matrices for different reaction runs always gave only three significant contributions, not four, which is the expected number of absorbing species. As an example, Table 1 shows the singular values obtained by SVD analysis of the experiment in which the PGE/aniline molar ratio was 2:1. The reason for this rank-deficiency is that the concentration profiles of the species are not linearly independent. The rank of three is in agreement with a reaction network process of two reactions (see section 3.1); i.e. with a process which can be described as A+B→C, A+C→D, where A = PGE, B = aniline, C is an intermediate (secondary amine) and D is the final product (tertiary amine), and the rate constant for the first reaction is larger than the rate constant of the second reaction but not by much, so the reactions cannot be considered consecutive.

Rank deficiency has been broken and the rank has been increased by column-wise matrix augmentation [4,5,7]. This rank augmentation by matrix augmentation has been

obtained by joining various matrices from various process runs that started with different initial molar ratios for the reagents, PGE and aniline. For each additional matrix, the rank of the augmented matrix can increase by one unit until the maximum value is equal to the total number of absorbing species. No further rank increase can be obtained.

Table 1 shows the singular values for the augmented matrices $\mathbf{M_1}$ and $\mathbf{M_2}$. It can be seen that the fourth singular value is higher than the singular values of individual data matrices. Therefore, the rank-deficiency was broken by using this strategy since the rank of the augmented matrices matched the number of absorbing species. Thus, four species could be resolved from MCR-ALS analysis. This topic has already been discussed in a previous study [18].

The ALS optimization algorithm was performed under constraints such as non-negativity (in both concentration and spectra profiles), unimodality and closure for the concentration profiles. The closure constraint applied imposes the fulfillment of a mass balance equation. Although the reaction is carried out without mass exchange between the reacting mixture and the environment, the number of moles varies throughout the reaction in an unknown way. Therefore, this balance is only fulfilled in terms of mass. Thus, only one closure was implemented and this meant that the sum of the amounts (in weight) of all the components in the reaction was constant. The constant value selected was set to one in all the reaction runs. Since only one set of spectra was recovered by ALS in the simultaneous analysis of all reaction runs (see below), concentration profiles in each reaction run are obtained accordingly scaled.

The ALS results are expressed in mass units so the corresponding values in moles were obtained by dividing each concentration profile by the corresponding molecular weight, assuming that each species and their molecular weight are known. Then, these results were normalized against the number of initial moles of aniline, which is the same in

all the experiments. In this way, it was easier to make a comparative analysis of the concentration profiles, when the molar ratios for the reactants were different.

Number of Factor	A_5	$M = [A_1;A_5]$	$M = [A_1;A_2;A_3;A_4;A_5]$
1	67.09	78.31	118.62
2	8.01	9.86	15.04
3	1.06	3.78	4.69
4	0.06	1.35	1.83
5	0.01	0.15	0.48
6	<0.01	0.09	0.22

Table 1: Rank analysis of matrix $\mathbf{A_5}$ and the column-wise augmented matrices $\mathbf{M_1}$ and $\mathbf{M_2}$.(the first six singular values are shown).

Figs. 2 and 3 show the concentration profiles obtained by ALS for $\mathbf{M_1}$ (lack of fit = 0.88%, explained variance = 99.99%) and $\mathbf{M_2}$ (lack of fit = 0.38%, explained variance = 100.00%) matrices. The concentration profiles of the four compounds (PGE, aniline,secondary and tertiary amines) are given for each reaction run using different initial molar ratios.

The resolved concentration profiles basically reproduced the molar ratios that were initially used for the reagents in each experiment, except for small differences in the experiments 1.25:1 and 1:1 in matrix $\mathbf{M_1}$ and 2:1 in matrix $\mathbf{M_2}$, where the solutions were not far from the expected values. During the first 100 minutes of the reaction, it can be

observed (see Figs. 2 and 3) that the variation of the concentration with respect to the time is approximately the same for PGE and aniline, since only the first reaction is taking place (see Fig. 1).

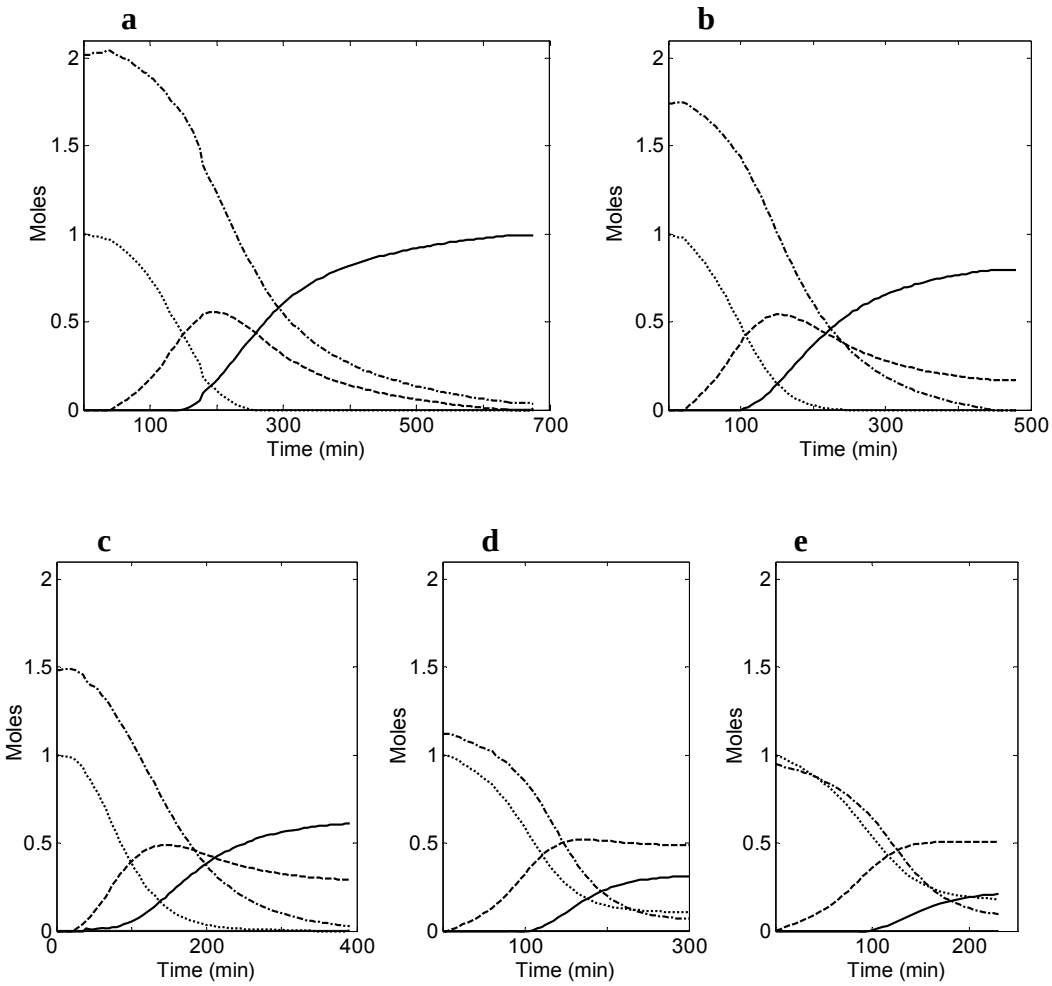

Fig. 2. Concentration profiles recovered, in moles, for matrix $\mathbf{M_1}$ for the five different PGE/aniline molar ratios: a) 2:1, b) 1.75:1, c) 1.5:1, d) 1.25:1 and e) 1:1. Aniline (dotted line), PGE (dash-dot line), secondary amine (dashed line) and tertiary amine (solid line).

When the aniline has reacted completely, the variation in PGE slows down since the process is controlled by the kinetic rate constant of the second reaction (note that $k_1>k_2$). This can be observed clearly in experiments 2:1, 1.75:1, and 1.5:1 for the $\mathbf{M_1}$ matrix, and 2:1 for $\mathbf{M_2}$ matrix. Also in these experiments, from the moment that the aniline has reacted completely, the variation over time for the secondary and tertiary amines is the same, but negative for the secondary amine and positive for the tertiary amine. This behaviour is expected, since in the second reaction, a mol of secondary amine give rise to a mol of tertiary amine. At the end of the experiment 2:1 (in both $\mathbf{M_1}$ and $\mathbf{M_2}$ matrices), the concentration of tertiary amine reached the value predicted by the stoichiometry of the reaction.

The concentration profiles for the common experiments in matrices $\mathbf{M_1}$ and $\mathbf{M_2}$ (i.e. 2:1 and 1:1) were compared and were found to be very similar, with correlation values always higher than 0.997.

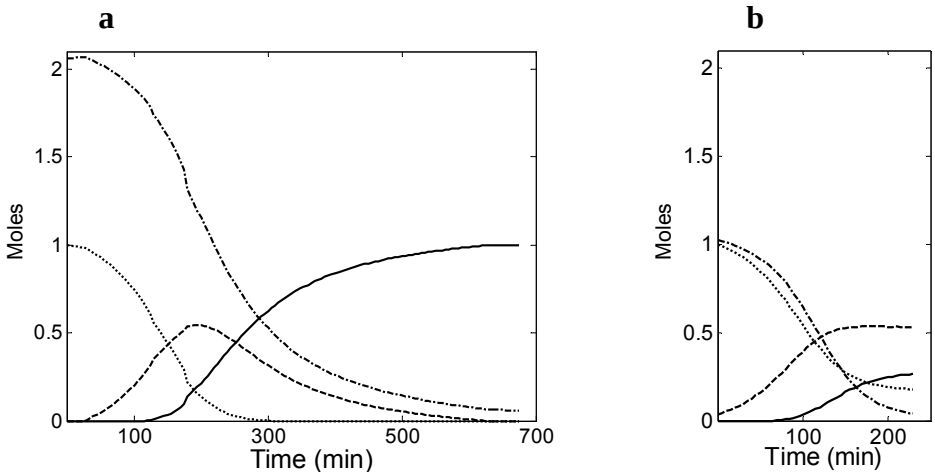

Fig. 3. Concentration profiles recovered, in moles, for matrix $\mathbf{M_2}$ for two different PGE/aniline molar ratios: a) 2:1 and b) 1:1. Aniline (dotted line), PGE (dash-dot line), secondary amine (dashed line) and tertiary amine (solid line).

Only one set of spectra corresponding to the four absorbing species that take part in the reaction was recovered by ALS, and it was unique for all the experimental runs that made up the augmented matrix. Recovered spectral profiles for both $\mathbf{M_1}$ and $\mathbf{M_2}$ matrices also presented high correlation values. As an example, Fig. 4 shows the spectral profiles obtained for matrix $\mathbf{M_1}$, after ALS optimization.

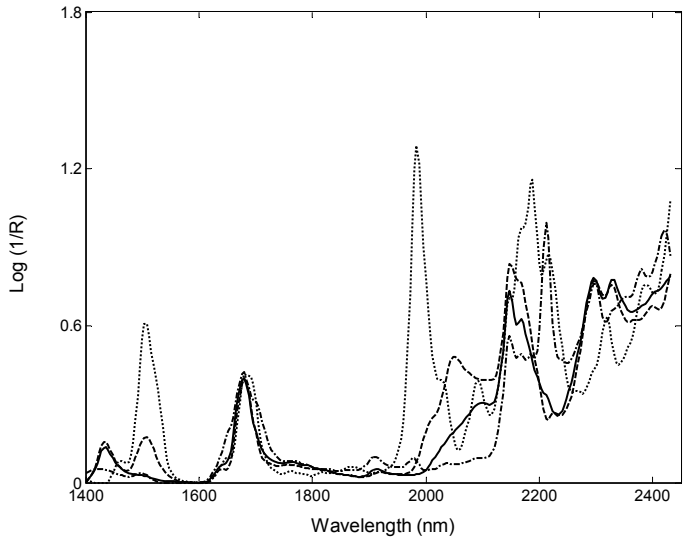

Fig. 4. Recovered spectra for matrix $\mathbf{M_1}$ relative to aniline (dotted line), PGE (dash-dot line), secondary amine (dashed line) and tertiary amine (solid line).

The characteristic spectral bands of the functional groups of the system studied (primary and secondary amines, oxirane and hydroxyl groups) have been resolved [17, 18]. The correlation (similarity) [17,18] between the recovered spectra and the experimentally obtained pure spectra for PGE, aniline and the tertiary amine (final product) has been studied. The similarity coefficients obtained when matrix $\mathbf{M_1}$ was analysed were: 0.998 for

the PGE, 0.994 for the aniline and 0.999 for the tertiary amine. Also, when these coefficients were calculated for the recovered spectra of matrix $\mathbf{M_2}$, the correlation values were: 0.999, 0.991 and 1.000 for PGE, aniline and the tertiary amine, respectively. The recovered spectrum for the tertiary amine was compared with the last spectrum from the experiment in which the PGE/aniline molar ratio was 2:1, since the reaction is considered to have ended. The correlation coefficients were high in all the cases, which make it possible to assume that the recovered spectrum of the secondary amine is similar to the real spectrum. This latter spectrum could not be obtained directly by means of instrumental techniques.

Figs. 5 and 6 show the band boundaries of feasible solutions associated to the concentration profiles obtained by ALS when matrices $\mathbf{M_1}$ and $\mathbf{M_2}$ were respectively analyzed.

Within these band boundaries, there is the set of solutions that fits the data equally well and fulfils the applied constraints. The band boundaries give the set of rotationally ambiguous solutions. For all the species in each experiment, except for the secondary amine in matrix $\mathbf{M_2}$ (see Fig. 6), at least one of the band boundaries matches the ALS solutions; for example, the concentration profiles for aniline coincide exactly with the minimum band boundaries and the concentration profiles for PGE coincide exactly with the maximum band boundaries.

For PGE, the bands narrow significantly when aniline concentration is practically zero. This corresponds to the moment at which the first of the two reactions postulated in Fig. 1 ends. From this point on, the ambiguity associated to the ALS solution diminishes for all concentration profiles because new conditions of local rank are established when aniline is consumed.

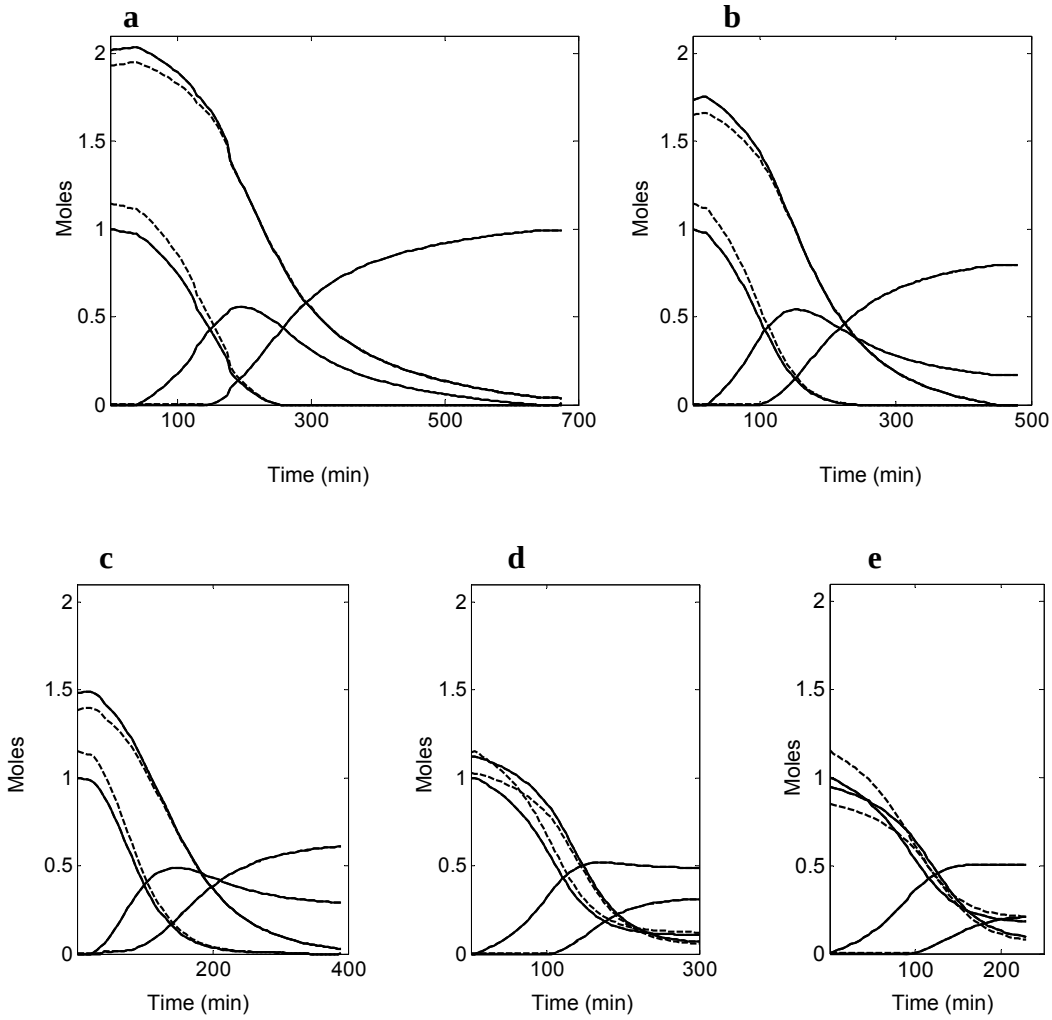

Fig. 5. Band boundaries of feasible solutions, expressed in moles, for concentration profiles obtained for matrix $\mathbf{M_1}$. Solid line: ALS solution. Dotted line: Band boundaries of feasible solutions

If the band boundaries of feasible solutions for matrices $\mathbf{M_1}$ and $\mathbf{M_2}$ (see Figs. 5 and 6) are compared, it can be seen clearly that the bands for matrix $\mathbf{M_2}$ are wider than the ones

for matrix $\mathbf{M_1}$. A detailed inspection of the recovered concentration profiles of both $\mathbf{M_1}$ and $\mathbf{M_2}$ matrices shows that the concentration of PGE only reaches zero in the experiment with molar ratio 1.75:1, although it should be zero at the end of the reaction for all the experiments. This has already been described in a previous study [18]. One possible explanation for this unexpected behaviour is that the NIR spectra for each experiment were recorded until the band corresponding to the oxirane group (2208 nm) disappeared; and the reaction is considered to have finished at this point. The NIR spectra may show that the band disappears at 2208 nm, but the reaction has not really stopped, and a small quantity of epoxide has still not reacted. This did not happen in experiment 1.75:1, which is long enough for the reaction to end. So, from the point of view of the curve resolution, in the experiment with molar ratio 1.75:1 there are new local rank conditions in which only the secondary and tertiary amine are present. This decreases the ambiguity and, therefore, the bands for matrix $\mathbf{M_1}$ (which include the experiment with molar ratio 1.75:1) are narrower than for $\mathbf{M_2}$ matrix.

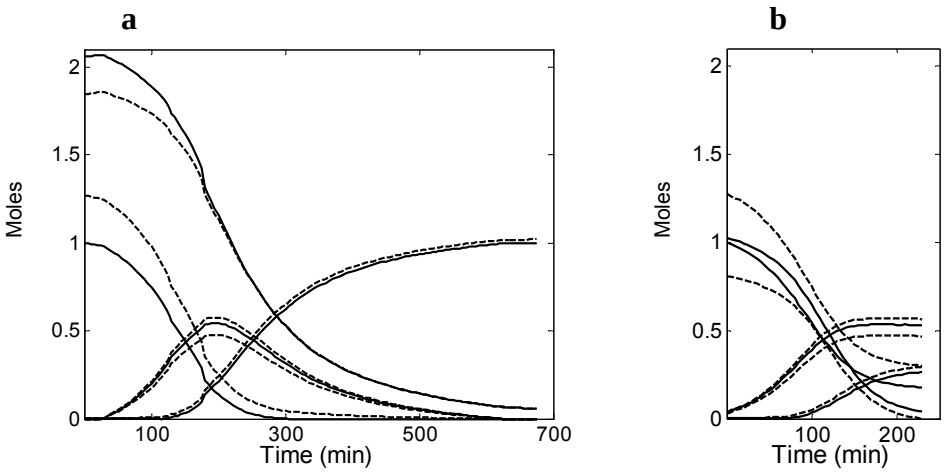

Fig. 6. Band boundaries of feasible solutions, expressed in moles, for concentration profiles obtained for matrix $\mathbf{M_2}$. Solid line: ALS solution. Dotted line: Band boundaries of feasible solutions.

In order to determine whether this decrease in the ambiguity of matrix $\mathbf{M_1}$ is exclusively due to the presence of this kind of local rank information, the band boundaries of feasible solutions were calculated (although these calculations are not shown in this paper) for an augmented matrix formed by the experiments with molar ratio 1.75:1 and 1:1. Despite having the additional local rank information, the ambiguity for these profiles was greater than the ambiguity found for both $\mathbf{M_1}$ and $\mathbf{M_2}$. This indicates that good local rank information by itself is not sufficient to diminish the ambiguity. It is important that the experimental design be appropriate for choosing the experiments to be included in the augmented matrix.

In the same way, the band boundaries associated to the spectral profiles were obtained. For matrix $\mathbf{M_1}$, the recovered spectrum for the aniline was the only profile with wide bands (see Fig. 7 a)). On the other hand, for matrix $\mathbf{M_2}$ the ambiguity was present in both aniline and secondary amine spectra (see Fig. 7 b) and c)). In addition, the ambiguity associated to the aniline spectra was higher in this last case.

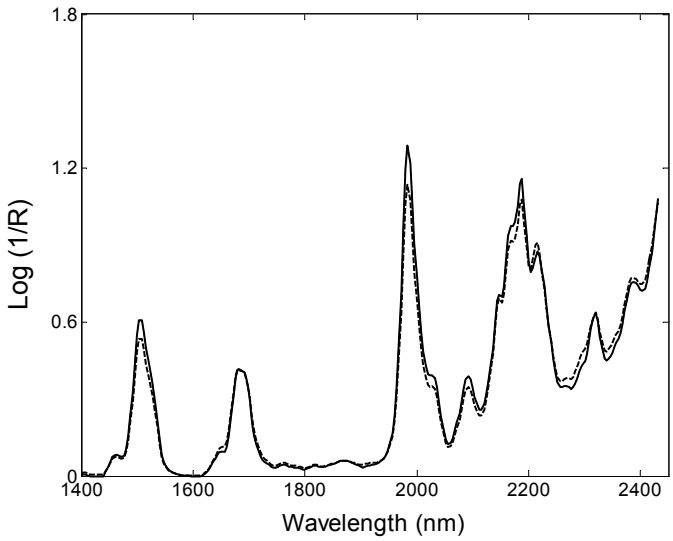

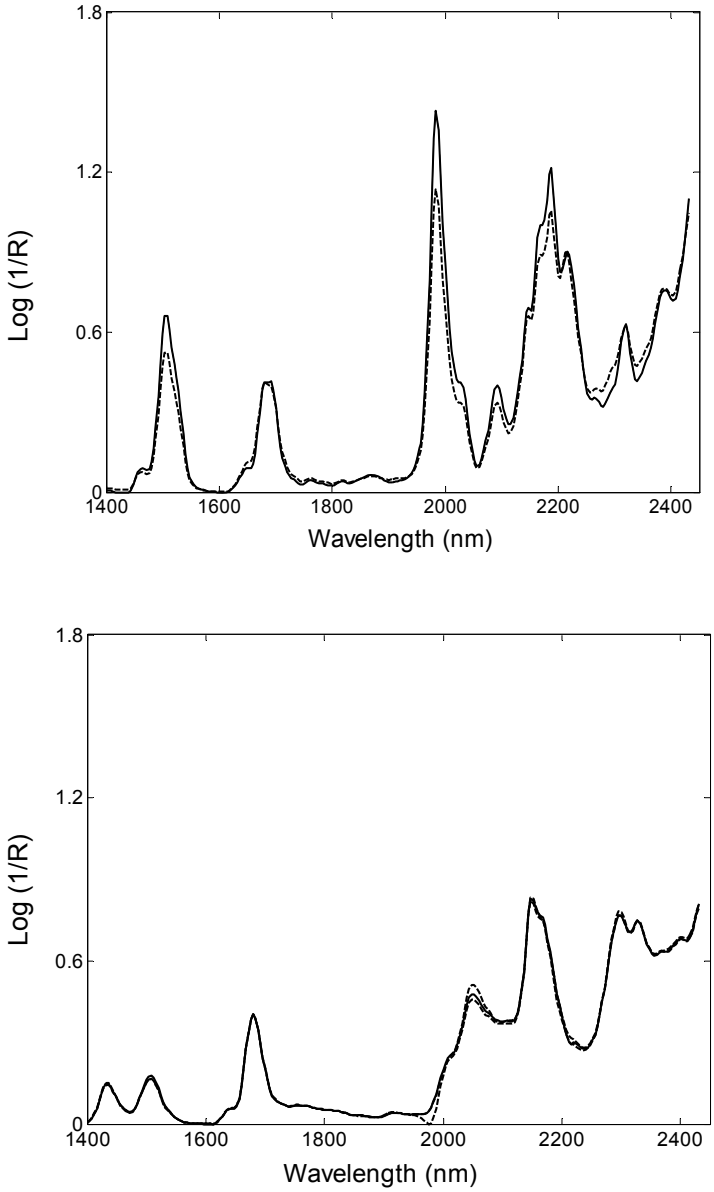

Fig. 7. a) Band boundaries of feasible solutions for the spectral profile recovered for aniline when matrix $\mathbf{M_1}$ was analyzed. b) Band boundaries of feasible solutions for the spectral profile recovered for aniline when matrix $\mathbf{M_2}$ was analyzed. c) Band boundaries of feasible solutions for the spectral profile recovered for secondary amine when matrix $\mathbf{M_2}$ was analyzed.

For both $\mathbf{M_1}$ and $\mathbf{M_2}$ matrices, the spectra for PGE and tertiary amine were recovered without any ambiguity. The spectrum of secondary amine was also recovered with no ambiguity when matrix $\mathbf{M_1}$ was analyzed. A possible explanation for this ambiguity in spectral profiles is the presence of selectivity and local rank conditions in the corresponding concentration profiles, compelling new linear combinations between profiles to be present (see above).

5. Conclusions

The application of a previously developed algorithm to calculate band boundaries of feasible solutions has been shown to provide satisfactory results in the study of a complex rank deficient chemical reaction concerning a curing process.

The rotational ambiguities associated with the calculation of spectra and concentration profiles of the resolved reaction species were considerably reduced by applying constraints and matrix augmentation. results can only be good if the experimental design is suitable for selecting the appropriate experiments for the augmented matrix.

The decrease in the ambiguity of the recovered solution is closely related to the presence of favorable local rank conditions within the set of matrices analyzed. Linked to this, it is important that monitoring continues until the reaction totally stops. In this way, the information (regions of selectivity and/or local rank information) about the system is more complete.

From the results obtained in this study, it has been possible to deduce the composition of the reacting mixture at any time during the curing process, and to estimate possible errors in the spectra and concentration profiles associated to rotational ambiguities.

Aknowledgements

The authors would like to acknowledge the economic support provided by the MCyT (project Nº BQU 2003-01142).

References

[1] J. H. Hamilton and P. J. Gemperline, J. Chemometrics 4, (1990), 1-13.

[2] A. de Juan, E. Casassas and R. Tauler, Encyclopedia of Analytical Chemistry: Instrumentation and applications. 'Soft-modelling of analytical data', Wiley, New York, 2000.

[3] R. Tauler, A. Izquierdo-Ridorsa and E. Casassas, Chemom. Intell. Lab. Syst., 18, (1993), 293-300.

[4] A. Izquierdo-Ridorsa, J. Saurina, S. Hernández-Cassou and R. Tauler, Chemom. Intell. Lab. Syst., 38, (1997), 183-196.

[5] J. Saurina, S. Hernández-Cassou, R. Tauler and A. Izquierdo-Ridorsa, J. Chemometrics, 12, (1998), 183-203.

[6] E. R. Malinowski, Factor Analysis in Chemistry ,3rd Edn., Wiley, New York, 2002.

[7] M. Amrhein, B. Srinivasan, D. Bonvin and M. M. Schumacher, Chemom. Intell. Lab. Syst., 33, (1996), 17-33.

[8] R. Tauler, A. Smilde and B. R. Kowalski, J. Chemometrics, 9, (1995), 31-58.

[9] R. Gargallo, F. Cuesta-Sanchez, D. L. Massart and R. Tauler, Trends Anal. Chem., 15, (1996), 279-286.

[10] A. De Juan, Y. Vander Heyden, R. Tauler and D. L. Massart, Anal. Chim. Acta, 346, (1997), 307-318.

[11] R. Manne, Chemom. Intell. Lab. Syst., 27, (1997), 89-94.

[12] R. C. Henry and B. M. Kim, Chemom. Intell. Lab. Syst., 8, (1990), 205-216.

[13] P. D. Wentzell, J. H. Wang, L. F. Loucks and K. M. Miller, Can. J. Chem., 76, (1998), 1144-1155.

[14] B. M. Kim and R. C. Henry, Chemom. Intell. Lab. Syst., 49, (1999), 67-77.

[15] P. J. Gemperline, Anal. Chem., 71, (1999), 5398-5404.

[16] R. Tauler, J. Chemometrics, 15, (2001), 627-646.

[17] M. S. Larrechi and F. X. Rius, Appl. Spectrosc. 58, (2004), 47-53.

[18] M. Garrido, I. Lázaro, M. S. Larrechi and F. X. Rius, Anal. Chim. Acta, 515 (2004), 65-73.

[19] R. Tauler, Chemom. Intell. Lab. Syst., 30, (1995), 133-146.

[20] C. Billaud, M. Vandeuren, R. Legras and V. Carlier, Appl. Spectrosc. 56, (2002), 1413-1421.

[21] J. Mijovic, A. Fishbain and J. Wijaya, Macromolecules 25, (1992), 979-985.

[22] C.A. May, Epoxy resins: chemistry and technology, Marcel Dekker, New York, 1988, pp.293-305.

[23] L. Matějka and K. Dušek, J. Polym. Sci. Part A: Polym. Chem. 33, (1995), 461-472.

[24] J. Mijovic and S. Andjelic, Macromolecules 28, (1995), 2787-2796.

[25] The Mathworks, MATLAB Version 6.5, Natick, MA, 2002.

[26] The Mathworks, Optimization Toolbox, 2.0 version, Natick, MA, 1998.

[27] J.J. Kelly, C. H. Barlow, T. M. Jinguji and J. B. Callis, Anal. Chem. 61, (1989), 313-320.

[28] D. L. Massart, B. G. M. Vandeginste, L. M. C. Buydens, S. de Jong, P. J. Lewi and J. Smeyers-Verbeke, Handbook of Chemometrics and Qualimetrics : Part A, Elsevier, Amsterdam, 1997.

[29] W. Windig and J. Guilment, Anal Chem. 63, (1991), 1425-1432.

4.5 Validation of the concentration profiles obtained from the NIR/multivariate curve resolution monitoring of reactions of epoxy resins using HPLC as a reference method

submitted

M. Garrido, M. S. Larrechi, F. X. Rius*

Department of Analytical and Organic Chemistry, Faculty of Chemistry, Rovira i Virgili University, Marcel·lí Domingo s/n (43005), Tarragona, Spain

Abstract

This paper reports the validation of the results obtained by the combination of near infrared spectroscopy and multivariate curve resolution-alternating least squares using high performance liquid chromatography as a reference method, for the model reaction of phenylglycidylether and aniline. The results are obtained as concentration profiles over the reaction time. The trueness of the proposed method has been evaluated in terms of lack of bias. The joint test for the intercept and the slope showed that there were no significant differences between the profiles calculated spectroscopically and the ones obtained experimentally by means of the chromatographic reference method at a global level of confidence of 5%. The uncertainty of the results obtained was estimated by using information derived from the process of assessment of trueness. In addition, some operational aspects such as cost and availability of the instrumentation, time and cost of the analysis were evaluated. The proposed method represents a good choice to monitor the reactions of epoxy resins, obtaining the variation of all the species throughout the time.

1. Introduction

The soft-modelling methods, such as the Multivariate Curve Resolution-Alternating Least Squares method (MCR-ALS) [1,2], can provide the description of reaction processes without explicitly using the underlying chemical model linked to them [3]. When MCR-ALS is applied to bilinear spectroscopic data obtained from monitoring a chemical reaction, it make it possible to estimate the concentration profiles of each species involved in the reaction as well as the corresponding pure spectra [4]. In addition the concentration profiles obtained by soft-modelling approaches can be useful to design a suitable reaction model and to support the model chosen for a hypothetical reaction under study [5,6]. Consequently, it is important to verify the validity of the soft-modelling concentration profiles in order to reliably use them as a monitoring technique and as a guide for choosing a possible reaction mechanism for the reacting system.

Specifically, MCR-ALS was already applied to the NIR data from the monitoring of reactions of epoxy in a previous study [7]. Concretely, the reaction studied were the one between phenylglycidylether (PGE) and aniline. The recovered concentration profiles were helpful in order to establish a kinetic model to estimate the corresponding kinetic rate constants [8]. Although the results obtained were comparable with concentration profiles and kinetic rate constants reported in the bibliography, no validation studies were carried out for the applied method. The aim of the present paper is, therefore, to assess the validity of the concentration profiles obtained by NIR/MCR-ALS for the reaction between PGE and aniline, using HPLC as a reference method.

In accordance with ISO [9], validating implies the verification that a determined method fulfills a series of particular requirements for a specified purpose. These requirements are not only related to statistically-based performance criteria (e.g. trueness,

precision, etc.) but also to other feasibility characteristics such as easy of operation, cost or sample throughput [10]. The extent to which a laboratory has to undertake validation of a method (i.e. which of the criteria have to be studied) depends on the existing status of the method, the competence of the laboratory and of the customer requirements [9].

In the present paper the performance criteria analyzed are: trueness (i.e. verification of presence of method bias), precision (intermediate precision) and uncertainty. The bias of an analytical method can be determined by comparing the response of the method under validation with a value obtained by a reference method [11], with smaller bias indicating greater trueness. When the bias is analyzed for several values corresponding to a concentration profiles, the concentration range and the number of comparisons are large. In the case under study, the two methods to be tested (i.e. NIR/MCR-ALS and HPLC) were compared by using bivariate linear regression [12]. In this way, when the values of the method under validation were regressed on the results obtained by the reference method, a straight line was expected. So, the trueness was assessed by applying the joint confidence interval test for the slope and the intercept to the straight line obtained [13]. If the slope and the intercept values of the straight line both are not significantly different from the theoretical values of unity and zero, respectively, we can conclude that there is not method bias for a certain level of confidence preestablished.

The estimation of the precision was carried out by varying certain operational conditions among the runs, in order that different normal situations in the laboratory were represented [11]. Thus, different runs were performed by changing day, operator and reagents. The intermediate precision obtained gives a notion of the variability that should be expected in the laboratory when the method under validation is applied, and it is an essential component of the overall uncertainty of the results. Because the precision varied with time and analyte concentration, instead a value of precision for the method, a band of intermediate precision was obtained for the concentration profile of each species.

Uncertainty was estimated following the procedure proposed by Maroto et al. [14], which make use of the information generated in the assessing of the accuracy (trueness and precision) of the analytical method. So, besides the uncertainty arising from the experimental variation, the uncertainty originated in the process of assessment of trueness must be also considered. In the case under study, instead of the typical way for expressing an analytical result (i.e. Value± Uncertainty), a concentration profile for each species was obtained, surrounded by a band of overall uncertainty associated to these experimental values.

Also, other operational aspects that can be interesting for users were evaluated. Concretely, amount of reagents used instrumentation (cost and availability), time and cost of the analysis.

2. Theory

2.1 Trueness

Trueness is defined as the closeness of agreement between the average value obtained from a large set of test results and an accepted reference value [15]. The evaluation of trueness, in terms of assessing the absence of bias, need therefore reference values. As it has been mentioned above, monitoring the reaction produces a series of concentration profiles over time corresponding to the different species that intervene in the reaction. Therefore, comparing the results obtained by the method to be tested with those obtained by a reference method is an appropriate choice to assess the trueness. Several comparisons based on different statistical tests could be performed [16]. In this case, the

analytical results obtained by the method to be tested are regressed on the results obtained by the reference method. In this way, a straight line is expected. The ordinary least squares technique (OLS) is often used to find the regression coefficients. However, OLS assumes the presence of constant random errors in only one of the methods being compared (normally in the method represented on the y-axis), considering the other method free of random errors. This is not the real situation, because the errors are commonly present in both methods. Bivariate least squares (BLS) could be considered an appropriate technique because consider errors in both axes [12]. If the slope and the intercept of this regression line do not differ significantly form unity and zero, respectively, the results produced by the both methods will not be statistically different at a given level of significance α. In order to test whether there are significant differences between the regression coefficients and the theoretical values of zero intercept and unity slope, the joint confidence interval test for the slope and the intercept can be used [13]. The joint test consist of verifying the presence of the theoretical point zero intercept and unity slope within the limits of the elliptical-shaped joint confidence region defined by:

$$\sum_{i=1}^{n}\frac{1}{w_i}(\hat{a}-a)^2+2\sum_{i=1}^{n}\frac{x_i}{w_i}(\hat{a}-a)(\hat{b}-b)+\sum_{i=1}^{n}\frac{x_i^2}{w_i}(\hat{b}-b)^2=2\hat{s}^2F_{1-\alpha(2,n-2)} \quad \text{Eq./(1)}$$

where $F_{1-\alpha(2,n-2)}$ is the tabulated F-value at a level of confidence α with 2 and n-2 degrees of freedom, n indicates the overall number of samples analyzed (i.e. the number of (x_i,y_i) experimental data points) and w_i is the weighting factor for each data point. Likewise, $\hat{s}^2$ is the estimate of the experimental error, a and b are the true values of the BLS regression coefficients and $\hat{a}$ and $\hat{b}$ are their respective estimated regression coefficients.

2.2 Precision

Precision is defined as "the closeness of agreement between independent test results obtained under stipulated conditions" [17]. These stipulated conditions are related to the different factors that could be changed for each method run. Depending on the factors changed, three types of precision can be obtained: the repeatability, the intermediate precision and the reproducibility [18]. The precision can be estimated by the corresponding standard deviation, obtained under the specified conditions: repeatability standard deviation indicates the variability observed within a laboratory, over a short time, using a single operator, the same instrument and reagents, etc; intermediate precision relates to the variation in results when one or more factors, such as time, instrumentation and operator, are varied within a laboratory and reproducibility standard deviation shows the variability obtained when different laboratories analyze the same sample. For a single-laboratory, precision under repeatability conditions (s_r) and precision under run-to-run conditions ($s_{I(run)}$, intermediate precision) could be taken into account.

2.3 Uncertainty

The uncertainty is defined as "a parameter, associated with the result of a measurement, that characterizes the dispersion of the values that could reasonably be attributed to the measurand" [19]. An important step in the assessment of the uncertainty consists of the identification of all sources of error that affect the dispersion of the values. Uncertainty and trueness are closely related. Assuring that a result is included within a certain interval (given for the uncertainty of the estimated result) is not possible if the trueness of the analytical method is not assessed previously. Therefore, the uncertainty generated during the process of assessment of trueness has to be considered, as well.

Thus, the overall uncertainty can be calculated as the sum of four terms [14]:

$$U = k\sqrt{u_{proc}^2 + u_{assessment}^2 + u_{preproc}^2 + u_{other\ therms}^2} \qquad \text{Eq. (2)}$$

The term u_{proc} is the standard uncertainty arising from the analytical procedure, which is related to the experimental errors. The u_{proc} can be estimated by the run-different intermediate precision ($s_{I(run)}^2$), which considers the experimental variation due to the conditions of the measurement.

The second term, $u_{assessment}$ considers the uncertainty of the assessment of trueness. This uncertainty is calculated as:

$$u_{assessment} = \sqrt{\frac{s_{I(run)}^2}{n} + u(ref)^2} \qquad \text{Eq. (3)}$$

where $s_{I(run)}^2$ is the run-different intermediate precision, n is the number of times that the reference sample is analyzed in the assessment of trueness and $u(ref)$ is the standard uncertainty of the reference sample. When a reference method is used, $u(ref)$ can be calculated as $s_{ref} \big/ \sqrt{n}$, where s_{ref} is the standard deviation of the n results obtained when a sample is analyzed by the reference method.

The third component in Eq. (2) takes into account the uncertainty of the pretreatments carried out and the fourth term considers the sources of uncertainty not

considered in the former terms. The coverage factor *k* is often used instead of the two-sided *t*-tabulated when there is no information about the degrees of freedom of some of the components in Eq. (2).

3. Experimental Part

The reactions that take place between PGE and aniline are depicted in Scheme 1. Primary amine reacts with the epoxide to form a secondary amine and, in a further reaction, the secondary amine reacts with epoxide to form a tertiary amine. The experimental procedure for the reaction involved mixing the necessary amounts of aniline (from Aldrich, distilled before using it) and PGE (Aldrich) at room temperature to obtain the desired molar ratio. Initial molar ratios between PGE and aniline were chosen and the temperature was set at 95 ºC to ensure that the reactions under study were the only ones taking place and that there were no collateral etherification or homopolymerization reactions [20,21].

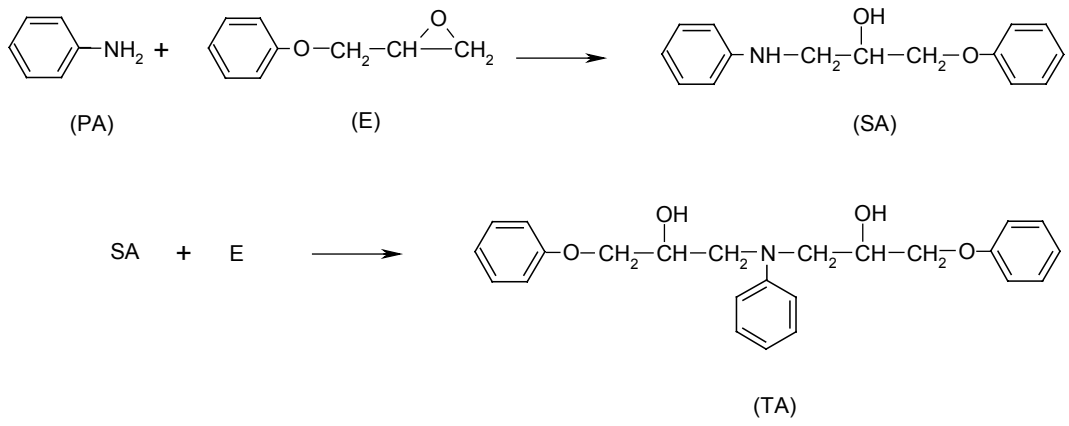

Scheme 1. Reaction between phenylglycidylether (PGE) and aniline. E: PGE, PA: aniline, SA: Secondary amine and TA: Tertiary amine.

3.1 Monitoring of epoxy-amine reactions by NIR and MCR-ALS

Experiments with different molar ratios between the reactants (i.e. PGE and aniline) were performed. In these experiments the molar ratios between the reactants were varied to obtain the following PGE/aniline ratios: 1:1, 1.25:1, 1.5:1, 1.75:1 and 2:1. The procedure involved mixing the necessary amounts of aniline and PGE at room temperature to obtain the desired molar ratio and, immediately after, injecting 1 mL of this mixture into the cell for liquids of the NIR spectrophotometer. The cell temperature was set at 95ºC.

The NIR spectra were recorded throughout the reaction every 4 nm, between 1100 and 2500 nm with an InfraAlizer 500 spectrophotometer from Bran-Luebbe. For each experiment, we acquired data at intervals of 5 minutes until the end of the reaction. The reaction was considered to be complete when no changes were observed in the spectra throughout the time. NIR spectra of the pure reactants (aniline and PGE) were also recorded in the same experimental conditions. The recorded spectra were exported and converted into MATLAB binary files [22].

In order to eliminate the vertical shift caused by using a NIR spectrophotometer with only one light beam, all the spectra were pretreated with an *off-set* correction [23]. Wavelength selection was performed by selecting the wavelengths of interest and ignoring those in which no variation over time was observed because they provide no information about the reaction under study. The regions of the spectrum in which only noise was detected were also eliminated. The MCR-ALS method has been applied as in a previous article [7].

The entire procedure (See the left part in Scheme 2) has been repeated seven times in the same laboratory but under different experimental conditions obtained by changing some variables such as operator, day and reagents.

3.2 High Performance Liquid Chromatography

For the monitoring by HPLC, the reaction was carried out under stoichiometric proportions (i.e. PGE/aniline molar ratio of 2:1) into a thermostatic bath (PolyScience, USA) at 95 ± 0.2 ºC and the temperature of the reacting mixture was controlled with an immersion probe thermometer (Crison).

The chromatographic separation was performed by reversed-phase HPLC using a Hewlett Packard series 1100 chromatographic system with UV detector set at 254 nm to monitor eluted species. The samples (nineteen samples withdrawn from the reacting mixture at different times, analyzed by triplicate) were prepared by weighing 10-25 mg of reacting mixture and dissolving them with methanol to 10 mL. Aliquots of this solution (20 μL) were injected on an analytical phase-reverse column Hypersil ODS (5 μm particle size), 200 mm x 4.6 mm i.d. (Agilent Technologies). The temperature of the column was kept at 20 ºC. HPLC analyses were carried out by gradient elution of methanol-water system (both solvents of HPLC grade from SDS) with a flow rate of 1.75 mL min^{-1}. The gradient ranged from 20% to 100% of methanol within 10 min.

Concentration of the species under study was calculated from the peak areas using the calibration curves of pure compounds. Phenylglycidylether and aniline were commercially available. Secondary amine product was prepared by reacting PGE with excess aniline (1:10 molar ratio) at 80 ºC for 12 h. The excess of aniline was distilled off under reduced pressure. Tertiary amine was obtained form the stoichiometric mixture (i.e. PGE/aniline 2:1) reacted at 120 ºC for 20 h. The standard solutions for the calibration curves were made by triplicate and taking into account the range of concentration of each species throughout the process. The areas of the chromatographic peaks had a linear relationship with respect to the concentration of the species in the mobile phase.

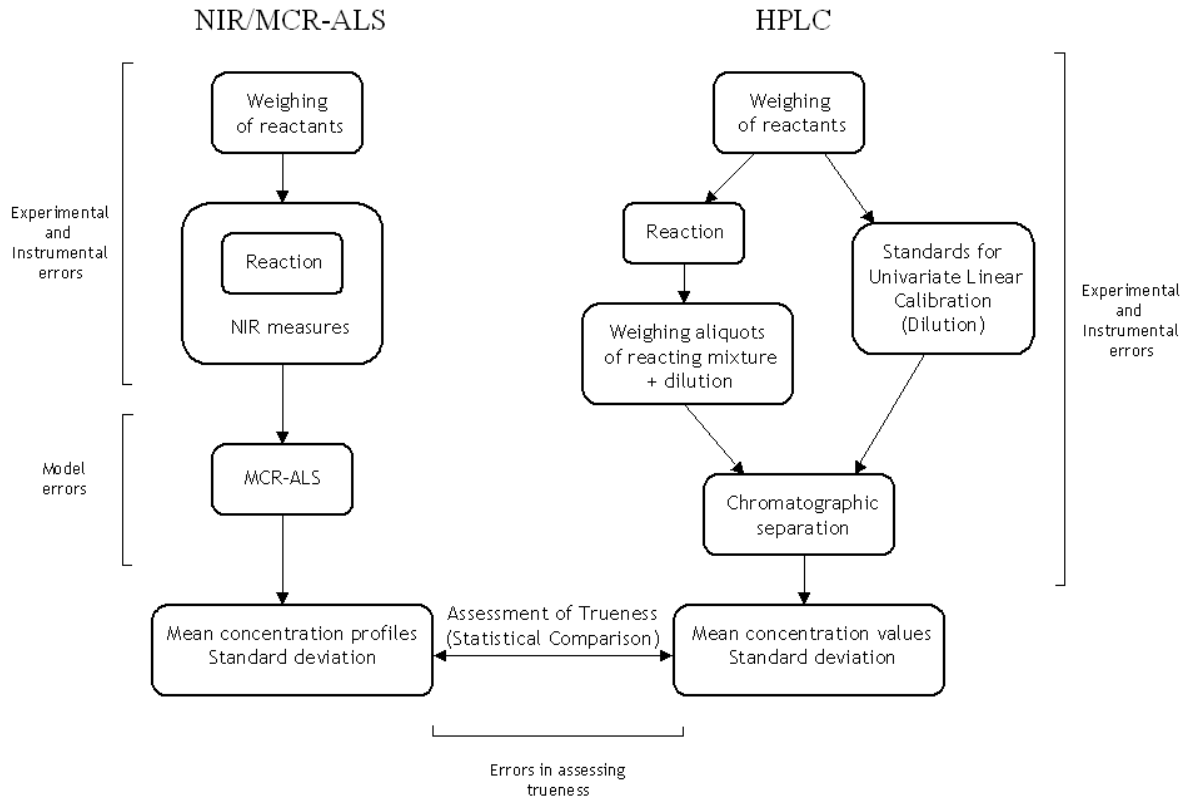

Scheme 2. Sources of error in the NIR/MCR-ALS procedure (on the left) and in the HPLC procedure (on the right).

4. Results and Discussion

4.1 Trueness

Fig. 1 shows a superposition of the concentration profiles obtained by NIR/MCR-ALS (the mean profiles of the seven runs performed) and the mean of the triplicate concentration values obtained by HPLC, for the reaction with a PGE/aniline molar ratio of 2:1. This molar ratio was selected because in this situation is possible to obtain information about the entire process, since both reactions (see Scheme 1) can be considered finished.

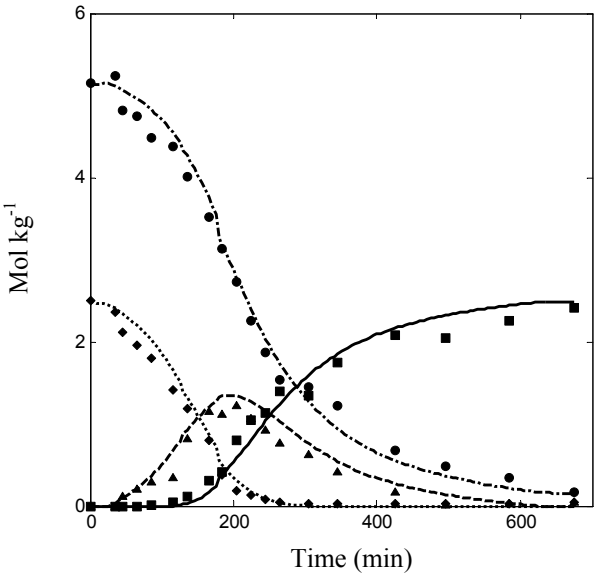

Fig. 1. Superposition of the mean concentration profiles (n = 7) obtained by NIR/MCR-ALS and the values obtained by HPLC for the reaction between PGE and aniline (molar ratio of 2:1). For the NIR/MCR-ALS concentration profiles (···) aniline, (-·-) PGE, (---) secondary amine and (—) tertiary amine. In HPLC values (♦) aniline, (●) PGE, (▲) secondary amine and (■) tertiary amine.

An *a priori* visual inspection of Fig. 1 makes it possible to observe that there is a good correspondence between the profiles obtained by NIR/MCR-ALS and the obtained ones by HPLC. Considering that the evolution of each species is related to each other by the underlying mass balance, the trueness was jointly analyzed for the four concentration profiles corresponding to the species involved in the reaction.

When the values of concentration recovered by NIR/MCR-ALS were plotted vs. the values of concentration obtained by HPLC, a straight regression line was obtained by bivariate least square technique, with a slope near to 1 and an intercept near to 0 (y = 0.97x + 0.01). The qualitative similarity between the profiles obtained by both methods was evaluated in terms of correlation coefficient of this straight line, obtaining a value of 0.991.

The statistical joint interval test of slope and intercept was used to test for the presence of bias. If there are no significant differences between the results obtained by both techniques, the value 1 for the slope and 0 for the intercept should fall within the elliptical confidence region centered on the values of slope and intercept of the obtained straight regression line. Because the validation involved comparisons of values at different concentration levels, the level of significance had to be corrected by using the Bonferroni adjustment [16], in accordance with the following expression:

$$\alpha' = 1(1-\alpha)^{1/k} \qquad \text{Eq. (4)}$$

where α' is the significance level for the individual comparisons, α the overall significance level and *k* the number of comparisons. Therefore, to make a joint confidence statement with 95% probability the results obtained by both techniques were not significantly

different, each individual comparison had to be performed at a significance level α' ≈ 0.001, considering k = 76 comparisons (concentration values of the four species for each one of the nineteen samples compared).

The results show (see Fig. 2) that there is not a significant statistical difference between the concentration profiles obtained by both techniques, considering an α = 0.05 as the overall significance level.

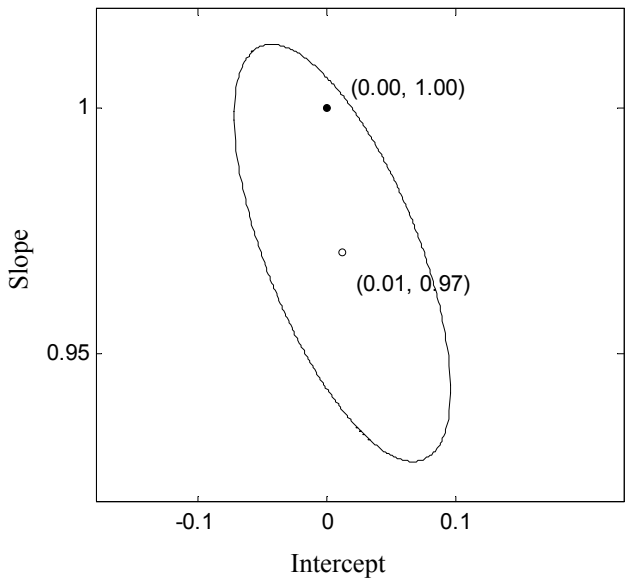

Fig. 2. Joint confidence region for the BLS regression coefficients at a global level of significance of 5%. (○) represents the estimated $\hat{a}$ and $\hat{b}$ valued and (●) corresponds to the theoretical value of zero intercept and unity slope.

From these results it is possible to conclude that there is no bias in the evolution of the species over time obtained by the combination of NIR and MCR-ALS compared to the reference concentration profiles obtained by HPLC.

4.2 Precision

Precision for the NIR/MCR-ALS method has been calculated in terms of intermediate precision conditions for the seven method runs performed in different days and changing the operator and the reagents used. The values of $s_{I(run)}$ ranged between 0.011 and 0.326 mol kg^{-1} for the PGE, 0 – 0.219 mol kg^{-1} for the aniline, 0 – 0.112 mol kg^{-1} for the secondary amine and 0 – 0.136 mol kg^{-1} for the tertiary amine. The largest deviations were found in experiments with molar ratio PGE/aniline 1:1 and 1.25:1 while the lower values were obtained for the experiment with PGE/aniline molar ratio of 2:1.

4.3 Uncertainty

In multivariate curve resolution three sources of error can be found: model errors, instrumental noise and experimental errors [24]. In addition, when the uncertainty is estimated on the basis of the information obtained during the assessment of trueness, also the errors committed during validation should be taken into account (see Scheme 2). As described in a previous article [7], NIR/MCR-ALS applied a bilinear model, which followed the Lambert-Beer law and the number of factors were appropriately selected after the correction of rank deficiency. In addition, the evaluation of the band boundaries of feasible solutions has demonstrated that the rotational ambiguities have been minimized [25], therefore is expected that the magnitude of the model errors was less important than the other components of uncertainty [24]. The uncertainty derived from the model errors

was estimated through the band boundaries of feasible solutions (calculated as in ref [25]) obtained for each of the seven experiments. Since the solutions within the band boundaries fit the experimental data equally well, all of them have a constant probability and, therefore, follow a rectangular (or uniform) distribution. Thus, the uncertainty due to the model errors can be expressed as $u_{model} = \sqrt{\sum u_i^2 / n^2}$, where n = 7 is the number of runs performed to obtain the mean concentration profiles and u_i is the uncertainty of each individual run due to the rotational ambiguities, calculated as the half of the difference between the maximum and the minimum band boundaries, divided by $\sqrt{3}$ because of the rectangular distribution [26]. The values of u_{model} ranged between 8.0 x 10^{-7} – 0.018 mol kg^{-1} for PGE, 7.0 x 10^{-9} – 0.026 mol kg^{-1} for aniline, 2.0 x 10^{-9} – 2.0 x 10^{-5} mol kg^{-1} for the secondary amine and 1.0 x 10^{-9} – 8.0 x 10^{-5} mol kg^{-1} for the tertiary amine. The influence of instrumental noise and experimental errors has been evaluated by performing run-different intermediate precision experiments. The uncertainty of the mean concentration profiles arising from instrumental and experimental errors, u_{exp}, has been estimated by the run-different intermediate precision ($s^2_{I(run)}$) for the seven replicates of the NIR/MCR-ALS procedure.

Thus, in the estimation of the overall uncertainty (see Eq. (2)), the first term, u_{proc}, was calculated as:

$$u_{proc} = ((u_{exp})^2 + (u_{model})^2)^{½} = (s^2_{I(run)} / n) + \sum u_i^2 / n^2)^{½} \qquad \text{Eq. (5)}$$

Finally, the u_{proc} ranged between 0.007 – 0.123 mol kg^{-1} for PGE, 7.0 x 10^{-9} – 0.083 mol kg^{-1} for aniline, 2.0 x 10^{-9} – 0.042 mol kg^{-1} for the secondary amine and 6.0 x 10^{-6} – 0.052 mol kg^{-1} for the tertiary amine.

The $u_{assessment}$ were calculated in accordance with Eq. (3), considering that each reference sample was analyzed three times during the assessment of trueness (n = 3) and the values of *u(ref)* of HPLC for each species were 0.046 mol kg^{-1} for PGE, 0.052 mol kg^{-1} for aniline, 0.021 mol kg^{-1} for the secondary amine and 0.022 mol kg^{-1} for the tertiary amine. The values of *u(ref)* for each species were the mean of the *u(ref)* calculated at each concentration level, because the values were comparable (at a level of confidence of 5%) along the whole range of concentration. So, the $u_{assessment}$ fluctuate between 0.046 – 0.194 mol kg^{-1} for PGE, 0.052 – 0.137 mol kg^{-1} for aniline, 0.021 – 0.068 mol kg^{-1} for the secondary amine, 0.022 – 0.082 mol kg^{-1} for the tertiary amine.

In the estimation of overall uncertainty, only the two first terms under the square root Eq. (2) were considered because no preprocessing steps were carried out and no other source of variation had to be considered. On the basis of these considerations and using a coverage factor k = 2, the overall uncertainty was calculated and the results were depicted in Fig. 3.

The overall uncertainty ranged between 0.095 – 0.460 mol kg^{-1} for PGE, 0.103 – 0.320 mol kg^{-1} for aniline, 0.042 – 0.160 mol kg^{-1} for secondary amine and 0.044 – 0.193 mol kg^{-1} for tertiary amine. From Fig. 3 it can be seen that the largest uncertainties are found in the experiences with lower PGE/aniline molar ratio. If the contribution of each source of error is analyzed (see Scheme 2), nearly a 70 % of the overall uncertainty arises from the errors produced during the process of assessment of trueness, while the other 30 % corresponds to the uncertainty of the procedure (i.e. experimental and instrumental errors and model errors). However, the model errors contribute with less than 1 % to the overall uncertainty.

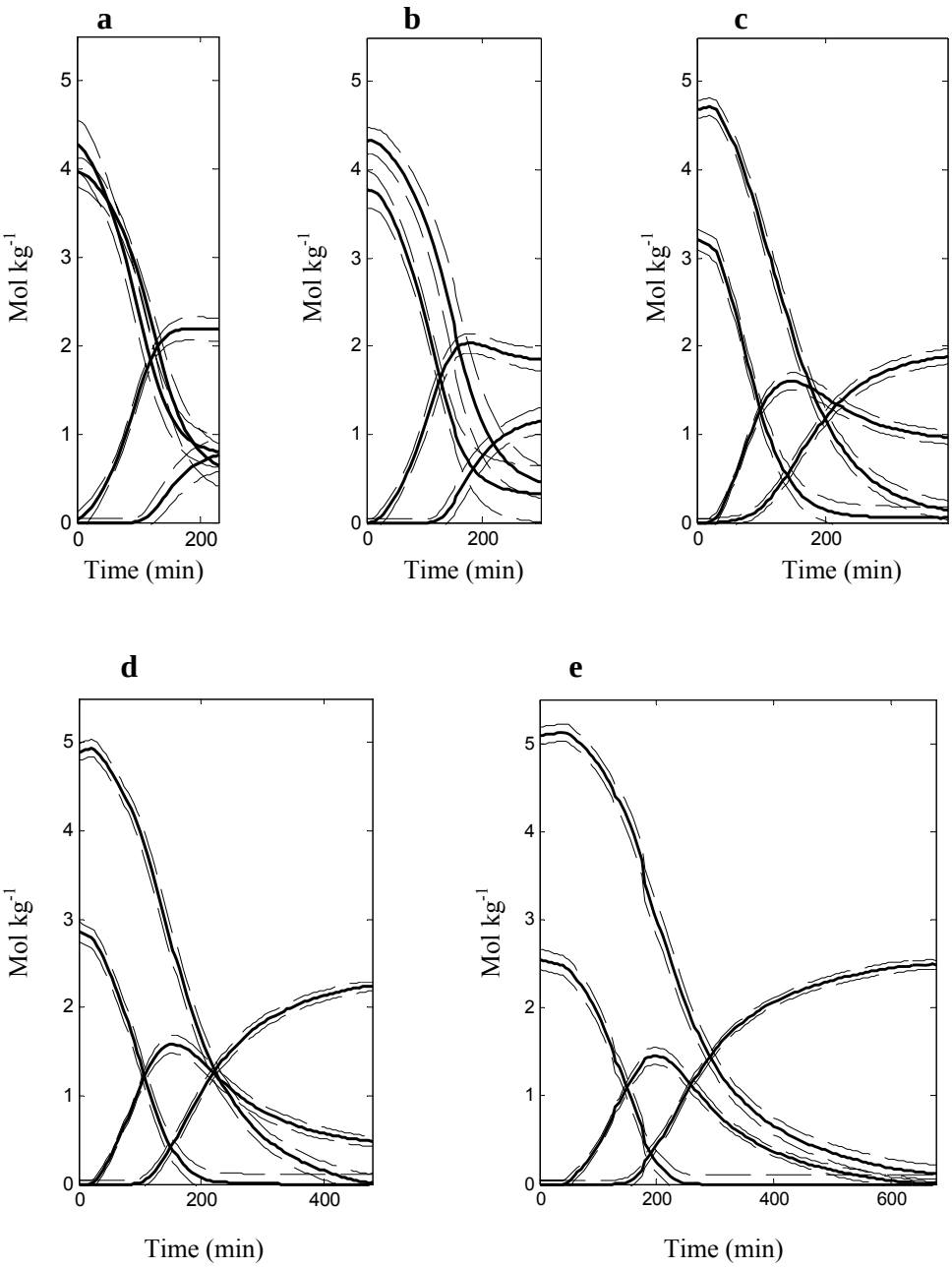

Fig. 3. Uncertainty associated to the results of NIR/MCR-ALS. Solid line: mean concentration profiles (n = 7), dashed line: uncertainty intervals.

4.3 Operational aspects

The amount of reagents consumed, the cost of the instrumentation and its availability, the time spent during the analysis and the cost of the analysis, that includes all the aspects related to the analysis (reagents, personnel costs, etc.) except the instrumentation cost have also been considered. NIR/MCR-ALS does not require any sample pretreatment, therefore, the time devoted to preprocessing the samples is minimal and the use of additional solvents are avoided. Furthermore, if the appropriate accessories are available, the monitoring can be carried out *in situ*. Regarding to the instrumentation cost and availability, depending on the characteristics of the instrument, a near infrared spectrophotometer can be considered affordable in most of industrial laboratories.

The time consumed for the reaction is an inherent characteristic of the system under study and, therefore independent of the analytical technique used for monitoring the reaction. However, the monitoring by NIR is carried out on-line, and during 12 hours of reaction (e.g. when aniline and PGE react in a molar ratio of 2:1) could be possible to automatically record about of 670 NIR spectra. On the other hand, the data treatment by MCR-ALS is moderately elaborate, but when the method is well established and the operator has the appropriate chemometric knowledge, the time consumed in data treatment is slightly longer than the time used for the monitoring of the reaction.

Finally, the cost of the analysis is closely related to the cost in personnel and this is proportional to the time consumed in the analysis. Moreover, the NIR/MCR-ALS is susceptible to be completely automated, which means that the cost of the analysis is drastically reduced.

5. Conclusions

The results obtained from a multivariate data analysis have been validated. Using bivariate least squares and the joint confidence interval test, the absence of bias in the NIR/MCR-ALS method has been assessed. The results indicate that there are no significant differences between NIR/MCR-ALS and HPLC, used as a reference method. In this manner the trueness of the proposed method has been validated.

Likewise, the overall uncertainty of the NIR/MCR-ALS was estimated taking the information obtained during the assessment of trueness into account. The different sources of error that contribute to the overall uncertainty were identified and the relative contribution of each of them has been evaluated.

In addition, some operational characteristics such as capability of automation and short time of analysis make this method an interesting alternative for the monitoring of reactions of epoxy resins.

NIR/MCR-ALS has, therefore, appropriately validated and represents a useful tool to achieve information about the evolution of all species, especially for the developing of kinetic studies.

Acknowledgements

The authors would like to acknowledge financial support provided by the MCyT (project Nº BQU 2003-01142).

References

[1] R. Tauler, A. Izquierdo-Ridorsa and E. Casassas, Chemom. Intell. Lab. Syst., 18, (1993), 293.

[2] A. Izquierdo-Ridorsa, J. Saurina, S. Hernández-Cassou and R. Tauler, Chemom. Intell. Lab. Syst., 38, (1997), 183.

[3] A. de Juan, E. Casassas, and R. Tauler, "Soft-modelling of analytical data" in *Enciclopedia of analytical Chemistry: Instrumentation and Applications*, (Wiley, New York, 2000), p. 9800.

[4] J. Saurina, S. Hernández-Cassou, R. Tauler and A. Izquierdo-Ridorsa, J. Chemometrics, 12, (1998), 183.

[5] A. de Juan, M. Maeder, M. Martínez, and R. Tauler, Chemom. Intell. Lab. Syst. 54, (2000), 123.

[6] Y. Neuhold and M. Maeder, J. Chemometrics 16, (2002), 218.

[7] M. Garrido, I. Lázaro, M. S. Larrechi, F. X. Rius, Anal. Chim. Acta. 515, (2004), 65.

[8] M. Garrido, M. S. Larrechi, F. X. Rius, Appl. Spectrosc. 2, (2006), 174.

[9] ISO, International Organization for Standardization, (1994b) ISO Guide 8402: Quality-Vocabulary, Geneva.

[10] "The fitness for Purpose of Analytical Methods", EURACHEM Secretariat, Internet Version. http://www.eurachem.ul.pt/guides/valid.pdf

[11] M. Thompson, S. L. R. Ellison R. Wood, *Pure Appl. Chem.* 74, (2002), 835.

[12] A. Martinez, J. Riu, O. Busto, J. Guasch, F. X. Rius, Anal. Chim. Acta 406, (2001), 257.

[13] J. Riu, F. X. Rius, Anal. Chem. 68 (1996) 1851.

[14] A. Maroto, J. Riu, R. Boqué, F. X. Rius, Anal. Chim. Acta 391, 1999, 173.

[15] ISO, International Organization for Standardization, (1993) ISO 3534-1. Statistics, Vocabulary and Symbols, ISO Geneva.

[16] D. L. Massart, B. G. M. Vandeginste, L. M. C. Buydens, S. de Jong, P. J. Lewi and J. Smeyers-Verbeke, Handbook of Chemometrics and Qualimetrics: Part A, Elsevier, Amsterdam, 1997.

[17] ISO, International Organization for Standardization (1993) ISO 3534-1, "Statistics, Vocabulary and symbols", ISO, Geneva.

[18] ISO, International Organization for Standardization (1994) ISO 5725 "Precision of Test Methods", ISO, Geneva.

[19] BIPM, IEC, IFCC, ISO, IUPAC, IUPAP, OIML (1993) International Vocabulary of basic and general terms in Metrology, VIM, ISO, Geneva.

[20]C. A. May, *Epoxy Resins*, (Marcel Dekker, New York, 1988).

[21] J. Mijović, A. Fishbain, J. Wijaya, Macromolecules 25, (1992), 979.

[22] The Mathworks, MATLAB Version 6.5, Natick, MA, (2002).

[23] J.J.Kelly, C. H.Barlow, T. M. Jinguji, J. B.Callis, Anal. Chem. 61, (1989), 313.

[24] J. Jaumot, R. Gargallo, R. Tauler, J. Chemometrics 18, (2004), 327.

[25] M. Garrido, M. S. Larrechi, F. X. Rius, R. Tauler, Chemom. Intell. Lab. Syst. 76, (2005), 111.

[26] EURACHEM/CITAC Guide, Quantifying Uncertainty in Analytical Measurement, ed. S. L. R. Ellison, M. Rösslein and A. Williams, 2nd edn., 2000, p. 102, EURACHEM, Berlin (htttp://www.measurementuncertainty.org/mu/guide).

4.6 Conclusiones

En base a los resultados obtenidos para el estudio del sistema modelo PGE/anilina, es posible concluir que la espectroscopía NIR es una técnica instrumental adecuada para el seguimiento *in situ* de las reacciones de resinas epoxy ya que, debido a sus características, no se requiere realizar tratamientos previos a la muestra y las medidas pueden realizarse directamente sobre la mezcla de reacción.

La deficiencia de rango que presentaba el conjunto de datos experimentales fue resuelta exitosamente mediante la estrategia de matrices aumentadas, en dos variantes diferentes (aumentando la matriz de datos con información espectral de los reactivos de partida, o agregando conjuntos de datos correspondientes a la monitorización del mismo proceso pero bajo diferentes condiciones iniciales). Por lo tanto, una vez resuelta la deficiencia de rango, es posible detectar tantas fuentes de variabilidad como especies absorbentes se esperaba encontrar en el sistema químico

La aplicación de MCR-ALS a los datos NIR procedentes de la monitorización ha hecho posible la extracción de información cualitativa, en forma de espectros puros de cada compuesto que participa en la reacción, y al mismo tiempo información cuantitativa que permite conocer la evolución de la concentración de cada especie a lo largo del tiempo, incluso para productos intermedios de la reacción.

La ambigüedad típica de las descomposiciones de datos bilineares fue evaluada para las soluciones obtenidas. La aplicación de restricciones inherentes a la naturaleza química del proceso en estudio permitió reducir considerablemente el número de soluciones posibles, sin embargo sólo con la aplicación de restricciones de igualdad (utilizando sólo unos pocos valores de concentración correspondientes a tres de las especies presentes, procedentes del seguimiento de la reacción mediante ^{13}C RMN) fue posible obtener soluciones únicas para todas las especies en ambos modos (de concentración y espectral).

La veracidad de los perfiles de concentración obtenidos fue evaluada utilizando HPLC como técnica de referencia. Mediante la utilización de mínimos cuadrados bivariantes y el test conjunto de la pendiente y la ordenada al origen fue posible corroborar la ausencia de sesgo (con un nivel de confianza del 5%).

Asimismo, para la estrategia presentada en la sección 4.2 se realizó un estudio de validación para otros parámetros analíticos como la precisión y la incertidumbre, identificando las diferentes fuentes de error y evaluando su contribución a la incertidumbre global.

Las características que ofrece la combinación de NIR y MCR-ALS hacen de las estrategias propuestas una buena alternativa para la monitorización cuantitativa de las reacciones de resinas epoxy, aún cuando las reacciones estudiadas son sistemas modelo que no evolucionan hacia productos sólidos, es decir, que no polimerizan.

4. Estimación de Constantes Cinéticas

5.1 Introducción

La determinación de mecanismos de reacción y constantes de velocidad es de fundamental importancia en química [94] y es una práctica habitual en la química analítica de procesos [95,96]. La cinética de reacción en procesos químicos ha sido estudiada tradicionalmente tomando muestras de la mezcla de reacción y analizándolas externamente mediante técnicas como la cromatografía y, posteriormente, ajustando los datos obtenidos a un modelo cinético mediante métodos de regresión no lineal. Sin embargo, para muchos sistemas de reacción, las muestras pueden ser inestables o puede resultar complicado obtener muestras representativas de la mezcla de reacción. Además, existe la posibilidad de que la reacción continúe desarrollándose durante el tiempo transcurrido entre la toma de muestra y el posterior análisis. Estos problemas pueden ser resueltos realizando medidas espectroscópicas *in situ*.

La monitorización espectroscópica de una reacción puede proveer gran cantidad de información acerca de la reacción química. Habitualmente la información espectral se utiliza de manera univariante, asignando una banda espectral a cada compuesto en la mezcla de reacción. Sin embargo, en la mayoría de los casos, no existen longitudes de onda selectivas para cada una de las especies existentes. Por el contrario, frecuentemente existe solapamiento espectral entre las bandas correspondientes a algunos compuestos. En los últimos tiempos, también se han realizado estudios cinéticos ajustando el modelo cinético directamente a los datos espectrales multivariantes [97,98]. Esto permite solucionar algunos de los problemas mencionados y analizar sistemas de mayor complejidad.

El modelado matemático de datos espectroscópicos puede realizarse de dos maneras diferentes: analizando los datos mediante métodos de modelado blando, donde no es necesario el conocimiento del modelo cinético vinculado a la reacción estudiada, o a

través de métodos de modelado duro, que requiere la postulación previa de un esquema de reacción.

La utilización de métodos de modelado blando (por ejemplo, MCR-ALS) evita los errores causados por asumir un modelo incorrecto y permite modelar las señales originadas por analitos que no siguen un esquema de reacción bien definido, o que no participan del proceso estudiado. La principal desventaja de estos métodos es la ambigüedad rotacional asociada con los perfiles obtenidos. Este problema es especialmente importante en espectroscópicos correspondientes al seguimiento de reacciones quimicas, donde es común la ausencia de regiones de selectividad [33]. Además, los métodos de modelado blando permiten obtener perfiles cinéticos que describen la evolución de cada especie con respecto al tiempo, pero no se obtienen parámetros cinéticos como las constantes de velocidad de reacción.

Los métodos de modelado duro están basados en un mecanismo de reacción postulado para el sistema en estudio [64] que deriva en un modelo cinético expresado a través de ecuaciones diferenciales cuyas variables son las absortividades molares de las diferentes especies y las constantes cinéticas. El modelo cinético es ajustado a los datos experimentales para obtener las constantes cinéticas. Este proceso se puede realizar mediante diversos métodos de ajuste no lineal [64]. Esto significa que el ajuste se realiza teniendo en cuenta los parámetros no-lineales (constantes cinéticas) y descartando los parámetros lineales (absortividades molares de cada especie a cada longitud de onda). Esta considerable reducción de los parámetros a ajustar es lo que confiere robustez a los métodos de modelado duro. El principal inconveniente de estos métodos radica en la determinación correcta del modelo cinético. La selección del modelo adecuando, a falta de experimentos suplementarios o de un conocimiento químico profundo del sistema en estudio, normalmente consiste en un procedimiento de “prueba y error” que puede resultar tedioso. Otra de las desventajas de los métodos de modelado duro es que no operan correctamente en presencia de artefactos como deriva de la línea de base o ruido espectral.

Otra posibilidad para el análisis de datos espectroscópicos procedentes de la monitorización de reacciones consiste en una estrategia capaz de combinar los métodos de modelado blando y duro. Así, la flexibilidad ligada a los métodos de modelado blando permite modelar contribuciones diferentes a aquellas relacionadas con el proceso de reacción estudiado (derivas en la línea de base, ruido espectral, especies absorbentes que no participan en el proceso de reacción) o analizar simultáneamente experimentos diferentes mientras que, gracias al modelado duro, es posible obtener las constantes cinéticas vinculadas a la reacción.

Esta combinación o "modelado blando-duro" puede implementarse de dos formas diferentes. Uno de estos procedimientos implica, en un primer paso, la resolución del sistema mediante un método de modelado blando. En un segundo paso, los perfiles de concentración de las especies ligadas a la reacción en estudio, obtenidos mediante el modelado blando, se ajustan a un modelo cinético (modelado duro). El otro procedimiento comprende la resolución del sistema mediante un método de modelado blando pero aplicando, en cada iteración del algoritmo, una restricción sobre los perfiles de concentración de las especies que intervienen en la reacción, consistente en el cumplimiento de un modelo cinético establecido. Ambas estrategias de combinación de los métodos de modelado duro y blando permiten obtener tanto los perfiles de concentración que satisfacen el modelo cinético propuesto, como las correspondientes constantes de velocidad de reacción.

La primera de las estrategias es útil cuando se posee un conocimiento profundo del sistema estudiado (mecanismo de reacción, concentraciones iniciales de los reactivos de partida) y todas las fuentes de variación observadas se deben sólo a la reactividad de las especies ligadas al modelo cinético postulado. La principal desventaja de esta estrategia es que los perfiles de concentración obtenidos mediante un método exclusivamente blando están afectados por la ambigüedad rotacional, lo que implica una propagación del error a las constantes cinéticas obtenidas.

La segunda estrategia permite minimizar (o incluso eliminar) la ambigüedad, puesto que el modelo cinético se utiliza como una restricción fuerte durante el proceso de optimización. Además, permite analizar sistemas de los cuales se desconoce la concentración de partida de los reactivos. Por otra parte, algunas de las especies presentes en el sistema pueden modelarse de manera blanda (aquellas que no están vinculadas al modelo cinético subyacente) mientras que las especies de interés son ajustadas al modelo cinético propuesto. De todas maneras, la obtención de buenos resultados está condicionada a la correcta selección del modelo que se emplea como restricción.

En este capítulo se han aplicado las dos estrategias de modelado blando-duro. La primera de las estrategias (MCR-ALS seguida de un paso de ajuste no lineal) se ha aplicado a dos sistemas modelo. En la sección 5.2 se muestra su aplicación al sistema PGE/anilina, mientras que en la sección 5.3 se ha estudiado el sistema PGTE/anilina, en el que el monómero epoxídico cambia un grupo éter por un grupo tioéter. La comparación de los resultados obtenidos permite evaluar la influencia de los heteroátomos ligados a la estructura de los monómeros en el proceso de reacción. La segunda estrategia (llamada HS-MCR, por Hard and Soft modelling) utiliza una modificación del algoritmo ALS que incluye el cumplimiento del modelo cinético como restricción y fue aplicada a datos precedentes de la monitorización NIR de la reacción entre GDMPS (monómero que contiene silicio en su estructura) y anilina. Los resultados, que se muestran en la sección 5.4, han sido comparados con los datos obtenidos de la monitorización de la reacción mediante ^{13}C RMN.

5.2 Multivariate Curve Resolution-Alternating Least Squares and kinetic modelling applied to near infrared data from curing reactions of epoxy resins. Mechanistic approach and estimation of kinetic rate constants

Applied Spectroscopy, 60(2), **2006**, 174-181

M. Garrido, M.S. Larrechi and F.X. Rius*

Department of Analytical and Organic Chemistry, Faculty of Chemistry, Rovira i Virgili University, Marcel·lí Domingo s/n (43007), Tarragona, Spain

(Received 20 May 2005; accepted 20 December 2005)

Abstract

This study describes the combination of Multivariate Curve Resolution-Alternating Least Squares with a kinetic modelling strategy, based on a kinetic model, for obtaining the kinetic rate constants of a curing reaction of epoxy resins. The reaction between phenyl glycidyl ether and aniline is monitored by near infrared spectroscopy under isothermal conditions for several initial molar ratios of the reagents. The data for all experiments, arranged in a column-wise augmented data matrix, are analyzed using Multivariate Curve Resolution-Alternating Least Squares. The concentration profiles recovered are fitted to a chemical model proposed for the reaction. The selection of the kinetic model is assisted by the information contained in the recovered concentration profiles. The non-linear fitting provides the kinetic rate constants. The optimised rate constants are in agreement with values reported in the literature.

1. Introduction

Epoxy resins have been widely studied in the past and continue receiving worldwide attention because of the increasing number of their industrial applications. The curing conditions strongly influence the intended properties of the epoxy resins, so optimising the curing requires a reliable kinetic model for the reactions that take place during the process. Research has therefore focused in determining the reaction mechanism and quantifying the kinetic parameters. Many mechanisms have been proposed[1-4] but, though the experiments have tried to verify these mechanisms, the real mechanism is still not fully understood.

The curing of epoxy resins, mainly with amines as a curing agent, has been monitored by several techniques. Calorimetric methods such as Differential Scanning Calorimetry (DSC)[5] obtain only the overall conversion of the reaction because of the assumption that the rate of heat release is proportional to the rate of the reaction. However, Modulated Temperature DSC (MTDSC)[6] provides more information because the heat capacity signal can be used to distinguish between the primary amine-epoxy and secondary amine-epoxy steps. Concentration profiles of the reaction have been obtained by High Performance Liquid Chromatography (HPLC),[6,7] which, though an essentially off-line technique, is often used for the kinetic investigation of reactions that do not evolve toward solid products.

Spectroscopic techniques, such as Fourier Transform Infrared Spectroscopy (FTIR)[8] or Near Infrared Spectroscopy (NIR),[9] provide information on the individual species of interest and, if the appropriate accessories are available, allow the cure reactions to be monitored *in situ*. However, NIR spectra are much simpler than mid-IR spectra,[10] and relatively large amounts of sample can be used, because molar absorptivities are much lower in this region.[11] In spite of this, the direct measurement of concentrations of reactive

species involves deciding on a baseline for peak integration in combination with appropriate reference bands, which means that the later stages of the cure are difficult to monitor. Also, some bands, for example those related to the secondary amine, have to be decomposed,[11,12] which requires further assumptions.

Some of these problems can be avoided by using Multivariate Curve Resolution methods such as Alternating Least Squares (MCR-ALS),[13-16] in which the NIR data from the monitoring of the reaction are all processed together and a large number of variables (wavelengths) are taking into account. Consequently, a set of pure spectra and concentration profiles of each species (showing their evolution over time) is obtained. These types of methods are often called 'soft-modelling approaches' because they can describe processes without explicitly using the underlying chemical model linked to them.[17]

To determine the kinetic parameters of the chemical system under study, the data from the monitoring of the reaction (obtained by any of the above-mentioned techniques), have to be fitted to a chemical model in a separate step.[6,7,9] This method is usually known as 'hard-modelling' and involves the non-linear least-squares (or similar) fitting of the parameters of a chemical model describing the data.

The most difficult aspect of hard modelling is determining the correct model. The simplest model, which suitably fits the data within the error limits of the measurements, is often chosen. But this does not guarantee that the model will be correct. Most soft-modelling approaches can be useful for designing a suitable reaction model and supporting the model chosen.[18,19]

Soft-modelling has already been combined with the hard-modelling approach either by incorporating a hard-modelling step into a MCR-ALS method[18,20] or by applying the hard-modelling approach after the MCR-ALS optimisation[21] but only for (pseudo) first-order kinetic models. The epoxy-amine reaction studied in this paper can be described as

pseudo-termolecular step consisting of two successive bimolecular reactions.[6] The chemical model is therefore rather complex.

In this study we propose a model for the cure reaction on the basis of the concentration profiles obtained by MCR-ALS from the near-infrared monitoring of the reaction between phenylglycidylether (PGE) and aniline.[16] We have also estimated the kinetic parameters (rate constants) by applying the 'hard-modelling' approach to the ALS concentration profiles.

2. Theory

In Multivariate Curve Resolution, a bilinear decomposition of the experimental data matrix is performed using the following model equation:

$$\mathbf{D} = \mathbf{C}\,\mathbf{S}^T + \mathbf{E} \qquad \text{Eq.(1)}$$

where the dimensions of the matrices are: **D**(NR,NC), **C**(NR,N), $\mathbf{S}^T$(N,NC); **E**(NR,NC), N is the number of components considered (chemical species contributing to the signal), NR is the number of rows (in spectroscopic data, NR is the number of spectra) in data matrix **D**, and NC is the number of columns (in spectroscopic data, NC is the number of wavelengths) in data matrix **D. C** is the matrix describing how the contribution of the N species changes in the different NR rows of the data matrix (concentration profiles). $\mathbf{S}^T$ is the matrix describing how the response of these N species changes in the NC columns of the data

matrix (pure spectra profiles). **E** is the residual matrix with the data variance unexplained by $\mathbf{C}\,\mathbf{S}^T$.

Multivariate resolution can be carried out by MCR-ALS. This is an iterative method that calculates in each cycle new **C** and $\mathbf{S}^T$ matrices that incorporate a set of constraints based on the chemical information available (non negativity, closure, unimodality, etc.) in order to minimize the residual matrix **E**. The process involves the following steps:

(1) Determination of the number of components, N, in the experimental data matrix **D**,
(2) Construction of the initial estimate of spectra, $\mathbf{S}^T$ (or concentration profiles, **C**),
(3) Given **D** and the initial estimate $\mathbf{S}^T$, least-squares calculation of **C** under the suitable constraints,
(4) Given **D** and **C**, least-squares calculation of $\mathbf{S}^T$ under the suitable constraints, and
(5) Reproduction of **D**, using **C** and $\mathbf{S}^T$. If the conversion criterion is fulfilled, the process is finished. If not, go back to step 3.

The correct resolution of the system is possible if the rank of the data matrix (chemical rank) is assumed to be equal to the number of absorbing species when no other contributions, such as instrumental noise, are present. Since matrix **D** can be considered as the product of two matrices ($\mathbf{D} = \mathbf{C}\mathbf{S}^T$), the rank obtained for matrix **D** can be understood from the following mathematical property of the rank: when matrix **D** can be decomposed into the product of two matrices, **C** and $\mathbf{S}^T$, then $\text{rank}(\mathbf{D}) \leq \min(\text{rank}(\mathbf{C}), \text{rank}(\mathbf{S}^T))$. When the systems analyzed come from processes in evolution, the data sets are often rank-deficient, i.e. their chemical rank is lower than the total number of absorbing compounds. Rank-deficiency can be broken by column-wise matrix augmentation, as has already been

demonstrated.[16,22] In all cases, the success of rank augmentation is linked to the strategy of choosing which individual data matrices must be included in the augmented one.

MCR-ALS is one of to the so-called soft-modelling methods because the spectral and concentration profiles can be obtained without using an explicit kinetic model. Information about kinetic parameters is therefore not available from the MCR-ALS results. However, MCR-ALS results can be useful for obtaining these kinetic parameters by applying a Non-Linear Least-Squares fitting.

In agreement with Beer's law, a matrix **D** (NR x NC) of spectroscopic data with *N* absorbing components can be decomposed into the product of a concentration matrix **M** (NR x N) and a matrix **A** of the molar absorptivities (N x NC) but, because of the instrumental noise of the measurements, the decomposition does not represent **D** exactly. Therefore, a matrix of residuals, **R**, is established as follows:

$$\mathbf{R} = \mathbf{MA} - \mathbf{D} \qquad \text{Eq.(2)}$$

Prior to the non-linear fitting, matrix **D** is decomposed by factor analysis following Eq. (1). In this paper we used the MCR-ALS method. It is assumed that the matrix **E** of residuals in Eq. (1) can be neglected because it does not contain relevant information. Therefore, almost all the variance in the experimental data is expressed by the product $\mathbf{CS}^T$.

$$\mathbf{R} = \mathbf{MA} - \mathbf{C}\,\mathbf{S}^T \qquad \text{Eq. (3)}$$

The aim of Non-Linear Least-Squares fitting is to find the set of parameters for

which the sum of the squares of all the elements of the matrix **R** of residuals is minimal.[23]

Matrix **M** is obtained by integrating the differential equations (by using Runge-Kutta method) of the suitable kinetic model, which quantitatively describes the reactions and concentrations of all components in the system. The model is expressed as a function of the kinetic rate constants, which are usually non-linear parameters. The matrix **A** is composed of the molar absorptivities of the reacting components, which are linear parameters. An important point is that linear parameters can be eliminated from the optimisation process. [18] They can be explicitly calculated as $\mathbf{A} = \mathbf{M}^{+}\mathbf{D}$, where $\mathbf{M}^{+}$ is the pseudo inverse of the matrix **M** (also $\mathbf{S}^{T} = \mathbf{C}^{+}\mathbf{D}$). [24] Therefore, only is necessary the fitting of the non-linear parameters.[18]

A function representing the sum of squares of **R** is optimised by using a multi-parameter minimum search based on the Nelder-Mead algorithm.[25] This function simulates the concentration profiles (matrix **M**) and calculates the difference between the simulated concentration profiles and the profiles resolved by MCR-ALS (matrix **C**). As a result, the optimized kinetic rate constants are obtained.

3. Experimental

3.1 Reaction conditions and procedure

The reaction between PGE and aniline, which acts as the curing agent was performed at 95º C. The molar ratio between PGE and aniline was chosen to ensure that only the reaction under study took place and that there were no collateral

etherification or homopolymerization reactions.[7,12] Five experiments were performed. In these experiments the molar ratios between the reactants were varied to obtain the following PGE/aniline ratios: 1:1, 1.25:1, 1.5:1, 1.75:1 and 2:1. The procedure involved mixing the necessary amounts of aniline and PGE at room temperature in order to obtain the desired molar ratio and then immediately injecting 1 mL of this mixture into the liquid cell of the NIR spectrophotometer. The cell temperature was set at 95ºC.

3.2 Data acquisition and pretreatment

The data obtained correspond to the NIR spectra recorded every 4 nm between 1100 and 2500 nm in an InfraAlyzer 500 Bran-Luebbe spectrophotometer. For each experiment, we acquired data at intervals of 5 minutes until the end of the reaction. The band at 2208 nm, which is characteristic of the oxirane group, was chosen as a reference. The reaction was considered to be completed when this band disappeared. In this way, the times of spectra recorded for each experiment, expressed in increasing order with respect to the proportion of epoxide, were: 230, 300, 390, 480 and 675 min.

All the spectra were corrected in order to eliminate the vertical shift caused by using a NIR spectrophotometer with only one light beam.[16,26] Also, selection of wavelengths was performed by selecting the wavelengths of interest and ignoring those with no variation over time, because these provide no information about the reaction under study. The regions of the spectrum in which only noise was detected were also eliminated. The selected wavelengths ranged from 1400 to 2432nm.

The pretreated data were arranged in matrices whose rows were the number of recorded spectra and whose columns were the wavelengths. The following matrices were thus obtained: $\mathbf{D_1}$ (47 x 259), $\mathbf{D_2}$ (61 x 259), $\mathbf{D_3}$ (79 x 259), $\mathbf{D_4}$ (97 x 259) and $\mathbf{D_5}$ (136 x

259). These corresponded to the experiments with PGE/aniline molar ratios of 1:1, 1.25:1, 1.5:1, 1.75:1 and 2:1, respectively. The number of rows in the matrices depends on the different reaction times in each experiment. The higher the PGE/aniline ratio, the higher the number of considered rows. All matrices had the same column length i.e. two hundred and fifty-nine NIR wavelengths, from 1400 to 2432 nm, every 4 nm. In the same conditions, the NIR spectra of the pure reactants were also recorded. The spectra recorded in the InfraAlyzer 500 were exported and converted into MATLAB binary files.[27,28]

3.3 Multivariate Curve Resolution-Alternating Least Squares optimisation (MCR-ALS)

The rank of all data matrices was analyzed with Singular Value Decomposition (SVD).[29] It is assumed that the singular values associated to the chemical components are much larger than other possible contributions such as instrumental drift or experimental error. The chemical rank was thus estimated by simply inspecting the tables of singular values for each data matrix analyzed. Rank deficiency of experimental data matrices was solved by column-wise matrix augmentation.[16,22] The column-wise augmented data matrix (420 x 259 in size) was constructed with the five sets of pretreated data (corresponding to the five experiments).

The initial estimate for the pure spectra was constructed, as in a previous article,[16] by applying the SIMPLISMA algorithm[30] to the augmented matrix and using the experimentally recorded pure spectra of the reactants (PGE and aniline).

The ALS algorithm[31] was iterated by applying a series of constraints in order to find a solution that was consistent with the chemical problem and restrict the number of possible solutions. These constraints were:

a) The values of the spectra of each component must be non-negative,

b) The values of the concentration profiles as a function of time must be non-negative,

c) The system must be closed related to the total analytic concentration, and

d) Each concentration profile must have only one maximum (unimodality).

Note that the pure spectra used to construct the initial estimate were not fixed throughout the resolution process.

3.4 Non-linear fitting

The computer program for non-linear optimization was *home-made* as follow: first, a function consisting of the differential equations of each compound present in the reaction was constructed in accordance with the chemical reaction model for the system. This model was based on our previous knowledge of the system and on the results of the MCR-ALS optimization. This function was integrated numerically using an ordinary differential equation solver (ODE23, a Runge-Kutta subroutine of MATLAB[27]) in order to obtain matrix **M** (see Theory section). The kinetic concentration profiles were therefore completely defined by the model, the rate constants and the intial concentration of the reacting compounds.

The multi-parameter minimum search (fminsearch, from Matlab Optimization Toolbox,[28]) based on the Nelder-Mead algorithm,[25] then found the rate constants that provided the best fit between the profiles obtained from the kinetic model (matrix **M**) and the MCR-ALS concentration profiles (matrix **C**). The fitting had to begin with reasonable initial guesses for the rate constants, which are refined iteratively. The initial estimates used for the rate constants were within the range of values cited in the bibliography.[5-7,9,32]

The goodness of the fitting can be evaluated by the % relative error:

$$RE = \sqrt{\frac{\sum_i \sum_j \left(m_{ij} - c_{ij}\right)^2}{\sum_i \sum_j \left(c_{ij}\right)^2}} \times 100 \qquad \text{Eq. (4)}$$

where m_{ij} represents the elements of matrix **M** (the profiles obtained by using the optimized rate constants) and c_{ij} represents the elements of matrix **C** (the MCR-ALS profiles).

4. Results and discussion

Fig. 1 shows the five concentration profiles obtained, when the augmented matrix was analyzed, by MCR-ALS for the four species that took part in the reaction. These concentration profiles correspond to the five reactions carried out with different PGE/aniline molar ratios. The concentration profiles recovered for the ALS algorithm were expressed in mass units, so the corresponding values in moles were obtained by dividing each concentration profile by the corresponding molecular weight and assuming that each species and their molecular weight are known. Note that these profiles were resolved without previous postulation of a chemical model and satisfactorily represent the evolution of each compound involved in the reaction.[16]

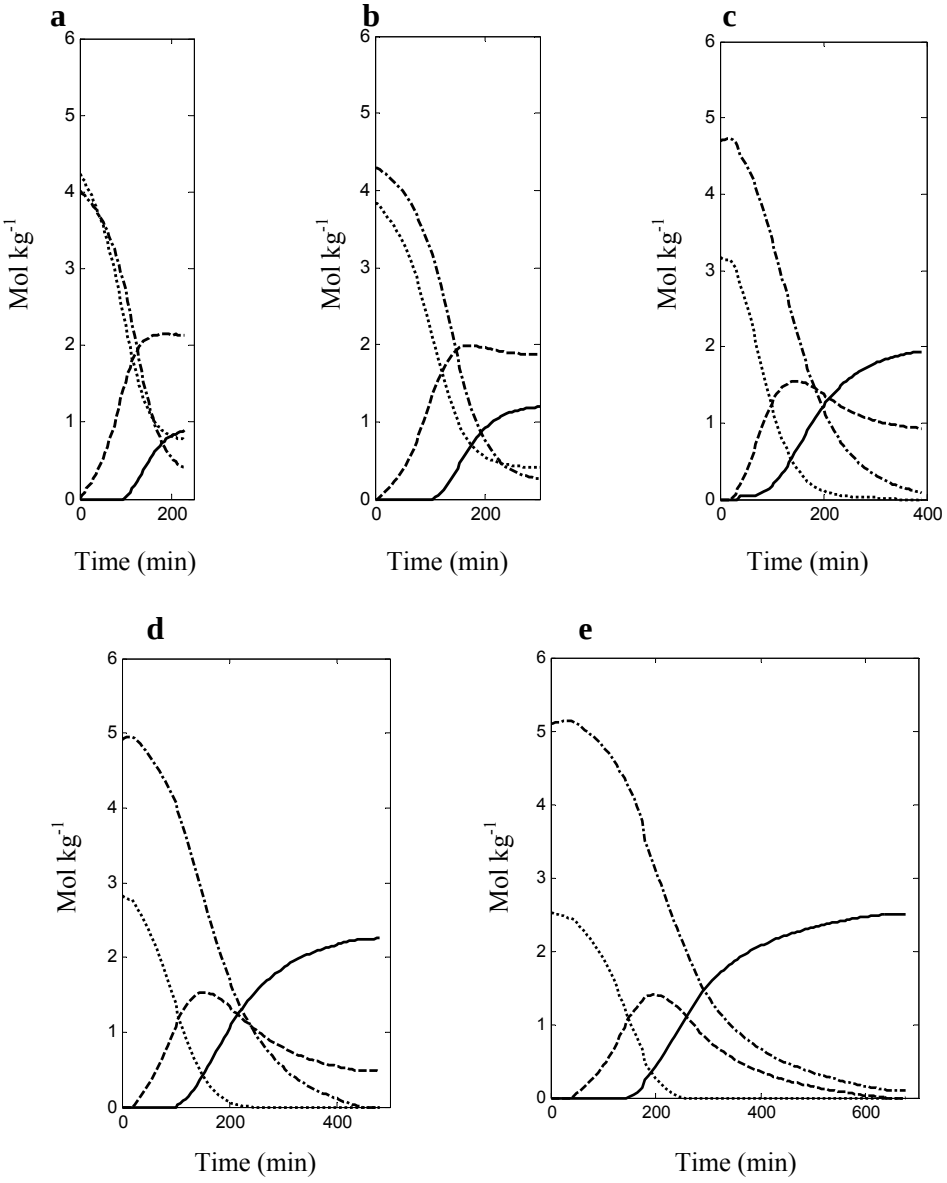

Fig.1. Concentration profiles (in mol kg^{-1}) obtained by MCR-ALS optimisation for the five PGE/aniline molar ratios: a) 1:1, b) 1.25:1, c) 1.5:1, d) 1.75:1 and e) 2:1. Aniline (dotted line), PGE (dash-dot line), secondary amine (dashed line) and tertiary amine (solid line).

Except for small differences in the experiments 1.25:1 and 1:1, where the solutions were not far from the expected values, the resolved concentration profiles basically reproduced the molar ratios that were initially used for the reagents in each experiment. In the first 100 minutes of the reaction, we can see (see Fig. 1) that the changes in concentration with respect to time are approximately the same for PGE and aniline, since the main reaction taking place is the one involving primary amine (see below).

When the aniline has reacted completely, the variation in PGE slows down because the reaction between secondary amine and PGE controls the process. This is clearly seen in experiments 2:1, 1.75:1, and 1.5:1. Also in these experiments, once the aniline has reacted completely, the variations over time for the secondary and tertiary amines are the same but negative for the secondary amine and positive for the tertiary amine. This behaviour is expected since a mol of secondary amine leads to a mol of tertiary amine (see below). At the end of experiment 2:1, the concentration of tertiary amine reached the value predicted by the stoichiometry of the reaction. The evolution of the species over time is similar to the behaviour in the HPLC profiles in the literature.[6]

To obtain the corresponding kinetic parameters, i.e. the kinetic rate constants, these profiles have to be fitted to a chemical model. Determining the correct chemical reaction model is critically important in this process and usually requires previous chemical knowledge.

The reaction between PGE and aniline can be represented by these two bimolecular reactions:

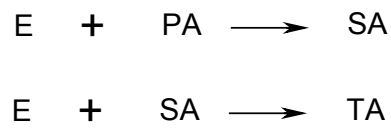

where E is the epoxide, PA is the primary amine, SA is the secondary amine, and TA is the tertiary amine. Only these reactions should be considered, since reactions like homopolymerization and etherification only take place when specific catalysts are present or when the curing is performed at elevated temperatures.[7,12,33] This approach is useful for describing the process in a general way but the formation of numerous intermediate complexes arising from donor-acceptor interactions makes the reaction mechanism more complex.[4]

Our analysis in this paper is based on the mechanism proposed by Xu et al.[9] It is well known that compounds containing oxygen-hydrogen and nitrogen-hydrogen bonds can play the role of catalysts for epoxy-amine reactions.[7] The mechanism involves an initial interaction between epoxy groups with proton donor molecules (OH or NH_2 groups), leading to the formation of hydrogen bond complexes (also named "reactive complexes") (Fig. 2 a and 2 b). The reaction between these reactive complexes and primary or secondary amines give a secondary or tertiary amine, respectively, in both cases through the formation of a termolecular intermediate (see Fig. 2 c-e). The formation of the termolecular intermediate is considered the rate controlling step in the reaction.[9]

In accordance with this mechanism, in the early stages of the reaction, when hydroxyls are absent, the amine groups can act both as an electrophilic and a nucleophilic agent. Since the hydroxyl group is a much stronger electrophilic agent than an amine, the catalysis carried out by amine groups is less effective and relatively unimportant during the course of the reaction. However, at the very beginning of the cure, this reaction path is important because the initiation of the mechanism depends on the catalytic ability of the amine groups (Fig. 2 c). As the reaction advances, the catalysis due to hydroxyl groups gains relevance (Fig. 2 d), and when the tertiary amine starts to form, significant amounts of hydroxyl groups already exist. Therefore, the reaction between epoxide and secondary

amine catalyzed by the amine group can be safely neglected because it is dominated by the hydroxyl-catalytic reaction path (Fig. 2 e).

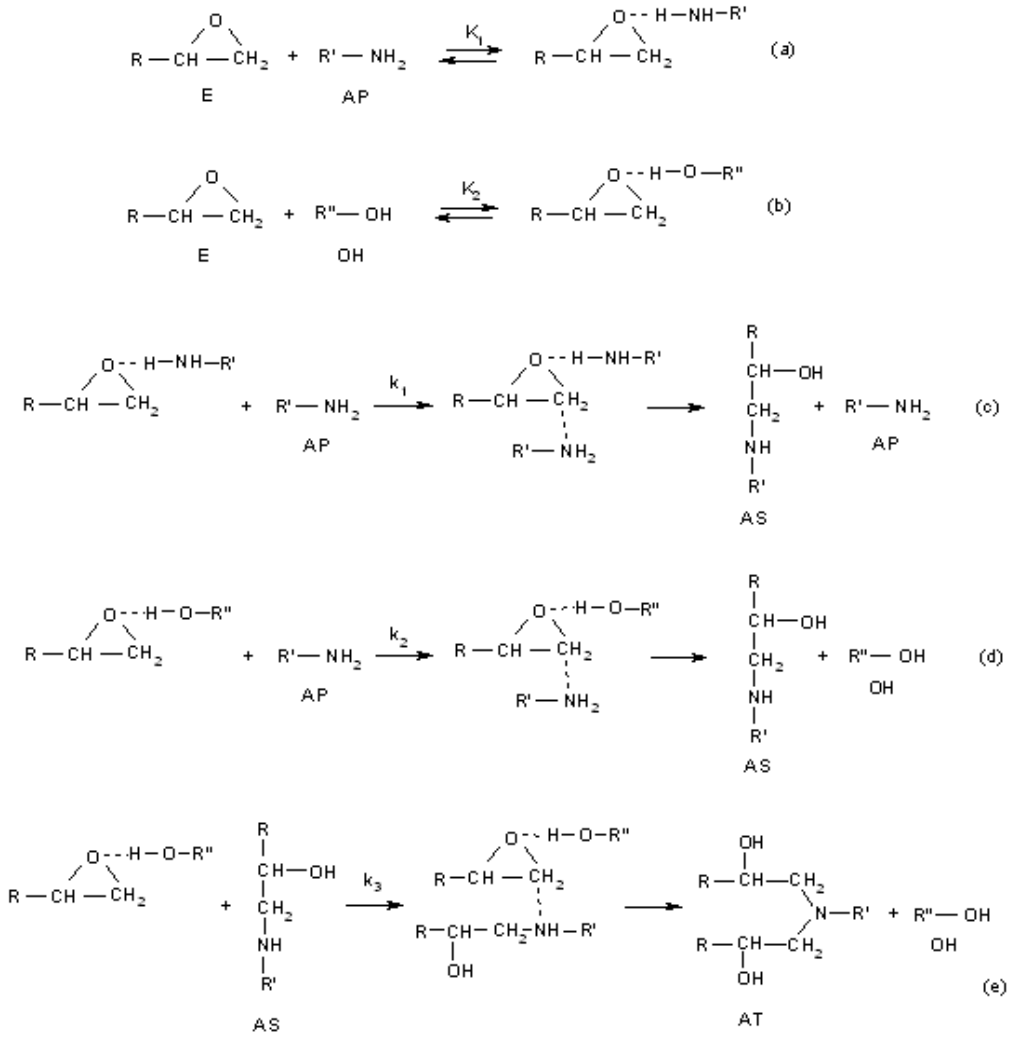

Fig. 2. Mechanism of the epoxy-amine reaction

Some authors take into account the formation of other complexes, called non-reactive complexes, between hydroxyl groups, amine groups and the ether group of epoxy (see Fig. 3 a-c).[4,6] While reactive complexes (see above) assist the reaction and cause an accelerated rate, the non-reactive complexes reduce the concentration of some of the reactive species, i.e. they slow down the reaction.

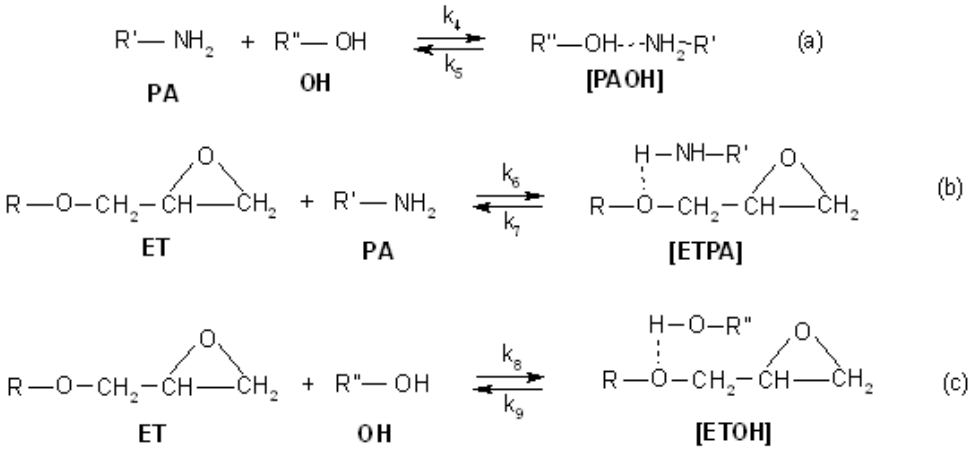

Fig. 3. Non-reactive complexes equilibria

From the assumption that the formation of the termolecular intermediate is the rate-determining step, and taking into account the reactive and non-reactive complexes, the following differential equations are derived:

$$d[PA]/dt = -k_1'[E][PA]^2 - k_2'[E][OH][PA] - k_4[PA][OH] + \\ + k_5[PAOH] - k_6[PA][ET] + k_7[ETPA] \qquad \text{Eq. (6)}$$

$$d[E]/dt = -k_1'[E][PA]^2 - k_2'[E][OH][PA] - k_3'[E]OH][SA] \qquad \text{Eq. (7)}$$

$$d[SA]/dt = k_1'[E][PA]^2 + k_2'[E][OH][PA] - k_3'[E]OH][SA] \quad \text{Eq. (8)}$$

$$d[TA]/dt = k_3'[E][OH][SA] \quad \text{Eq. (9)}$$

$$d[PAOH]/dt = k_4[PA][OH] - k_5[PAOH] \quad \text{Eq. (10)}$$

$$d[ETPA]/dt = k_6[PA][ET] - k_7[ETPA] \quad \text{Eq. (11)}$$

$$d[ETOH]/dt = k_8[ET][OH] - k_9[ETOH] \quad \text{Eq. (12)}$$

where $k_1' = K_1k_1$, $k_2' = K_2k_2$, $k_3' = K_2k_3$, OH represents the hydroxyl group, ET corresponds to the ether group of the epoxide and PAOH, ETPA and ETOH are the non-reactive complexes depicted in Fig. 3 a, b and c, respectively.

The iterative fitting of the parameters needs to be started with initial guesses for the rate constants. Normally convergence is satisfactory for any reasonable initial guesses. Table I shows the initial estimates used for the rate constants. The values for the equilibrium constants were found[6] but the values for the formation rate constants (k_4, k_6, k_8) and the dissociation rate constants (k_5, k_7, k_9) for the non-reactive complexes were not available in the literature. Different values for these latter rate constants were therefore tested in accordance with the following relationship: $k_{formation}/k_{dissociation} = K_{equilibrium}$ and assuming that the formation of non-reactive complexes are pseudoequilibria.[9]

The calculated optimal fit was verified by changing the value for the different rate constants and simulating the corresponding kinetic profiles. Both positive and negative changes with respect to the optimal value led to an increase in the sum of squares of the residuals **R'** Eq. (5). The values of the rate constants for the non-reactive complexes were varied in pairs in order to mantain the same value for the equilibrium constant.

Table I also shows the resulting rate constants after carrying out the fitting. The order of magnitude for k_2'and k_3' is in agreement with the values reported in the literature.[6,7,9,32] In table II the obtained rate constants are compared with the values reported in the literature for k_1', k_2', and k_3'. Moreover, the substitution effect (ρ), defined as the ratio of the consumption rates of epoxide groups by secondary and primary amine functionalities ($\rho = k_3'/k_2'$),[6,9] gives a value of 0.32, which is close to the theoretical value expected for aromatic amines.[34,35] On the other hand, the value for k_1' is over one order of magnitude slower than the value expected from other studies,[6,7,9,32] possibly because of the high purity of the reactants used in this study. It has been reported that the value of this rate constant is very sensitive to the purity of the reactants.[36] When no impurities are present in the reacting mixture, the reaction is slower at the beginning, and the value of k_1' es smaller.

	Initial Estimates	Fitted rate constants
$k_1' \times 10^3$ ($kg^2mol^{-2}min^{-1}$)	0.01	0.0075
$k_2' \times 10^3$ ($kg^2mol^{-2}min^{-1}$)	4	4.3
$k_3' \times 10^3$ ($kg^2mol^{-2}min^{-1}$)	1	1.4
$k_4 \times 10^3$ ($kg\ mol^{-1}min^{-1}$)	0.01	0.01
$k_5 \times 10^3$ (min^{-1})	0.045	0.041
$k_6 \times 10^3$ ($kg\ mol^{-1}min^{-1}$)	0.8	0.4
$k_7 \times 10^3$ (min^{-1})	3.6	4
$k_8 \times 10^3$ ($kg\ mol^{-1}min^{-1}$)	0.01	0.009
$k_9 \times 10^3$ (min^{-1})	0.045	0.05

Table I. Initial guesses for the rate constants and fitted rate constants.

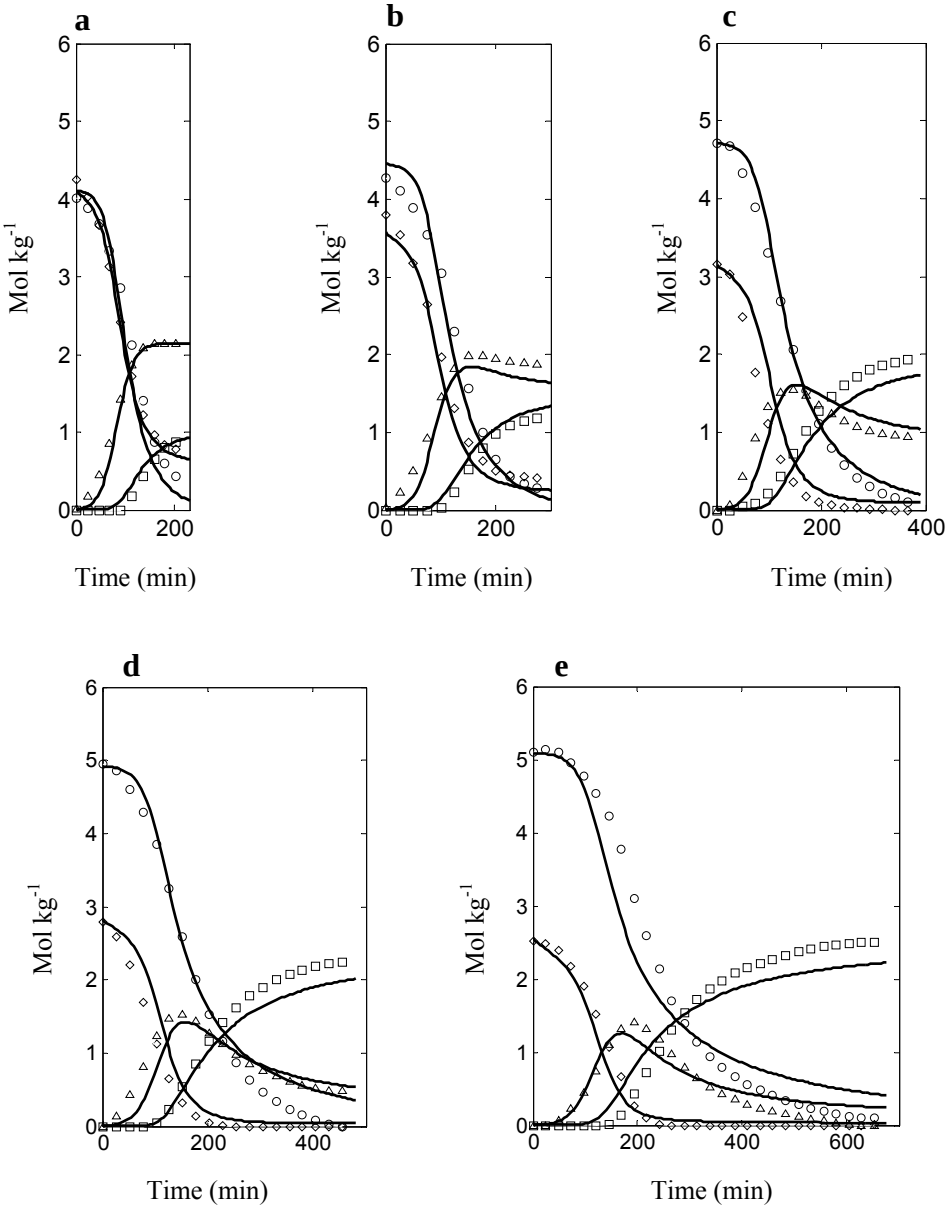

Fig. 4. Overlap of experimental concentration profiles recovered after MCR-ALS optimisation for PGE (○), aniline (◊), secondary amine (Δ) and tertiary amine (□), and the profiles obtained by integration of the proposed chemical model using the fitted rate constants (solid line).

Fig. 4 shows a comparison between the concentration profiles resolved by MCR-ALS and the profiles obtained by integration of the proposed chemical model using the fitted rate constants. Only the concentration profiles corresponding to PGE, aniline, secondary and tertiary amines are shown, because the profiles for non-reactive complexes can be considered negligible. The profiles obtained after the non-linear fitting show a good agreement with the ALS profiles in all experiments. The relative error (*RE*, Eq. (4)) for the profiles obtained after the optimization process was 2.03 %, while the *RE* calculated for the comparison between MCR-ALS profiles and the profiles generated using the initial rate constants was 19.31 %. As can be seen, the fitting was significantly improved. When the ALS concentration profiles were fitted to a model without taking into account the non-reactive complexes, the sum of squares was higher and the fitting was worse.

By using several matrices in the augmented column-wise data matrix we can not only solve the rank deficiency but also obtain a global fitting for all the experiments, corresponding to different molar ratios, thus avoiding the over-fitting that would occur when working with an individual data matrix. This means that experimental design is crucially important when using this method. In this case, it is important to select a suitable number of experiments with a suitable range of molar ratio for the reagents. The various experiments must provide enough information to guarantee the elimination of local optima and correlation between the adjustable model parameters. Indeed, when the model was fitted using an individual data matrix (for a particular initial molar ratio for the reagents), the kinetic rate constants did not suitably represent the behaviour of the species in the other experiments with different initial molar ratios.

5. Conclusions

Near-infrared spectroscopy and MCR-ALS, supported by a suitable experimental design, was a valuable guide for choosing a possible reaction mechanism for the reacting system. MCR-ALS combined with hard modelling satisfactorily estimated the rate constants when applied to data from reactions with complex mechanisms, such as curing reactions of epoxy resins. The rate constants found by this method are in agreement with values reported in the literature.

Using augmented data matrices assures that a global adjustment is obtained. In this way, over-fitting and optimal local minima are avoided and there is no correlation between the optimized parameters. Extrapolating this strategy to other reactions requires chemical knowledge of the system in order to construct a suitable kinetic model (i.e. the presence or absence of catalysts, the formation of intermediate complexes, side reactions, etc.). This is a topic for future research.

Aknowledgements

The authors would like to acknowledge financial support provided by the MCyT (project Nº BQU 2003-01142).

References

1. L. Schechter, J. Wynstra, and R. P. Kurkjy, Ind. Eng. Chem. **48**, 94 (1956).

2. I. R. Smith, Polymer **2**, 95 (1961).

3. Y. Tanaka and T. F. Mika, *Epoxy Resisns. Chemistry and Technology*, C. A. May, Y. Tanaka, Eds. (Marcel Dekker, New York, 1988), 2nd ed., pp. 298-300.

4. B. A. Rozenberg, Adv. Polym. Sci. **75**, 113 (1985).

5. H. J. Flammersheim, Themochim. Acta **310**, 153 (1998).

6. S. Swier and B. Van Mele, Termochim. Acta **411**, 149 (2004).

7. J. Mijovic, A. Fishbain, and J. Wijaya, Macromolecules **25**, 979 (1992).

8. F. Fraga, S. Burgo, and E. Rodríguez Núñez, J. Appl. Polym. Sci. **82**, 3366 (2001).

9. L. Xu, J. H. Fu, and J. R. Schlup, Ind. Eng. Chem. Res. **35**, 963 (1996).

10. J. H. Fu and J. R. Schlup, J. Appl. Polym. Sci. **49**, 219 (1993).

11. G. A. George, P. Cole-Clarke, N. St. John, and G. Friend, J. Appl. Polym. Sci. **42**, 643 (1991).

12. C. Billaud, M. Vandeuren, R. Legras, and V. Carlier, Appl. Spectrosc. **11**, 1413 (2002).

13. R. Tauler, A. Izquierdo-Ridorsa, and E. Casassas, Chemom. Intell. Lab. Syst. **18**, 293 (1993).

14. A. Izquierdo-Ridorsa, J. Saurina, S. Hernández-Cassou, and R. Tauler. Chemom. Intell. Lab. Syst. **38**, 183 (1997).

15. M. S. Larrechi and F. X. Rius, Appl. Spectrosc. **58**, 47 (2004).

16. M. Garrido, I. Lázaro, M. S. Larrechi, and F. X. Rius, Anal. Chim. Acta **515**, 65 (2004).

17. A. de Juan, E. Casassas, and R. Tauler, "Soft-modelling of analytical data" in *Enciclopedia of analytical Chemistry: Instrumentation and Applications*, (Wiley, New York, 2000), p. 9800.

18. A. de Juan, M. Maeder, M. Martínez, and R. Tauler, Chemom. Intell. Lab. Syst. **54**, 123 (2000).

19. Y. Neuhold and M. Maeder, J. Chemometrics **16**, 218 (2002).

20. E. Bezemer and S. C. Rutan, Chemom. Intell. Lab. Syst. **59**, 19 (2001).

21. E. Bezemer and S. C. Rutan, Anal. Chem. **73**, 4403 (2001).

22. M. Amrhein, B. Srinivasan, D. Bonvin, and M. M. Schumacher, Chemom. Intell. Lab. Syst. **33**, 17 (1996).

23. M. Maeder and A. D. Zuberbülher, Anal. Chem. **62**, 2220 (1990).

24. M. Otto, *Chemometrics: Statistics and Computer Application in analytical Chemistry*, (Wiley-VCH, Weinheim, 1999), p. 196.

25. J. A. Nelder and R. Mead, Comput. J. **7**, 308 (1965).

26. J.J. Kelly, C. H. Barlow, T. M. Jinguji, and J. B. Callis, Anal. Chem. **61**, 313 (1989).

27. The Mathworks, MATLAB Version 6.5, Natick, MA, 2002.

28. The Mathworks, Optimization Toolbox, 2.0 version, Natick, MA, 1998.

29. D. L. Massart, B. Vandeginste, L. Buydens, S. de Jong, P. Lewi, and J. Smeyers-Verbeke, *Handbook of Chemometrics and Qualimetrics : Part A*, (Elsevier, Amsterdam, 1997), p. 541.

30. W. Windig and J. Guilment, Anal Chem. **63**, 1425 (1991).

31. R. Tauler and A. de Juan, http://www.ub.es/gesq/mcr/ndownload.htm, Chemometrics and Solution Equilibria group, University of Barcelona, Department of Analytical Chemistry, 2003.

32. N. S. Enikolopiyan, Pure. Appl. Chem. **48**, 317 (1976).

33. L. Matějka and K. Dušek, J. Polym. Sci. Part A: Polym. Chem. **33**, 461 (1995).

34. K. Dušek, Adv. Polym. Sci. **78**, 1 (1986).

35. L. Matějka and K. Dušek, Macromolecules **22**, 2902 (1989).

36. J. Mijovic and J. Wijaya, Macromolecules **27**, 7589 (1994).

5.3 Curing Reaction of GlycidylThioether Resins: Kinetic Model Study by Near Infrared Spectroscopy and Multivariate Curve Resolution

Journal of Polymer Science, Part A: Polymer Chemistry, 44, **2006**, 4846-4856

M. Garrido, M. S. Larrechi, F. X. Rius, J. C. Ronda, V. Cadiz**

Department of Analytical and Organic Chemistry, Faculty of Chemistry, Rovira i Virgili University, Marcel·lí Domingo s/n (43007), Tarragona, Spain

(Received 24 April 2006; accepted 30 May 2006)

Abstract

The reactivity of sulphur-based epoxy monomers was studied by monitoring of a model system involving phenylglycidylthioether and aniline. The reaction was carried out under isothermal conditions and monitored *in situ* by Near Infrared Spectroscopy. Using Multivariate Curve Resolution-Alternating Least Squares made it possible to obtain the concentration and spectral profiles of each species throughout the reaction. To obtain the kinetic rate constants, the values of the recovered concentration profiles were fitted to a kinetic model proposed for the reaction in order to obtain the kinetic rate constants. Reactivity was evaluated by comparing the concentration profiles and kinetic rate constants obtained with the same parameters obtained for phenylglycidylether/aniline as a reference system.

1. Introduction

Glycidyl-type epoxy resins, which had been prepared mainly from Bisphenol A and other phenolic compounds with epichlorohydrin, have long been used as starting products in curing reactions. Several curing agent types, such as aromatic amines, have been used to achieve good results in reinforced plastic materials, moulding materials, coating, adhesives, insulation materials and foams.[1]

The heat resistance and thermal stability of polymers have been shown to depend on the structure of the elementary units. As well as the nature of the monomer and crosslinking agent affect the chemical structure of the network; the curing process of the epoxy resins also determines the final physical properties of the polymer.[2] There is therefore a need for a more detailed description of the curing process and a greater understanding of the relationships between structure, properties and processing.

Relatively less work has been carried out on sulphur-containing compounds. In a series of articles by Charmas et al.[3] on the synthesis of glycidylthioether resins, it was found that the thioderivatives can be cured using common hardeners for epoxy resins, such as aromatic amines, to yield products with often better properties than those of the resins cured from Bisphenol A. Similar results are also observed by Sergeev et al.[4]. More recently, Charmas[5] studied the relationship between the structure of the glycidylthioether resins and the stability and thermomechanical properties of different cured resins including photocured diglycidylthioetheracrylated resins.[6] Moreover, different new diglycidylthioether resins are reported to produce, on curing, optical resins possessing high refractive indices together with good mechanical properties.[7] The industrial interest of such a class of materials, in which the sulphur seems to play an important role, is reflected by the existence of several patents covering this field.[8]

In spite of this cure process itself has not been a subject of detailed investigation, Sultanova[9] studied the addition of amines to the model compound 1,2-epoxy-3-propylphenyl sulphide (phenilglycidylthioether, PGTE) on the basis of the IR spectra of the main final products. On the other hand the temperature promoted oxirane ring- opening were studied on the basis of model compounds using chromatography and IR and NMR spectral methods.[10] However, as far as we know, the only outstanding kinetic study on the curing behaviour of a glycidylthioether resin has been performed calorimetrically with the bis [3-(2,3-epoxypropylthio)phenyl] sulfona/trimercaptothioethylamine system.[11]

The epoxy-amine curing reaction has been monitored using several techniques, the most common of which are calorimetric methods such as differential scanning calorimetry (DSC).[12-14] However, these techniques do not provide direct information about the mechanism of the reaction. Concentration profiles of species involved in the curing reaction can be obtained by separation techniques such as high performance liquid chromatography.[15,16] Although this is essentially an off-line technique, it is often used for the kinetic investigation of reactions that do not evolve toward solid products. Spectroscopic techniques, such as Fourier transform infrared spectroscopy (FT-IR),[17,18] fluorescence[19,20] and near infrared spectroscopy (NIR)[21,22] enable the process to be monitored on-line and provide useful information about the kinetics of the curing reaction that can be used for mechanistic studies. In particular, NIR spectra are much simpler than mid-IR spectra. Also, relatively large amounts of sample can be used because molar absorptivities are much lower in this region.[17]

Most studies in the literature[17,22] use the spectral data in a univariate mode. This analysis provides data for evaluating the total degree of conversion but does not explain how many steps are involved in the overall process, how the concentration of the species evolves over time (concentration profiles), or what the spectral profile of each compound is. Much more complete information of this sort can be obtained from multivariate analysis

of the recorded data. Multivariate Curve Resolution methods such as Alternating Least Squares (MCR-ALS)[23-26] process the NIR data provided by the monitoring of the reaction all together and take into account a large number of variables (wavelengths). A set of pure spectra and concentration profiles is therefore obtained for each species. These methods are often called 'soft-modelling approaches' because they can describe processes without explicitly using the underlying chemical model to which they are linked.[27]

To determine the kinetic parameters of the chemical system under study, the data from the monitoring of the reaction (obtained by any of the above-mentioned techniques), have to be fitted to a chemical model in a separate step.[15,16,21] This method is usually known as 'hard-modelling' and involves the non-linear least-squares (or similar) fitting of the parameters of a chemical model that describe the data.

Curing is a multi-step chemical process that is complicated by physical phenomena such as gelation and/or vitrification. Therefore, model compounds have usually been used to investigate kinetic processes because the reactions are chemically-controlled and these physical changes do not have to be considered. In this paper we study the reaction between phenylglycidylthioether (PGTE) and aniline at 90 ºC using Near Infrared spectroscopy. The concentration profiles of the species involved in each reaction were obtained by applying the MCR-ALS algorithm to the NIR data. Also, the kinetic rate constants have been estimated by applying the 'hard-modelling' approach to the corresponding recovered concentration profiles. The reactivity of PGTE was compared with that of phenylglycidylether (PGE), an epoxy monomer that does not contain sulphur in its structure, to evaluate how the presence of sulphur affects the opening of the oxirane ring.

2. Experimental

Materials

All the organic and inorganic reagents were supplied by Fluka or Aldrich and used without previous purification as fitting. Solvents were purified by standard methods.

Monomer preparation

Phenylglycidylthioether

A solution of 50 g (1.25 mol) of NaOH in 200 mL water was added dropwise to a cool mixture of 110.2 g (1.0 mol) of thiophenol and 372 g (4.0 mL) of epiclorohydrin in 1 L of ethanol, keeping the temperature below 10ºC. Water was then added and the product was extracted with diethyl ether, washed, dried, concentrated and fractionated twice over CaH_2 to yield 156 g (93%) of a colourless liquid (b.p. 110-112ºC, 1 mmHg), (lit: 112-114ºC, 4 mmHg). [3d]

2.1 Sample preparation and measurements

The experimental procedure for the reaction involved mixing the necessary amounts of aniline and PGTE at room temperature to obtain the desired molar ratios (PGTE/aniline 1:1, 1.5:1 and 2:1). Then, 1 mL of this mixture was injected into the liquid cell of the NIR spectrophotometer to perform the NIR measurements. The cell temperature was set at 90ºC.

The NIR spectra were recorded throughout the reaction every 4 nm, between 1100 and 2500 nm using an InfraAlyzer 500 near infrared spectrophotometer (Bran-Luebbe). For each experiment, we acquired data at 5-minute intervals until no changes were observed in

the spectra throughout the time. In this way, the spectra were recorded for 355, 695 and 1435 min for the experiments with molar ratios of epoxy monomer to aniline of 1:1, 1.5:1 and 2:1, respectively.

2.2 Data pretreatment

To eliminate the vertical shift caused by using a NIR spectrophotometer with only one light beam, all the spectra were pretreated with an *off-set* correction.[28] Wavelength selection was performed by selecting the wavelengths of interest and ignoring those in which no variation over time was observed because they provide no information about the reaction under study. The regions of the spectrum in which only noise was detected were also eliminated. The selected wavelengths ranged from 1400 to 2432 nm.

The pretreated data corresponding to each experiment were arranged in matrices whose rows were the number of recorded spectra and whose columns were the wavelengths. The following matrices were thus obtained: $\mathbf{A_1}$ (72 x 259), $\mathbf{A_2}$ (140 x 259) and $\mathbf{A_3}$ (288 x 259). These matrices corresponded to the experiments with PGTE/aniline molar ratios of 1:1, 1.5:1 and 2:1, respectively. In the same conditions, the NIR spectra of the pure reactants (i.e. aniline and PGTE) were also recorded. The spectra recorded were exported and converted into MATLAB binary files.[29]

2.3 Optimization by Multivariate Curve Resolution-Alternating Least Squares (MCR-ALS)

Using Multivariate Curve Resolution methods makes it possible to obtain the concentration profiles of the species involved in the reaction as well as their

pure spectra profiles. This method is based on a bilinear decomposition of the experimental data matrix that is performed using the following model equation:[30]

$$\mathbf{D} = \mathbf{C}\,\mathbf{S}^{T} + \mathbf{E} \qquad \text{Eq. (1)}$$

where **D** is the data matrix obtained experimentally, **C** is the matrix that describes the changes in the concentrations of the species in the system under study, $\mathbf{S}^{T}$ is the matrix that contains the response profile of these species (spectra profiles) and **E** is the residual matrix with the data variance unexplained by $\mathbf{C}\,\mathbf{S}^{T}$.

Multivariate resolution can be carried out by MCR-ALS, which is an iterative method intended to minimize the residual matrix **E**.[23,24] The process involves the following steps:

*Determination of the number of components that contribute to the chemical information contained in the experimental data matrix **D** (i.e. chemical rank)*

In this study, the rank of all the data matrices was analyzed with singular value decomposition.[31] When the data analyzed are from chemical reactions, the data matrices are often rank-deficient, i.e. their chemical rank is lower than the total number of expected compounds. In our case, this problem was solved by column-wise matrix augmentation, which involves analyzing a matrix that joins the data matrices from several experiments that began with different initial conditions.[26,32] Thus, matrix **M** (500 x 259 in size) comprised $\mathbf{A_1}$, $\mathbf{A_2}$ and $\mathbf{A_3}$ matrices.

Construction of the initial estimate

The optimization of Eq. (1) requires an initial estimate either of the spectra in $\mathbf{S}^T$ or of the concentration profiles associated with these spectra. In this study, the initial estimate of $\mathbf{S}^T$ consisted of the experimentally recorded pure spectra of the reactants, i.e. aniline and PGTE, and the spectra of secondary and tertiary amine found applying SIMPLISMA algorithm[33] to the augmented matrix **M**.

Optimization by alternating least squares (ALS)

The ALS algorithm was iterated by applying a series of constraints in order to obtain a solution that was consistent with the chemical problem and to restrict the number of possible solutions. These constraints were as follows:

a) The values of the spectra and concentration profiles of each component must be non-negative.
b) The system must be closed with respect to the total analytic concentration.
c) Each concentration profile must have only one maximum (unimodality).

The pure spectra used in the construction of the initial estimate were not fixed throughout the resolution process.

2.4 Non-linear fitting

To obtain the kinetic rate constants for the PGTE/aniline system, a kinetic model was postulated based on the results of the MCR-ALS optimization and our prior knowledge

of the reaction between phenylglycidilether (PGE) and aniline. In this way, a function consisting of the differential equations of each compound taking part in the reaction was constructed, in accordance with the kinetic mechanism postulated. This function was integrated numerically by applying an ordinary differential equation solver (ODE23, a Runge-Kutta subroutine of Matlab[29]) and using initial guesses for the rate constants in order to obtain the concentration profiles related to the proposed model.

The kinetic rate constants were calculated by means of non-linear fitting. A multi-parameter minimum search based on the Nelder-Mead algorithm[34] then found the rate constants that provided the best fit between the profiles obtained from the kinetic model and the MCR-ALS concentration profiles. The fitting had to begin with reasonable initial guesses for the rate constants, which were refined iteratively. The optimized kinetic rate constants were thus obtained. No rate constants are reported for the system PGTE/aniline, so the kinetic rate constants used as initial guesses were taken from the PGE/aniline system[35] because this system is similar to the reaction under study.

3. Results and Discussion

The reaction between PGTE and aniline can be represented by the following two bimolecular reactions: the reaction of the primary amine to open the oxirane ring to form a secondary amine and the further reaction of the secondary amine with the oxirane ring to form a tertiary amine (see Scheme 1).

Only these reactions should be considered, since homopolymerization only takes place when specific catalysts are present (Lewis bases or acids)[16]. For a stoichiometric

molar ratio or when amine is present in excess, the etherification reaction is generally insignificant. Moreover, etherification is usually much slower than the amine-epoxy reactions and only becomes significant in epoxy-rich systems when the primary amine is sufficiently depleted.[36]

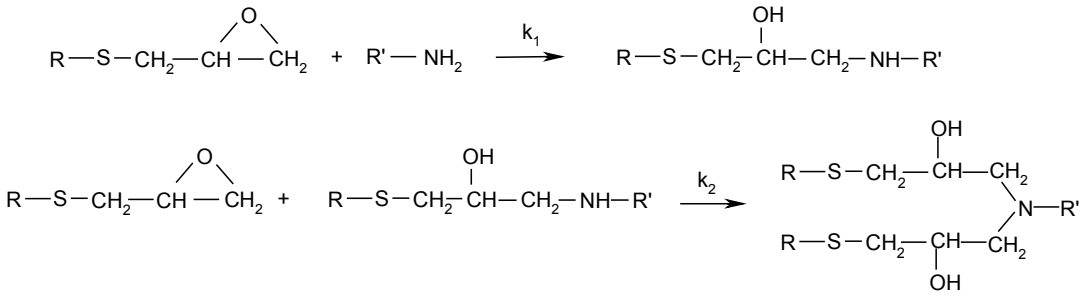

Scheme 1. General scheme of epoxy-amine reactions.

As an example, Fig. 1 shows the NIR spectra obtained by monitoring the experiment with a PGTE/aniline molar ratio of 2:1 at 90 ºC, after wavelength selection and off-set correction. As the reaction progresses, there is an increase in the band corresponding to the hydroxyl group at 1430 nm, which is in agreement with the reactions described above. On the other hand, the characteristic epoxy band (2210 nm) disappears because of the opening of the oxirane ring, and the primary (1978 nm and 1500 nm) and secondary (1500 nm) amine bands also decrease because of the reaction between epoxy and amine groups. On the basis of these considerations, four species were expected to be present in the system: epoxide, primary amine, secondary amine and tertiary amine. However, the rank analysis of the individual $\mathbf{A_1}$, $\mathbf{A_2}$ and $\mathbf{A_3}$ data matrices showed that there were three significant contributions for all the matrices but not four, which was the number of species involved in the process that absorb in the spectral zone. This occurs frequently in chemical reactions in

which more than one component (e.g. the reactants) exists when the reaction starts. So, instead of being able to detect all the components present at the beginning, only one can be mathematically derived. The spectrum of this component is a linear combination of the pure spectra of all the components present initially (in this case, PGTE and aniline)[37]. To eliminate this rank deficiency, the column-wise augmented matrix **M** was constructed. The rank analysis of matrix **M** gave four components, which matched the expected number of species. Adding new experiments with different initial conditions (i.e. different initial PGTE/aniline molar ratios) meant including more information about the variation of the reactants over time. In this way, rank deficiency was overcome.

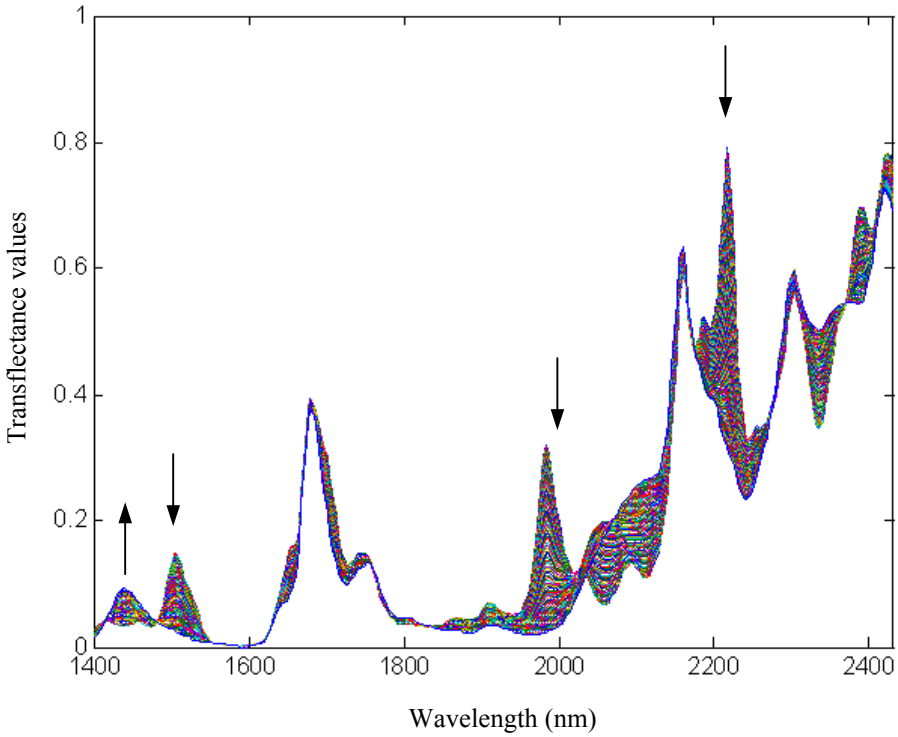

Fig. 1. NIR transflectance spectra of PGTE/aniline 2:1 system obtained every five minutes at 90ºC, after the application of the offset correction.

Fig. 2 shows the spectra for each of the four species recovered by MCR-ALS. The goodness of the spectra profiles recovered was evaluated quantitatively by calculating the similarity coefficients[26] between the recovered spectra and the pure spectra recorded for aniline and PGTE. The recovered spectrum for the tertiary amine was compared with the spectra recorded after 24 hours of reaction under the conditions stated in the procedure to ensure the completion of the reaction (molar ratio PGTE/aniline of 2:1). The values obtained were 0.992 for aniline, 0.999 for PGTE and 0.999 for the tertiary amine.

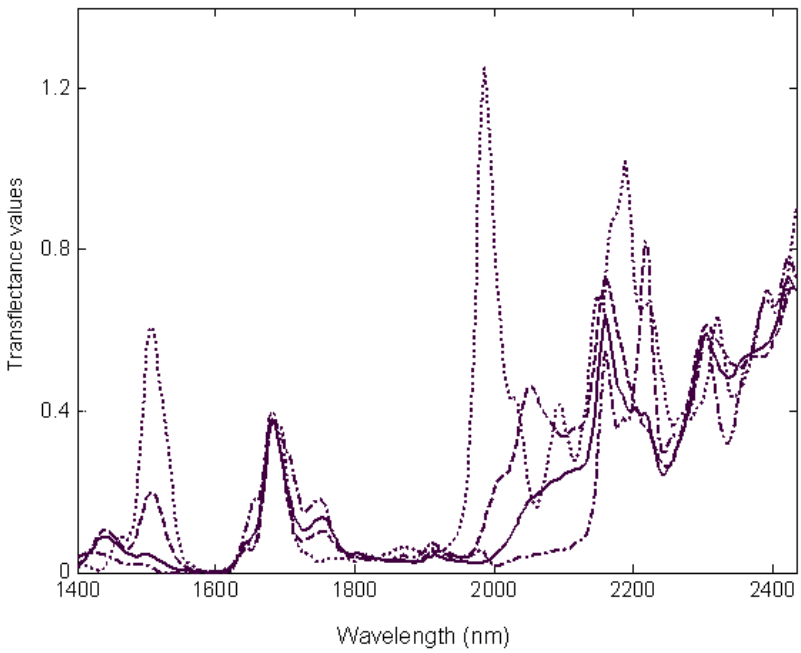

Fig. 2. Recovered spectra, after applying MCR-ALS to the experimentally recorded data matrix **D**. Aniline (····), PGTE (-·-·-), secondary amine (----) and tertiary amine (——).

The concentration profiles obtained by MCR-ALS for PGTE/aniline are shown in Fig. 3 a-c. The concentration profiles of the four compounds (PGTE, aniline, secondary amine and tertiary amine) are provided for each reaction run using the different initial molar ratios (1:1, 1.5:1, 2:1).

The resolved concentration profiles satisfactorily reproduced the molar ratios that were initially used for the reagents in each experiment. During the first minutes of the reaction, the change in concentration with respect to time is approximately the same for both the PGTE and the aniline, since only the first reaction (see Scheme 1) is taking place.

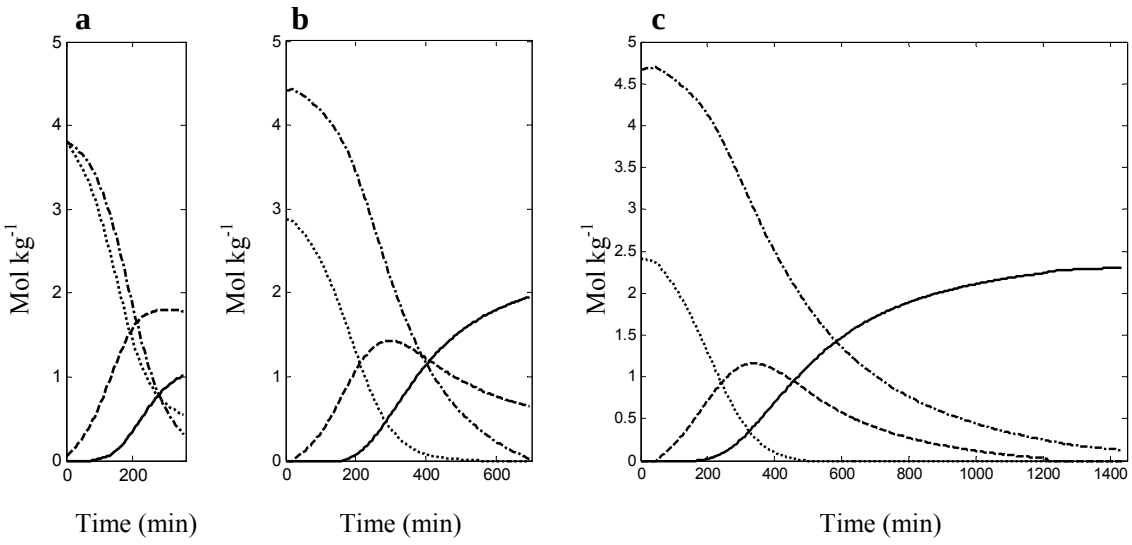

Fig.3. Concentration profiles for the curing reaction started at different PGTE/aniline molar ratios a) 1:1, b) 2:1. Aniline (····), PGTE (-·-·-), secondary amine (----) and tertiary amine (——).

When the aniline has reacted completely, the variation in PGTE concentration slows down because the kinetic rate constant of the reaction between epoxy and the secondary amine is lower than the rate constant of the reaction with primary amine. This can be clearly observed in the experiment with a molar ratio of 2:1. As the proportion of epoxy monomer increases, the tertiary amine appears later. This was also observed in the reaction between aniline and PGE.[26] For the PGE/aniline system, the behaviour of the tertiary amine may be explained by taking into account hydrogen-bonding interactions between hydroxyl groups, primary amine and ether groups of epoxy (see below). These H-bonded complexes reduce the ability of epoxy groups to react, so the formation of tertiary amine is delayed. [15,35,38] The same kind of complexes possibly appear in the PGTE/aniline system but involve the thioether group rather than the ether group.

The plots of the conversion (α) versus time for both systems (i.e. PGTE/aniline and PGE/aniline) are depicted in Fig. 4.

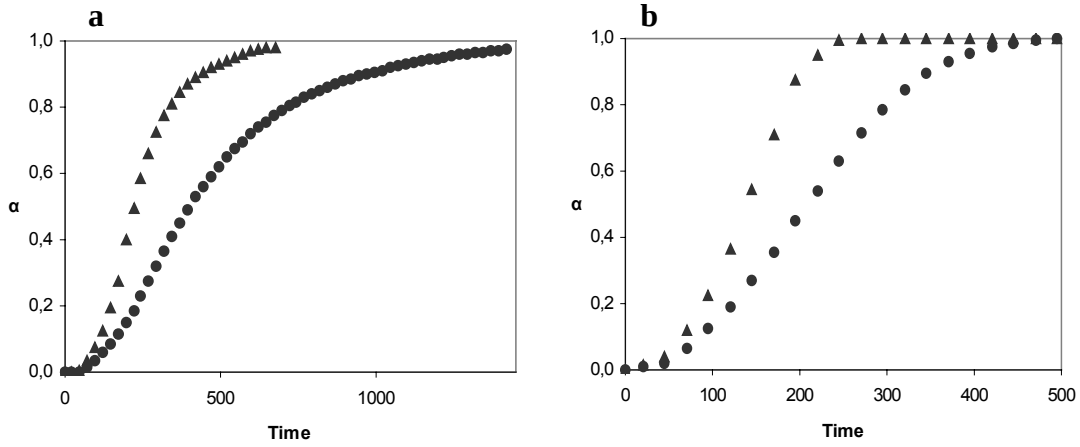

Fig.4. Plot of the conversion (α) versus time for systems with a 2:1 molar ratio: (a) epoxide (▲: PGE/aniline system, ●: PGTE/aniline system) and (b) primary amine (▲: PGE/aniline system, ●: PGTE/aniline system).

The values for the PGE/aniline system are based on the concentration profiles obtained in a previous study.[26] From this charts it is possible to analyse the reactivity of the PGTE in comparison with phenylglycidylether. The curves show a sigmoidal shape, typical of systems that follow an autocatalytic behaviour. The reactivity of PGTE is clearly lower than the reactivity of PGE. Higher conversions are reached in less time for PGE/aniline system, which implies that the openning of the oxirane ring take place more easily for PGE than for PGTE (see Fig. 4a). The early stages of the reaction can be analysed in the primary amine conversion plot (Fig. 4b). It also shows that the PGTE/aniline reaction is slower than the PGE/aniline reaction. The greater reactivity of PGE can be assigned to the more electronegative oxygen atom, which facilitates the nucleophilic attack on the oxirane ring by the amine.

Also, the plot of the reaction rate versus conversion shows the characteristic behaviour of the autocatalytic reactions (see. Fig. 5). The reaction rate increases initially as the reaction advances, passes through a maximum, and progressively slows down tending to zero.

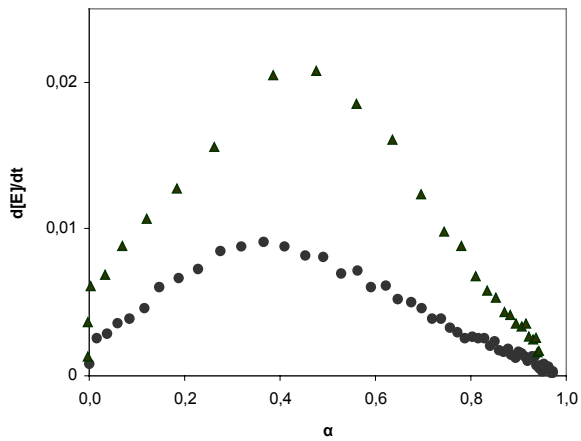

Fig. 5. Reaction rate vs. conversion (α), (▲: PGE/aniline system, ●: PGTE/aniline system). In both cases, [E] represents the concentration of epoxy, either PGE or PGTE.

The initial increase in the reaction rate is associated with the formation of hydroxyl groups, which acts as catalysts of the reaction. The maximum rate for both systems is observed at conversion between 30-40 %, as expected for autocatalytic reactions.[39]

The analysis carried out on the basis of the results obtained by the soft-modelling approach has been helpful for understanding the nature of the process taking place and constitute a guide for the postulation of a mechanism for the reaction under study. When information about rate constants is required, a kinetic model to describe the process is essential and a more detailed understanding of the mechanism is therefore needed.

Our analysis in this paper is based on the mechanism proposed by Xu et al. for the reaction between PGE and aniline [21] because of the resemblance between the PGE and PGTE structures and based on the similar autocatalytic behaviour of both reacting systems. It is known that compounds containing oxygen-hydrogen and nitrogen-hydrogen bonds can play the role of catalysts for epoxy-amine reactions.[16] The mechanism involves an initial interaction between epoxy groups with proton donor molecules (OH or NH_2 groups), thus leading to the formation of hydrogen bond complexes (also named “reactive complexes”) (Scheme 2a and 2b). The reaction between these reactive complexes and primary or secondary amines gives a secondary or tertiary amine, respectively, and in both cases this is through the formation of a termolecular intermediate (see Scheme. 2c-e). The formation of the termolecular intermediate is considered the rate-controlling step in the reaction.[21]

In accordance with this mechanism, in the early stages of the reaction, when hydroxyls are absent, the amine groups can act as both an electrophilic and a nucleophilic agent. Since the hydroxyl group is a much stronger electrophilic agent than an amine, the catalysis carried out by amine groups is less effective and relatively unimportant during the course of the reaction. However, at the very beginning of the reaction, this pathway is important because the initiation of the mechanism depends on the catalytic ability of the amine groups (Scheme 2 c). As the reaction advances, the catalysis due to hydroxyl groups

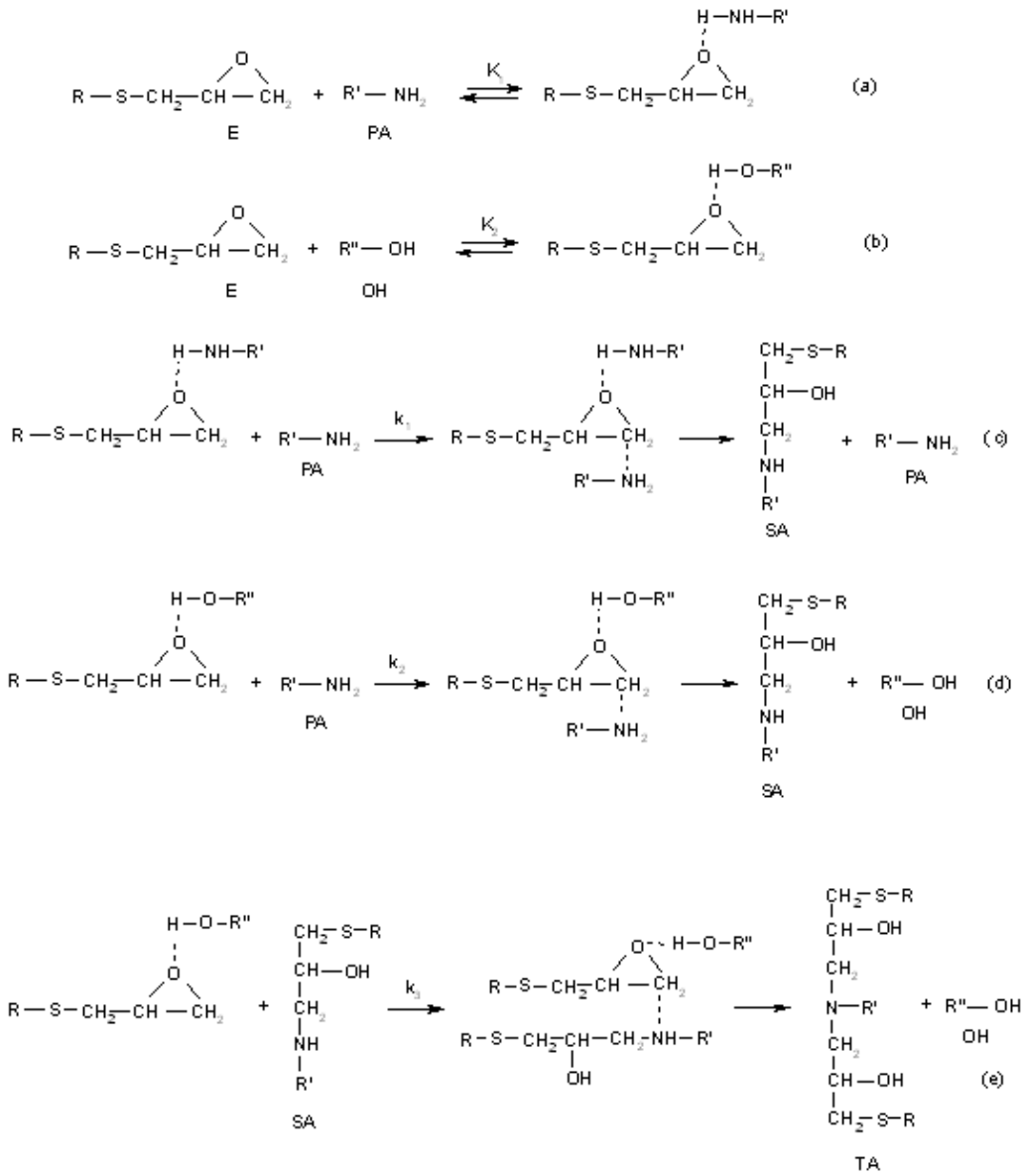

Scheme 2. Mechanism of the epoxy-amine reaction.

gains importance (Scheme 2 d) and, when the tertiary amine starts to form, significant amounts of hydroxyl groups already exist. Therefore, the reaction between epoxide and secondary amine catalyzed by the amine group (not shown in Scheme 2) can be safely neglected because it is dominated by the hydroxyl-catalytic reaction path (Scheme 2 e).

The formation of other hydrogen bond complexes, called "non-reactive complexes", such as the complex between hydroxyl group and amine group, amine and ether group and hydroxyl group and ether group have been reported in the reaction of PGE and aniline[15,38]. While reactive complexes assist the reaction and increase the reaction rate, the non-reactive complexes reduce the concentration of some of the reactive species, i.e. they slow down the reaction. Some studies about hydrogen bond conclude that sulphur is nearly as capable as oxygen as a hydrogen bond acceptor.[40,41] The general opinion that hydrogen bonds to oxygen are stronger result from the observation that H bonds are dominated by electrostatic effects that are larger in O···H-O than in S···H-O interactions. However, some theories point out that the dispersion effects are higher in the S-containing systems and this compensates the loss in the electrostatic contribution.[40] Other authors also remark that the surprising strength of the sulphur hydrogen bond may be due to the more polarizable sulphur atom and to the basicity of the sulphur lone pair.[41]

Considering these assumptions, and based on the similarity between this system and the PGE/aniline system, similar non-reactive hydrogen bond complexes could be expected in the reaction between PGTE and aniline (See Scheme 3). So, a model was proposed involving the following differential equations:

$$d[PA]/dt = -k_1'[E][PA]^2 - k_2'[E][OH][PA] - k_4[PA][OH] + \\ + k_5[PAOH] - k_6[PA][S] + k_7[SPA] \qquad \text{Eq.(2)}$$

$$d[E]/dt = -k_1'[E][PA]^2 - k_2'[E][OH][PA] - k_3'[E][OH][SA] \qquad \text{Eq. (3)}$$

$$d[SA]/dt = k_1'[E][PA]^2 + k_2'[E][OH][PA] - k_3'[E][OH][SA] \quad \text{Eq. (4)}$$

$$d[TA]/dt = k_3'[E][OH][SA] \quad \text{Eq. (5)}$$

$$d[PAOH]/dt = k_4[PA][OH] - k_5[PAOH] \quad \text{Eq. (6)}$$

$$d[SPA]/dt = k_6[PA][S] - k_7[SPA] \quad \text{Eq. (7)}$$

$$d[SOH]/dt = k_8[S][OH] - k_9[SOH] \quad \text{Eq. (8)}$$

where $k_1' = K_1k_1$, $k_2' = K_2k_2$, $k_3' = K_2k_3$ (see Scheme 2) and PAOH, SPA and SOH are the non-reactive complexes depicted in Schemes 3 a, b and c, respectively.

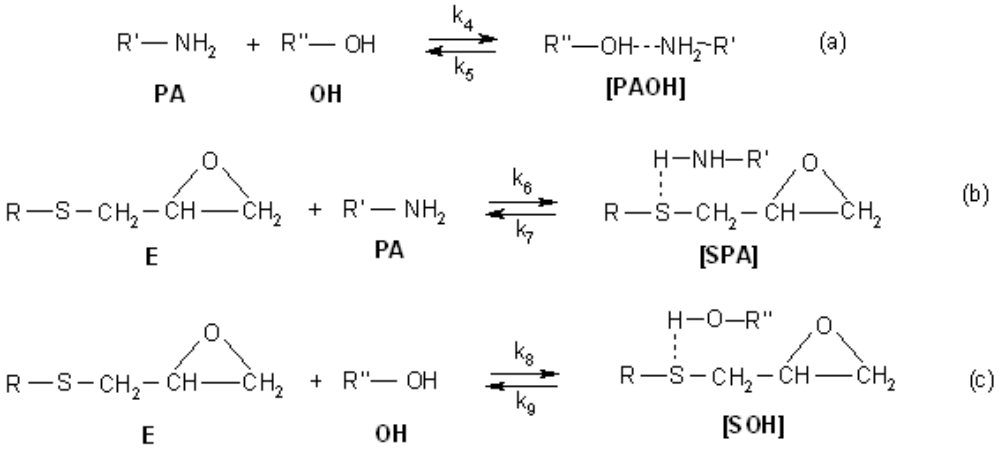

Scheme 3. Non-reactive complexes equilibria

Based on this kinetic model, non-linear fitting was carried out using the rate constants obtained for the PGE/aniline system in a previous study as initial guesses (see Table 1).[35]

Fig. 6 compares the concentration profiles resolved by MCR-ALS with the profiles obtained by integrating the proposed chemical model using the fitted rate constants (Table 1). Only the concentration profiles corresponding to PGTE, aniline, secondary amine and tertiary amine are shown because the profiles for non-reactive complexes can be considered negligible. The profiles obtained after the non-linear fitting show a good agreement with the MCR-ALS profiles in all experiments, with a relative error of 2.7%. The relative error was calculated in terms of difference of squares between the MCR-ALS profiles and the kinetic profiles obtained by non-linear fitting.

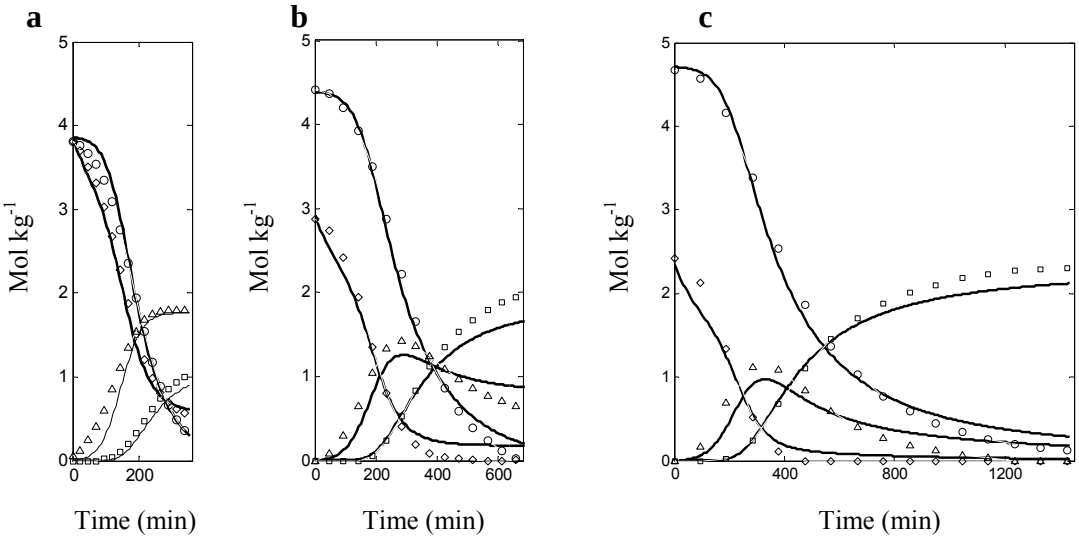

Fig. 6. Overlap of experimental concentration profiles recovered after MCR-ALS optimisation for PGTE (○), aniline (◊), secondary amine (Δ) and tertiary amine (□), and the profiles obtained by integration of the proposed chemical model using the fitted rate constants (solid line).

When the ALS concentration profiles were fitted to a model without taking into account the non-reactive complexes the fitting was worse and the relative error was 12.8%. As can be seen, the fitting was significantly improved when non-reactive complexes were taking into account.

	Initial Estimates	Fitted rate constants
k_1' x 10^3 ($kg^2mol^{-2}min^{-1}$)	0.0075	0.0049
k_2' x 10^3 ($kg^2mol^{-2}min^{-1}$)	4.3	2.9
k_3' x 10^3 ($kg^2mol^{-2}min^{-1}$)	1.40	0.98
k_4 x 10^3 ($kg\ mol^{-1}min^{-1}$)	0.010	0.010
k_5 x 10^3 (min^{-1})	0.041	0.069
k_6 x 10^3 ($kg\ mol^{-1}min^{-1}$)	0.4	0.5
k_7 x 10^3 (min^{-1})	4.0	3.1
k_8 x 10^3 ($kg\ mol^{-1}min^{-1}$)	0.009	0.005
k_9 x 10^3 (min^{-1})	0.05	0.06

Table 1. Initial guesses for the rate constants and fitted rate constants.

The values obtained for the rate constants k_1', k_2' and k_3' evidence the less reactivity of the oxirane ring due to the presence of sulphur in the structure of the epoxy monomer. On the other hand, the rate constants relative to the dissociation/formation of the non-reactive complexes do not show significant variations with respect to the corresponding constants in the PGE/aniline system. This is in accordance with the nearly

similar capacity of sulphur and oxygen as hydrogen bond acceptor, as has been postulated by some authors.[40,41]

4. Conclusions

The combination of near infrared spectroscopy and Multivariate Curve Resolution-Alternating Least Squares was succesfully used to monitor the curing processes and draw the corresponding concentration and spectra profiles. The concentration profiles provided by MCR-ALS were a valuable guide for choosing a possible reaction mechanism for the reacting system.

Our results clearly show a difference in reactivity between PGE and PGTE in their reaction with aniline. The lower reactivity can be attributed to the lower electronegativity of the S atom, which does not help to open the ring as efficiently as the O atom.

Nevertheless, both reactions seems to follow comparable pathways, and similar 'reactive' and 'non reactive' complexes may be involved in the reaction mechanism.

MCR-ALS combined with hard-modelling has made it possible to satisfactorily estimate the kinetic rate constants, which had been unpublished until now.

Aknowledgements

The authors thank the Comisión Interministerial de Ciencias y Tecnología, CICYT (MAT2005-01593) and MCyT (project Nº BQU 2003-01142).

References

1. Epoxy Resins: Chemistry and Technology; May, C. A., Ed., Marcel Dekker: New York, 1988.

2. Dusek, K. In Rubber-Modified Thermoset Resins; Riew, C. K.; Gillham, J. K., Eds.; Am. Chem. Soc.: Washington DC, 1989; Chapter 1.

3. (a) Charmas, W.; Podkościenly, W. J. Appl. Polym. Sci. 1982, 27, 1453-1463. (b) Charmas, W. J. Appl. Polym. Sci. 1982, 27, 2797-2807. (c) Charmas, W. J. Appl. Polym. Sci. 1985, 30, 411-421. (d) Charmas, W.; Podkościenly, W.; Brunn, J. J. Polym. Sci.:Part A: Polym. Chem. 1989, 27, 2397-2415. (e) Charmas, W.; Podkościenly, W.; Rudź, J. J. Appl. Polym. Sci. 1990, 39, 1623-1633.

4. Sergeev, V. A.; Nedelkin, V. I.; Novikov, V. U. Vysokomolekulyarnye Soedineniya, Seriya A 1984, 26, 208-211.

5. Charmas, W. Int. J. Polym. Mat. 2003, 52, 459-469.

6. Nowak, J.; Majewski, W.; Charmas, W. Annales Universitatis Mariae Curie-Skłodowska. Sectio AA. Chemia. 2004, 59, 108-120.

7. Cui, Z.; Lu, C.; Yang, B.; Shen, J.; Su, X.; Yang, H. Polymer 2001, 42, 10095-10100.

8. (a) Sergeev, V. A.; Nedelkin, V. I.; Novikov, V. U. (Institute of Heteroorganic Compounds, Academy of Sciences; All-Union Correpondence Polytechnic Institute) U.S.S.R. Patent SU 1043146, September 23, 1983, (b) Yamamoto, K.; Wakimura, K.; Suzuki, M.; Ikeda, K. (Sumitomo Seika K. K.) Japan patent JP 10324858, December 8, 1998, (c) Kasai, T. (Kyocera Chemical Corp.) Japan Patent JP 2005082666, March 31, 2005.

9. Sultanova, N. R.; Movsumzade, M.; Mamedov, F. N.; Vezirova, N. M. Organ. Soedin. Sery., 1980, 2, 37-43.

10. Charmas, W. Int. J. Polym. Mat. 2003, 52, 101-117.

11. Lu, C.; Cui, Z.; Yang, B.; Su, X.; Huo, C.; Shen, J. J. Appl. Polym. Sci. 2002, 86, 589-595.

12. Karkanas, P. I.; Partridge, I. K. J. Appl. Polym. Sci. 2000, 77, 1419-1431.

13. Riccardi, C. C.; Fraga, F.; Dupuy, J.; Williams, R. J. J. J. Appl. Polym. Sci. 2001, 82, 2319-2325.

14. Dean, K.; Cook, W. D. Macromolecules 2002, 35, 7942-7954.

15. Swier, S.; Van Mele, B. Termochim. Acta 2004, 411, 149-169.

16. Mijovic, J.; Fishbain, A.; Wijaya, J. Macromolecules 1992, 25, 979-985.

17. George, G.A.; Cole-Clarke, P.; St. John, N.; Friend, G. J. Appl. Polym. Sci. 1991, 42, 643-657.

18. Fraga, F.; Burgo, S.; Rodríguez Núñez, E. J. Appl. Polym. Sci. 2001, 82, 3366-3372.

19. Strehmel, B.; Strehmel, V.; Younes, M. J. Polym. Sci. Part B: Polym. Physics 1999, 37, 1367-1386.

20. Younes, M.; Wartewig, S.; Lellinger, D.; Strehmel, B.; Strehmel, V. Polymer 1994, 35, 5269-5278.

21. Xu, L.; Fu, J. H.; Schlup, J. R. Ind. Eng. Chem. Res. 1996, 35, 963-972.

22. Billaud, C.; Vandeuren, M.; Legras, R.; Carlier, V. Appl. Spectrosc. 2002, 56, 1413-1421.

23. Tauler, R.; Izquierdo-Ridorsa, A.; Casassas, E. Chemom. Intell. Lab. Syst. 1993, 18, 293-300.

24. Izquierdo-Ridorsa, A.; Saurina, J.; Hernández-Cassou, S.; Tauler, R. Chemom. Intell. Lab. Syst. 1997, 38, 183-196.

25. Larrechi, M. S.; Rius, F. X. Appl. Spectrosc. 2004, 58, 47-53.

26. Garrido, M.; Lázaro, I.; Larrechi, M. S.; Rius, F. X. Anal. Chim. Acta 2004, 515, 65-73.

27. De Juan, A.; Casassas, E.; Tauler, R. In Enciclopedia of analytical Chemistry: Instrumentation and Applications; Wiley: New York, 2000; p. 9800.

28. Kelly, J.J.; Barlow, C. H.; Jinguji, T. M.; Callis, J. B. Anal. Chem. 1989, 61, 313-320.

29. The Mathworks, MATLAB Version 6.5, Natick, MA, 2002.

30. De Juan, A; Tauler, R. Anal. Chim. Acta 2003, 500, 195-210.

31. Massart, D. L.; Vandeginste, B.; Buydens, L.; De Jong, S.; Lewi, P.; Smeyers-Verbeke, J. In Handbook of Chemometrics and Qualimetrics: Part A; Elsevier: Amsterdam, 1997; p. 541.

32. Amrhein, M.; Srinivasan, B.; Bonvin, D.; Schumacher, M. M. Chemom. Intell. Lab. Syst. 1996, 33, 17-33.

33. Windig, W.; Guilment, J. Anal Chem. 1991, 63, 1425-1432.

34. Nelder J. A.; Mead R. J. Comput. 1965, 7, 308-313.

35. Garrido, M.; Larrechi, M. S.; Rius, F. X. Applied Spectroscopy 2006, 60, 174-181.

36. Riccardi, C.C.; Williams, R.J.J. Polymer 1986, 27, 913-920.

37. Saurina, J.; Hernández-Cassou, S.; Tauler, R.; Izquierdo-Ridorsa, A. J. Chemometrics 1998, 12, 183-203.

38. Swier, S.; Van Assche, G.; Vuchelen, W.; Van Mele, B. Macromolecules. 2005, 38, 2281-2288.

39. Ghaemy, M.; Barghamadi, M.; Behmadi, H. J. Appl. Polym. Sci. 2004, 94, 1049-1056.

40. Wennmohs, F.;Staemmler, V.; Schindler, M. J. Chem. Pys. 2003, 119, 3208-3218.

41. Rablen, P. R.; Lockman, J. W.; Jorgensen, W. L. J. Phys. Chem. A 1998, 102, 3782-3797.

5.4 Kinetic analysis of reactions of Si-based epoxy resins by near-infrared spectroscopy, ^{13}C NMR and soft-hard modelling

Analítica Chimica Acta, in press

Mariano Garrido, Maria Soledad Larrechi, F. Xavier Rius,*
Luis Adolfo Mercado, Marina Galià[†]

Department of Analytical and Organic Chemistry, Faculty of Chemistry, Rovira i Virgili University, Marcel·lí Domingo s/n (43007), Tarragona, Spain

(Received 19 July 2006; revised 18 October 2006; accepted 26 October 2006)

Abstract

Soft- and hard-modelling strategy was applied to near infrared spectroscopy data obtained from monitoring the reaction between glycidyloxydimethylphenyl silane, a silicon-based epoxy monomer, and aniline. On the basis of the pure soft-modelling approach and previous chemical knowledge, a kinetic model for the reaction was proposed. Then, multivariate curve resolution-alternating least squares optimization was carried out under a hard constraint, that compels the concentration profiles to fulfil the proposed kinetic model at each iteration of the optimization process. In this way, the concentration profiles of each species and the corresponding kinetic rate constants of the reaction, unpublished until now, were obtained. The results obtained were contrasted with ^{13}C NMR. The joint interval test of slope and intercept for detecting bias was not significant (α = 5%).

1. Introduction

Nowadays, research into epoxy resins focuses on improving their characteristics so that they can respond to the requirements of new and advanced applications. A further requirement that has recently gained importance is the need for flame resistance. Traditionally, brominated compounds are used to make epoxy resins more flame retardant, but environmental problems now mean that non-halogenated flame retardants are receiving more attention [1-3]. In particular, introducing silicon into epoxy resins improves their electrical properties, thermal stability and flame retardancy [4,5].

Therefore, the intended properties of flame retardant epoxy resins depend on the flame retardant components, but they are also strongly influenced by the curing process. This curing process and the structure/property/processing relationships of the epoxy thermosets can be better understood by studying the reaction mechanism and quantifying the kinetic parameters. Although many mechanisms have been proposed for curing epoxy resins [6-9], the real mechanism is still not fully understood. Furthermore, so far, no mechanistic studies have analysed the effect caused by the presence of silicon on the kinetics of curing silicon-based epoxy resins. An important issue in epoxy-amine kinetics is how the reactivity of the secondary amine changes in comparison to that of the primary amine: the so-called substitution effect (ρ). This effect is normally calculated by the ratio of the reaction rate constant of an epoxide reacting with a secondary amine to that of an epoxide reacting with a primary amine. This value is important to perform an adequate description of the kinetics of network formation and, therefore, to know the morphology of the cured structure [10].

Among the various techniques used for monitoring the curing process, near-infrared (NIR) spectroscopy is one of the most suitable since it is non-destructive and, if the appropriate accessories are available, it enables the curing reactions to be monitored *in situ* [11,12]. Moreover, NIR absorptivities are small, which means that a relatively large

quantity of sample can be used and that the kinetics of the curing process can be easily studied [10,13,14]. In spite of these advantages, directly measuring of concentrations of reactive species means that a baseline for peak integration and appropriate reference bands must be decided on, and this in turn means that the later stages of the curing are difficult to monitor.

In addition, the primary amine and the secondary amine absorb in the same spectral region and their bands are completely overlapped. Therefore, the spectral bands have to be decomposed if they are to be quantified, which requires further assumptions [13]. An alternative is to extract the information about how species that have specific bands evolve over time, whereas the variation of the other species is inferred by mass balance equations [10].

These problems arise from a univariate use of the spectra and can be overcome by combining NIR with multivariate resolution techniques. In these methods, NIR data are all processed together, and a large number of variables (wavelengths) are taken into account. As a result, information about the spectra and concentrations of the species is obtained. Several useful approaches have been applied to NIR data, such as Iterative Target Testing Factor analysis (ITTFA) [15], Iterative Target Testing (TT) [16], SIMPLISMA [17], Self Modelling Curve Resolution (SMCR) [18], and Multivariate Curve Resolution-Alternating Least Squares (MCR-ALS) [19,20]. MCR-ALS, in particular, was successfully applied to NIR data from monitoring epoxy resins reactions [21,22]. One peculiarity of these methods, often called 'soft-modelling' approaches, is that they can describe the process without explicitly using the underlying chemical model to which they are linked [23]. Indeed, soft-modelling approaches can be useful for designing a suitable reaction model and supporting the model chosen [24].

The profiles obtained by soft-modelling methods, however, are subject to so-called ambiguities [25,26] and unless local rank conditions [27] or selectivity regions [26] are

present, unique solutions cannot be obtained. Another way to minimise the ambiguity associated to soft-modelling solutions is to impose a kinetic model as a constraint throughout the resolution process [24,28-30]. Thus, at each iteration of the soft-modelling optimization process, the concentration profiles obtained are used as input for a non-linear multivariate kinetic fit. This 'hard-modelling' step involves the non-linear least-squares (or similar) fitting of the parameters of a chemical model that describes the data. The fitting is done directly on the concentration profiles without taking into account the spectral contributions (linear parameters) [31]. The resulting fitted kinetic profiles update the profiles obtained by soft-modelling and the rate constants (non-linear parameters) of the process are obtained as additional information [24].

We apply a combination of MCR-ALS and hard-modelling following the strategy reported by de Juan et al. [24]. This 'hard and soft modelling' multivariate curve resolution (HS-MCR) strategy contains the advantages of both pure soft- and pure hard-modelling. Soft-modelling makes it possible to apply constraints in a flexible way, and helps to resolve systems that may eventually have instrumental responses that are different from those related to the reaction studied (e.g. in the case of epoxy resins, the presence of collateral etherification or homopolymerization reactions). On the other hand, hard-modelling makes it possible to resolve the system without ambiguities, and obtain the corresponding kinetic rate constants [24,28].

HS-MCR has already been used for first-order reactions [24,28], second order reactions in simulated data [29] and enzymatic reactions [32,33]. Other studies found in the bibliography apply the hard-modelling approach to the concentration profiles obtained by soft-modelling, but only after a process of optimization by Alternating Least Squares [34-36].

In the present study, HS-MCR was applied to more complex reactions. We used near infrared spectroscopy to monitor the reaction between glycidyloxydimethylphenyl

silane (GDMPS), a silicon-based epoxy monomer, and aniline. On the basis of initial concentration profiles obtained by MCR-ALS (the pure soft-modelling approach), a kinetic model involving two consecutive (pseudo) second-order reactions was proposed and discussed. This model was used as a hard-modelling constraint during ALS optimization (HS-MCR). In this way, new concentration profiles and a set of kinetic rate constants, unpublished until now, were obtained. The reaction was also monitored by ^{13}C NMR in order to verify the validity of the results obtained. To the best of our knowledge, no studies have been published on the use of ^{13}C NMR for the quantitative monitoring of epoxy resins reactions.

The results obtained made it possible to evaluate the influence of silicon on the substitution effect and provided useful information, which can be extrapolated to reactions that evolve toward crosslinked products.

2. Background

In this study, GDMPS was selected as a model compound so that the reactivity of silicon-containing epoxy monomers in curing reactions with primary amine hardeners could be explored. The curing process is a multi-step chemical process that is complicated by the physical processes of gelation and vitrification. The latter should not be considered in the reaction kinetics of this model system, since the product obtained is not a polymer. The main reactions that take place are between the primary amine and epoxy to form a secondary amine and the further reaction of the secondary amine with epoxy to form a tertiary amine (see Scheme 1). Other possible reactions include the homopolymerization of epoxy resins and the etherification between epoxy and hydroxyl groups. However, the

homopolymerization of epoxy groups is generally considered to be negligible in the absence of Lewis acid or base catalysts [37]. When the molar ratio is stoichiometric or there is an excess of amine, the etherification reaction is generally insignificant with respect to the reactions in Scheme 1. Moreover, etherification is usually much slower than amine-epoxy reactions and only becomes significant in epoxy-rich systems when the primary amine is sufficiently depleted [38].

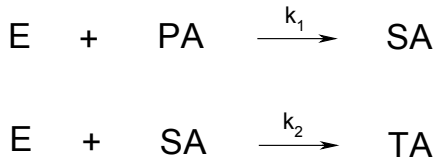

Scheme 1. General scheme of epoxy-amine reactions.

The reactions depicted in Scheme 1 are a general representation of the system, but do not reflect the underlying mechanism. The soft-modelling approach makes it possible to study the behaviour of each species and, consequently, to propose a mechanism for the reaction.

3. Experimental

3.1 Reagents, materials and instrumental

GDMPS was synthesized as in a previous article [22]. Aniline, supplied by Aldrich, was distilled before it was used. An analytical scale was used to weigh the reagents. A

thermostatic bath (PolyScience, USA) was used to set the appropriate reaction temperature, and an immersion probe (Crisson) was used to control the bath temperature during the reaction.

NIR spectra were recorded in an InfraAlyzer 500 Bran-Luebbe spectrophotometer equipped with a cell for liquids, operating in transflectance mode by using a stainless steel reflecting surface. ^{13}C NMR spectra were performed in a Varian Gemini 300 NMR spectrometer at 75.4 MHz operating with proton noise decoupling.

All chemometric data analyses were performed using MATLAB® [39,40], on an Intel Pentium IV computer with 2.8 GHz and 512 Kb of RAM. The software used to perform HS-MCR was a home-made modification of the MCR-ALS software provided by the Solution Equilibria and Chemometrics Group of Barcelona University, which is freely available on the Web [41].

3.2 Procedure

The experimental procedure for the reaction involved mixing the necessary amounts of aniline and GDMPS at room temperature to obtain two different molar ratios: GDMPS/aniline 2:1 (i.e the stoichiometric molar ratio) and GDMPS/aniline 1:1, a mixture with an excess of aniline. The reaction was isothermally carried out at 95ºC. In order to perform the NIR measurements, 1 mL of this mixture was injected into the liquid cell of the NIR spectrophotometer. Before the injection, the cell temperature was set to 95ºC.

The NIR spectra were recorded throughout the reaction every 4 nm operating in the transflectance mode. For each experiment, we acquired data at intervals of 5 min until the end of the reaction. The reaction was considered to be complete when no changes were

observed in the spectra throughout the reaction time. In this way, the times of the spectra recording were 230 min for the experiment with the molar ratio GDMPS/aniline 1:1 and 675 min for the experiment with the molar ratio GDMPS/aniline 2:1.

In order to eliminate the vertical shift caused by using a NIR spectrophotometer with only one light beam, all the spectra were pretreated by applying an *off-set* correction [42]. The wavelengths of interest were selected and those in which no variation over time was observed were ignored because they provide no information about the reaction being studied. The regions of the spectrum in which only noise was detected were also eliminated. The selected wavelengths ranged from 1400 to 2432 nm.

The pretreated data were arranged in matrices whose rows were the number of recorded spectra and whose columns were the wavelengths. The following matrices were thus obtained: $\mathbf{A_1}$ (47 x 259) and $\mathbf{A_2}$ (136 x 259), corresponding to the experiments with GDMPS/aniline molar ratios of 1:1, and 2:1, respectively. The same number of columns for all the matrices refers to the 259 NIR wavelengths from 1400 to 2432 nm, every 4 nm. And the rows are the number of spectra recorded every five minutes, so the acquisition time for $\mathbf{A_1}$ was 230 min while for $\mathbf{A_2}$ it was 675 min. In the same experimental conditions, the NIR spectra of the pure reactants were also recorded.

The spectra recorded in the InfraAlyzer 500 were exported and converted into MATLAB binary files.

3.3 Kinetic model

The kinetic model for the system was postulated by considering previous knowledge about curing reactions. It was based on the shape of the concentration profiles obtained after the pure soft-modelling approach had been applied. The soft-modelling was

carried out by applying MCR-ALS under the constraints of non-negativity, closure and unimodality, as in a previous article [22].

In order to describe the reaction pathway, a function consisting of the differential equations representing the variation in concentration of the species over time was constructed in accordance with the kinetic mechanism proposed. An ordinary differential equation solver (ODE23) that comes with MATLAB was used to solve the differential equations [39,43]. It required some initial information: the starting concentrations for each of the species considered in the model, a vector specifying the various time points for the reaction times and an initial estimate of the kinetic rate constants. A multi-parameter minimum search procedure, based on the Nelder-Mead algorithm [44] found the rate constants that provided the best fit between the profiles obtained from the kinetic model and the resolved concentration profiles during each iteration of the ALS optimization.

3.4 HS-MCR approach

The rank of data matrices $\mathbf{A_1}$ and $\mathbf{A_2}$ was analyzed with Singular Value Decomposition (SVD) [45] and Evolving Factor Analysis (EFA) [46]. Both methods provided an identical number of components. It is assumed that the singular values associated to the chemical components are much larger than other possible contributions such as instrumental drift or experimental error. The chemical rank was thus estimated by simply inspecting the tables of singular values for each data matrix analyzed. When the systems analyzed come from evolving processes, the data sets are often rank-deficient, (i.e. their chemical rank is lower than the total number of absorbing compounds) [47]. In our case, the rank deficiency of experimental data matrices was solved by means of column-wise matrix augmentation [48]. A column-wise augmented data matrix (183 x 259 in size) was constructed with the two sets of pretreated data ($\mathbf{A_1}$ (47x269 in size) and $\mathbf{A_2}$ (136x269 in size) matrices).

The initial estimate for the pure spectra, which ALS needs to start the optimization process, was obtained by applying the SIMPLISMA algorithm [49] to the augmented matrix and using the experimentally recorded pure spectra of the reactants (GDMPS and aniline). The procedure was the same as in a previous article [22].

The hard-modelling step in the ALS optimization requires an initial estimate of the kinetic rate constants. These initial estimates were obtained in a separate step that used a non-linear least squares optimization to fit the concentration values obtained by pure soft-modelled concentration profiles to the proposed kinetic model. Finally, the ALS algorithm was iterated by applying the non-negativity constraint to both the spectral and concentration profiles, and imposing the fulfilment of the kinetic model. The closure constraint was not implemented because the kinetic model already includes inherent mass balance [29]. The pure spectra used to construct the initial estimate were not fixed throughout the resolution process.

3.5 ^{13}C NMR analysis

In order to verify the validity of the concentration profiles obtained, the reaction was monitored by ^{13}C NMR. Therefore, the reaction was carried out under stoichiometric proportions (i.e. GDMPS/aniline molar ratio of 2:1) in a thermostatic bath at 95 ± 0.2 ºC, and the temperature of the reacting mixture was controlled with an immersion probe thermometer. The starting concentrations of the reagents were weighed on the analytical scale, but changes in the third decimal do not cause any significant variations in the desired molar ratio. Samples of the reacting mixture (about 150 mg) were withdrawn at particular times and dissolved with $CDCl_3$. ^{13}C NMR spectra of the samples were recorded at room temperature at 75.4 M Hz with proton noise decoupling. The spectrum of each sample was the average of 64 scans.

In order to quantitatively integrate the signals, the NMR spectra were acquired using inverse-gated decoupling and a relaxation time delay of about $5T_1$. This value (T_1) was the relaxation time of the carbons located in the *ortho* position with respect to the silicon atom, which were used as the reference signal. It was the slowest relaxing nucleus of all the signals used in the quantification.

Relative quantification was carried out using the invariable signal of the reference carbon and assuming that, in all spectra, this signal has a concentration of 3.93 mol kg^{-1} (quantity of GDMPS that is initially present in the 2:1 GDMPS/aniline reacting mixture).

4. Results and discussion

Figs. 1a and 1b show the soft-modelled concentration profiles obtained when MCR-ALS was applied to the augmented data matrix (formed by $\mathbf{A_1}$ and $\mathbf{A_2}$ matrices, 183 x 259 in size). Note that the constraints imposed were related to the physical and chemical characteristics of the system, and no kinetic information was required. The corresponding fitting parameters are: % of lack of fit = 0.49, explained variance = 99.998 %. The evolution of the concentrations of the chemical species involved in the reaction is depicted for the two experiences with different GDMPS/aniline molar ratios: 1:1 and 2:1.

The recovered profiles satisfactorily reproduced the molar ratio that was initially used in each experiment. GDMPS can be considered to have been totally consumed by the end of each experiment, whereas an excess of aniline in the reaction with GDMPS/aniline molar ratio 1:1 can be clearly seen in Fig. 1a.

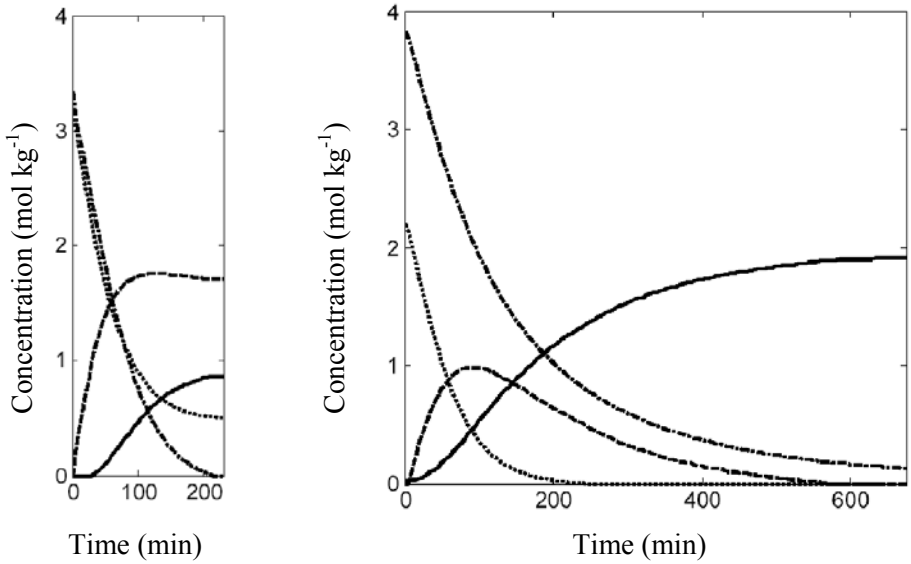

Fig. 1. Concentration profiles obtained by pure soft-modelling approach for the reaction between GDMPS and aniline started with (a) 1:1 and (b) 2:1 GDMPS/aniline molar ratios: (···) aniline, (-·-) GDMPS, (---) secondary amine and (—) tertiary amine.

On the other hand, the concentration of tertiary amine at the end of the experiment with GDMPS/aniline molar ratio 2:1 (see Fig. 1b) reaches the value predicted by the stoichiometry. In this latter figure, the profile of the tertiary amine appears early, almost at the beginning of the reaction, which indicates that the reactivities of the primary and secondary amine are similar. It can also be seen that the profiles of aniline and GDMPS do not display the typical behaviour of an autocatalytic reaction (slow at the beginning and

then faster, due to the presence of OH groups that catalyze the reaction). Instead, both reactants are rapidly consumed just from the very beginning of the reaction.

The higher conversions indicate that the opening of the oxirane ring takes place easily. One possible explanation for this is the effect of silicon on the epoxide structure. The higher reactivity of the oxirane group in GDMPS is probably due to electronic effects. The silicon atom acts as a π-acceptor, withdrawing electronic density from the oxygen atom [22]. Thus, the electronic density of this oxygen atom is low, and its electron-withdrawing character is high, which increases the electrophilic character of the oxiranic carbons. This facilitates the attack of the amine and enhances the reactivity of GDMPS (see Scheme 2a).

The reaction may also follow a catalytic pathway by forming termolecular complexes between the hydroxyl, amino and epoxy groups (see Scheme 2b and 2c) [50]. In the early stages of this reaction, when hydroxyls are absent, the amine groups can act both as electrophilic and nucleophilic agents. Although at the very beginning of the reaction, this reaction path can be important, hydroxyl groups are much stronger electrophilic agents than amines. Therefore, the catalysis carried out by amine groups is less effective and relatively unimportant during the course of the reaction. As the reaction progresses, the catalysis due to hydroxyl groups gains in importance because of the significant number of hydroxyl groups generated. Therefore, the reaction between epoxide and secondary amine catalyzed by the amine group can be safely neglected (see the reaction indicated by dotted lines in Scheme 2c) because it is dominated by the hydroxyl-catalytic reaction path. On the other hand, when the secondary amine reaction predominates in the reaction path (i.e. after the maximum of the secondary amine in Fig. 1b), the species evolve as they do in reactions involving monomers that do not have silicon in their structure [22]. Therefore, the effect of silicon seems to be more important at the beginning of the reaction.

a)

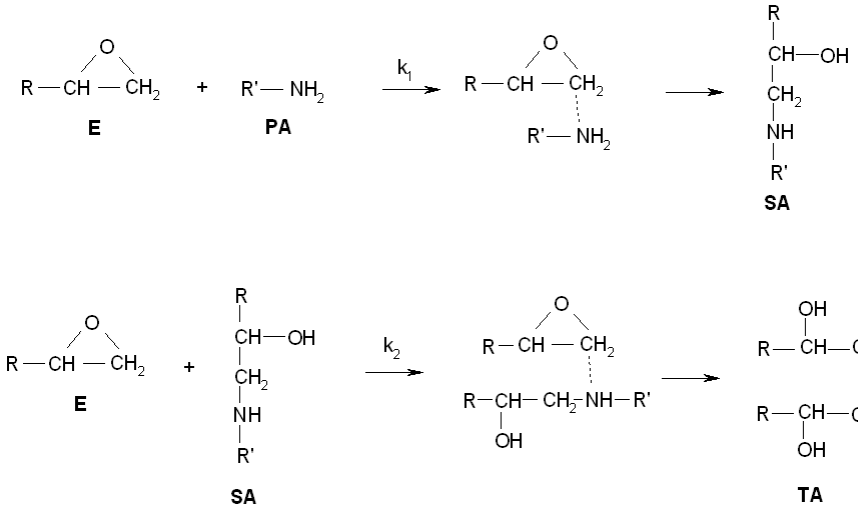

b)

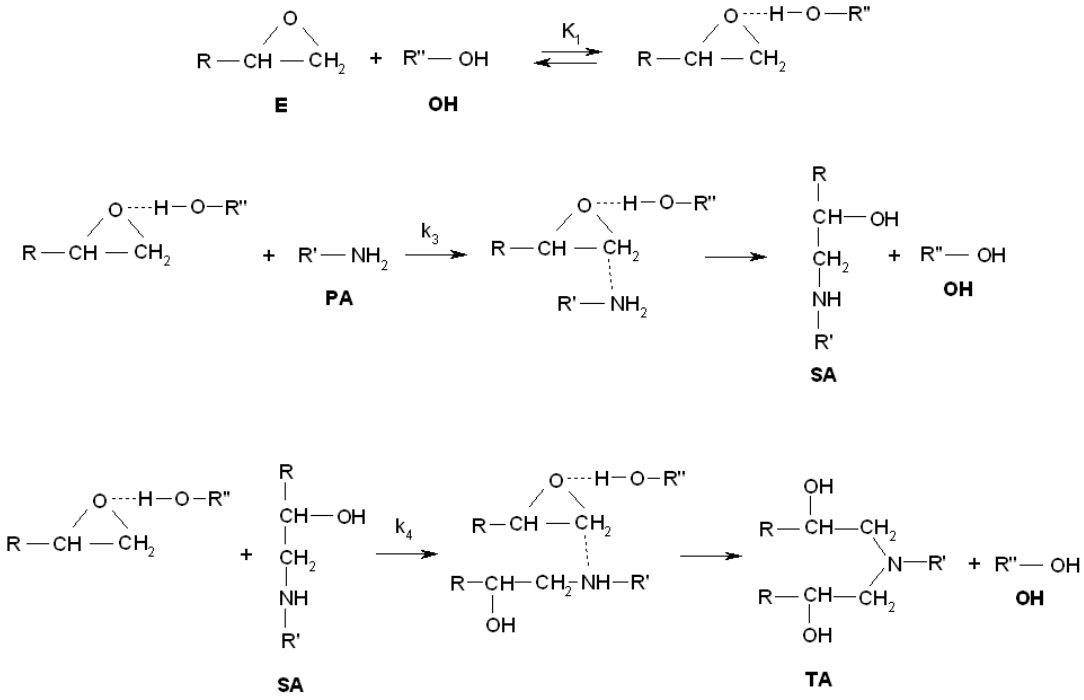

c)

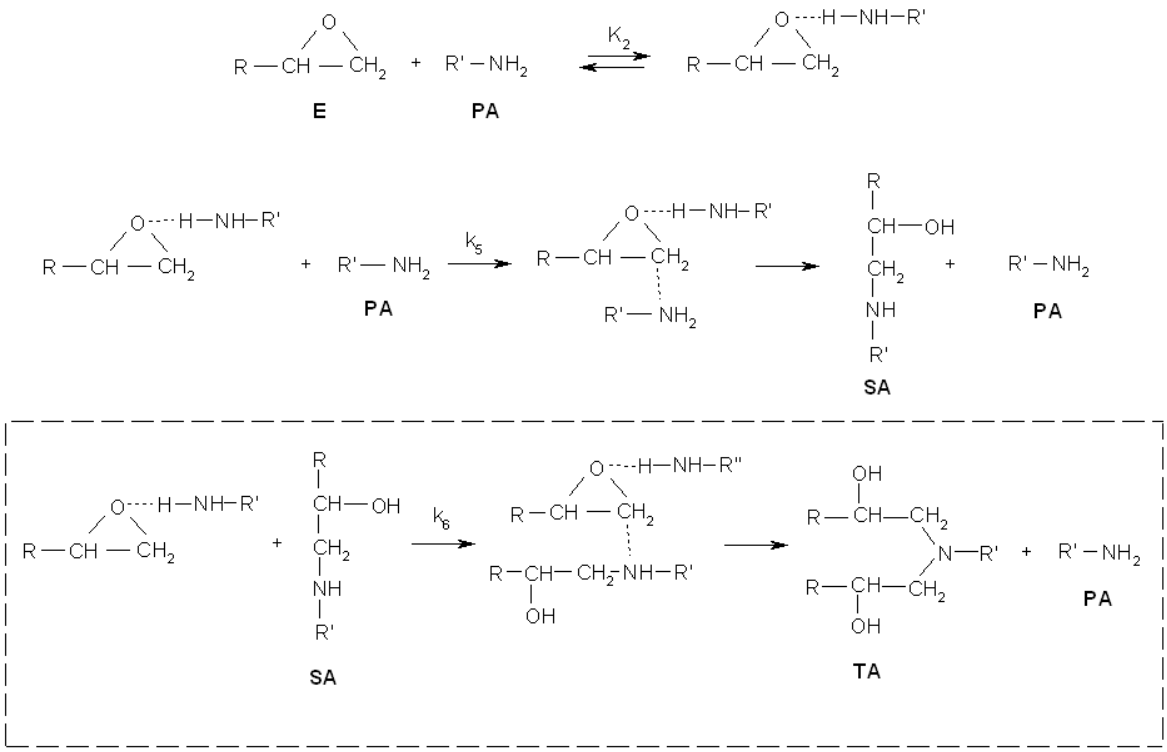

Scheme 2. Mechanism of the epoxy-amine reaction. a) Non-catalytic pathway, b) Reaction path catalyzed by OH group, c) Reaction path catalyzed by amino group.

On the basis of these considerations, a kinetic model was postulated. The model includes three pathways for the reaction between epoxy and primary amine: one non-catalytic pathway and two catalyzed by the OH and amino groups (see Scheme 2). It also considers two possible pathways for the reaction between epoxy and secondary amine: a non-catalytic reaction path and a step catalyzed by OH groups. The differential equations for the model are the following:

$$d[E]/dt = -k_1[E][PA] - k_1'[E][PA][OH] - k_1''[E][PA]^2 - k_2[E][SA] - k_2'[E][SA][OH] \quad \text{Eq. (1)}$$

$$d[PA]/dt = - k_1[E][PA] - k_1'[E][PA][OH] - k_1''[E][PA]^2 \quad \text{Eq. (2)}$$

$$d[SA]/dt = k_1[E][PA] + k_1'[E][PA][OH] + k_1''[E][PA]^2 - k_2[E][SA] - k_2'[E][SA][OH] \quad \text{Eq. (3)}$$

$$d[TA]/dt = k_2[E][SA] + k_2'[E][SA][OH] \quad \text{Eq. (4)}$$

where E is the epoxy, PA is the primary amine, SA is the secondary amine and TA is the tertiary amine. The kinetic rate constant k_1 corresponds to the non-catalytic path for the reaction between epoxy and primary amine, whereas $k_1' = K_1k_3$ and $k_1'' = K_2k_5$ correspond to the pathway catalyzed by OH groups and amino groups, respectively, for the same reaction. On the other hand, k_2 is the kinetic rate constant of the non-catalytic path for the reaction between epoxy and secondary amine and $k_2' = K_1k_4$ is the corresponding catalyzed step.

When the proposed model was used as a hard constraint at each step of the MCR-ALS optimization, the following kinetic rate constants were obtained: $k_1 = 2.43 \times 10^{-3}$, $k_1' = 3.55 \times 10^{-3}$, $k_1'' = 3.87 \times 10^{-6}$, $k_2 = 2.53 \times 10^{-5}$ and $k_2' = 2.75 \times 10^{-3}$. These values agree with what has been said above about the evolution of the species in the pure soft-modelling profiles (see above). In the reaction between the primary amine and the epoxide, the order of magnitude for k_1 and k_1' is similar, which means that the reaction can follow both a non-catalyzed and a catalyzed pathway. A comparison of the values shows that the contribution of the pathway catalysed by the primary amine can be neglected, as can be seen from the value of the rate constant k_1'', which is about three orders of magnitude lower than k_1 and

k_1'. The importance of k_1 may be related to the presence of silicon in the monomer structure, which facilitates the opening of the oxirane ring without the help of the catalysts. However, the value of the catalyzed pathway is slightly higher.

The reaction between the secondary amine and the epoxy monomer seems to follow a catalytic pathway. The number of OH groups generated during the reaction mean that the catalytic pathway more is important than the non-catalytic reaction path. Consequently, the value of k_2 is about two orders of magnitude lower than k_2'. The substitution effect (ρ) can be calculated as the ratio of the rate constants for the reaction between the secondary amine and the epoxide and the rate constants for the reaction between the primary amine and the epoxide (i.e. $\rho = (k_2 + k_2')/(k_1 + k_1' + k_1'')$). In the reaction being studied, ρ has a value of 0.46, which means that the substitution effect is almost absent. This indicates that the primary amine and the secondary amine have similar reactivities. This information is important if the behaviour is extrapolated to situations involving silicon-based monomers that form crosslinked networks. The negative substitution effect (i.e. $\rho << 0.5$) indicates that the reaction of the primary amine group is preferred to the reaction of the secondary amine group and it gives rise to linear chains before the branching during polymerization. In the present case, the nearly non-existent substitution effect (i.e. $\rho \sim 0.5$) results in extensive formation of branching and crosslinking right from the beginning of the reaction [51]. This is in agreement with the concentration profiles obtained after the optimization by MCR-ALS (% of lack of fit = 0.30, explained variance = 99.999 %) under the kinetic model constraint (see Fig. 2), in which both the secondary and the tertiary amine start to form early. Fig. 3 shows the spectra recovered by HS-MCR. The goodness of the spectral profiles was evaluated by calculating the similarity coefficients [21] between the recovered spectra and the spectra recorded for the reactants (i.e. GDMPS and aniline), respectively. The values were: 0.996 for the GDMPS and 0.993 for the aniline. In the same manner, the recovered spectrum for the tertiary amine was compared with the last spectrum recorded for the reacting system. The conversion was

assumed to be almost 100 %. The similarity coefficient for the tertiary amine was 0.999. The similarity coefficients were high in all cases, which suggested that the recovered spectrum of the secondary amine was similar to its real spectrum.

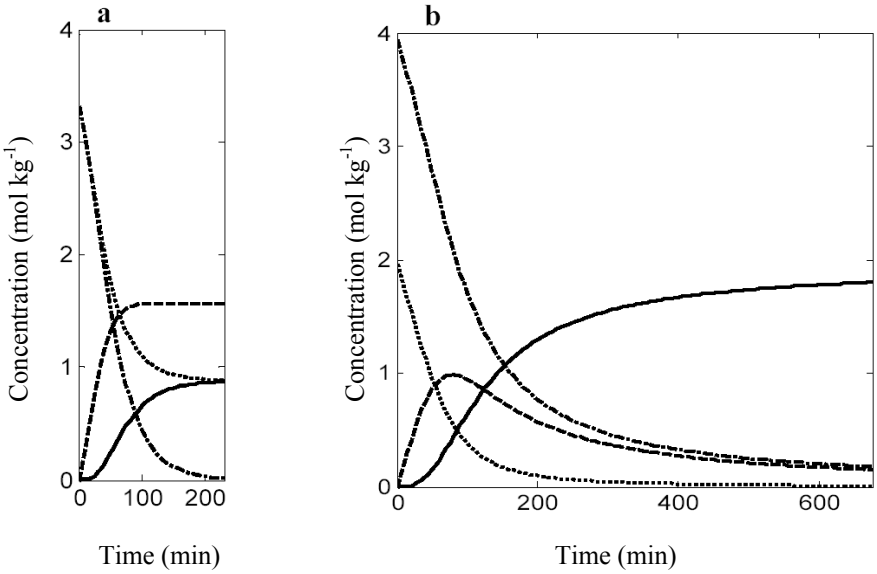

Fig. 2. Concentration profiles obtained by combining HS-MCR approach for the reaction between GDMPS and aniline started with (a) 1:1 and (b) 2:1 GDMPS/aniline molar ratios: (···) aniline, (-·-) GDMPS, (---) secondary amine and (—) tertiary amine.

In order to assess the validity of the concentration profiles obtained, the reaction was monitored by ^{13}C NMR. Fig. 4 shows, as an example, the ^{13}C NMR spectra of the reaction between GDMPS and aniline at three different times. The signals were assigned in accordance with the spectra reported in the literature for the reaction between aniline and phenylglycidylether (PGE), an epoxy monomer similar to GDMPS [52,53]. Fig. 4 a shows the spectrum obtained at the beginning of the reaction, when GDMPS and aniline have still not significantly reacted.

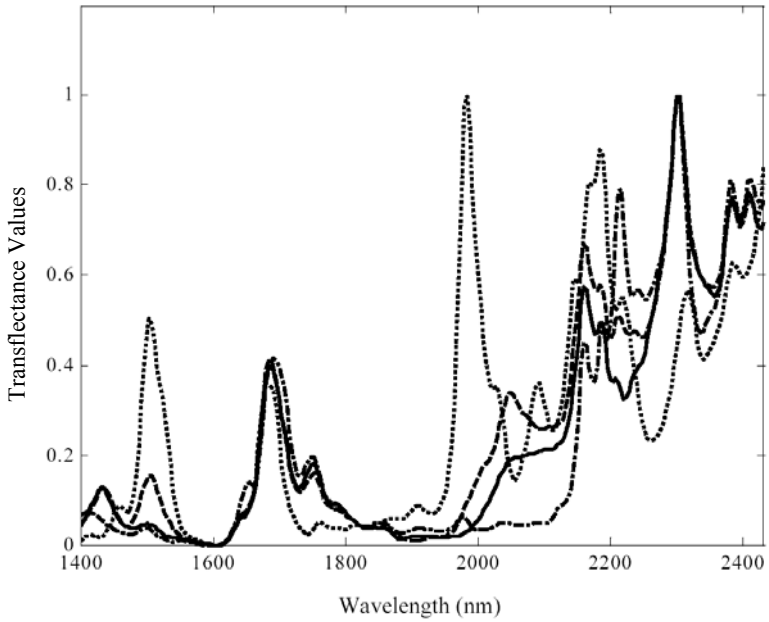

Fig. 3. Recovered spectra after HS-MCR optimization relative to (···) aniline, (-·-) GDMPS, (---) secondary amine and (—) tertiary amine.

When the secondary amine starts to form, new signals are detected (Fig. 4 b) which totally disappeared by the end of the reaction, when the tertiary amine has formed almost completely. The evolution of GDMPS was monitored by three signals: A, B and C. The secondary amine was monitored through the signals of the I, J and K carbons and the tertiary amine was monitored through the L, M and N signals (see Fig. 4). The L, M and N carbons lead to double peaks because of the different stereoisomeric forms of the tertiary amine. The tertiary amine consists of a mixture of RR, RS and SS stereoisomers at a molar ratio of 1:2:1. The RR and SS isomers produce the same NMR spectra that are different from those produced by the RS isomer. Therefore, Fig. 4 (c) shows two signals of similar intensities in several carbons of the tertiary amine [52]. This indicates that the reaction is not stereoselective. So, to calculate the concentration vales of the tertiary amine, the signals of the L, M and N carbons were added together.

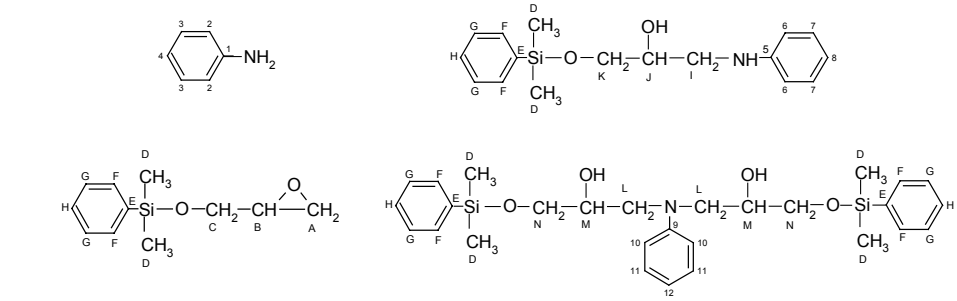

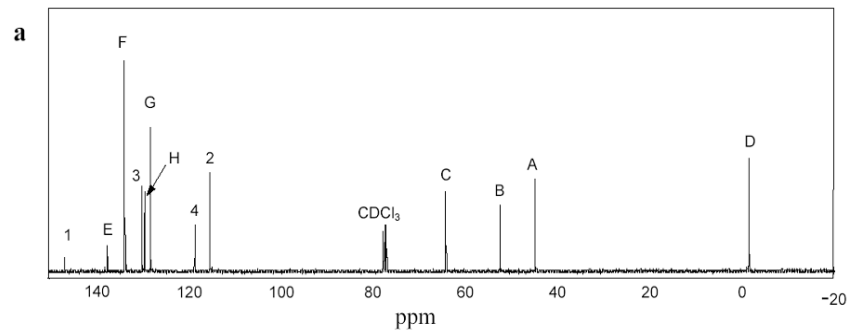

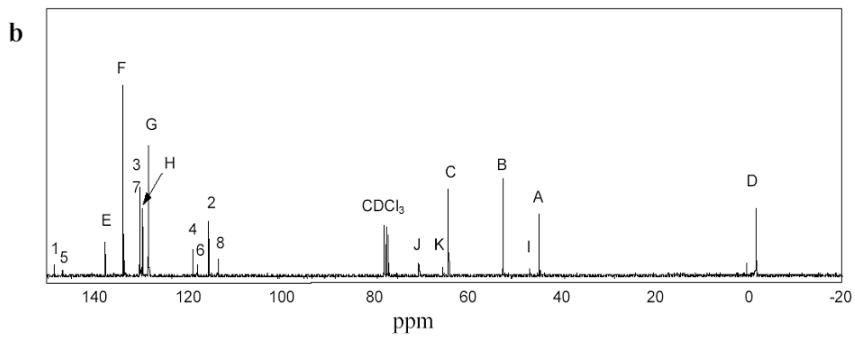

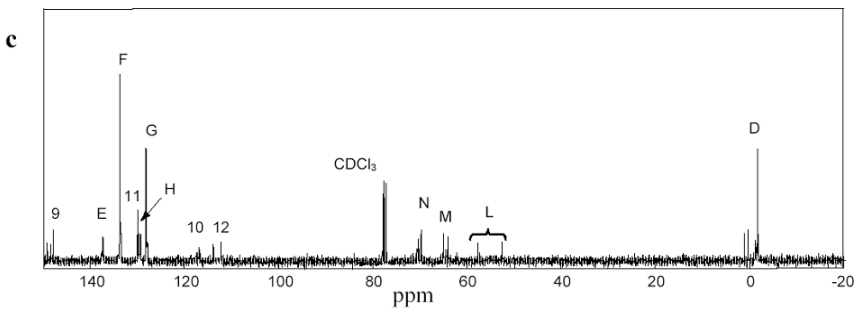

Fig. 4. ^{13}C NMR spectra of the reacting mixture at different times of reaction. a) 0 min, b) 45 min, c) 675 min.

Signals 1-4 could be useful for monitoring aniline, but their relaxation times are so large that the quantitative results would not be trustworthy (relaxation times > 5 s). Therefore, only the profiles for GDMPS, the secondary amine and the tertiary amine can be reliably monitored by ^{13}C NMR.

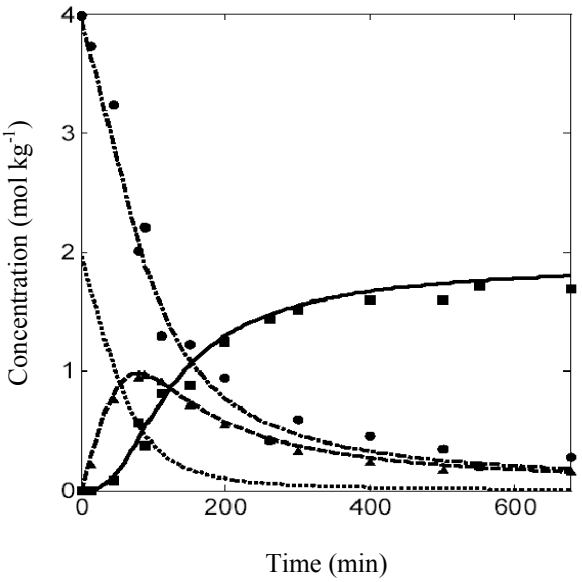

Fig. 5. Superposition of the concentration profiles obtained by soft- and hard-modelling strategy and the values obtained by ^{13}C NMR for the reaction between GDMPS and aniline (molar ratio of 2:1). For the soft-and hard-modelling concentration profiles (···) aniline, (-·-) GDMPS, (---) secondary amine and (—) tertiary amine. In ^{13}C NMR values (●) GDMPS, (▲) secondary amine and (■) tertiary amine.

Fig. 5 shows the concentration profiles obtained by the strategy of soft- and hard-modelling and the concentration values obtained by ^{13}C NMR for the epoxide and the

secondary and tertiary amines. A preliminary visual inspection makes it possible to conclude that there is a good correlation between the profiles obtained by NIR/soft- and hard-modelling strategy and those obtained by ^{13}C NMR. The evolutions of each species are related by the underlying mass balance so the concentration profiles have been analyzed together. When the concentration values recovered by soft-hard modelling were plotted vs. the concentration values obtained by ^{13}C NMR, the resulting straight line had a slope near to 1 and an intercept near to 0 for the three concentration profiles ($y = 0.97x + 0.03$). The similarity between the profiles obtained by both methods was evaluated in terms of the correlation coefficient of this straight line, and the value obtained was 0.987. The joint interval test of slope and intercept [54] was used to test for the presence of bias. The results show that there are no significant differences between the concentration profiles obtained by both techniques ($\alpha = 5\%$).

5. Conclusions

The set of concentration profiles obtained by the pure soft-modelling approach was a valuable guide for postulating a kinetic model for the GDMPS/aniline system.

The combination of soft- and hard-modelling (HS-MCR) was successfully used to obtain concentration profiles and estimate the kinetic rate constants for the reaction. On the basis of the kinetic rate constants, information was extracted about the reactivity of the silicon-based epoxy monomer studied. The kinetic information obtained could be extrapolated to reactions that evolve toward crosslinked products so that the characteristics of the final network can be inferred.

The concentration profiles obtained were compared to those calculated from ^{13}C NMR data, and there was a good correlation between them. Likewise, ^{13}C NMR has proved to be a good technique for monitoring epoxy resins reactions, even though some species require long analysis times if they are to be reliably quantified.

Acknowledgements

L. A. Mercado and M. Galià express their thanks to the Comisión Interministerial de Ciencia y Tecnología (CICYT) (project MAT2005-01593) for providing financial support. M. Garrido, M. S. Larrechi and F. X. Rius acknowledge the financial support provided by the Ministerio de Ciencia y Tecnología (MCyT) (project BQU 2003-01142).

References

[1] S. Y. Lu, I. Hamerton, Prog. Polym. Sci., 27 (2002) 1661.

[2] E. D. Weil, S. Levchik, J. Fire Sci., 22 (2004) 25.

[3] S. V. Levchik, E. D. Weil, Polym. Int., 53 (2004) 1901.

[4] G. H. Hsiue, W. J. Wang, F. C. Chang, J. Appl. Polym. Sci., 73 (1999) 1231.

[5] W. J. Wang, L. H. Perng, G. H. Hsiue, F. C. Chang, Polymer, 41 (2000) 6113.

[6] L. Schechter, J. Wynstra, R. P. Kurkjy, Ind. Eng. Chem., 48 (1956) 94.

[7] I. R. Smith, Polymer, 2 (1961) 95.

[8] Y. Tanaka, T. F. Mika, in: Epoxy Resins Chemistry and Technology, C. A. May, Y. Tanaka (Eds.), Marcel Dekker, New York, 1973.

[9] B. A. Rozenberg, Adv. Polym. Sci., 75 (1986) 113.

[10] L. Xu, J. H. Fu, J. R. Schlup, Ind. Eng. Chem. Res., 35 (1996) 963.

[11] K. Dean, W. D. Cook, L. Rey, J. Galy, H. Sautereau, Macromolecules, 34 (2001) 6623.

[12] Q. Wang, B. K. Storm, L. P. Houmøller, J. Appl. Polym. Sci., 87 (2003) 2295.

[13] G. A. George, P. Cole-Clarke, N. St. John, G. Friend, J. Appl. Polym. Sci., 42 (1991) 643.

[14] J. Mijovic, S. Andjelic, Macromolecules, 28 (1995) 2787.

[15] L. Stordrange, A. A. Christy, O. M. Kvalheim, H. Shen, Y. Z. Liang, J. Phys. Chem. A, 106 (2002) 8543.

[16] E. Furusjo, L. G. Danielsson, Chemom. Intell. Lab. Syst., 50 (2000) 66.

[17] S. Šašić, Y. Ozaki, A. Olinga, H. W. Siesler

[18] P. J. Gemperline, E. Cash, Anal. Chem. 75 (2003) 4236.

[19] S. Navea, A. de Juan, R. Tauler, Anal. Chem. 75 (2003) 5592.

[20] M. Blanco, M. Castillo, A. Peinado, R. Beneyto, Appl. Spectrosc. 60 (2006) 641.

[21] M. Garrido, I. Lázaro, M. S. Larrechi, F. X. Rius, Anal. Chim. Acta, 515 (2004) 65.

[22] L. A. Mercado, M. Galià, L. A. Reina, M. Garrido, M. S. Larrechi, F. X. Rius, J. Polym. Sci.: Part A: Polym. Chem., 44 (2006) 1447.

[23] A. de Juan, E. Casassas, R. Tauler, in: Enciclopedia of analytical Chemistry: Instrumentation and applications. 'Soft-modelling of analytical data', Wiley, New York, 2000.

[24] A. de Juan, M. Maeder, M. Martínez, R. Tauler, Chemom. Intell. Lab. Syst., 54 (2000) 123.

[25] R. Tauler, Chemom. Intell. Lab. Syst., 30 (1995) 133.

[26] R. Tauler, A. Smilde, B. R. Kowalski, J. Chemometrics, 9 (1995) 31.

[27] R. Manne, Chemom. Intell. Lab. Syst., 27 (1995) 89.

[28] A. de Juan, M. Maeder, M. Martínez, R. Tauler, Anal. Chim. Acta, 442 (2001) 337.

[29] E. Bezemer, S. C. Rutan, Chemom. Intell. Lab. Syst., 59 (2001) 19.

[30] A. R. Carvalho, J. Wattoom, L. Zhu, R. G. Brereton, Analyst, 131 (2006) 90.

[31] M. Maeder, A. D. Zuberbülher, Anal. Chem., 62 (1990) 2220.

[32] J. M. Amigo, A. de Juan, J. Coello, S. Maspoch, Anal. Chim. Acta, 567 (2006) 236.

[33] J. M. Amigo, A. de Juan, J. Coello, S. Maspoch, Anal. Chim. Acta, 567 (2006) 245.

[34] E. Bezemer, S. C. Rutan, Anal. Chem., 73 (2001) 4403.

[35] M. Garrido, M. S. Larrechi, F. X. Rius, Appl. Spectrosc., 60 (2006) 174.

[36] M. Garrido, M. S. Larrechi, F. X. Rius, J. C. Ronda, V. Cádiz, J. Polym. Sci.: Part A: Polym. Chem., 44 (2006) 4846.

[37] S. Swier, G. Van Assche,W. Vuchelehn, B. Van Mele, Macromolecules, 38 (2005) 2281.

[38] L. Matějka, Macromolecules, 33 (2000) 3611.

[39] The Mathworks, MATLAB Version 6.5, Natick, MA, 2002.

[40] The Mathworks, Optimization Toolbox, 2.0 version, Natick, MA, 1998.

[41] J. J. Kelly, C. H. Barlow, T. M. Jinguji, J. B. Callis, Anal. Chem., 61 (1989) 313.

[42] Group of Solution Equilibria, University of Barcelona, MCR Homepage, URL: http://www.ub.es/gesq/mcr/ndownload.htm.

[43] L. F. Shampine, in: Numerical solutions of ordinary differential equations, Chapman & Hall, London, 1994.

[44] L. A. Nelder, R. Mead, Comput. J., 7 (1965) 308.

[45] D. L. Massart, B. Vandeginste, L. Buydens, S. De Jong, P. Lewi, J. Smeyers-Verbeke, in: Handbook of Chemometrics and Qualimetrics : Part A, Elsevier, Amsterdam, 1997.

[46] H. R. Keller,D. L. Massart, Chemom. Intell. Lab. Syst., 12 (1992) 209.

[47] E. R. Malinowski, in: Factor Analysis in Chemistry, 3rd ed., Wiley, New York, 2002.

[48] M. Amrhein, B. Srinivasan, D. Bonvin, M. M. Schumacher, Chemom. Intell. Lab. Syst., 33 (1996) 17.

[49] W. Windig, J. Guilment, Anal Chem., 63 (1991) 1425.

[50] J. Mijovic, A. Fishbain, J. Wijaya, Macromolecules, 25 (1992) 979.

[51] C. C. Riccardi , R. J. J. Williams, Polymer, 27 (1986) 913.

[52] T. Dyakonov, Y. Chen, K. Holland, J. Drbohlav, D. Burns, D. Vander Velde, L. Seib, E. J. Soloski, J. Kuhn, P. J. Mann, W. T. K. Stevenson, Polym. Degrad. Stabil., 53 (1996) 217.

[53] H. Jullien, A. Petit, C. Mérienne, Polymer, 37 (1996) 3319.

[54] N. Draper, H. Smith, in: Applied Regression Analysis, 2nd ed., John Wiley and Sons, New York, 1981.

5.5 Conclusiones

Los resultados obtenidos a través de los métodos de modelado blando (MCR-ALS) representan una valiosa información y un soporte sólido para postular mecanismos de reacción en base a los cuales es posible formular modelos cinéticos adecuados para describir los sistemas en estudio. Dichos modelos cinéticos son utilizados para llevar a cabo el modelado duro de los datos experimentales, a fin de obtener las constantes cinéticas de interés.

La combinación de MCR-ALS con los métodos de modelado duro, ha permitido estimar constantes cinéticas para sistemas tan complejos como las reacciones de resinas epoxi, ya sea ajustando al modelo cinético los perfiles de concentración obtenidos mediante modelado blando después de la optimización por ALS, o bien aplicando el modelado duro como una restricción en cada iteración del proceso de optimización, de tal manera que los perfiles recuperados se ven obligados a satisfacer el modelo cinético.

Los sistemas estudiados, si bien corresponden a reacciones de resinas epoxi, tienen diferencias en cuanto a la reactividad de los monómeros epoxídicos frente a la anilina. Esto queda reflejado en los perfiles de concentración obtenidos mediante la combinación de los modelados blando y duro, y permite analizar los efectos que puede tener la presencia de diferentes heteroátomos en el mecanismo del proceso de curado de resinas epoxi.

Asimismo, las constantes cinéticas obtenidas (algunas de ellas reportadas por primera vez para este tipo de reacciones) permiten extraer información acerca de la reactividad de los monómeros estudiados, como es el caso del parámetro llamado efecto de sustitución. La extrapolación de esta información cinética a reacciones de polimerización puede brindar una idea acerca de las características de la red tridimensional del producto del curado, las cuales están directamente relacionadas con las propiedades del polímero final.

6. Consideraciones a la metodología propuesta para el seguimiento de procesos de curado

6.1 Introducción

En el capítulo 2 ya se ha hecho mención a la íntima relación que existe entre la variación en la concentración de las especies que participan de un proceso de curado y los cambios físicos que tienen lugar durante la polimerización (ver apartado 2.1.3). El aumento en la viscosidad de una resina epoxi, cuando ésta se aproxima al punto de gelificación, está ocasionado por el extenso entrecruzamiento entre las cadenas poliméricas formadas. La consiguiente restricción en la movilidad de las cadenas y el aumento en la rigidez de los enlaces se ven reflejados en los espectros NIR registrados durante la monitorización de la reacción de curado.

La frecuencia de vibración de las moléculas no sólo depende de las masas de los átomos involucrados sino también de la fuerza del enlace que los une. La fuerza del enlace, por su parte, se ve afectada por la aparición de interacciones inter y/o intramoleculares, como las interacciones dipolo-dipolo, asociaciones moleculares y puentes de hidrógeno [99]. Precisamente, el aumento en la viscosidad de polímeros como las resinas epoxy está estrechamente ligado a la aparición de puentes de hidrógeno que involucran, principalemente, los grupos hidroxilo [100,101]. Cuando un grupo O-H participa en una interacción del tipo puente de hidrógeno, la frecuencia de la vibración de estiramiento disminuye, puesto que el átomo de hidrógeno está "retenido" por dos centros electronegativos (ver Fig. 6.1 a). Esto ocasiona un desplazamiento de la banda de absorción del grupo O-H hacia mayores longitudes de onda. Lo contrario ocurre con la frecuencia de vibración de flexión: el enlace del grupo hidroxilo se ve debilitado puesto que la densidad electrónica está parcialemente deslocalizada entre los dos centros electronegativos (ver Fig. 6.1 b), con lo que la flexión se ve favorecida. El aumento en la frecuencia ocasiona un desplazamiento en la banda hacia regiones de menor longitud de onda [120,121]. En el espectro NIR, estos efectos se aprecian como ensanchamientos y aparición de hombros y colas en los picos relacionados con los grupos funcionales afectados.

Estiramiento Flexión

Fig. 6.1 Representación esquemática de las vibraciones de estiramiento (a) y flexión (b) cuando el grupo OH se ve afectado por una interacción de tipo puento de hidrógeno.

Es importante tener en cuenta estas consideraciones cuando se aplica la resolución multivariante de curvas a los datos NIR registrados durante la monitorización de una reacción de curado. Los cambios operados en el espectro NIR a raiz de las variaciones en la viscosidad ocasionan una variabilidad en los datos experimentales que no está directamente relacionada con la reactividad de las especies químicas. Dicho en otras palabras, el modelo en el cual se basa la aplicación de los métodos de resolución de curvas a datos espectroscópicos (la ley de Lambert-Beer) deja de cumplirse, puesto que se pierde la relación de proporcionalidad entre los cambios en la absorbancia (o transflectancia, según sea el caso) y los cambios en la concentración de las especies absorbentes presentes en el sistema en estudio. Por lo tanto, la aplicación de MCR-ALS con el objeto de describir los perfiles de concentración y espectrales para una reacción de curado, conduciría a resultados erróneos.

La capacidad de la espectroscopia NIR para detectar los cambios en la viscosidad que tienen lugar durante un proceso de curado ha sido estudiada en esta Tesis a través los experimentos llevados a cabo para el sistema DGEBA/DDM. Los resultados que se comentan en la sección 6.2, muestran la existencia de una relación entre los espectros NIR y la viscosidad compleja que permite establecer un modelo de calibrado para la predicción de dicha propiedad.

6.2 Modeling of complex viscosity changes in the curing of epoxy resins from near infrared spectroscopy and multivariate regression analysis

Applied Spectroscopy, 58(12), **2004**, 1424-1430

M. Garrido, M.S. Larrechi and F.X. Rius*

Department of Analytical and Organic Chemistry, Faculty of Chemistry, Rovira i Virgili University, Pl. Imperial Tàrraco, 1, 43005 Tarragona (Spain)

(Received 23 April 2004; accepted 26 July 2004)

Abstract

The present study investigates the relationship between the changes in complex viscosity and near infrared spectra. Principal component regression analysis is applied to a near infrared data set obtained from the *in situ* monitoring of the curing of diglycidyl ether of bisphenol A with the diamine 4,4'-diaminodiphenylmethane. The values of complex viscosity obtained by dynamical mechanical analysis during the cure process were used as a reference. The whole near infrared spectra recorded throughout the reaction, unlike the univariate data analysis at some wavelengths of the spectra, contain a sufficient amount of information to estimate the complex viscosity. The relationship found was high and the results demonstrate the quality of the fitted model. Also, a simple user-friendly procedure for applying of the model focused to the user is shown.

1. Introduction

Nowadays, thermosetting resins are among the most important polymer materials in use. Epoxy resins are a particularly important class of thermosetting materials, because of their chemical resistance, notable adhesive characteristics, and good mechanical and physical properties. The reactions that have most been studied are those based on diglycidyl ether of bisphenol A (DGEBA).[1,2] These epoxy resins are typically cured with the aid of crosslinking agents or hardeners. The most common procedure is a reaction with polyfunctional amines, e.g. 4,4'diaminodiphenylmethane (DDM).

Epoxy-amine polymers are often used in the construction, electronic, and aerospace industries as well as in medicine and odontology.[3-6] In these applications, the curing process of the epoxy resins affects the chemical structure of the network and, hence, determines the final physical properties.[5-7] This dependence explains the numerous studies that investigate the mechanism and quantify the kinetics of cure reactions.[8-13] Consequently, there is a need for a more detailed understanding of the curing process and the structure-property relationship of cure epoxy resins in order to control the curing economically and to optimise the physical properties of the final product.

During the curing reaction the polymer undergoes several transformations: it starts as a liquid, passes through its gel point, where it is transformed into a rubber, and then through its vitrification point, where it is transformed into the vitreous state. The molecular mobility in the system decreases as the cure reaction proceeds. These transformations can be followed by such techniques as differential scanning calorimetry (DSC),[14,15] dielectric and mechanical relaxation,[16-18] dynamic mechanical analysis (DMA),[19-21] and several spectroscopic methods, e.g., infrared,[21-22] Raman[23] and fluorescence.[24-26]

Spectroscopic techniques make it possible to monitor the process on-line and they provide data about the conversion degree of the reagents. Moreover, DMA and DSC provide information about parameters such as gelation and vitrification times or glass transition temperature (Tg), but they cannot control the process *in situ*. It has been demonstrated that different methods can be combined to understand crosslinking behaviour better.[21,26]

The spectroscopic techniques based on vibrational spectroscopy are the most suitable since they are non-destructive and monitor the epoxy resin curing *in situ*.[11,21,22] Near infrared spectroscopy, in particular, has a wavenumber domain in which the absorption bands are overtones or combinations of fundamental vibrations observed in the mid-infrared region. Therefore, their absorptivities are much lower and each band can be readily isolated from the neighbouring bands.This means that a relatively large quantity of sample can be used and that the kinetics of the curing process can be studied.[8,10,12,20,27,28]

Most of the studies in the bibliography that apply near infrared spectroscopy to monitor of curing reactions use the data in a univariate way, relating the variation in the peak area (or height) to a percentage of conversion of the reagents in the polymeric product.[12,21,22] When working with multivariate data, the sources of variability found in the spectra not only correspond to the changes in concentrations of the species in the reaction, but also reflect other phenomena, during the curing process, such as the viscosity changes, which are no directly related to the reactivity of the species.

Several authors have reported a relationship between NIR spectra and the changes caused by hydrogen bonds during the curing process because of the increase in viscosity.[8,10,29] So we have investigated the relation between viscosity and NIR spectra.

The aim of this paper is to show that there is a relation between the viscosity measurements obtained by DMA and the NIR spectra recorded on-line throughout the

curing reaction for the same process, using a principal components regression model. With only one NIR spectrum of the reaction mixture, the proposed model can also help to determine in which stage the curing process is (liquid-gel-vitreous). The application to the reaction of curing epoxy resin between DGEBA and DDM is presented.

2. Background

In general, the mechanism of the addition reaction between epoxies and amines has two stages[30,31] (see Fig. 1). However, depending on the conditions of reaction (temperature, concentration of the reactive groups, the presence or absence of catalysts) and the type of the epoxy-amine system, other collateral reactions such as etherification, cyclization or homopolymerization can also occur.

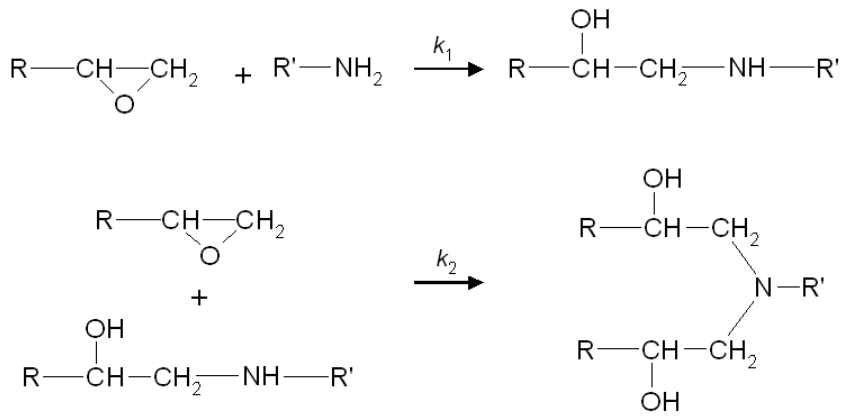

Fig. 1. Scheme of the curing reaction of epoxy resin with an amine as curing agent.

After the chemical reaction with the appropriate curing agent, the epoxy resin produces a three-dimensional network and, during this process, the material changes from a viscous liquid to a hard solid. Because of the interactions between kinetic chemistry and the changes in the physical properties of the reaction environment it is not easy to analyse the evolution of the curing reaction.

The curing reaction is generally characterised by gelation and vitrification processes. Viscosity increases dramatically as gelation is approached, and the molecular weight goes to infinite.[32] Then, when the polymer reaches the region of vitrification, the reaction becomes slower and, finally, stops. Therefore, the changes in viscosity after vitrification are negligible.

The variations in viscosity are closely related to the appearance of hydrogen bonding in the reactive mixture.[8,33] This can be corroborated by means of infrared spectroscopy. In general, the formation of hydrogen bonds affects the vibrational spectra of the groups involved by decreasing the frequency of stretching modes and increasing the frequency of bending modes.[34] In particular, when epoxy resins curing is followed by near infrared spectroscopy, the bands corresponding to the OH group have been well studied. The free OH band appears at 1435 nm and the peak maximum does not shift, while the hydrogen bonding species form a tail at longer wavelengths (1460 – 1480 nm) in the later stages of the curing process.[8] A build-up in the base line is also observed from 1540 to 1615 nm. This would correspond to the hydrogen-bond of hydroxyl group from the opening of the epoxy ring.[10] Other authors[35] attribute the relative change in the base line to variations in refractive index of the sample. As the curing reaction progresses, the band at 2040 nm, which corresponds to the OH combination of stretching and bending modes, shifts approximately 10 nm to a lower wavelength. This is in agreement with the increase of the intermolecular hydrogen bonding.[10]

3. Experimental

3.1 Reaction conditions

Diglycidyl ether of bisphenol A (Epikote 828 from Shell, EEW 190 g/mol) was cured with 4,4'-diaminodiphenylmethane (99% from Aldrich) at curing temperature of 70ºC. The molar ratio of DGEBA and DDM was 2:1. The necessary amounts of the starting materials were manually mixed for 3 minutes at the cure temperature. Then, the mixture was transferred into the reaction cell (either NIR or DMA), whose temperature was fixed at 70ºC.

3.2 NIR measurements

NIR transflectance measurements were taken every 4 nm between 1100 and 2500 nm in an InfraAlyzer 500 Bran+Luebbe spectrophotometer. The spectra were recorded at intervals of 5 min for approximately 4 hours, until no significant changes in two consecutive spectra were observed. The measurements were performed by using a "home-made" cell consisting in a thin plate of glass (where a drop of sample is placed) that is located on a stainless steel diffuse reflecting surface. The cell is closed by using a quartz window. The reaction under study was monitored several times in order to test the reproducibility. No significant changes were observed if the measurement time was well controlled.

3.3 DMA measurements

The complex viscosity was measured with a Dynamic Mechanical Analyser 2980 DMA V1.40 from TA Instruments equipped with a shear sandwich clamp and using a fixed frequency of 1Hz (amplitude 30 μm). The measurements were taken isothermally at 70ºC. A glass fiber support (10 x 10 x 0.34 mm^3) was impregnated with the reacting mixture. The curve of complex viscosity as a function of time was obtained (see Fig. 2). The reproducibility of DMA measurements, as far as the transition points are concerned, is very good.[36,37]

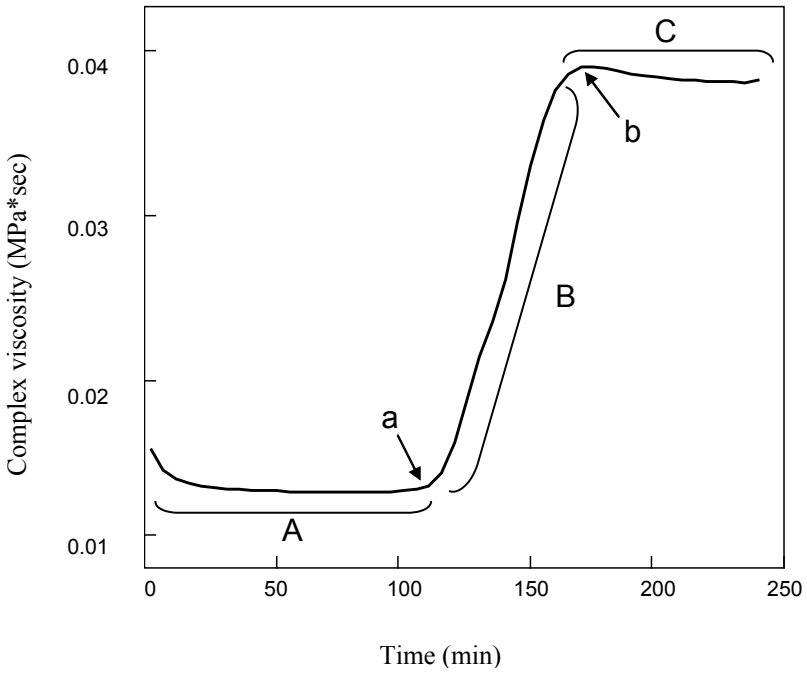

Fig. 2. Complex viscosity curve obtained by DMA. a = gel point, b = vitrification point. A, B and C, see the text.

3.4 Calibration model and validation

The NIR data were arranged to conform a matrix of dimensions 49x351. There is one row for each of the spectra recorded every five minutes. Each row, then, corresponds to different reaction times. The columns are the number of wavelengths at which the spectra were recorded, i.e. 351 NIR wavelengths recorded between 1100 and 2500 nm, every 4 nm. All the original spectra were corrected. This was to eliminate any vertical shift in the spectra during the course of the experiment caused by using a NIR spectrophotometer with only one light beam. This pre-treatment involves subtracting the lowest value of log(1/R) for each individual spectrum from the values of log(1/R) recorded at each wavelength.[38]

The viscosity data were acquired every five minutes so that both NIR and DMA measurements could be compared over time. The complex viscosity values were arranged into a matrix of dimensions 49x1. The rows correspond to the same times as for the NIR.

In order to build the multivariate regression model relating viscosity to NIR spectra, the zone corresponding to significant changes in viscosity was selected (see region B in Fig. 2). This corresponds to the range between 115 and 165 min.

Two regression models were performed. In the first, wavelengths were selected using the information found in the literature about which wavelengths are affected by the hydrogen bonding produced by the increases in viscosity (see section 2). The selected regions of the spectrum were between 1460 and 1488 nm,1540 and 1636 nm, and 2020 and 2140 nm. In total they are 64 wavelengths. Therefore, the matrix of predictor variables used in the calibration model was $\mathbf{X_1}$ (11x64). The second model was performed using all the wavelengths of the spectra, so the matrix of predictor variables was $\mathbf{X_2}$ (11x351). The matrix of predicted variables was $\mathbf{Y}$ (11x1). In all matrices the number of rows correspond to the selected interval of time, every 5 min. Before the principal components regression model was constructed, all the matrices were centred.

To select the optimal number of factors for the models, a leave-one-out cross

validation model with a different number of factors was performed and the prediction residual error sum of squares (PRESS) was calculated for each model using Eq. (1)

$$PRESS = \sum_{i=1}^{n} \left(\hat{y}_i - y_i \right)^2 \qquad \text{Eq.(1)}$$

where n is the total number of calibration samples, $\hat{y}_i$ represents the estimated viscosity, and y_i is the experimentally measured viscosity value for the ith sample left out of the calibration during cross validation.

The model that yields the minimum PRESS is used as the benchmark. All models with fewer factors are compared with this benchmark by means of an F-test.[39] The objective of this comparison is to find the model with the fewest factors whose PRESS is not significantly larger than that PRESS of the benchmark.

The overall ability of the model to make predictions can be measured by the root mean square error of cross validation (RMSECV), which is defined by Eq. (2):

$$RMSECV = \left(\frac{PRESS}{n} \right)^{\frac{1}{2}} \qquad \text{Eq. (2)}$$

where n is the total number of calibration samples. The smaller the error of cross validation is, the greater the agreement between the predicted and the measured values, and the more appropriate the model is.

In order to detect the presence of outliers in the set of NIR spectra used to construct the model, the T^2 plots were made. Hotelling's T^2_{limit} statistic was calculated[40,41] so that when the T^2 values of a particular spectrum are larger than the T^2_{limit}, it is rejected. The same procedure is followed to evaluate if a new NIR spectrum can be introduced into the model to predict the value of viscosity. Again, if the T^2 value of the new spectrum is greater than the T^2 limit, it cannot be used to predict values of viscosity.

The joint interval test of slope and intercept[42] was used to test for the presence of bias in the models. The predicted results from the model are regressed against the measured results. If there are no significant differences between them, the values for the slope and the intercept of the straight regression line should fall within the elliptical confidence region (considering an $\alpha = 5\%$) centred on the theoretical values of 1 slope and 0 intercept. The following software was used: Unscrambler version 7.5 (Camo ASA, Norway) and Matlab 6.1 (The MathWorks, Inc., USA).

4. Results and discussion

Figure 3 shows all the NIR spectra corresponding to the monitoring of the curing reaction. The principal bands that characterise the different functional groups involved in the reaction can be seen. The bands of the oxirane group (1648 and 2212 nm), and the primary (1982 nm and 1502 nm) and secondary (1502 nm) amines disappear as the reaction progresses, and the band corresponding to the hydroxyl group (1432 nm) appears.[8,27]

Also, the same regions are affected by the hydrogen bonds generated in the course of the reaction when viscosity increases. The band at 1432 nm, which corresponds to O-H

stretching, is not affected since it characterises free OH groups (see section 2). The hydrogen-bonded hydroxyl group absorbs at longer wavelength than the free hydroxyl group (see Fig. 4). The effect is that a "tail" appears between 1460 and 1485 nm. Fig. 4 shows the build-up of the base line from 1540 to 1630 nm, a shift that can also be attributed to the changes in the refractive index of the sample as the viscosity is increasing (see also section 2).

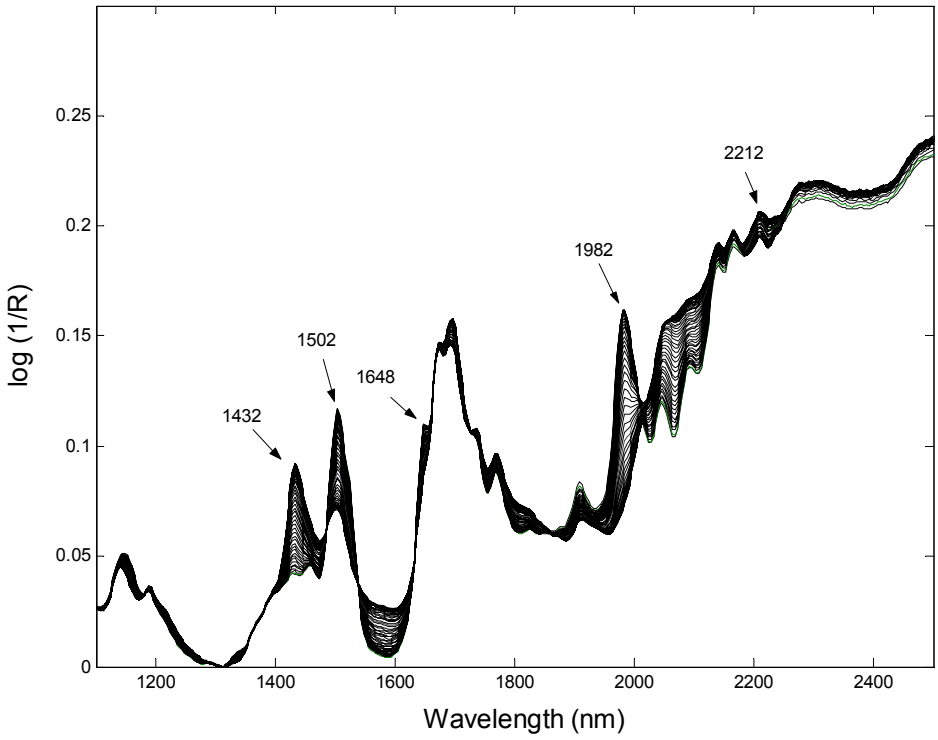

Fig. 3. NIR spectra relative to the DGEBA/DDM 2:1 system at 70ºC, after the application of the offset correction.

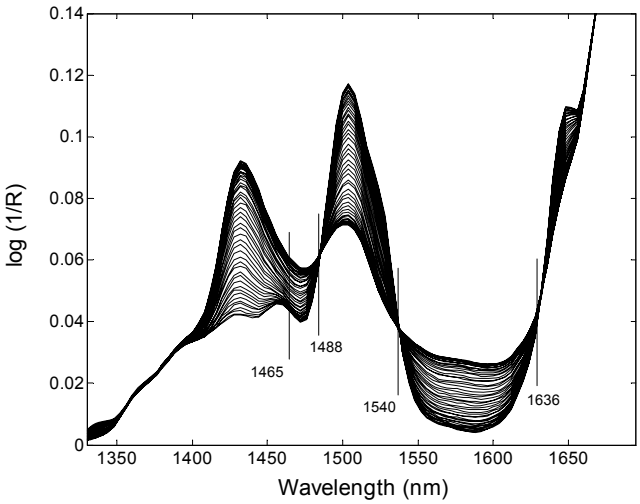

Fig. 4. Enlarged view of zone between 1325 and 1675 nm of the NIR spectra of a DGEBA/DDM system at 70 ºC, showing the effect of hydrogen bonds on the base line of this region.

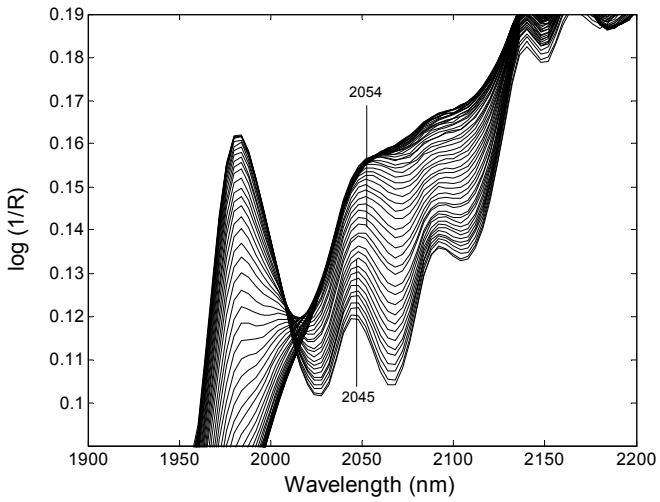

Fig. 5. Overlapped spectra of DGEBA/DDM system at 70 ºC, showing a decrease in the primary amine band (1982 nm) and the growth and shift of the hydroxyl band (2045 nm)

The wide band at 2045 nm is the result of a combination of the O-H stretching and bending modes. As curing proceeds, the maximum shifts by approximately 10 nm to longer wavelength throughout the gelation. This is related to the increase in intermolecular hydrogen bonding (Fig. 5).

Figure 2 shows how complex viscosity evolves over time, measured by DMA. In region A, the changes in viscosity are negligible. At this stage, the monomer molecules react to form linear chains followed by extensive branching. As the curing process continues, the chains in the polymer crosslink and when the gel point is reached (see Fig. 2 point 'a'), the polymer becomes insoluble. The criterion used for determining the gel point was, fundamentally, the time at which the peak of the tan δ reaches the maximum, in other words, the point at which the material begins to develop mechanical properties characteristic of elastic solids.[32] The calculated gel point was 115 min, which is in agreement with the literature.[21] From this moment, the complex viscosity increases drastically (region B), and continues to increase until the reaction becomes slower (because of the loss of mobility in the chains) at the vitrification point (see Fig. 2, point 'b'). Vitrification was defined as the moment at which the storage modulus became constant or almost constant and represents the maximum state of cure.[32] The calculated vitrification point was 170 min, which also agrees with the values found in other studies.[21] From this moment, the curing process stops (region C). This was also reflected by the NIR spectra, since the changes produced after the vitrification point were negligible.

The relation between the measures of viscosity and the set of NIR spectra selected (115-165 min) was close. Only two factors were needed for both models, which means that the 351 variables (the wavelengths) can be compressed into 2 variables. These two sources of variability may be due, first, to the changes in the epoxy resin caused by the reactivity of the functional groups that take part in the reaction and, second, to the changes in viscosity throughout the curing process.

When the regression model was constructed with all the NIR wavelengths, the percent variance explained was 99.23 % for the NIR data, i.e. almost all the information was collected in these two factors, which are a linear combination of the original variables. For the viscosity data, the two-factors model expressed 99.05% of the variation present in the original measurements.

Figure 6 shows the plot of measured complex viscosity vs. predicted complex viscosity. The slope was 0.9881 and the intercept was 3 x 10^{-4}, with a coefficient of correlation (R^2) of 0.9882. The RMSECV was 8.9 x 10^{-4}.

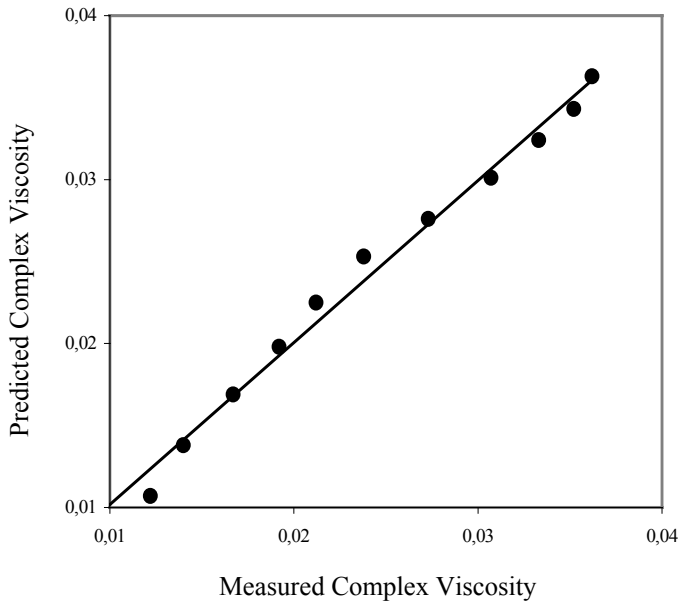

Fig. 6. Predictions from the principal components regression model/NIR spectra versus the expected value measured by DMA. a) with selection of wavelengths b) with complete spectra

For the model in which the wavelengths were selected, the values for the slope and the intercept were 0.9755 and 6 x 10^{-4}, respectively. The explained variances was 100% for the NIR measures and 98.89% for the complex viscosity data. In this case the RMSECV was 1.33 x 10^{-3}. The coefficient of correlation (R^2) was 0.9737.

In both cases there is a close relationship between NIR spectra and viscosity but the values of the slope, the intercept and the RMSECV show that the model with selection of wavelengths is worse. This means that the complete spectrum includes some relevant information that does not appear in the wavelength ranges selected. The loadings plot could be useful as a variable diagnostic, and represent the relative contribution of the variables in the model. In Fig. 7 the plot of the principal components loadings versus wavelengths is shown. In the first principal component, the more important contributions are linked with the characteristic absorption bands corresponding to the functional groups that are formed or consumed throughout the reaction: oxirane (1648 and 2212 nm), primary amine (1982 and 1502 nm), secondary amine (1502 nm) and OH groups (1432 nm and the wide band around 2072nm). It can also be observed a shoulder at 1468 nm that corresponds to the hydrogen-bonded OH groups and a broad band at 1572 nm related to the build-up of the base line in this region of the spectrum caused by the changes in the refractive index of the sample (see section 2). The main characteristic of the second principal component loadings is its noisy structure along the recorded wavelengths. However, a wide band at 2050 nm can be observed. This band is related to the shift observed in the spectrum due to the increase of hydrogen-bonded OH groups (see also section 2). At the same time, some contribution at 1502 and 1982 nm (corresponding to amine groups) and 2212 nm (oxirane groups) can be seen. The physical changes that take place during the curing process also affect the overall reaction rate. The rate of increasing or decreasing of the characteristic absorption bands become slower, and these variations are collected in the principal components. Thus, the information present in the bands assigned to the hydrogen bonding is not the only one related to the viscosity.

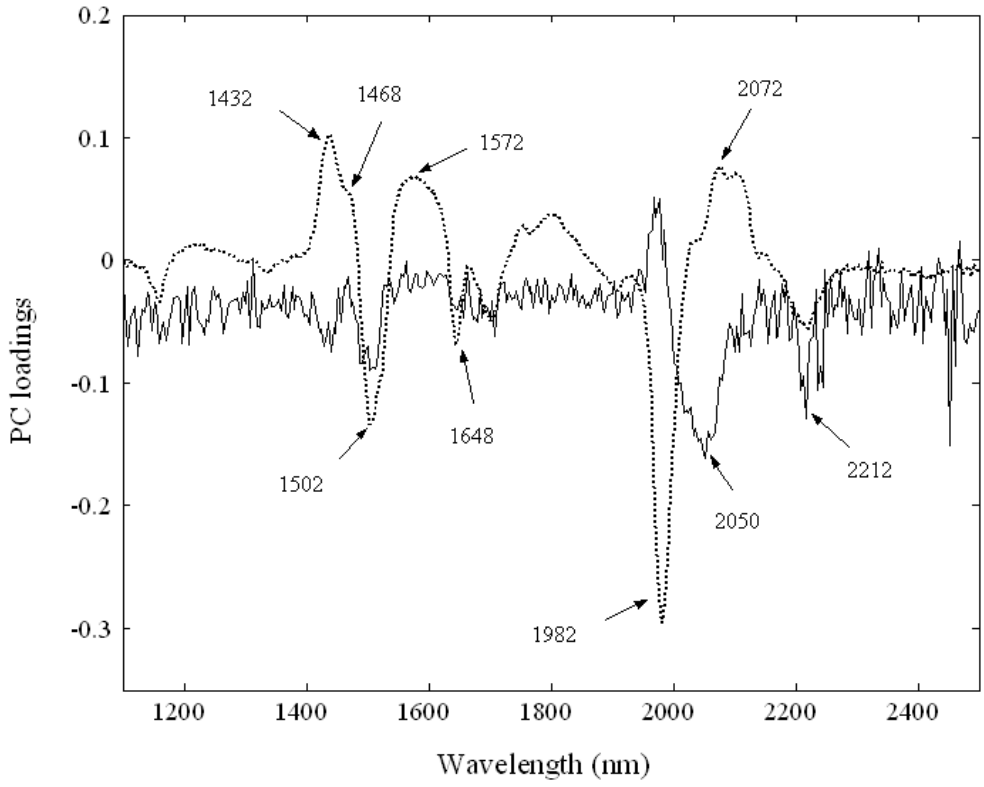

Fig. 7. Loadings plot. Dotted line: loadings for the first principal component. Solid line: loadings for the second principal component.

On the other hand, some changes can occur in the spectrum because of the variations in the refractive index of the sample when the viscosity is increasing. This effect depends on the type of experimental arrangements used to obtain the NIR spectra of the resin (transmission, reflectance, transflectance, attenuated total reflection). In this study, since the sample is a liquid which evolves into a transparent solid resin, the NIR spectra were acquired by transflectance. When the light reaches the sample, part of this radiation can exhibit specular and diffuse reflection, but a significant proportion of the original intensity is transmitted through the sample. The extent of this effect depends on the

chemical characteristics of the sample, variations in the refractive index and the presence of particles having size comparable to the wavelength of the light.[35] Thus, as the resin is uring, the change in the refractive index can produce changes in the whole range of wavelengths, and this can be observed as variations in the base line of the spectrum (away from an absorption band).

Therefore, the model constructed with all the wavelengths is chosen for this study. The model shows very good agreement between the reference method measurements and the predicted values of viscosity. This demonstrates that there is a relationship between NIR spectra and complex viscosity.

The presence of bias for the selected model was found to be not significant by means of the joint interval test of slope and intercept at a significance level of $\alpha = 5\%$ (see Fig.8).

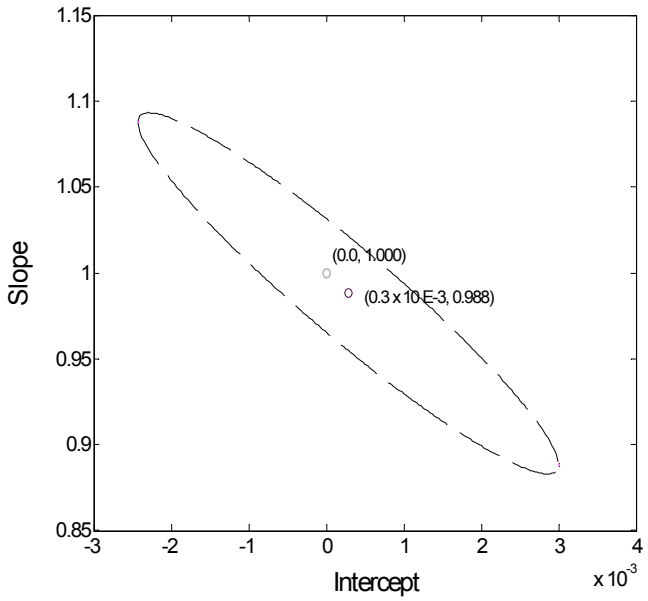

Fig. 8. Joint interval test for the slope and the intercept

Fig. 9 shows the T^2 plot for the NIR spectra corresponding to the samples used in the model. The T^2 limit was calculated with $\alpha = 5\%$, and its value was 9.46. All the samples used in the construction of the model were under the limit. The value of T^2 obtained for sample 7 is higher than the values for the rest of the samples. In comparison with the NIR spectra of other samples, there is a change in the increase (or decrease) of the bands corresponding to the functional groups that take part in the reaction. This sample corresponds to a time of 145 min which is also the point of inflection in the curve of complex viscosity (Fig. 2). One reason for this may be that, from this point on, the control of the curing process by diffusion begins to be important, and the reaction rate changes. Anyway, the sample was not considered to be an outlier, since its value of T^2 does not surpass the T^2 limit and, therefore, it was used to construct the model.

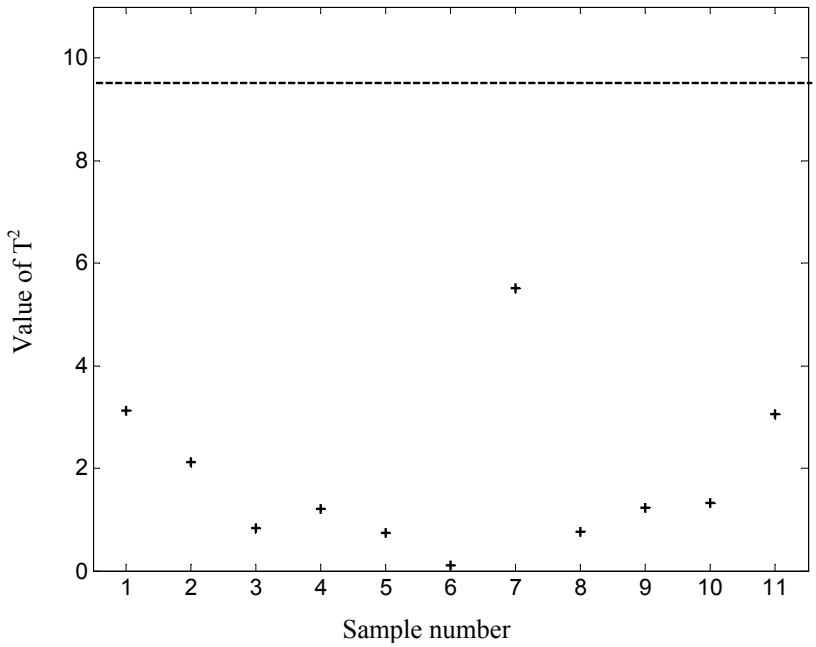

Fig. 9. T^2 plot for the samples used in the construction of the model.

The T^2 values were also calculated for the spectra belonging to the interval of time between 0 and 110 min (times correspond to the A region in the viscosity plot). The T^2 values were always over the limit. Therefore, they cannot be used to predict the viscosity with the model. On the other hand, the T^2 values calculated for the spectra recorded between 170 and 240 min were under the T^2 limit. These spectra correspond to the so called "zone of vitrification", and their shapes are very similar to the shape of the last spectrum used in the model (165 min) because the reaction practically stops because of the typical decrease in mobility in the vitreous state. The predicted complex viscosity for these spectra is the same as the complex viscosity predicted for a spectrum recorded at 165 min.

The proposed model makes it possible to know the extent of the curing process, with only one NIR spectrum of the reaction mixture (see scheme in Fig. 10). The procedure consists of recording a NIR spectrum of the reacting mixture, at a particular stage of the curing process, and calculating the corresponding T^2 value. If the value is under the T^2 limit, the principal components regression model must be performed. The value obtained makes it possible to enter in the complex viscosity curve and to determine either the time that the epoxy resin will still take to reach the vitrification point or if the polymer has vitrified. This is possible because both the DMA and NIR measurements are highly reproducible, particularly as far as time is concerned. On the other hand, if the value of T^2 is above to the limit, the model cannot be used to predict the complex viscosity. In this case, the information that is obtained is that the polymer is still in the A zone (see Fig. 2), before the gel point, but it is not possible to establish how much time must elapse before gelation. It should be remembered that of all the spectra obtained throughout the reaction, the only ones that had T^2 values greater than the T^2 limit were those recorded between 0 and 110 minutes, i.e. in the A zone.

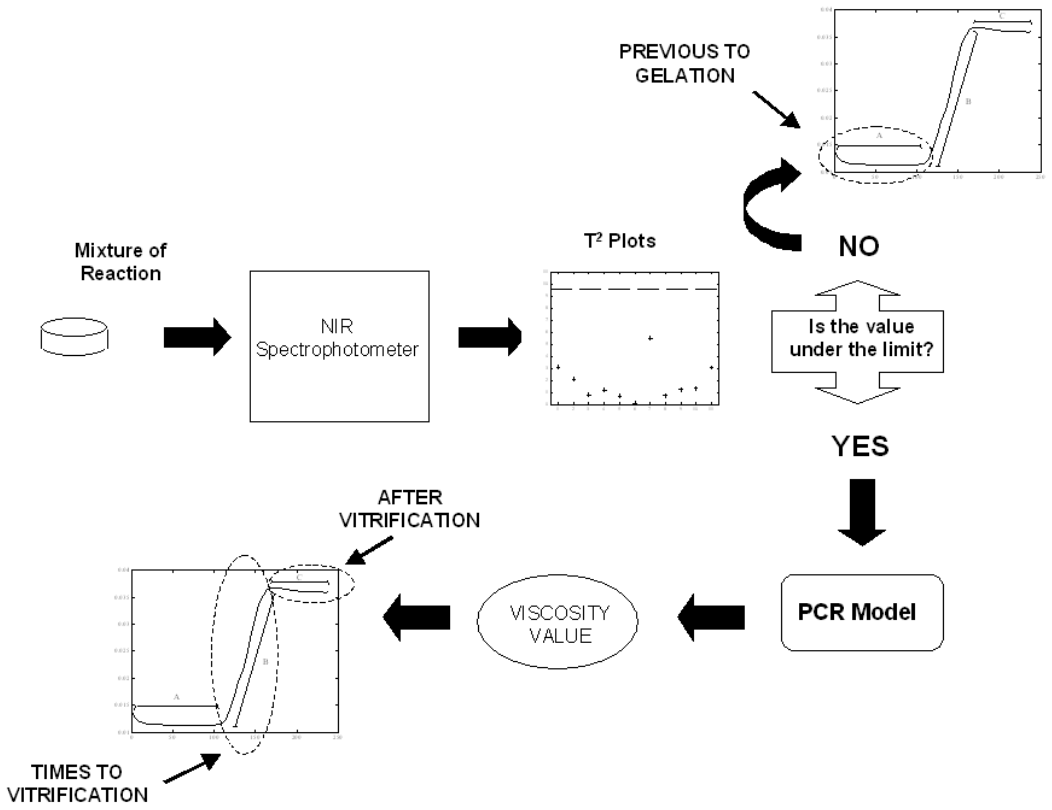

Fig. 10. Scheme for the proposed practical procedure.

5. Conclusions

We have shown that the increase in the viscosity of samples involved in a polymerization process is detected by NIR spectroscopy. Univariate data analysis of the spectra has been unable to detect this so far. Therefore, a multivariate data analysis

technique should be applied to processes that involve a fairly broad range of viscosity.

A multivariate relationship can be established between NIR spectra and complex viscosity measurements. The quality parameters demonstrate that the model is adapted to predict the viscosity from NIR measurements.

The relationship found indicates that viscosity is a significant source of variability in the recorded spectra. Consequently, if factor analysis is applied to this type of data, the factors found cannot be related only to the reaction process and the changes in the concentration of the species. This aspect is relevant when techniques such as multivariate curve resolution are applied to describe the concentration profile of the reaction.

Acknowledgements

We would like to thank Luis Adolfo Mercado, Marina Galià and Virginia Cádiz from the Area of Organic Chemistry of the Rovira i Virgili University, for their collaboration in the preparation of this paper. Likewise, we would like to acknowledge the economic suport provided by the MCyT (project Nº BQU 2003-01142).

References

1. B. A. Rozenberg, Adv. Polym. Sci. **75**, 113 (1985).
2. K. Dušek, Adv. Polym. Sci. **78**, 1 (1986).
3. R. J. Morgan, and J. E. O'Neal, Polym. Plast. Technol. Eng. **10**, 49 (1978).
4. E. F. Oleinik, Pure Appl. Chem. **53**, 1567 (1981).
5. B. Ellis, *Chemistry and Technology of Epoxy Resins*, (Blackie Academic & Professional, New York, 1993).
6. C. A. May, *Epoxy Resins*, (Marcel Dekker, New York, 1988).
7. E. F. Oleinik, Adv. Polym. Sci. **80**, 49 (1986).
8. J. Mijovic, and S. Andjelic, Macromolecules **28**, 2787 (1995).
9. J. Mijovic, S. Andjelic, C. F.W. Yee, F. Belluci, and L. Nicolais, Macromolecules **28**, 2797 (1995).
10. G. A. George, P. Cole-Clarke, N. St. John, and G. Friend, J. Appl. Polym. Sci. **42**, 643 (1991).
11. V. Strehmel, and T. Scherzer, Eur. Polym. J. **30**, 361 (1994).
12. J. Mijovic, A. Fishbain, and J. Wijaya, Macromolecules **25**, 979 (1992).
13. P. Musto, E. Martuscelli, G. Ragosta, P. Russo, and P. Villano, J. Appl. Polym. Sci. **74**, 532 (1999).
14. J. M. Barton, Adv. Polym. Sci. **72**, 111 (1985).
15. C. J. de Bakker, N. A. St. John, and G. A. George, Polymer **34**, 716 (1993).
16. M. T. Aronhime, and J. K. Gillham, Adv. Polym. Sci. **78**, 83 (1987).
17. I. C. Choy, and D. J. Plazek, J. Polym. Sci., Part B: Polym. Phys. **24**, 1303 (1986).
18. H. Kim, and K. Char, Bull. Korean Chem. Soc. **20**, 1329 (1999).
19. L. Barral, J. Cano, J. López, I. López-Bueno, P. Nogueira, C. Ramírez, A. Torres, and M. J. Abad, Thermochimica Acta **344**, 137 (2000).
20. N. A. St. John, and G. A.George, Polymer **33**, 2679 (1992).
21. K. Dean, W. D. Cook, L. Rey, J. Galy, and H. Sautereau, Macromolecules **34**, 6623 (2001).

22. Q. Wang, B. K. Storm, and L. P. Houmøller, J. Appl. Polym. Sci. **87**, 2295 (2003).
23. J. F. Aust, K. S.Booksh, C. M. Stellman, R. S. Parnas, and M. L. Myrick, Appl. Spectrosc. **51**, 247 (1997).
24. K. Hakala, R. Vatanparast, S.Y. Li, C. Peinado, P. Bosch, F. Catalina, and H. Lemmetyinen, Macromolecules **33**, 5954 (2000).
25. B. Strehmel, V. Strehmel, and M.Younes, J. Polym. Sci., Part B: Polym. Phys. **37**, 1367 (1999).
26. M. Younes, S. Wartewig, D. Lellinger, B. Strehmel, and V. Strehmel, Polymer **35**, 5269 (1994).
27. M. S. Larrechi, and F. X. Rius, Appl. Spectrosc. **58**, 47 (2004).
28. M. Garrido, I. Lázaro, M. S. Larrechi and F. X. Rius, Anal. Chim. Acta, 515 (2004), 65-73.
29. G. Lachenal, Vib. Spectrosc. **9**, 93 (1995).
30. L. Matějka, and K. Dušek, Macromolecules **22**, 2902 (1989).
31. L. Matějka, Macromolecules **33**, 3611 (2000).
32. J. López, C. Ramírez, A. Torres, M. J. Abad, L. Barral, J. Cano, and F. J. Diez, J. Appl. Polym. Sci. **83**, 78 (2002).
33. M. S. Lin, and R. J. Chang, J. Appl. Polym. Sci. **46**, 815 (1992).
34. E. Mertzel, and J. L. Koenig, Adv. Polym. Sci. **75**, 73 (1986).
35. B. Degamber, G. F. Fernando, MRS Bull. **27**, 370 (2002).
36. M. C. S. Perera, U. S. Ishiaku, and Z. A. M. Ishak, Polymer Degrad. Stab. **68**, 393 (2000).
37. H. C. Wang, D. G. Thompson, J. R. Schoonover, S. R. Aubuchon, and R. A. Palmer, Macromolecules **34**, 7084 (2001).
38. J. J. Kelly, C. H. Barlow, T. M. Jinguji, and J. B. Callis, Anal. Chem. **61**, 313 (1989).
39. D. M. Haaland, and E. V. Thomas, Anal. Chem. **60**, 1193 (1988).
40. F. Mc Lennan, and B. R. Kowalski, *Process Analytical Chemistry*, (Chapman & Hall, London, 1995).

41. B. Vandeginste, D. L. Massart, L. Buydens, S. de Jong, P. Lewi, and J. Smeyers-Verbeke, *Handbook of Chemometrics and Qualimetrics: Part B*, (Elsevier, Amsterdam, 1998).

42. N. Draper, and H. Smith, *Applied Regression Analysis*, (Wiley, New York, 1981), 2nd ed.

7. Conclusiones

Durante el transcurso de esta Tesis ha sido posible profundizar en la problemática de las reacciones de resinas epoxi con aminas, y en las capacidades de la espectroscopía NIR, en conjunto con técnicas quimiométricas como los métodos de resolución de curvas, para la investigación de la cinética de dichas reacciones.

La utilización conjunta de la espectroscopia NIR y los métodos de resolución de curvas ha resultado ser una opción válida y atractiva para el seguimiento cuantitativo de las reacciones de resinas epoxi y el estudio cinético de las mismas. Como se ha mostrado a lo largo de esta Tesis, es posible lograr una descripción satisfactoria y completa de los sistemas estudiados, incluyendo la obtención de perfiles de concentración de las especies a lo largo del tiempo y los correspondientes espectros puros, la postulación de modelos cinéticos y la estimación de las constantes cinéticas asociadas. Todo ello con ventajas adicionales, tales como el corto tiempo de análisis post-reacción, la ausencia de solventes orgánicos y la capacidad de automatización del método. Cabe destacar la complejidad de los mecanismos de reacción de los sistemas estudiados, que presentan cinéticas de pseudo segundo orden no estudiadas hasta ahora con este tipo de metodologías.

La aplicación de estas metodologías a sistemas modelo tiene una gran utilidad a nivel del desarrollo de nuevos materiales. La modificación de la estructura de ciertos monómeros es, hoy en día, una práctica común en la búsqueda de materiales con nuevas propiedades mecánicas y físicas. Es, por lo tanto, importante conocer los efectos que puede tener los cambios en la estructura de un monómero en la reactividad de un sistema químico.

A pesar de que los métodos propuestos se adaptan de forma adecuada al estudio de reacciones modelo, todavía permanece sin solución el reto de la extrapolación de estas estrategias de estudio cinético a reacciones de polimerización. Como se ha señalado, el espectro NIR se ve afectado por los cambios de viscosidad que tienen lugar durante las reacciones de curado, por lo que no es posible obtener resultados confiables cuando se

aplica este tipo de métodos multivariantes ya que, para datos espectroscópicos, su correcta utilización está supeditada al cumplimiento de la Ley de Beer. Evidentemente, el camino para solucionar estos problemas está ligado a la utilización de una técnica de análisis que no se vean afectadas por los cambios en la viscosidad de la mezcla de reacción. Investigaciones futuras en este sentido estarán orientadas a la utilización de técnicas como la resonancia magnética nuclear para sólidos.

De cualquier manera, es importante destacar el potencial de la combinación de la espectroscopía de infrarrojo cercano con los métodos de resolución de curvas para la monitorización de otros procesos químicos en los que no se produzcan cambios en la viscosidad, tanto en medio gaseoso como líquido. En cuanto a las reacciones en solución, es importante considerar que, cuando se trabaja con soluciones acuosas, la matriz puede interferir seriamente en la señal de ciertos grupos funcionales. El único requisito para las especies a monitorizar es que puedan experimentar un cambio neto en su momento dipolar para poder absorber energía infrarroja.

Referencias

[1] D. J. T. Hill, G. A. George, D. G. Rogers, *Polym. Adv. Technol. 13*, **2002**, 353.

[2] C.A. May, *Epoxy resins:chemistry and technology*, 2nd ed.; Marcel Dekker, New York, **1988**.

[3] B. Ellis, *Chemistry and Technology of Epoxy Resins*, Blackie Academic & Professional, New York, **1993**.

[4] H. J. Flammersheim, *Thermochim. Acta* 310, **1998**, 153.

[5] S. Swier, B. Van Mele, *Thermochim. Acta* 411, **2004**, 149.

[6] P. Musto, G. Ragosta, P. Russo, L. Mascia, *Macromol. Chemo. Phys.* 202, **2001**, 3445.

[7] B. Strehmel, V. Strehmel, M. Younes, *J. Polym. Sci. Part B* 37, **1999**, 1367.

[8] R. E. Lyon, K. E. Chike, S. M. Angel, *J. Appl. Polym. Sci.* 53, **1994**, 1805.

[9] R. E. Challis, M. E. Unwin, D. L. Chadwick, R. J. Freemantle, I. K. Partridge, D. J. Dare, P. I. Karkanas, J. *Appl. Pol. Sci.* 88, **2003**, 1665.

[10] J. Mijovic, A. Fishbain, J. Wijaya, *Macromolecules* 25, **1992**, 979.

[11] G. A. George, P. Cole-Clarke, N. St. John, G. Friend, *J. Appl. Polym. Sci.* 42, **1991**, 643.

[12] V. Strehmel, T. Scherzer, *Eur. Polym. J.* 30, **1994**, 361.

[13] J. Mijovic, S. Andjelic, *Macromolecules* 28, **1995**, 2787.

[14] J. Mijovic, S. Andjelic, C. F.W. Yee, F. Belluci, L. Nicolais, *Macromolecules* 28, **1995**, 2797.

[15] L. Xu, J.H. Fu, J. Schlup, *Ind. Eng. Chem. Res.* 35, **1996**, 963.

[16] C. Billaud, M. Vandeuren, R. Legras, V. Carlier, *Appl. Spectrosc.* 56, **2002**, 1413.

[17] T. Amari, Y. Ozaki, *Appl. Spectrosc.* 56, **2002**, 350.

[18] K. Dean, W. Cook, L. Rey, J. Galy, H. Sautereau, *Macromolecules* 34, **2001**, 6623.

[19] R. Tauler, A. Izquierdo-Ridorsa, E. Casassas, *Chemom. Intell. Lab. Syst.* 18, **1993**, 293.

[20] A. Izquierdo-Ridorsa, J. Saurina, S. Hernández-Cassou, R. Tauler. *Chemom. Intell. Lab. Syst.* 38, **1997**, 183.

[21] R. Tauler, A. Smilde, B. Kowalsky, *J. Chemometrics* 9, **1995**, 31.

[22] M. Gui, S. C. Rutan, A. Agbodjan, *Anal Chem.* 67, **1995**, 3293.

[23] J. Saurina, S. Hernández-Cassou, R. Tauler, *Anal Chem.* 69, **1997**, 2329.

[24] J. Jaumot, M. Vives, R. Gargallo, R. Tauler, *Anal. Chim. Acta* 490, **2003**, 253.

[25] M. Blanco, M. Castillo, A. Peinado, R. Beneyto, *Appl. Spectrosc.* 60, **2006**, 641.

[26] B. Y. Li, J. M. Zhang, Y. Hu, Y. Z. Liang, Y. Ozaki, *Appl. Spectrosc.* 60, **2006**, 155.

[27] J. M. Amigo, A. de Juan, J. Coello, S. Maspoch, *Anal. Chim. Acta* 567, **2006**, 245.

[28] J. Saurina, C. Leal, R. Compano, R. Tauler, M. D. Prat, *Anal. Chim. Acta* 409, **2000**, 237.

[29] R. H. Uibel, J. M. Harris, *Appl. Spectrosc.* 58, **2004**, 934.

[30] E. R. Malinowski, *Factor Analysis in Chemistry* ,3ra Ed., Wiley, New York, **2002**.

[31] J. Saurina, S. Hernández-Cassou, R. Tauler, A. Izquierdo-Ridorsa, *J. Chemometrics* 12, **1998**, 183.

[32] A. de Juan, E. Casassas, and R. Tauler, "Soft-modelling of analytical data" in *Enciclopedia of analytical Chemistry: Instrumentation and Applications*, (Wiley, New York, 2000), p. 9800.

[33] A. de Juan, M. Maeder, M. Martínez, and R. Tauler, *Chemom. Intell. Lab. Syst.* 54, **2000**, 123.

[34] G. Puxty, M. Maeder, K. Hungerbühler, *Chemom. Intell. Lab. Syst.* 81, **2006**, 149.

[35] J. M. Amigo, A. de Juan, J. Coello and S. Maspoch, *Anal. Chim. Acta* 567, **2006**, 236.

[36] K. Dušek, *Adv. Polym. Sci.* 78, **1986**, 1.

[37] B. A. Rozemberg, *Adv. Polym. Sci.* 75*,* **1985***,* 113.

[38] K. E. Hassan, P. C. Robery, L. Al-Alawi, *Cem. Concr. Compos.***22**, (2000), 453.

[39] J. T. Carter, G. T. Emmerson, C. Lo Faro, P. T. McGrail, D. R. Moore, *Compos. Pt. A-Appl. Sci. Manuf.,* **34**, (2003), 83.

[40] M.Sham, J. Kim, *Compos. Pt. A-Appl. Sci. Manuf.,* **35***,* (2004)*,* 537.

[41] J. A. Simões, A. T. Marques, G. Jeronimidis, *Compos. Sci. Technol.*, **60**, (2000), 559.

[42] K. A. Schulze, S. J. Marshall, S. A. Gansky, G. W. Marshall, *Dent. Mater.***19**, (2003), 612.

[43] L. Matějka, *Macromolecules* 33, **2000**, 3611.

[44] Riccardi , C.C.; Williams, R.J.J. *Polymer* **1986**, *27*, 913-920.

[45] J. Mijovic, A. Fishbain, J. Wijaya, *Macromolecules* 25, **1992**, 979.

[46] L. Matějka, K. Dušek, *Macromolecules* 22, **1989**, 2902.

[47] H. J. Flammersheim, *Thermochim. Acta* 310, **1998**, 153.

[48] S. Swier, B. Van Mele, *Thermochim. Acta* 411, **2004**, 149.

[49] L. Xu, J.H. Fu, J. Schlup, *Ind. Eng. Chem. Res.* 35, **1996**, 963.

[50] J. López, C. Ramírez, M. Torres, J. Abad, J. Barral, F. Cano, J. Diez, *J. Appl. Polym. Sci.* 83, **2002,** 78.

[51] J. Lange, N. Altmann, C. T. J. Kelly, P. J. Halley, *Polymer* 41, **2000**, 5949.

[52] J. M. Cuevas, J. M. Laza, M. Correa, J. L. Vilas, M. Rodríguez, L. M. León, *J. Appl. Polym. Sci.* 41, **2003**, 1965.

[53] K. Dean, W. Cook, L. Rey, J. Galy, H. Sautereau, *Macromolecules* 34, **2001**, 6623.

[55] J. M. G. Cowie, *Polymers: Chemistry & Physics of Modern Materials*, 2ª Ed. Blackie Academic & Profesional, London, **1994**, 247-273.

[55] S. Swier, B. Van Mele, *Thermochim. Acta* 411, **2004**, 149.

[56] B. G. Osborne, T. Fearn, P. H. Hindle, *Practical NIR spectroscopy with application in food and beverage analysis*, Longman Scientific & Technical, 2da Ed. Harlow, England, **1993**.

[57] V. I. Bakhmutov, *Practical NMR Relaxation for chemists*, John Wiley & Sons, Chichester, **2004**.

[58] R. B. Bates, W. A. Beavers, *Carbon-13 NMR Spectral Problems*, The Humana Press, Clifton, **1981**.

[59] H. H. Willard. L. L. Merrit, J. A. Dean, F. A. Settle, *Instrumental methods of analysis*, 6ª edición, Wadsworth Publishing Company, Belmont, **1981**.

[60] E. Tenailleau, P. Lancelin, R.J. Robins, S. Akoka, Anal. Chem. 76 (2004) 3818–3825.

[61] E. A. Turi, *Thermal Characterization of Polymeric Materials*. Vol. 1. Academic Press, San Diego, **1997**.

[62] J. M. Cuevas, J. M. Laza, M. Correa, J. L. Vilas, M. Rodríguez, L. M. León, *J. Polym. Sci.: Part B: Polym. Phys.*41, **2003**, 1695-1977.

[63] V. A. Hackley, C. F. Ferraris, *Guide to rheological nomenclature for Liquid-based particle systems,* NIST special publication 946, NIST, 2001. URL: http://ciks.cbt.nist.gov/%7Egarbocz/SP946/SP946.htm.

[64] D. L. Massart, B. G. M. Vandeginste, L. M. C. Buydens, S. de Jong, P. J. Lewi, J. Smeyers-Verbeke, *Handbook of Chemometrics and Qualimetrics : Part A*, Elsevier, Amsterdam, **1997**.

[65] E. V. Thomas, D. M. Haaland, *Anal. Chem.* 62, **1988**, 1091.

[66] E. V. Thomas, D. M. Haaland, *Anal. Chem.* 62, **1988**, 1202.

[67] H. Martens, T. Naes, *Multivariate Calibration*, John Wiley & Sons, Chichester, **1989**.

[68] K. R. Beebe, B. R. Kowalsky, *Anal. Chem.* 59, **1989**, 1007A.

[69] R. Tauler, B. Kowalsky, S. Fleming, *Anal. Chem.* 65, **1993**, 2040.

[70] J. C. Hamilton, P. J. Gemperline, *J. Chemometrics* 4, **1990**, 1.

[71] W. Windig, *Chemom. Intell. Lab. Syst.* 16, **1992**, 1.

[72] K. V. Mardia, J. T. Kent, J. M. Bibby, *Multivariate Analysis*, Academic Press, London, **1980**.

[73] B. M. G. Vandeginste, D. L. Massart, L. M. C. Buydens, S. de Jong, P. J. Lewi, J. Smeyers-Verbeke, *Handbook of Chemometrics and Qualimetrics : Part B*, Elsevier, Amsterdam, **1998**.

[74] R. G. Brereton, *Chemometrics: Data Analysis for the Laboratory and Chemical Plant*, Wiley, Chichester, **2003**.

[75] R. Cela, *Avances en Quimiometría Práctica,* Universidade de Santiago de Compostela, Santiago de Compostela, **1994**.

[76] H. Gampp, M. Maeder, C. J. Meyer, A. Zuberbühler, *Talanta* 12, **1985**, 1133.

[77] H. R. Keller, D. L. Massart, *Chemom. Intell. Lab. Syst.* 12, **1992**, 209.

[78] W. Windig, J. Guilment, *Anal. Chem.* 63, **1991**, 1425.

[79] O. S. Borgen, B. R. Kowalski, *Anal. Chim. Acta* 246, **1991**, 379.

[80] M. C. Antunes, J. E. J. Simão, A. C. Duarte, R. Tauler, *Analyst* 127, **2002**, 809.

[81] R. Tauler, *Chemom. Intell. Lab. Syst.* 30, **1995**, 133.

[82] G. H. Golub, Ch. F. Van Loan, *Matrix Computations*, The John Hopkins university Press, Baltimore, **1989**.

[83] C. Mason, M. Maeder, A. Whitson, *Anal. Chem.* 73, **2001**, 1587.

[84] R. Tauler, *J. Chemometrics* 15, **2001**, 627.

[85] A. de Juan, Y. Vander Hieden, R. Tauler, D. L. Massart, *Anal. Chim. Acta* 346, **1997**, 307.

[86] C. L. Lawson, R. J. Hanson, *Solving Least Squares Problems*, Prentice-Hall, Englewood Cliffs, NJ, **1974**.

[87] R. Bro, S. Jong, *J. Chemometrics* 11, **1997**, 393.

[88] A. de Juan, R. Tauler, *Anal. Chim. Acta* 500, **2003**, 195.

[89] The Mathworks, MATLAB Versión 6.5, Natick, MA, 2002, http://www.mathworks.com.

[90] Camo Process AS, The Unscrambler Versión 9.0, Oslo, Norway, 2004, http://www.camo.no.

[91] Mestrelab research, MestRe-C Versión 2.3a, Departamento de Química Orgánica, Universidad de Santiago de Compostela, Santiago de Compostela, España, 2000, http://www.mestrec.com.

[92] R. Tauler, A. de Juan, Chemometrics and Solution Equilibria, Universidad de Barcelona, Barcelona, España, 1999, http://www.ub.es/gesq/mcr/ndownload.htm.

[93] M. Amrhein, B. Srinivasan, D. Bonvin, M. M. Schumacher, *Chemom. Intell. Lab. Syst.* 33, **1996**, 17.

[94] S. R. Crouch, A. Scheeline, E. S. Kirkor, *Anal. Chem.* 72, **2000**, 53R.

[95] J. Workman, D. J. Veltkamp, S. Doherty, B. B. Anderson, K. E. Creasy, M. Koch, J. F. Tatera, A. L. Tobinson, L. Bond, L. W. Burgess, G. N. Bokerman, A. H. Ullman, G. P. Darsey, F. Mozayeni, J. A. Bamberger, M. S. Greenwood, *Anal. Chem.* 71, **1999**, 121R.

[96] J. Workman, M. Koch, D. J. Veltkamp, *Anal. Chem.* 75, **2003**, 2859.

[97] K. J. Mohillo, M. Maeder, M. M. Schumacher, *Chemom. Intell. Lab. Syst.* 46, **1999**, 221.

[98] A. Zogg, U. Fischer, K. Hungerbülher, *Chemom. Intell. Lab. Syst.* 71, **2004**, 165.

[99] D. Kendall, *Applied Infrared Spectroscopy*, Reinhold Publishing Corporation, New York, **1966**.

[100] J. Mijovic, S. Andjelic, Macromolecules 28, **1995**, 2787.

[101] M. S. Lin, and R. J. Chang, J. Appl. Polym. Sci. 46, **1992**, 815.

[102] G. Lechenal, *Vibrational Spectroscopy* 9, **1995**, 93.

[103] E. Mertzel, J. L. Koenig, *Adv. Polym. Sci.* 75, **1986**, 73.

Anexo

Anexo I: Otros trabajos derivados de esta Tesis:

- "Reactivity of silicon-based epoxy monomers as studied by Near Infrared Spectroscopy and Multivariate Curve Resolution methods", L. A. Mercado, M. Galià, J. A. Reina, M. Garrido, M. S. Larrechi, F. X. Rius, J. Polym. Sci. Part A: Polym. Chem. 2006, 44, 1447-1456.

- "Influence of viscosity on NIR spectra obtained by monitoring of curing epoxy resins. Consequences for the application of Multivariate Curve Resolution methods", M. Garrido, M. S. Larrechi, F. X. Rius, en preparación.

- "Near infrared spectroscopy and multivariate curve resolution-alternating least squares for in situ quantitative monitoring of epoxy resins reactions". M. Garrido, M. S. Larrechi, F. X. Rius, en preparación.

- "Analytical methodologies for quantitative monitoring of epoxy resins reactions" M. Garrido, M. S. Larrechi, F. X. Rius, V. Cadiz, M. Galià, en preparación.

Anexo II: Listado de Acrónimos y símbolos

ALS : Mínimos cuadrados alternados

BLS: Mínimos cuadrados bivariantes

DDM: Diaminodifenilmetano

DGEBA: Diglicidiléter de Bisfenol A

DMA: Análisis Dinamomecánico

DSC: Calorimetría diferencial de barrido

EEW: Peso equivalente epóxido

EFA: Análisis de factores emergentes

FTIR: Infrarrojo con transformada de Fourier

GDMPS: Fenilglicidiloxidimetilsilano

HPLC: Cromatografía Líquida de Alta Eficacia

HS-MCR: Resolución multivariante de curvas con combinación de modelados duro y blando

ISO: Organización Internacional para la Estandarización

ITTFA: Iterative Target Testing Factor Analysis

Lof: Falta de ajuste

Mcr: Resolución multivariante de curvas

MTDSC: Calorimetría diferencial de barrido con temperatura modulada

NIR: Espectroscopía de infrarrojo cercano

NOE: Efecto nuclear Overhauser

OLS: Mínimos cuadrados ordinarios

PCA: Análisis de componentes principales

PCR: Regresión en componentes principales

PGE: Fenilglicidiléter

PGTE: Fenilglicidiltioéter

PRESS: Suma de cuadrados del error de predicción

RMN: Resonancia magnética nuclear

RMSECV: raiz cuadrada de la media de los errores de validación cruzada

ρ: Efecto de sustitución

SIMPLISMA: SIMPLe-to-use Interactive Self-modelling Mixture Analysis

SMCR: Self Modeling Curve Resolution

SVD: Descomposición en valores singulares

T_1: Tiempo de relajación spin- lattice

T_2: Tiempo de relajación spin- spin

Tg: Temperatura de transición vítrea

TGA: Análisis termogravimétrico

TT: Iterative Target Testing